Analysis of the South Westland Basin, New Zealand.

A thesis
submitted in partial fulfilment
of the requirements for the Degree
of
Master of Science in Earth Sciences
at the
University of Waikato
by

Keith Nicholas Sircombe

University of Waikato

1993

Abstract

Running parallel to the thrust front of the Southern Alps, an elongate, predominantly offshore and relatively deep basin, considered to have originated as a foreland basin, has previously been identified in South Westland, South Island, New Zealand. An integrative approach to basin analysis has been undertaken in this thesis to test the hypothesis that this basin has been formed by the loading of the Pacific Plate onto the Australia Plate during the Late Cenozoic. The two principal approaches to this problem undertaken in this thesis are seismic mapping of industry acquired seismic reflection profiles available for the basin and geodynamical analysis of the basin geometry and its stratigraphy.

Seismic mapping reveals a thick sedimentary section that can be divided broadly into five sequences. The thickness distribution of these units have been digitized into a computer database for subsequent modelling and mapping. The five sequences are titled Sequence E through to A from the basement to the surface. The lowermost sequence, Sequence E, is a thin sheet of marginal marine sediments thickening toward the west. It is believed to have formed in a rift margin setting during the Late Cretaceous–Eocene, overlain by a regionally extensive limestone formed during a marine transgression in the Oligocene. Sequence D has a sheet-like form comprising turbiditic systems deposited in bathyal depths between around 30 Ma and 15 Ma. This is coincident with increasing convergence across the Alpine Fault and initial loading of the Australia Plate, and Sequence D may represent the early underfill stage of foreland basin development. Sequence C is wedge-like in form, consisting of deep water turbiditic systems rapidly deposited between 5 Ma and 3.1 Ma. This corresponds with the uplift of the inner margin of the basin along the South Westland Fault Zone. Sequence B is a prominent lensoidal form prograding facies consisting of mudstone with frequent coarser beds deposited between 3.1 Ma and 1.2 Ma. Sequence A tops the section with a possible eustatically controlled and predominantly slumped deposit of mudstone with thick units of bioclasts near the present surface.

Geodynamic analysis reveals an early stage of thermal subsidence due to late Cretaceous rifting that preceded Tasman Sea spreading. It is compatible with a lithospheric stretching factor of 1.25. Increasingly rapid subsidence since 15–10 Ma is interpreted as possible fault-controlled subsidence due to strike-slip deformation combined with loading resulting from increased convergence across the Alpine Fault. This is followed by the uplift of the inner margin of the basin around 5 Ma to form the presently exposed coastal strip. This event probably also contributed to the loading of the Australia Plate. Flexural analysis of the basement structure of the Australia Plate reveals an unusually weak lithosphere with a rigidity around 9.79×10^{20} Nm. Several alternative interpretations are presented to explain this unusually weak lithosphere, such as high heat flows, lithospheric decoupling and inherited structures. The complex evolution of the basin from rift margin, through strike-slip to foreland basin is believed to have left behind structures that may constrain and/or enhance the flexural response of the Australia Plate.

Acknowledgements

I would like to thank all the people who have made completion of this thesis possible:

✓ Dr Peter Kamp for the formulation of this challenging and rewarding topic, and his continued enthusiasm during the supervision of this thesis.

✓ Professor Cam Nelson for encouraging the computer-orientated side of this project.

✓ Ian R Brown Associates Limited for providing the TECHBASE program, and Miranda Nelson, Pete Manning and Bill Leask for continued software support.

✓ Ray Wood, of the Institute of Geological and Nuclear Sciences, for providing his geohistory program to me, that was further developed in this thesis.

✓ The Earth Sciences Department technicians, Steve Bergin and Ian Whitehouse for technical assistance with computing and thesis preparation. Dr Mark Tippett is also thanked for useful discussions.

✓ My fellow students from many years (and in no particular order: Glen Hughes, Lisa Paton, Sarah Parsons, Gerry & Chris Spanninga, Tony Haworth, Niall Dinning, Steve Hood, Matt Middleton, Dave Phizacklea, Brett Roberts, Dougall Gordon, Helen Neil, Tim Naish) for their friendship and humour at all times.

✓ The untold number of people that have enriched my life through University. Especially Roger Foote, Carolyn Wait and Lyn Brassington for their friendship and support.

✓ My family, Mum, Dad, Amanda, Uncle Peter & Grandma for their total support throughout my education and this thesis.

Table of Contents

Chapter 4: Application and Observations of Basin Analysis in South Westland.

Chapter 5: Interpretation and Discussion of Basin Analysis in South Westland.

List of Figures

List of Tables

Chapter 1

Introduction

1.0 Introduction

An active zone of oblique continental convergence crosses the South Island of New Zealand. The Alpine Fault marks the boundary between the converging plates, the Australia Plate to the west and the Pacific Plate to the east (Figure 1.1). The Alpine Fault originated as a transform fault at about 25 Ma (Kamp, 1986, 1991; Cooper et al., 1987), and the compressive component of the oblique-slip displacement started at about 9.8 Ma (Stock & Molnar, 1982). The amount of lithospheric shortening normal to the continental convergence zone has been estimated at about 70 km in the central part of the South Island (Allis, 1986). This shortening has partially resulted in the uplift of the Southern Alps and the building of an associated 'root' of continental crust. Contrasting with the extreme amount of uplift in the Southern Alps is an elongate sedimentary basin trending parallel to the modern coastline and having a maximum depth to basement immediately offshore of about 3.5–4.0 km (Nathan et al., 1986, Figure 1.1). Kamp et al. (1992) noted several features of this sedimentary basin:

(1) The basin is parallel to the main thrust (Alpine Fault) and mountain belt (Southern Alps).

(2) The basin is asymmetric in cross section, deepening toward the mountain front.

(3) The basin started to form at about 13 Ma, about the time the plate boundary became obliquely convergent.

(4) The basin subsided rapidly, as distal submarine fan turbidites overlie a basal 10 m thick bioclastic shelf limestone.

(5) Typical molasse facies including glacial moraines, and thick conglomerates have been deposited along the SE margin of the predominantly marine basin during the Quaternary.

These features suggest that the basin has formed as the result of the Australia plate being loaded by the Pacific plate (Kamp et al., 1992). Such basins originating from the flexure (bending) of the lithosphere are termed foreland basins.

The broad aim of this thesis is to undertake an analysis of industry acquired seismic reflection profiles to test the idea that the basin formed in a foreland setting. This study includes geodynamical modelling.

1.1 Study objectives

The objectives of this study are:

❶ To identify and describe seismic stratigraphic features in the South Westland Basin.

❷ Compile a digitized database of seismic stratigraphic information for further processing.

❸ Develop a geohistory and geodynamic analysis package for studying the exploration wells in the study area.

❹ Expand the geohistory and geodynamic analysis for application to the digitized database and thus the studied area.

❺ Produce structure maps of basement, overlying sediment thicknesses and the evolution of the basin through time.

❻ Interpret the geological features of the South Westland basin with those of 'classical' foreland basins.

1.2 Location

The study area is bounded to the east by the Alpine Fault, between 10–15 km inland from the coastline (see Figure 1.1). The western boundary is undefined as the sedimentary sequences of the basin simply thin onto the Challenger Plateau, although any sediments beyond around 120 km from the coastline are not covered in this study. The township of Hokitika marks the northern extent of the study area and coincides with a pronounced widening of onshore South Island NW of the Alpine Fault, and the southern end of the Marlborough Fault Zone. To the south, Jackson Bay marks the southern limit of this study due to a paucity of quality data further south. The southern end of the basin coincides with the transition from early Paleozoic continental crust underlying the Challenger Plateau to Late Cretaceous oceanic crust of the Tasman Sea, which has been subducted to a depth of about 150 km beneath Fiordland (Davey & Smith, 1983; Figure 1.1). Although the principal area of interest lies offshore in the modern continental shelf and slope, onshore geology is still important for regional correlation.

Onshore, the topography of South Westland is extremely rugged and relatively inaccessible. The geology is dominated by the dextral obliquely convergent Alpine Fault and the resultant uplifted Southern Alps rising to Mt Cook at a height of 3754 m (McSaveney et al., 1992). The Southern Alps are largely responsible for the huge rainfall in the area by trapping moisture laden air from the prevailing southwesterly weather systems. The high rainfall in association with the high uplift rate in the Southern Alps

combine to produce rapid weathering and erosion, and thus a vast volume of sediment is being transported down the numerous rivers to the continental shelf. Offshore, relatively limited bathymetry shows a general smooth lying shelf becoming more rugged to the southwest and toward the Puysegur Trench off Fiordland.

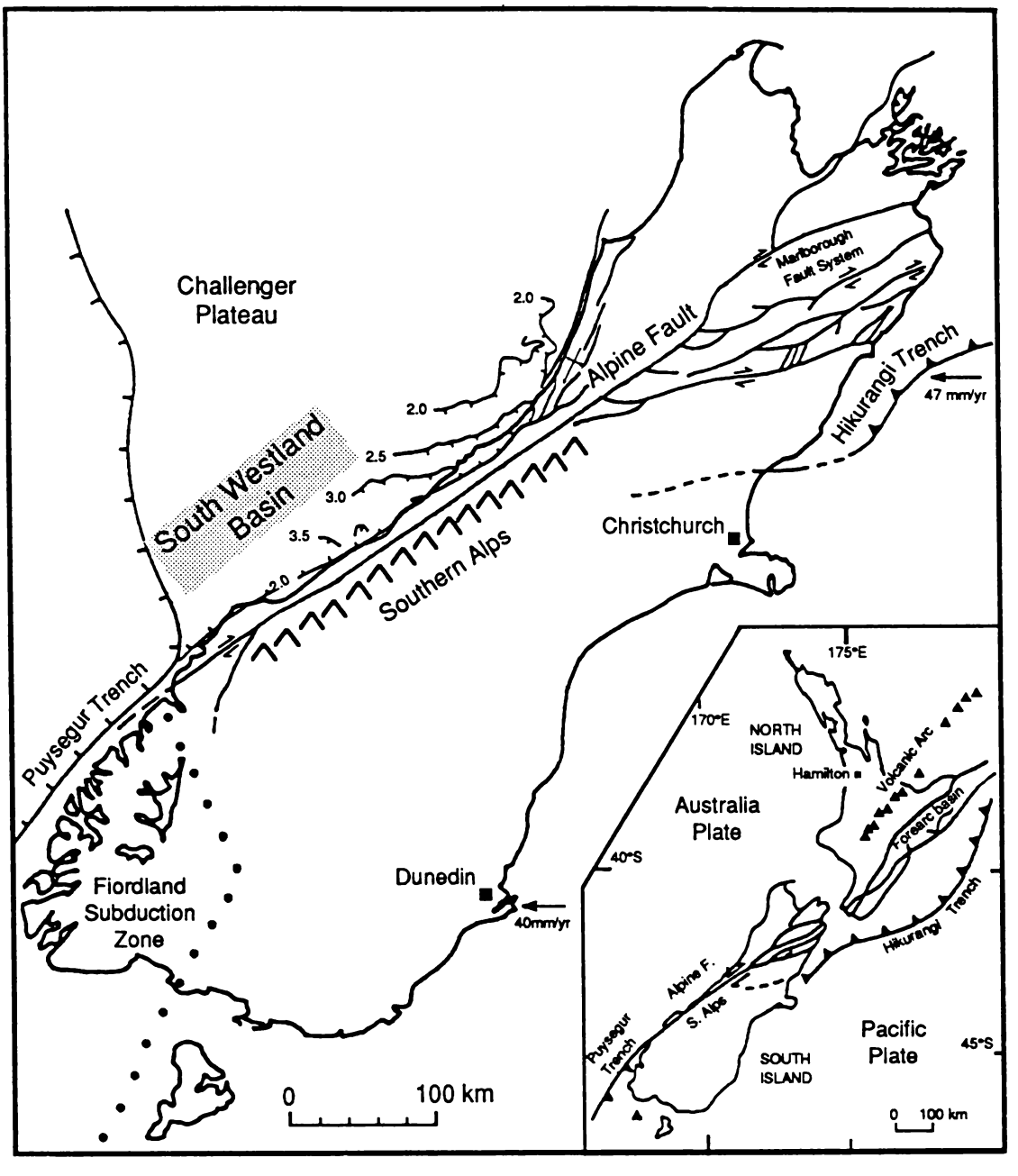

FIGURE 1.1: Map of the South Island, New Zealand, showing key tectonic features. Depth (in kilometres) to basement in the basin is from Nathan et al. (1986). Arrows indicate directions and rates of convergence (from Walcott, 1984b). Inset is a map of New Zealand showing character of the Australia-Pacific plate boundary. (From Kamp et al., 1992)

1.3 Previous studies

The West Coast region of South Island has been extensively geologically mapped due to the presence and exploitation of three major and several minor coalfields, oil and gas seepages and numerous metalliferous prospects. A combination of mountainous terrain, thick forest cover, intense rainfall and relative inaccessibility has prevented geological examination of South Westland on the same intensity as the better known Greymouth–Murchison area to the north in Westland.

Most previous work in South Westland has mostly been in a reconnaissance framework (e.g. Hector, 1863 & Haast, 1879, *in* Nathan, 1978; Wellman & Willett, 1942), often with an aim to tie local geology with the better known geology of the north. The onshore area is covered in the 1:250,000 series Geological Map of New Zealand by Sheet 17 — Hokitika (Warren, 1967); Sheet 19 — Haast (Mutch & McKellar, 1964); and Sheet 20 — Mt. Cook (Gair, 1967). Complementing the geological maps a number of geophysical maps have also been compiled to display gravity anomalies both onshore (Syms, 1978 & 1979) and offshore (Davy & Davey, 1985; Rose & Davey, 1985; Rose, 1986). Magnetic studies have also been done (Woodward, 1975).

Petroleum exploration in the late 1960's and early 1970's produced the majority of the seismic reflection profiles in the area (Shell B.P., 1967; Esso Exploration, 1968; Magellan Petroleum, 1971; N.Z. Petroleum, 1971, 1974; Australian Gulf, 1973). Three exploration wells were also drilled, two onshore (Harihari-1 and Waiho-1) and one offshore (Mikonui-1). All were dry and abandoned, although extensive reports were written about their findings (N.Z. Petroleum, 1971, 1972; Diamond Shamrock, 1981). Further investigation of the seismic and exploration well data appears to have been limited at the time when favourable plays were not easily found. From seismic data, McNaughton and Gibson (1970) suggested the presence of reef-like structures in the mid-Tertiary sequence, and Norris (1978) undertook an extensive review of the structures seen in near surface seismic profiles on the West Coast Shelf. Nathan et al. (1986) used various Open-file Petroleum Reports submitted by the exploration operators to produce a broad scale map of basement depth in the offshore basin.

Due to the inaccessibility of most of the region and lack of outcrop under dense bush, a number of studies have also focussed on the Cenozoic coastal and near coastal sections exposed between Gillespie Point through Jackson Bay, at the southern end of this study area, to Milford Sound (Cotton, 1956; Young, 1968; Nathan, 1977, 1978; Adams, 1987; Aliprantis, 1987; Sutherland, 1992; Figure 1.2). The stratigraphy of these rocks is of great relevance to a regional synthesis of geological information in the South Westland Basin.

The most intensive compilation of South Westland geology is the Cretaceous-Cenozoic sedimentary basins study done in the West Coast Region by Nathan et al. (1986). The following geological setting is largely based on the synthesis presented by Nathan et al.

A number of studies have also focussed on the nearby Southern Alps in regards to the character and kinematics of the collision zone in the South Island (e.g. Walcott & Cresswell, 1979; Wellman, 1979; Allis, 1981, 1986; Koons, 1989, 1990; Norris et al., 1990). Katz (1979) noted that subsidence in 'foredeep' basins along the western coast of New Zealand and orogenic uplift in adjacent mountain ranges appear to be linked, but no specific mechanism was discussed. Recent work in the Geochronology Research Unit, Department of Earth Sciences, University of Waikato on the Southern Alps (Kamp et al., 1992; Tippett, 1992) has developed a considerable pool of information about the evolution of the Southern Alps and therefore the implications for the various models of the continental collision zone. It is hoped that this study will complement and add a new dimension to this work.

1.4 Geological setting

The South Westland Basin occurs in the West Coast Region of the South Island, New Zealand, defined by Nathan et al. (1986) as the onshore area and adjacent continental shelf west of the Alpine Fault and Waimea-Flaxmore Fault System (Figure 1.1). The region is broadly divided into two major tectonic units, the West Coast Basin-and-Range Province and the Western Platform. The West Coast Basin-and-Range Province constitutes most of the onshore extent of the West Coast Region. The structure of Westland is dominated by a strong N-NNE structural trend which appears to date back to at least the Early Paleozoic and controls the structure of the present mountain ranges and inter-montane basins. The Western Platform is largely offshore to the west of the Cape Foulwind and South Westland Fault Zones and thus includes the South Westland Basin. The area is considered the southern continuation of the relatively stable area to the west of the Taranaki Graben which is northeast of Westland.

The time-stratigraphic subdivisions used in this thesis are summarised in Figure 1.2 (Edwards et al., 1988). The New Zealand stages are based on the range of fossils in marine sequences, and a summary is given by Suggate et al. (1978) and Hoskins (1982).

The existing geological interpretation of South Westland is largely derived from onshore outcrop exposures at or near the coast. The onshore stratigraphy of the main late Cretaceous and Tertiary lithostratigraphic units in the South Westland area are illustrated in Figure 1.3. The broad distribution of the various groups of rocks is shown in Figure 1.4. The geological history of South Westland also needs to be viewed in context of

the evolution of the plate boundary through the New Zealand continental block, particularly the displacement and timing of movement on the Alpine Fault. Numerous reconstructions of the plate boundaries have been complied by various authors (Walcott, 1984a, 1987; Kamp, 1986a; Spörli & Ballance, 1989). A summary of these reconstructions is given in Figure 1.5.

1.4.1 Pre-Cretaceous rocks

The pre-Cretaceous geology of the South Island can be broadly divided into two major litho-tectonic subdivisions: a western Tuhua Orogen, also termed the Foreland Province, representing a fragment of the Gondwana super-continent, consisting mainly of crystalline rocks with ages ranging from around 680 Ma (Nathan, 1986, p.16) to late Mesozoic; and the Rangitata Province, representing an accumulation of Carboniferous to Jurassic sediments grouped in distinctive terranes that were docked to the Tuhua Orogen during the Rangitata Orogeny.

The West Coast Region is largely underlain by rocks of the Tuhua Orogen, consisting of gneisses, metasediments and intrusive granites. An Early Paleozoic sedimentary sequence ranging from the Cambrian to Devonian is widespread through the region. This sequence is broadly divided into three sedimentary belts, the eastern and central belts are restricted to northwest Nelson, but the western belt extends over much of the region. The western belt occurs through the South Westland area and consists mainly of the Ordovician aged Greenland Group, a uniform and distinctive greenish-grey quartzose flysch-type sequence and is considered similar to exposures in North Westland (Laird, 1972; Laird & Shelley, 1974; Nathan, 1977).

Only a small area, east of Nelson, is underlain by terranes of the Rangitata Province. To the immediate east of the Alpine Fault lies the Haast Schist, a metamorphically derived terrane from the Rangitata Province. The intrusive rocks of the West Coast Region are grouped into two main periods of plutonic activity, at 280-370 Ma (Late Devonian-Carboniferous) and 80-120 Ma (Cretaceous). Both are interpreted as resulting from the plutonic phases of the Tuhuan and Rangitata Orogeny respectively.

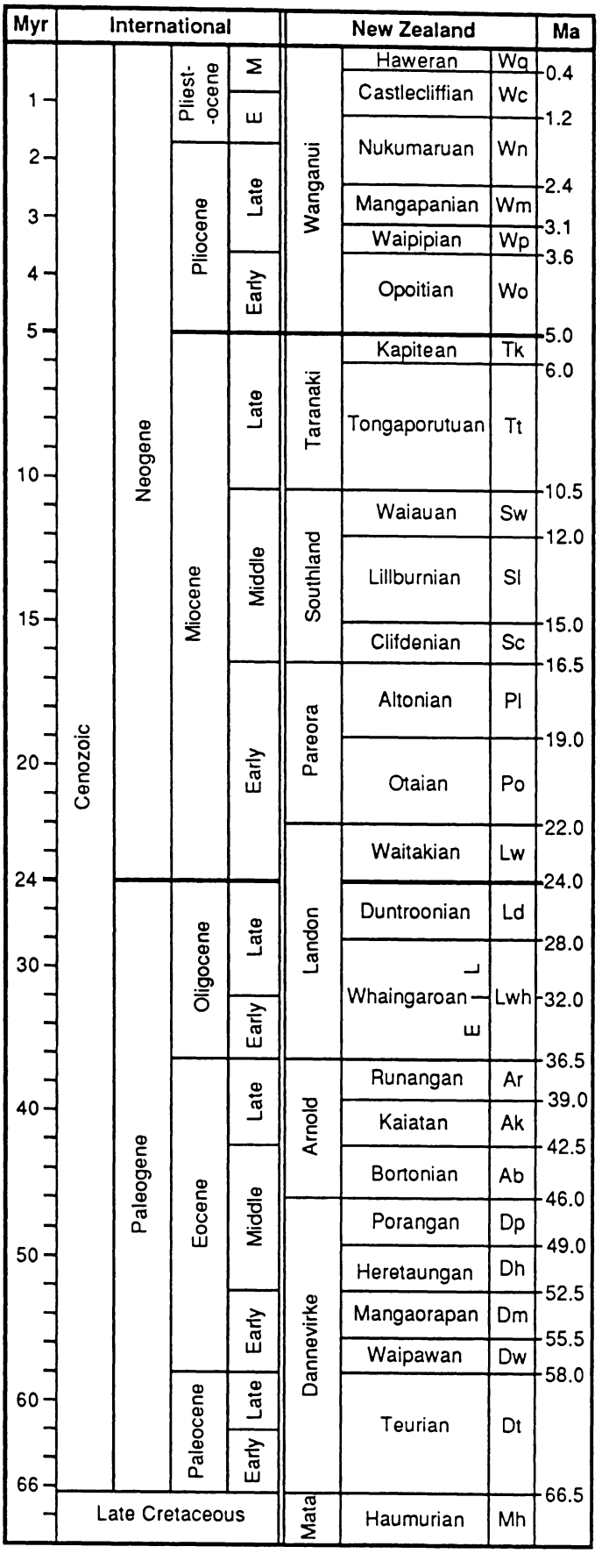

FIGURE 1.2: Geological time scale for Late Cretaceous and Cenozoic time, showing international and New Zealand subdivisions. (After Edwards et al., 1988)

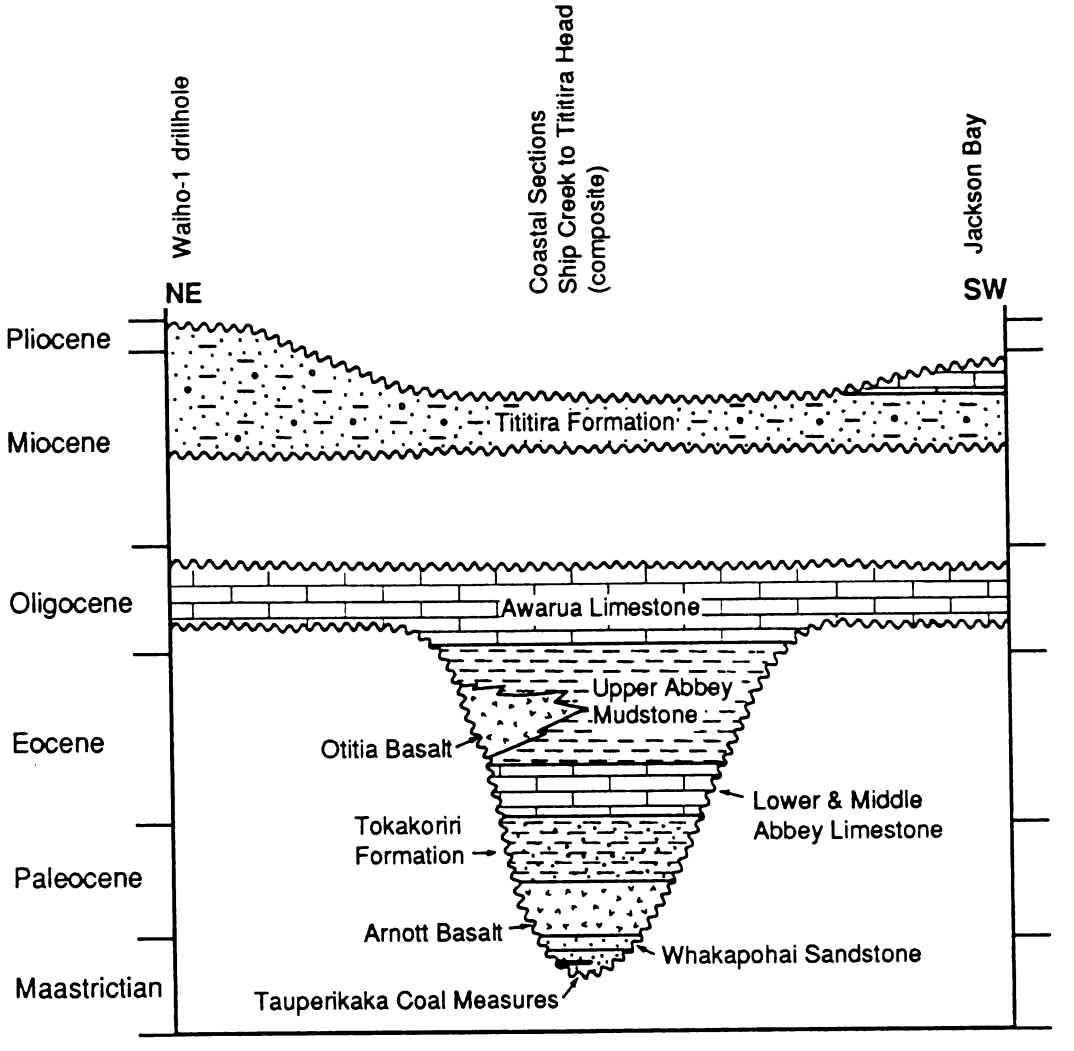

FIGURE 1.3: Stratigraphic diagram of the age and overall lithology of the main latest Cretaceous and Cenozoic lithostratigraphic units seen in onshore sections in South Westland (from Map 17, Nathan et al., 1986)

1.4.2 Cretaceous rocks

Two distinct phases of active rifting occurred during the Cretaceous. The first, about 100 Ma is associated with the continental rifting precursor to the creation of the Tasman Sea spreading ridge. Sedimentary evidence for this event is found in the Pororari Group and indicates that deposition of coarse sediments derived from granitic sources occurred in rapidly formed half grabens, with some lateral gradation locally to fluvio-lacustrine sediments. In South Westland, the Pororari Group is represented by the Otumotu Formation which consists of a basal breccia grading upwards to an interbedded sandstone, conglomerate and carbonaceous mudstone with scattered lenses of coal (Nathan, 1977; Nathan et al., 1986)

The second rifting event occurred in the Late Cretaceous (75-65 Ma). The origin of this event is poorly understood and may have been associated with some crustal weakness derived from the active Tasman Sea sea-floor spreading zone. Sediments were deposited in four main recognisable basins through the West Coast Region: the South Westland Embayment, the Paparoa Trough, Pakawau Basin and the Greville Basin. The latter three basins are dominantly fault controlled, but the Late Cretaceous–Paleocene sediments in South Westland have irregular margins and thus the term 'South Westland Embayment' is adopted (Nathan et al., 1986).

The basal unit of this sequence are dominantly fluvio-lacustrine coal-measures (Tauperikaka Coal Measures), grading upwards through a marine transgressive sequence containing interbedded volcanics that are interpreted as being derived from rift volcanics (Whakapohai Sandstone and Arnott Basalt, Fig.1.4; Sewell & Nathan, 1987). Overlying these units is a thin deep-water marine sequence of bioturbated calcereous muddy sandstone (Tokakoriri Formation, Fig.1.4). Adams (1987) noted that the thick sequences of Cretaceous rocks in the onshore sections may imply the existence of a former sedimentary basin lying eastward of a basement high.

1.4.3 Eocene–Oligocene

The early Cenozoic in the West Coast Region was marked by the development of a peneplain, due to thermal subsidence and tectonic quiescence of the New Zealand micro-continent as it drifted away from the active spreading zones. The only deposition occurred in the basin remnants of the late Cretaceous rifting event previously mentioned. In South Westland a deep-water marine sequence continued to accumulate (Lower & Middle Abbey Limestone and Upper Abbey Mudstone, Fig.1.4). A short period of local uplift and erosion is suggested by the presence of clasts of older units in the Upper Abbey Mudstone. Intraplate volcanism was also intermittent through the Eocene with basaltic breccia and scattered flows interbedded with the mudstone (Otitia Basalt, Fig.1.4; Sewell & Nathan, 1987). Elsewhere in the West Coast Region deposition was interrupted by the development of the peneplain. A marine transgression across the peneplain began in the mid-Eocene as evidenced by the deposition of the regional extensive Brunner Coal Measures in other parts of the West Coast Region. A number of basins also began to subside rapidly due to NE-SW extension caused by the branching of the Southeast Indian Ridge into the western margin of the New Zealand micro-continent (Kamp, 1986b). This resulted in spreading in the Emerald Basin (Fig. 1.5), which effectively isolated the South Westland Embayment as a wedge of continental crust between two spreading centres. This tectonic configuration may explain the thickening of Late Cretaceous–Eocene sediments to the east of a basement high as noted by Adams (1987). Renewed extension resulted in the

reactivation of the late Cretaceous rift structures and the formation of the Paparoa Trough/Tectonic Zone, Victoria (Reefton) and Murchison Basin in North Westland. The Oligocene saw continued, but gradually declining, subsidence in the West Coast Region. The Oligocene sediments are dominantly calcareous with regional extensive limestones being deposited. Limestone lithologies are simplified into two main grouping termed Platform Facies (shallow-water bioclastic limestones) and Basinal Facies (calcareous mudstone dominated by deep-water foraminifera). In South Westland the Platform Facies is represented by the regionally extensive, but relatively thin Awarua Limestone (Fig. 1.4). The Awarua Limestone is inferred as a similar age as the extensive Cobden Limestone further north, though possibly extending into the Waitakian (early Miocene). Early studies refer to the Awarua Limestone as a Cobden Limestone 'equivalent'. This limestone often occurs on or near the basement surface and is a prominent feature in seismic reflection profiles in the area.

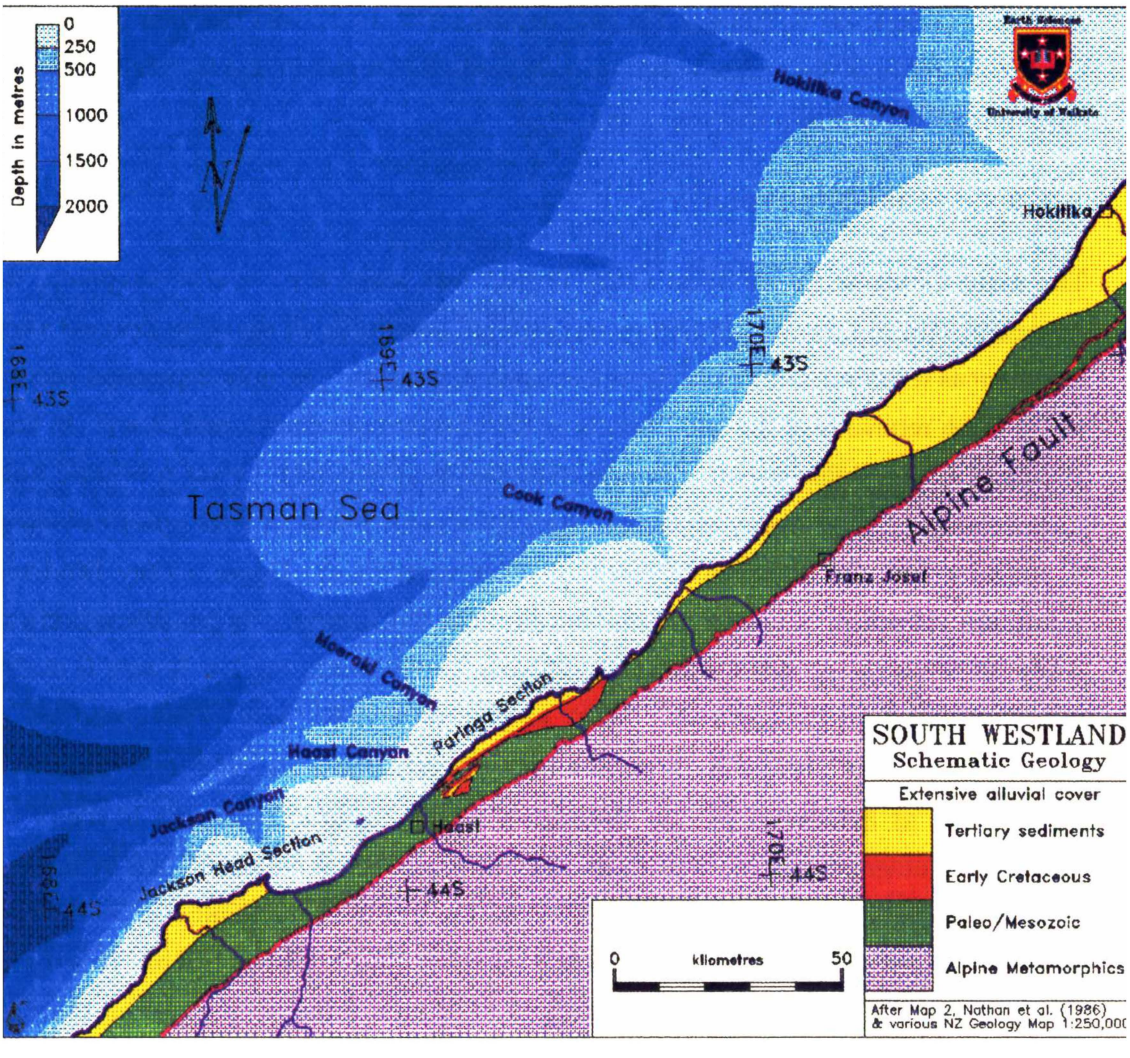

FIGURE 1.4: Schematic geology and bathymetry of the South Westland region. Note locations of Paringa and Jackson Head Sections as studied by various authors. (After Mutch & McKellar, 1964; Gair, 1967; Warren, 1967; Map 2, Nathan et al., 1986)

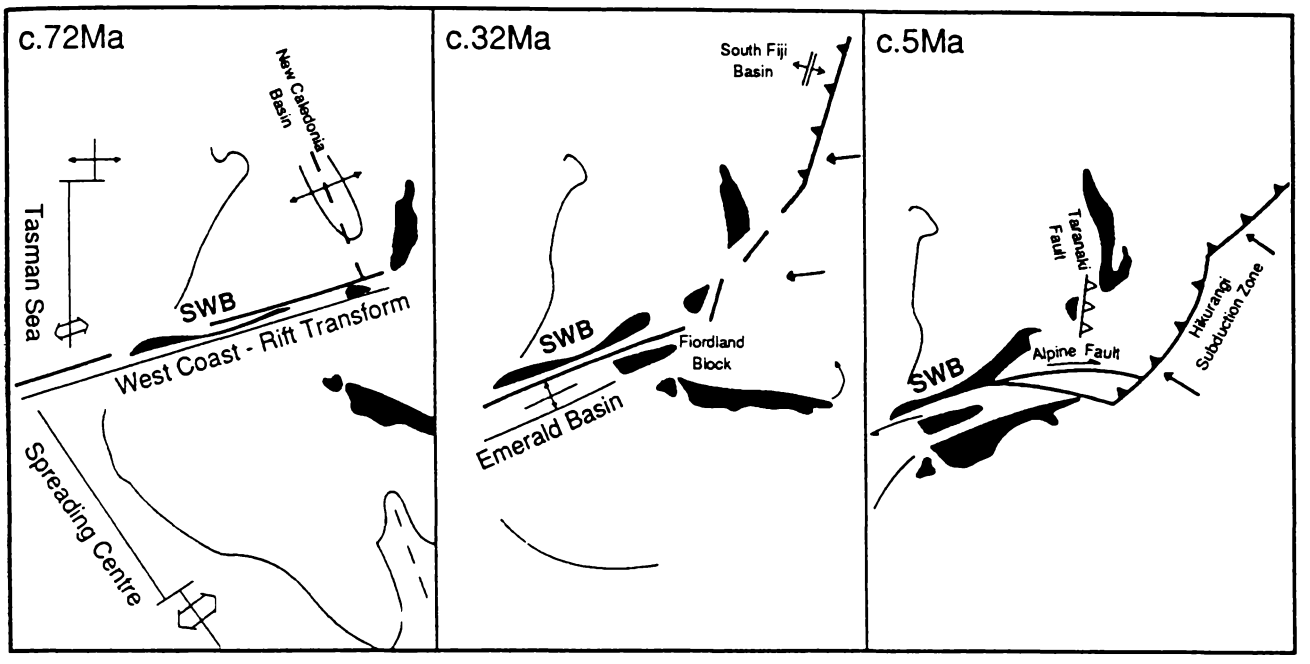

FIGURE 1.5: A schematic summary of the changing geometry and style of the Australia/Pacific plate boundary through New Zealand (after Fig.4, King, 1990); SWB = South Westland Basin.

1.4.4 Miocene–Quaternary

Major tectonic changes began to occur in the early Miocene, spreading on the Southeast Indian Ridge extension ceased and due to spreading differences between the Antarctic and Australian plates, and the Antarctic and Pacific plates, the Alpine Fault was incepted through the New Zealand micro-continent to relieve the tectonic stress about 23 Ma (Kamp, 1986).

In the West Coast Region the Alpine Fault cut directly across the old rift structures. Even though the Alpine Fault at first was largely a strike-slip transform fault, due to its close proximity the regional tectonic character changed from extensional to compressional. As the basin bounding faults had their sense of movement reversed the pre-Alpine basins ceased subsidence and began to be everted, with the exception of the Murchison Basin which continued to subside. New basins began to form between the now rising mountain ranges in North Westland. The sediments of the time illustrate a marine regression as movement on the Alpine Fault became increasingly oblique. In South Westland, the extensive Tititira Formation consists of deep-water turbidites from the mid-Miocene, deposited in a deep basin that rapidly subsided during the mid to late Miocene. These sediments are exposed onshore in a narrow, steeply dipping discontinuous strip along the coast known as the Coastal Monocline (Cotton, 1956). The Tititira Formation is continuous through the Wanganui Series in the two onshore wells, with numerous beds of coarser sand

found in the mudstones. Exotic blocks and foraminifera from the Arnold and Landon Series are found in sediments of Opoitian age in Waiho-1. Nathan (1978) interpreted these as originating from the erosion of the uplifted and deformed Coastal Monocline, thus placing movement on the Monocline around the Miocene–Pliocene boundary at 5 Ma. This coincides well with increased convergence across the Alpine Fault through the Late Miocene and onwards. A tectonic event at around 5 Ma would also correspond well with the fission track derived age of the uplifted block to the east of the Monocline (Kamp et al., 1992).

Interpretation of the recent tectonic structure of South Westland has been dominated by the presence of the Alpine Fault, and the large offsets that have occurred across it. This has resulted in a hypothesis of steeply dipping strike-slip faulting being employed to interpret the structures seen in South Westland (Wellman, 1955; Cotton, 1956; Nathan, 1977). Adams (1987) argues that the numerous low-angle faults and deformation seen in the Paringa area is better explained as the result of a thrust sheet emplacement, and that the Coastal Monocline is an antiformal stack thrust duplex (after the nomenclature of Boyer & Elliot, 1982). Adams sites examples of similar structures overseas and on the Alpine Fault itself further north. An example of comtemporary low-angle thrusting can be seen in the northern end of the study area where the Fraser Fault splays off the Alpine Fault (Rattenbury, 1986).

There are a number of implications of this alternative thrust model of the tectonic structure of South Westland. The sole and roof thrusts of the thrust sheet are inferred to extend beyond the coastline into the South Westland Basin. The amount of structural deformation in the sedimentary sequence, probably decreases offshore away from the Alpine Fault, the source of the compressive tectonic regime. Therefore, a relatively undeformed sequence with horizontal reflectors, representing the leading thrust planes are expected in the seismic charts offshore (Adams, 1987). The monoclinal fold of Cotton (1956) is interpreted by Nathan (1977) as extending from Milford Sound to Buttress Point and on geophysical evidence (McNaughton & Gibson, 1970) continues northwards for over 100 km. This implies the thrust system of Adams (1987) in the Paringa area may also extend a considerable distance both to the south and the north of the described area. The thrust system "may be a presently unrecognised feature of the whole Alpine Fault Zone" and "further thrust sheets may lie above and below those exposed" (Adams, 1987).

The series of glaciations from the Nukumaruan onwards (Suggate, 1990) have had a dramatic effect on the topography of the South Westland area, and numerous glaciers and icefields still remain in the central Southern Alps. Glaciers advanced down through valleys into the lowlands, and often beyond the modern coastline as evidenced by buried glacial moraines seen in shallow seismic records offshore (Norris, 1978). Thick

fluvioglacial gravels accumulated during and after each glacial retreat to fill the valleys created by the glaciers (Adams, 1980) and cover much of the lowlying areas of South Westland.

At present, the geological processes of South Westland are dominated by the high rates of precipitation of generally over 3200 mm per annum, possibly reaching 15000 mm in higher parts of the Southern Alps (Griffiths & McSaveney, 1983). Understandably, this high precipitation rate in combination with the uplift of the Southern Alps leads to high rates of erosion and transportation of sediments via the numerous river systems. Accordingly the West Coast (from Karamea to Fiordland) of the South Island contributes a substantial amount of sediment to the continental shelf, estimated to be 212 ± 40 tonnes.yr^{-1} (Griffiths & Glasby, 1985). This is about 55% of the total contribution to the New Zealand continental shelf. In the study area alone, the estimates of Griffiths & Glasby (1985) give a sediment load of 109 tonnes per annum, greater than the estimated sediment loads for the entire North Island.

1.5 Thesis format

The body of the thesis is contained in 6 chapters.

Chapter 1 *Introduction*

Chapter 2 *Basin Analysis*

The theory and methodology of the integrative approach in sedimentary basin studies is given. Methodologies discussed include the principles of seismic stratigraphy, geohistory analysis, geodynamical modelling and the handling and processing of seismic data unique to this study.

Chapter 3 *Characteristics of Foreland Basins*

The characteristics of foreland basins cited in various literature sources are discussed. Features discussed include geophysical features, structural control and stratigraphy, sedimentology, subsidence history and petrography.

Chapter 4 *Application and Observations of Basin Analysis in South Westland*

The methodologies outlined in Chapter 2 are applied to the seismic and exploration well data in the South Westland basin. Observations from the seismic data are given.

Chapter 5 *Interpretation and Discussion of Basin Analysis in South Westland*

The observations of Chapter 4 are interpreted and comparisons are made with various geodynamical models. The interpretation of the observations and geodynamical models are discussed.

Chapter 6 *Summary and Conclusions*

Appendices

Data and information appendices are included in this volume. These include further details of the seismic lines used in the study and more detailed information about the TECHBASE databases and associated subsidiary algorithms used in the processing of the seismic data.

Chapter 2

Basin Analysis

2.0 Introduction

Basin analysis is an integration of a broad spectrum of earth science disciplines, combining to study sedimentary basins as geodynamical entities. Basin analysis research involves aspects of geophysics, structural geology, stratigraphy (outcrop and seismic), sedimentology, geochemistry and mathematical and physical modelling organised in a framework to understand the geological and thermal evolution of a sedimentary basin (Klein, 1987; Welte & Yalçin, 1987).

Sedimentary basins contain strata from which the structural, stratigraphic and tectonic evolution of the basin and surrounds are inferred. This information held in the strata can also be used in the study of lithospheric deformation in the context of contemporary plate tectonic theories. Sedimentary basins are also the sites of almost all the world's commercial hydrocarbons and some minerals (Allen & Allen, 1990).

Each of the earth science disciplines integrated into basin analysis is a complete scientific pursuit in its own right. Thus this chapter will only cover a few principle topics in any detail, namely seismic stratigraphy, geodynamical modelling, the integral tool of geohistory analysis and an overview of computer data processing. These disciplines and techniques are subsequently used and applied in analysis of the South Westland Basin.

2.1 Seismic stratigraphy principles

2.1.0 Overview

Acoustic impedance is a bulk physical property of a rock and the fluids it contains, and is a function of the density of the rock multiplied by the velocity of the acoustic waves passing through it. Seismic reflections are generated along surfaces of acoustic impedance contrast, with the strength of the reflection increasing as the difference in impedance between two superimposed rock layers increases (Cross & Lessenger, 1988; Sheriff, 1989, p.311).

Using this geophysical phenomenon, sub-surface 'surveys' can be undertaken using an energy source to generate seismic waves in or above the strata and a line or lines of geophones to record the reflected seismic energy over time. Seismic surveys can be carried out on land or at sea. Internationally, land seismic surveys are more common than marine surveys (Sheriff, 1989, p.25), however this study uses about 1715 km of seismic lines, only 104 km of which are on land.

The acquired seismic data is processed by various means to correct the data for noise or distortion due to earth properties at the survey site. Further processing can be undertaken

to improve the clarity of the data or to extract and visualise specific information about amplitude and/or velocity. The objective of such processing is to produce a display of data from which geologic information can be interpreted (Sheriff, 1989, p.390).

Seismic stratigraphy is now a routine method used in the interpretation and modelling of stratigraphy, sedimentary facies and geologic history from seismic reflection data. The principles and descriptive parameters of seismic stratigraphy are outlined below.

2.1.1 Fundamental axiom of seismic stratigraphy

A fundamental precept of seismic stratigraphy is that primary seismic reflections are produced by stratal surfaces and unconformities which are formed at particular times during deposition or non-deposition. Therefore seismic reflections are chronostratigraphically significant in the sense that all rocks above a horizon are younger than those below (Mitchum, Vail & Thompson, 1977; Vail et al., 1977; Cross & Lessenger, 1988).

The universality of the assumption that a seismic horizon will separate older from younger strata is challenged by Christie-Blick et al. (1987, *in* Cross & Lessenger, 1988), who demonstrated two examples from deep marine and alluvial-fan environments where strata above an unconformity at one location would be older than strata below it at another location. Also, intuition would suggest that seismic reflections can be generated at sedimentary facies boundaries which can cross time lines, and thus their associated seismic reflections would also cross time lines. Cross & Lessenger (1988) undertake a lengthy discussion on this issue, concluding that seismic reflections are generated in both instances, but that conventional seismic displays emphasis laterally continuous surfaces of sharp impedance contrasts and thus time-significant (and generally laterally continuous) surfaces are emphasized. Facies changes and associated boundaries can be detected by studying subtle waveform changes along or between reflectors.

2.1.2 Seismic sequence stratigraphy model

The concepts of seismic sequence stratigraphy and seismic facies analysis as collated by the authors in *Seismic Stratigraphy—applications to hydrocarbon exploration* (Payton, 1977) and outlined below, have continued to develop since that compilation. One of the major driving forces to further research was the construction of a chart of global relative sea level through time by a group of geologists from Exxon, headed by P.R. Vail. Vail et al. (1977a,b) used the depositional limits of the coastal facies of marine sequences to interpret sea level histories along various continental margins. The apparent

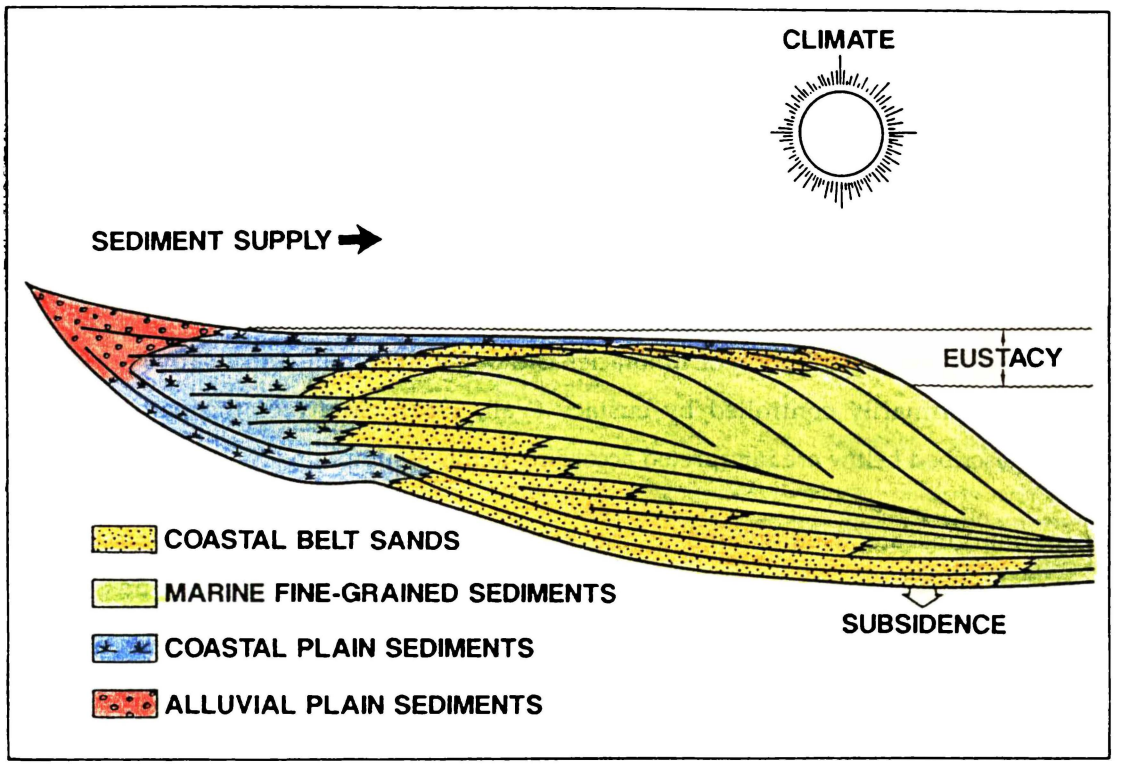

FIGURE 2.1: Diagram of seismic reflections, lithofacies, and major variables affecting stratigraphy (from Vail, 1987, Fig. 3)

synchroneity of sea level changes led to the construction of the charts—and continuing lively debate (Haq et al., 1987).

A significant recent advance in seismic stratigraphic concepts is the development of depositional models of genetically related sediments during various phases of the sea level cycle as detailed by various authors, both in seismic section (Wilgus et al., 1988) and outcrop (Van Wagoner et al., 1990), and summarised below.

There are three major variables that control the stratal patterns and lithofacies distributions within sedimentary deposits (Fig 2.1; Jervey, 1988; Allen & Allen, 1990):

- *Tectonic subsidence* creates the space where sediments can be deposited. Tectonic subsidence changes slowly with respect to eustacy and can be treated as linear with time.
- *Eustatic sea level change* which is believed to be a major control over the stratal patterns and distribution of lithofacies.
- *Sediment supply* controls the amount and type of sediment entering the depositional area and contributes to water depth in that zone. Sediment supply is a function of the sediment source area and the *climate* driving the weathering, erosion and transportation processes. Sediment supply is often assumed time-constant in the following depositional models.

The combination of tectonic subsidence and eustatic sea level change produces a relative change of sea level (Fig. 2.2). The relative sea level change curve represents the amount of space or *accommodation* available for incoming sediment in the depositional area. In effect, the higher the relative sea level the greater amount of space available for sediments to be deposited; the lower the relative sea level the less space available. The tectonic contribution is mainly attributed to the creation of long-term space for sedimentary deposits and the preserved thickness of those deposits. The depositional stratal patterns and distribution of lithofacies is thought to responsd to relative sea-level and is thus primarily controlled by eustacy (Vail, 1987). Many of the patterns and features described below are interpreted according to this assumption.

Passive margins are usually used as the geodynamical setting for this approach to stratigraphic modelling (Fig. 2.2), although stratigraphic modelling in foreland basins can also be achieved (Swift et al., 1987; Jervey, 1991). The originators of modern seismic sequence stratigraphy also emphasis the generality of their depositional models, and that local factors such as climate, sediment supply and tectonics must be incorporated into a model before application to a particular basin (Posamentier, Jervey & Vail, 1988). The great emphasis on eustatic controls, especially in regions and depositional settings clearly dominated by tectonic processes, should also be noted as a point of concern in this relatively new and still developing stratigraphic model (Sloss, 1988).

The basic unit of seismic stratigraphy is the *depositional sequence*, defined as a stratigraphic unit composed of a relatively conformable succession of genetically related strata and bounded at its top and base by unconformities or their correlative conformities (Mitchum, Vail & Thompson, 1977) (Fig. 2.3).

The concept of seismic sequences were modified from earlier stratigraphic sequences as defined and identified by Sloss (1963), being units traceable over wide areas and bounded by unconformities of 'interregional scope'. The depositional sequences of Mitchum, Vail & Thompson (1977) are an order of magnitude smaller than those of Sloss, requiring the Sloss sequences to be re-termed *supersequences*.

Depositional sequences are chronostratigraphically significant as they are bounded at top and bottom by time-tied boundaries, and were thus deposited during a given interval of geologic time. This total interval of geologic time during which a sequence is deposited is termed a *sechron* (Fig 2.3; Mitchum, Vail & Thompson, 1977, p.55).

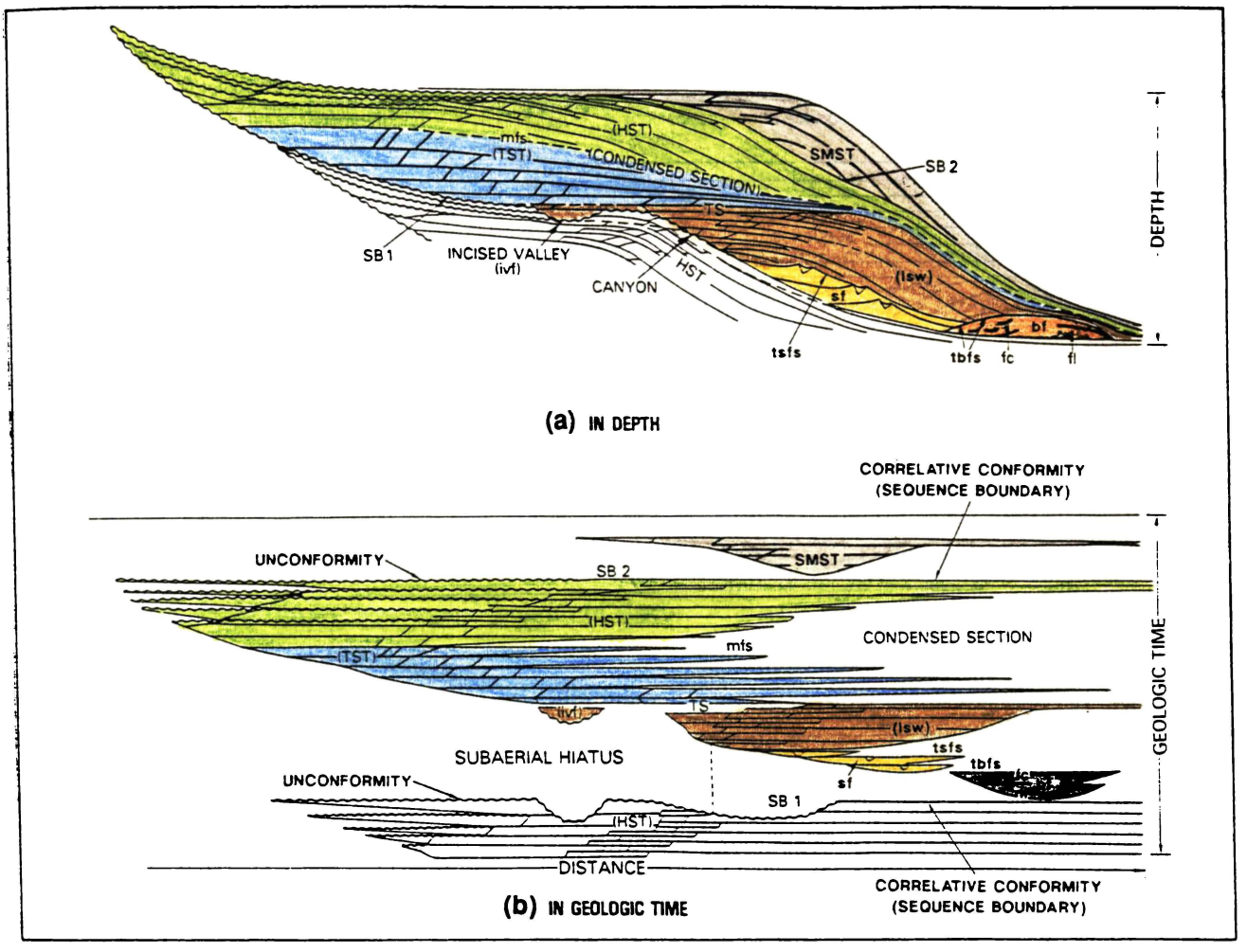

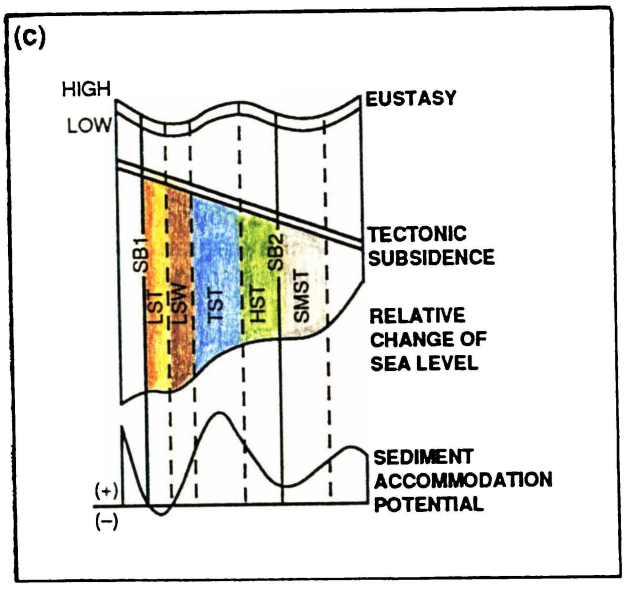

LEGEND

SURFACES

(SB) SEQUENCE BOUNDARIES
- (SB1) = Type 1
- (SB2) = Type 2

(DLS) DOWNLAP SURFACES
- (mfs) = maximum flooding surfaces
- (tbfs) = top basin floor fan surface
- (tsfs) = top slope fan surface

(TS) TRANSGRESSIVE SURFACE
(First flooding surface above maximum progradation)

SYSTEMS TRACTS

HST = HIGHSTAND SYSTEMS TRACT

TST = TRANSGRESSIVE SYSTEMS TRACT
- ivf = incised valley fill

LST = LOWSTAND SYSTEMS TRACT
- ivf = incised valley fill
- lsw = lowstand wedge-prograding complex
- sf = lowstand slope fan
- bf = lowstand basin floor fan
- fc = fan channels
- fl = fan lobes

SMST = SHELF MARGIN SYSTEMS TRACT

FIGURE 2.2: Sequence stratigraphy diagrammatic section, showing sequences and systems tracts in **(a)** depth and **(b)**geologic time. Stratal pattern relationship to eustacy, tectonic subsidence, sediment accommodation potential, and relative change of sea level **(c)**. (from Vail, 1987, Fig. 4; Sarg, 1988, Fig. 1)

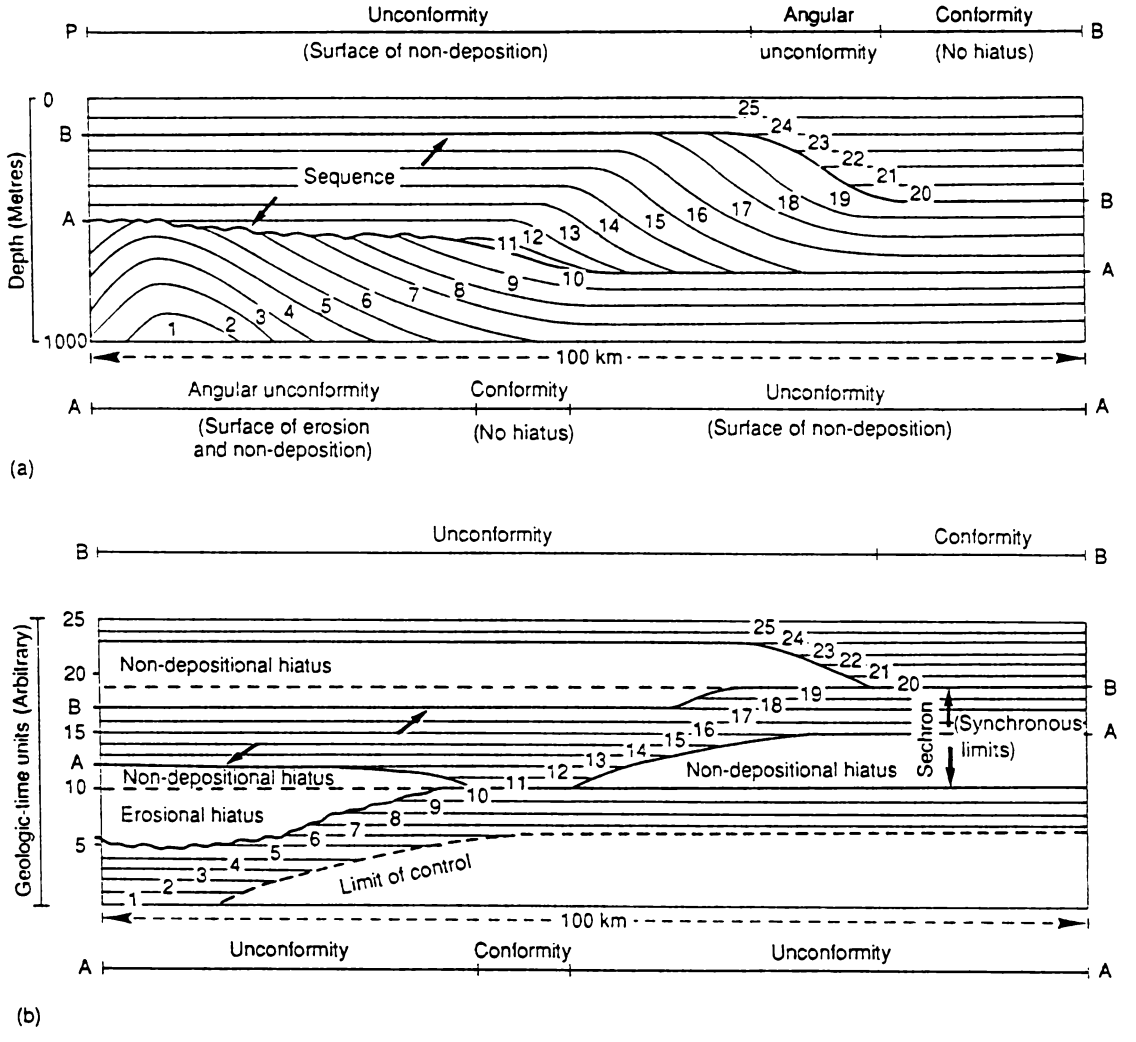

FIGURE 2.3: The basic concept of the depositional sequence as outlined by Vail et al. (1977a) (from Allen & Allen, Fig. 6.1, p.144).
(a) Generalised stratigraphic section of depositional sequence. Sequence boundary A changes from an angular unconformity (onlap surface) in the left half of the diagram to a conformity in the centre to a lateral conformity (downlap surface). Unconformities are dated at the points they have become laterally conformable.
(b) Generalised chronostratigraphic section of the same stratigraphic sequence in (a). Charts of this type are also termed 'Wheeler diagrams' following Wheeler (1958).

Depositional sequences can be subdivided into smaller units of chronostratigraphic significance. These small units are termed *systems tracts* (Brown & Fisher, 1977; Van Wagoner et al., 1988), which in turn are composed of *parasequences sets* and *parasequences* (Van Wagoner et al., 1987). Parasequences are relatively conformable succession of genetically related beds or bedsets bounded by marine-flooding surfaces and their correlative surfaces. A parasequence set is a succession of genetically related parasequences which form a distinctive stacking pattern that is bounded, in many cases, by major marine-flooding surfaces and their correlative surfaces. Systems tracts are a linkage

of contemporaneous depositional systems and correspond closely with particular segments of the relative sea level curve (Posamentier et al., 1988).

2.1.3 Seismic surfaces, boundaries and disconformities

Boundaries of sequences, parasequence sets, and parasequences provide a crucial chronostratigraphic framework for correlating and mapping sedimentary rocks. Sequences and systems tracts are defined and identified by the geometrical relationship of reflectors, including the continuity of surfaces bounding the units, and reflection configuration patterns within the unit (Van Wagoner et al., 1987).

Originally, unconformities were the principal subdividers in seismic sequence concepts, and followed the terms introduced by Dunbar and Rogers (1957) to describe the angularity or parallelism of strata above and below an unconformity. As the concepts of seismic stratigraphic analysis developed, the original definition of an unconformity as "a surface of erosion or nondeposition that separates younger strata from older rocks and represents a significant hiatus" (Mitchum, 1977, p.211), did not sufficiently differentiate between sequence and parasequence boundaries. Recent conceptual developments use *surfaces of discontinuity* (Vail, 1987) to describe a choronstratigraphically significant boundary in the seismic data. There are a number of such surfaces, representing a variety of depositional or erosional processes (Vail, 1987):

Sequence boundaries

- Type 1 Sequence boundary
- Type 2 Sequence boundary

Marine-flooding surfaces

- Downlap / Maximum flooding surface
- Trangressive surface
- 'Condensed Section'

These surfaces are identified by the geometric relation of the strata to the surface itself. Discordant relationships between internal strata and sequence boundaries giving reflection terminations are the principal criteria for recognition of surfaces and are termed *lapout* (lateral termination at depositional pinchout) or *truncation* (lateral termination due to erosion). Such relationships also form the basis for the interpretation of the surfaces, in particular whether they were formed by erosion or nondeposition. Mitchum, Vail & Thompson (1977) defined a number of terms to describe the geometrical relationships of strata to a sequence boundary and can apply equally to the patterns associated with other surfaces (Fig 2.4). These patterns are described below.

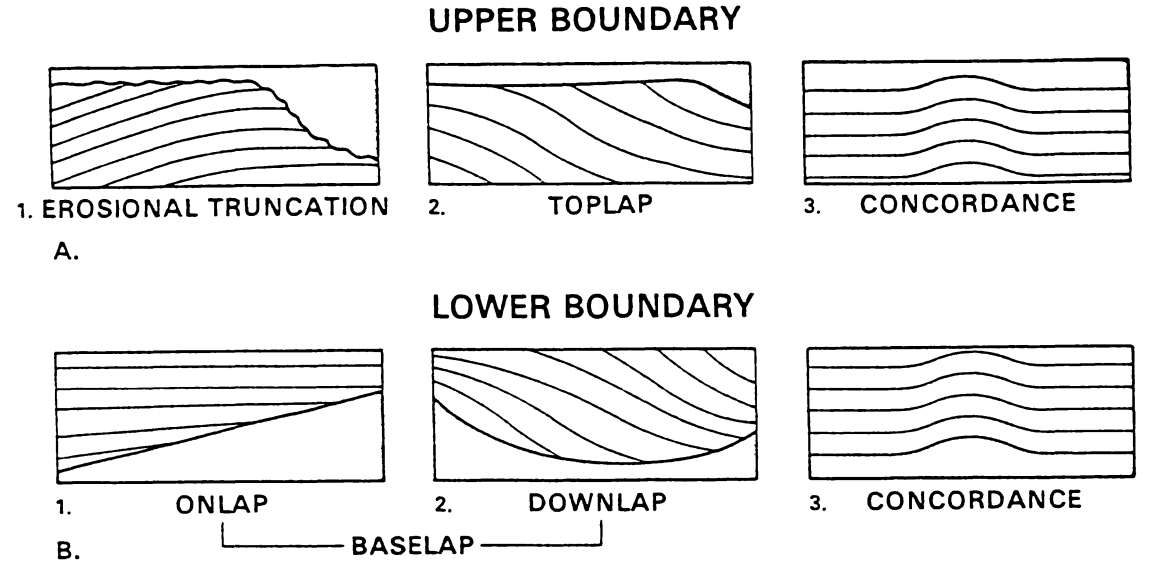

FIGURE 2.4: Relations of strata to discontinuity surfaces. **(A)** Relations of strata to upper surface of a unit. **(B)** Relations of strata to lower surface of a unit. See text for details of each pattern. (After Mitchum, Vail & Thompson, 1977)

Baselap: Onlap, Downlap

Two important types of lapout at the base of an unit are recognized, collectively termed *baselap* (Mitchum, Vail & Thompson, 1977; Allen & Allen, 1990). Successive terminations of strata along a depositional surface produce an increasing nondepositional hiatus in the direction of onlap or downlap (see Fig 2.3).

Onlap is baselap where initially horizontal stratum laps out against an initially inclined surface, or where initially inclined stratum laps out against a surface with greater inclination (Fig 2.4B1). Onlap is an indicator of a nondepositional hiatus and landward sediment progradation.

Downlap is baselap where initially inclined stratum terminates downdip against an initially horizontal, irregular or inclined surface (Fig 2.4B2). Downlap is an indicator of a nondepositional hiatus and seaward sediment progradation.

In some complex situations the distinction between onlap and downlap may be practically impossible, and the general term of baselap is used.

Toplap

Toplap is the termination of strata against the upper boundary of an unit. Inclined features, such as foreset beds and clinoforms, may show is pattern. Lateral terminations updip may taper and approach the upper boundary in a near parallel fashion. In some

seismic sections, resolution may be such that reflections appear to terminate at a high angle against the upper boundary (Mitchum, Vail & Thompson, 1977) (Fig 2.4A2).

Toplap is evidence of a nondepositional hiatus. It is produced by the depositional base level being too low to allow formation of the strata updip. Strata progrades below base level during the development of toplap, while sediment bypassing and some minor erosion occurs above base level. Toplap is commonly associated with shallow marine deposits such as deltaic complexes and deep marine fans depositionally controlled by turbidity currents (Mitchum, Vail & Thompson, 1977, p. 59)

Truncation: Erosional and Structural

Erosional truncation is the lateral termination of stratum by erosion at the upper boundary of a depositional sequence, and may occur over a large area or be restricted to a channel. The distinction between toplap and erosional truncation may be difficult in some cases, but in the latter strata tends to maintain parallelism as they terminate abruptly against the upper boundary rather than taper to it. Erosional truncation is evidence of an erosional hiatus (Mitchum, Vail & Thompson, 1977, p.59) (Fig 2.4A1).

Structural truncation is the lateral termination of stratum by structural disruption produced by faulting, gravity sliding, salt flowage, or igneous intrusion. The distinction between structural and erosional truncation should be made in interpretation as structural truncation has only minor, if any, chronostratigraphic significance with respect to unconformities and hiatuses (Mitchum, Vail & Thompson, 1977, p.59) (Fig 2.4A1).

Once seismic surfaces have been identified, the actual type of surface is interpreted from the relation of patterns above and below that surface. As listed above, a number of surfaces are recognised (Van Wagoner et al.., 1987; 1988).

A sequence boundary is characterised by regional onlap above and truncation below. A Type-1 sequence boundary is a regional surface characterised by subaerial exposure and concurrent subaerial erosion. This sequence boundary is interpreted to form when the rate of eustatic fall exceeds the rate of tectonic subsidence, producing a relative fall of sea level at that location. This causes the drainage base level to fall, rejuvenating streams, promoting erosion and incising valleys. A Type-2 sequence boundary is also marked by subaerial exposure, however it lacks both subaerial erosion and a basinward shift in facies. This sequence boundary is interpreted to form when the rate of eustatic fall is less than the rate of tectonic subsidence, so no relative fall in sea level occurs. These two types of sequence boundary are also used to define two types of sequence, namely a Type-1 sequence, bounded below by a Type-1 sequence boundary and above by a Type-1 or a Type-2

sequence boundary; and a Type-2 sequence, bounded below by a Type-2 sequence boundary and above by a Type-1 or a Type-2 sequence boundary.

A marine flooding surface separates younger from older strata, across which there is evidence for an abrupt increase in water depth. The marine-flooding surface commonly has a correlative surface in the coastal plain and on the shelf. In particular, downlap surfaces are marine-flooding surfaces onto which the bottomset of prograding clinoforms downlap, and are commonly identified by regional downlap on a seismic display. This surface indicates the change from retrogradational to aggradational deposition and is the surface of maximum flooding during a eustatic cycle. While not strictly a marine-flooding surface, the condensed section is the basinward correlative of a marine-flooding surface, consisting of a facies of thin marine beds of hemipelagic or pelagic sediments deposited at very slow rates. Condensed sections are most extensive during regional transgression and play a fundamental role in stratigraphic correlation, both regionally and globally (Loutit et al., 1988).

2.1.4 Seismic facies analysis

After sequences have been seismically defined within the chronostratigraphic framework of sequence boundaries, the environment and lithofacies of a seismic unit can be interpreted from seismic and geologic data. *Seismic facies analysis* is the description and geologic interpretation of seismic reflection parameters, including configuration, continuity, amplitude, frequency, and interval velocity (Mitchum, Vail & Sangree, 1977; Sangree & Widmier, 1979). In addition paleotopographic elements, directions of progradation or fluvial channel flow, and relative changes of sea level can be detected (Cross & Lessenger, 1988). Each parameter provides information on the geology of the subsurface (Table 2.1)

A *seismic facies unit* is defined as a three-dimensional restricted group of reflectors whose parameters are distinguishable from those of adjacent groups (Mitchum, Vail & Sangree, 1977; Sangree & Widmier, 1979; Cross & Lessenger, 1988). The combination of external form and internal configuration parameters must be described to understand the geometric interrelation and depositional setting of the facies units.

Three principle criteria are used in the identifying, classifying and mapping of seismic facies (Cross & Lessenger, 1988): the geometry of reflections and reflection terminations to the unit boundaries; reflection configuration within the unit; and, the three-dimensional external form of the seismic facies. The form and interpretation of unit boundaries is described above (see Fig 2.4). The two other seismic facies criteria are outlined below.

Seismic Facies Parameters	Geologic Interpretation
Reflection Configuration	• Bedding Patterns • Depositional Processes • Erosion and Paleotopography • Fluid Contacts
Reflection Continuity	• Bedding Continuity • Depositional Processes
Reflection Amplitude	• Velocity–Density Contrast • Bed Spacing • Fluid Content
Reflection Frequency	• Bed thickness • Fluid Content
Interval Velocity	• Estimation of Lithology • Estimation of Porosity • Fluid content
External form and areal association of seismic facies units	• Gross Depositional Environment • Sediment Source • Geologic Setting

TABLE 2.1: Seismic reflection parameters used in seismic facies analysis and their geologic significance, (after Mitchum, Vail & Sangree, 1977; Sangree & Widmier, 1979). The top four parameters (bold type) can be visually assessed directly or by computer enhancement from seismic reflection data.

2.1.4.1 *Reflection configuration patterns*

Reflection patterns within the sequence reveal stratification patterns and infer depositional processes. Some observed patterns may be complex and require further description with modifying terms. The definitions and geologic interpretation of these reflection configuration patterns is given below.

Parallel and Subparallel

These reflection configurations (Fig 2.5) suggest uniform rates of deposition on a uniformly subsiding shelf or stable basin plain setting (Mitchum, Vail & Sangree, 1977; Sangree & Widmier, 1979).

Divergent

This reflection configuration (Fig 2.5) is distinguished by a wedge-shaped unit in which lateral thickening is due to thickening of individual cycles within the unit, rather than by reflection termination against a sequence boundary. Internal convergence of reflectors

within the unit commonly causes lateral termination as the strata progressively thin below seismic resolution.

Divergent configurations suggest areal variations in the rate of deposition or progressive tilting of the depositional surface (Mitchum, Vail & Sangree, 1977; Sangree & Widmier, 1979).

Prograding Reflection Configurations

Several more complex reflection configurations occur (Fig 2.6), formed through progressive development, or *progradation*, of depositional surfaces, called *clinoforms*, that slope from gently dipping, relatively shallow water areas into deeper water. Such patterns are also termed *offlap* in recent papers (Vail, 1987). The clinoform surface is one of the most common depositional features. The configuration may also be divided into upper, middle and lower zones corresponding to Rich's (1951) undaform, clinoform and fondoform zones respectively, or topset, foreset and bottomset segments respectively (Sangree & Widmier, 1979). Prograding clinoforms occur in the variety of forms given below as described in Mitchum, Vail & Sangree (1977).

Sigmoid

A sigmoid progradational configuration is a prograding clinoform pattern formed by superimposed sigmoid (S-shaped) reflections. Topset segments have horizontal or near horizontal dips and are concordant with the upper boundary of the sequence. The foreset segments have successively younger lenses superimposed laterally in a depositional downdip direction forming an overall prograding pattern. Depositional angles are quite low, usually less than 1°. The bottomset segments show real or apparent downlap truncation against the base sequence boundary (Fig 2.6a).

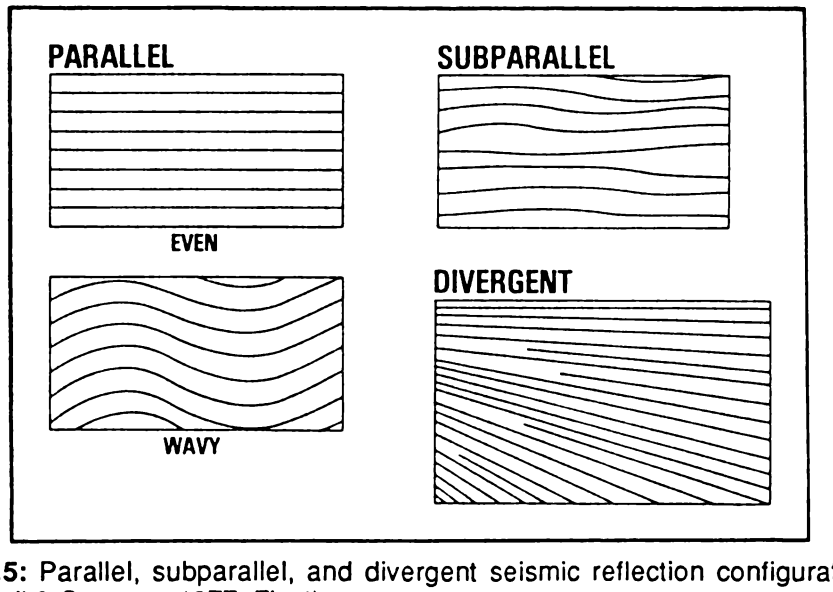

FIGURE 2.5: Parallel, subparallel, and divergent seismic reflection configurations (after Mitchum, Vail & Sangree, 1977, Fig.4).

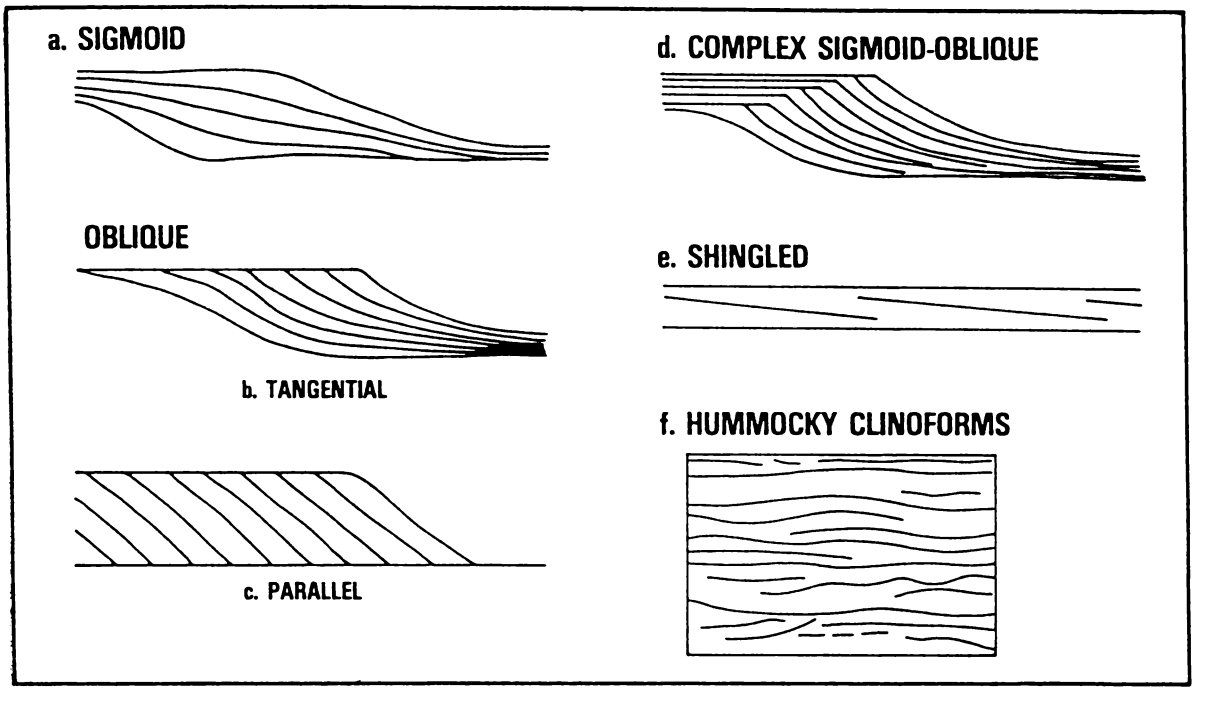

FIGURE 2.6: Seismic reflection patterns interpreted as prograding clinoforms (from Mitchum, Vail & Sangree, 1977, Fig. 6).

The parallelism of the topset reflectors is the most distinctive feature of the sigmoid reflection configuration, suggesting a continued upbuilding (aggradation) of the topset deposits coevally with the prograding of the foreset deposits. This is interpreted as a relatively low-energy, low sediment supply, relatively rapid basin subsidence, and/or rapid sea level rise to deposit and preserve the topset units (Mitchum, Vail & Sangree, 1977).

Oblique

Oblique progradational reflection configuration ideally consists of relatively steep-dipping strata terminating updip by toplap against the upper boundary, and downdip by downlap onto the lower boundary. Topset beds are characteristically absent. Foreset segments build laterally from a constant upper surface in a depositionally downdip direction. Depositional dips are intrinsically higher than in the sigmoid configuration, and may approach 10°. Baseset segments thin from the foreset units, or terminate against the lower boundary at a relatively high angle (Fig 2.4b & c).

In tangential oblique progradation patterns, dips decrease gradually in the lower parts of the foreset strata, forming concave-upward patterns. Reflections terminate tangentially against the lower boundary of the seismic facies unit. In the parallel oblique

progradational pattern, the steep parallel foreset strata terminate by downlap at a high angle against the lower boundary.

Oblique progradational configurations infer depositional environments with a combination of relatively high sediment supply, slow or no basin subsidence, and a standstill of sea level to allow rapid basin infill and sedimentary bypassing or scouring of the upper depositional surfaces—thus preventing the formation of topset units (Mitchum, Vail & Sangree, 1977, p.128).

Complex sigmoid-oblique

Prograding reflection configurations may also be a complex combination of variably alternating oblique and sigmoid progradational patterns within the single seismic facies unit (Fig 2.6d). The topset segment is distinguished by a complex alternating horizontal sigmoid topset patterns and oblique toplap termination patterns. This variability infers topset strata with a history of alternating aggradation and sediment bypassing within a high energy depositional environment. The other segments of this configuration are similar to the sigmoid configuration (Mitchum, Vail & Sangree, 1977)

Shingled

A shingled progradational reflection configuration (Fig 2.6e) resembles the parallel oblique progradational configuration, except that the thickness of the unit is at the point of seismic resolution. Upper and lower boundaries are commonly parallel, with gently dipping parallel, and occasionally discontinuous, internal reflectors terminating by apparent toplap and downlap. Shingled configurations are interpreted as depositional units prograding into shallow water (Mitchum, Vail & Sangree, 1977).

Hummocky

A hummocky clinoform reflection configuration (Fig 2.6f) consists of irregular discontinuous subparallel reflectors forming a random hummocky pattern marked by nonsystematic reflection terminations and splits. Relief on the hummocks is low, approaching the point of seismic resolution. The overall reflection pattern is interpreted as strata forming small, interfingering clinoform lobes prograding into shallow water in a prodelta or inter-deltaic position (Mitchum, Vail & Sangree, 1977).

Chaotic Reflection Configuration

Chaotic patterns are discontinuous, discordant reflections inferring a derangement of reflection surfaces (Fig 2.7a & b). They are interpreted as strata deposited in a variable,

relatively high energy setting, or deformed, but initially continuous strata. Some chaotic patterns may be interpreted as original configuration patterns still identifiable after deformation. Other patterns are so disrupted that identification and interpretation is practically impossible. Slump structures, cut-and-fill channel complexes, and highly faulted, folded, or contorted zones my display chaotic seismic reflection (Mitchum, Vail & Sangree, 1977).

Reflection-Free Areas

Some seismic data may display reflection-free areas (Fig. 2.7c). These are interpreted as homogeneous, nonstratified, highly contorted, or steeply dipping units, for example large igneous bodies or thick seismically homogeneous shales or sandstones (Mitchum, Vail & Sangree, 1977).

Modifying terms

Some variations in the basic reflection configuration patterns may be described by common modifying terms which are illustrated in Figure 2.8. Such terms outlined by Mitchum, Vail & Sangree (1977) as wavy, even, hummocky, lenticular, disrupted, contorted, regular, irregular, uniform and variable are self-explanatory.

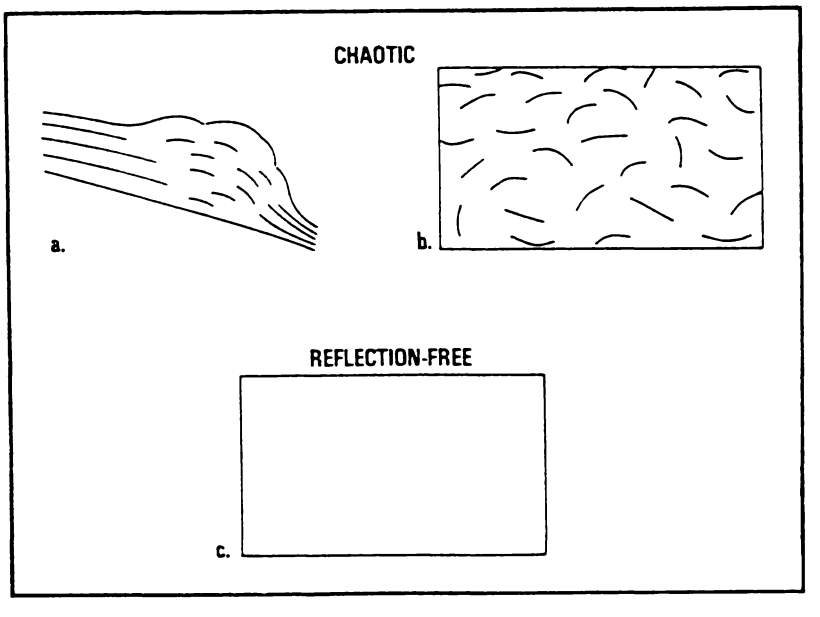

FIGURE 2.7: Diagrams of chaotic and reflection-free seismic reflection patterns. **(a)** represents a chaotic pattern that may still be identified as original features remain after deformation; **(b)** no recognisable stratal patterns can be interpreted; **(c)** represents a reflection-free area (from Mitchum, Vail & Sangree, 1977, Fig.9).

2.1.4.2 *External forms*

Also important to the analysis of seismic facies units is an understanding of their three dimensional forms and areal associations. Figure 2.9 illustrates some the important external forms. Sheets, wedges and banks are the most common shelf seismic facies comprised of a variety of parallel, divergent, and prograding patterns within the internal reflection configuration of the unit. Sheet drapes commonly comprise parallel reflections in a pattern suggesting uniform, low-energy, deep-marine deposition independent of bottom relief. Lenses may occur in any seismic facies unit, but are most common as external form of prograding clinoforms (Mitchum, Vail & Sangree, 1977). Mounds and fills are seismic forms produced by strata with a variety of origins, forming prominences, such as reefs or banks, or filling depressions on depositional surfaces, such as submarine canyons or drowned alluvial valleys (Cross & Lessenger, 1988).

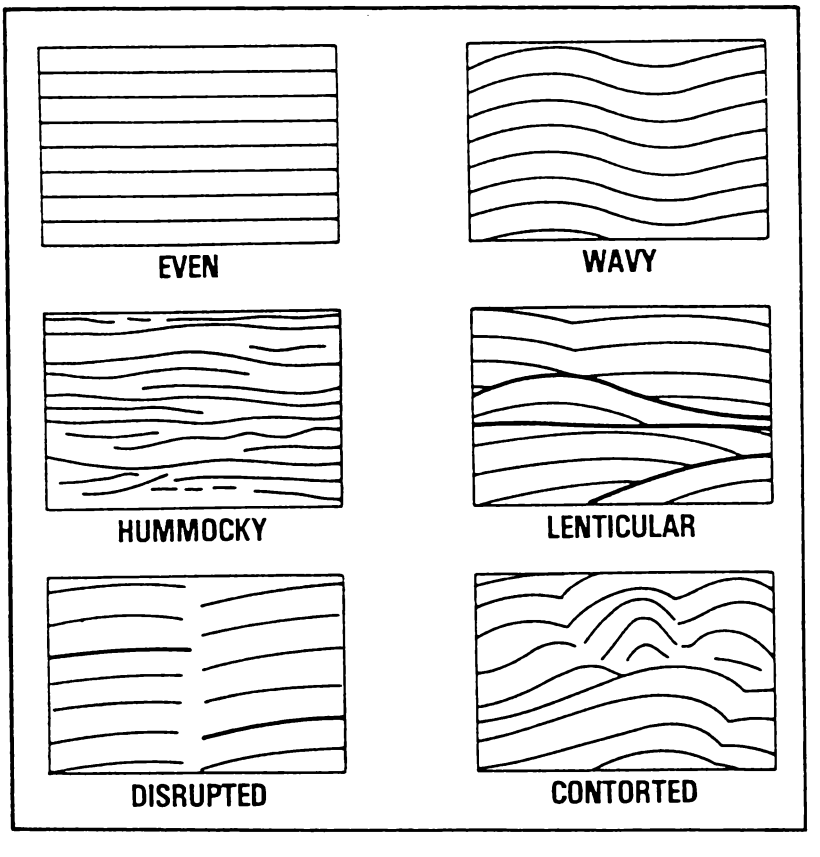

FIGURE 2.8: Some modifying seismic reflection configurations (from Mitchum, Vail & Sangree, 1977)

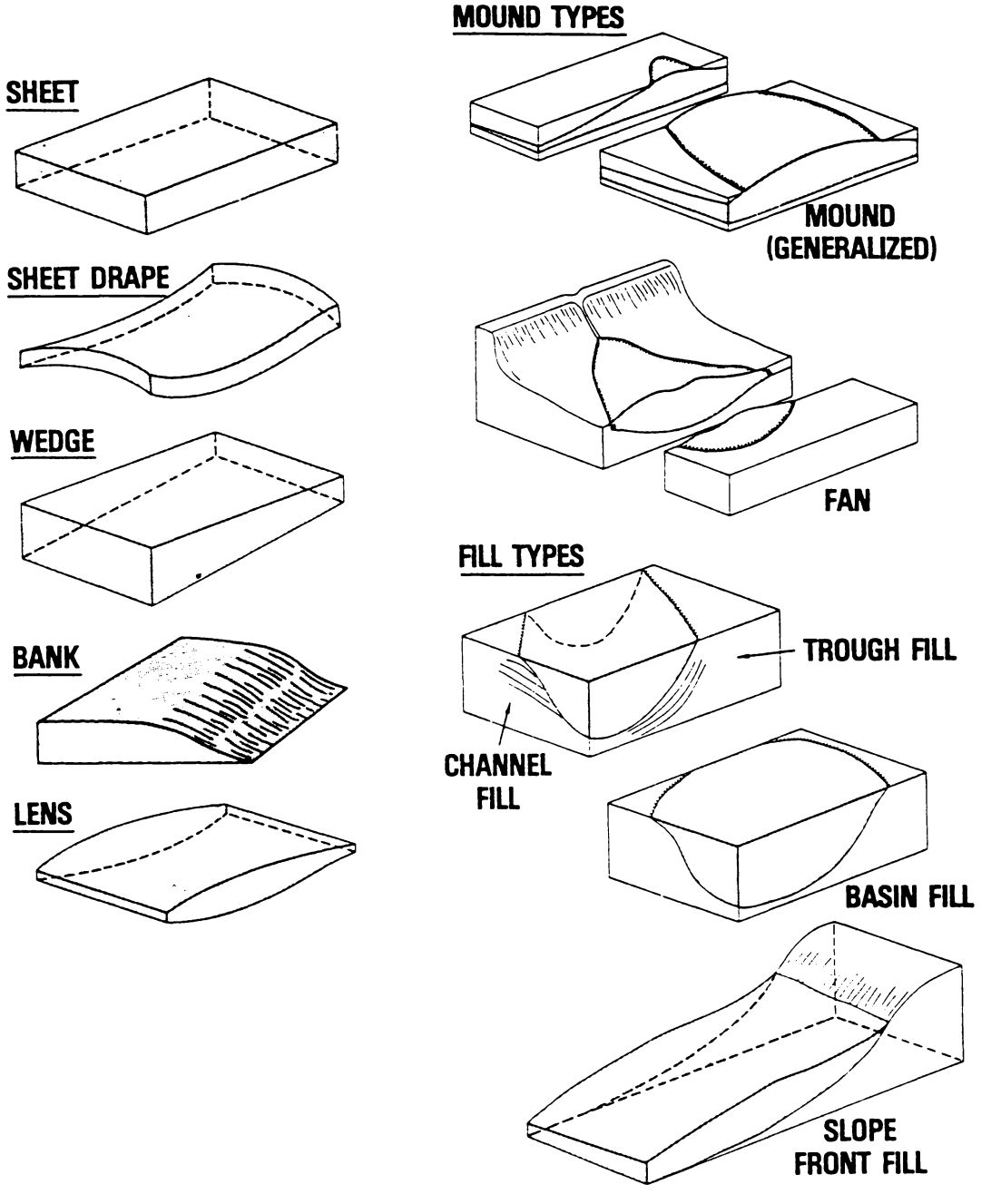

FIGURE 2.9: External forms of some seismic facies units (from Mitchum, Vail & Sangree, 1977)

2.1.4.3 *Mapping seismic facies*

Sangree & Widmier (1979) proposed a mapping convention in which the three attributes describing a seismic facies unit are combined.

The coding system has the form

$$\frac{A - B}{C}$$

where

A = relationship of reflections to upper boundary
- **Er** - Erosional truncation
- **Top** - Toplap truncation
- **C** - Concordant

B = relationship of reflections to lower boundary
- **On** - Onlap
- **Dwn** - Downlap
- **C** - Concordant

C = internal reflection configuration
- **P** - Parallel
- **D** - Divergent
- **Ch** - Chaotic
- **W** - Wavy
- **M** - Mounded
- **Ob** - Oblique progradational
- **Sig** - Sigmoid
- **Rf** - Reflection free

Assuming a relation between seismic and sedimentary facies, seismic facies maps can be interpreted in a similar way to geologic maps. However this assumed relation between seismic and sedimentary facies is a major limitation of seismic facies analysis due to a paucity of literature on the subject (Cross & Lessenger, 1988).

2.1.5 Relation of systems tracts to eustacy

Of particular importance in determining the stratigraphic response of depositional systems to relative sea level fluctuations is the *rate* of sea level change (Fig 2.2; Vail, 1987; Allen & Allen, 1990). Aggradation will dominate depositional processes when the rate of addition of new space increases, effectively trapping sediments closer to the source and starving distal area of the basin. The greatest increase of new space occurs at the inflection point of the rising limb of the relative sea level curve. Progradational processes will dominate when the rate of addition of new space or accommodation slows down and the sediment supply easily fills the available space, causing surplus sediment to be bypassed. The greatest decrease in new space occurs at the inflection point of the falling limb of the relative sea level curve. This falling inflection point also marks the period when sediments in the basin plain and shelf may be subject to erosion and the formation of an unconformity, which depending on the speed of the sea level fall will produce a Type-1 (rapid fall) or Type-2 (gradual fall) sequence boundary. Thus the sequence boundaries of a depositional sequence are intrinsically linked to falling sea level. Vail (1987) and Posamentier et al. (1988) link other bounding disconformity surfaces to particular points in time on the relative sea level curve, and the systems tracts within those intervals represent the rocks deposited within that time interval (Fig 2.2d).

Systems tracts can be broadly divided into four classes according to their relationship to specific parts of the relative sea level curve: lowstand, transgressive, highstand and shelf margin (Vail, 1987; Van Wagoner et al., 1987; Posamentier et al., 1988; Allen & Allen, 1990).

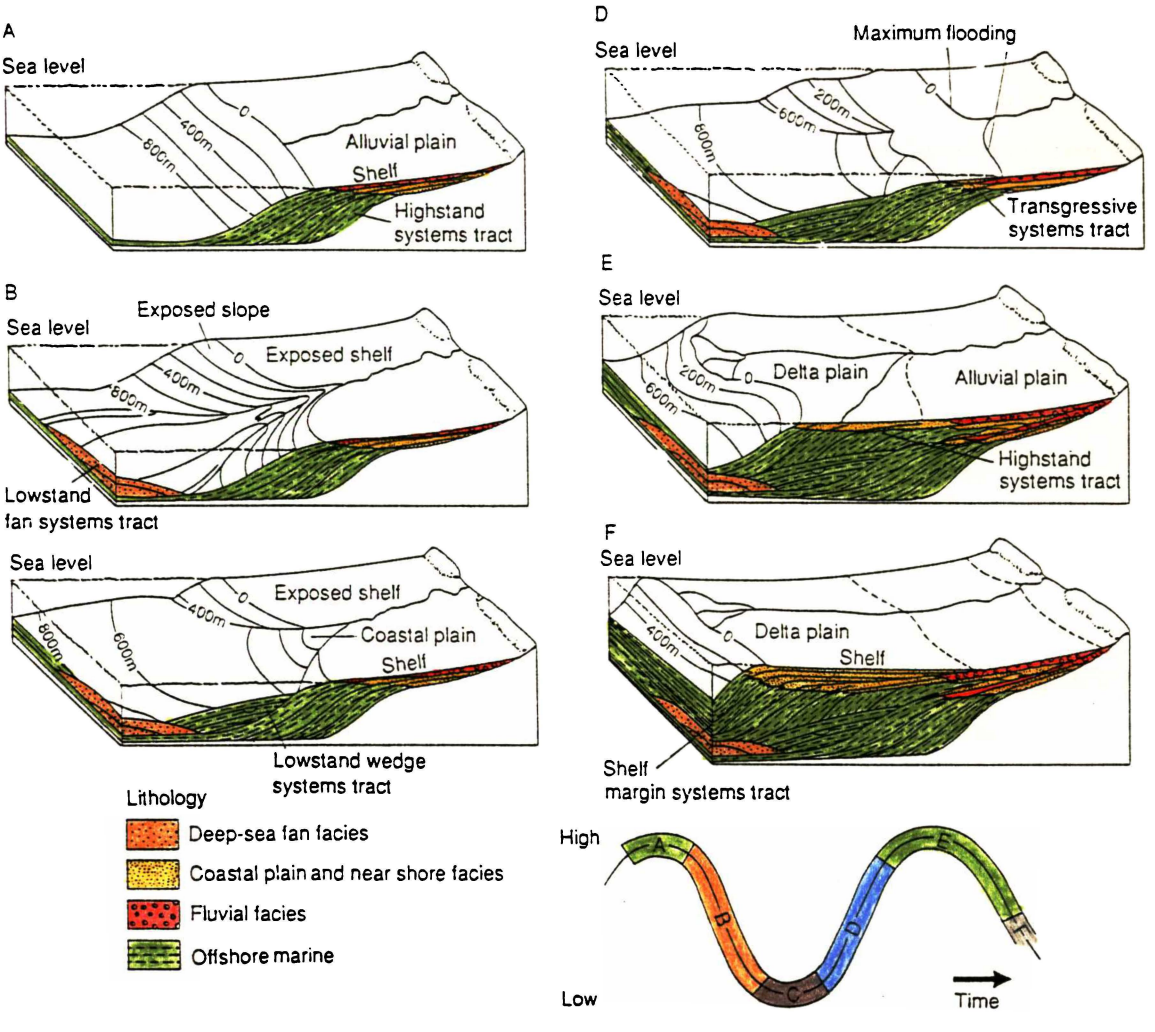

FIGURE 2.10: Characteristic systems tracts and their relation to the eustatic curve, according to the Exxon Group (Posamentier et al., 1988). These block diagrams are extremely idealised and have strong vertical exaggeration (from Allen & Allen, 1990, Fig 6.36)

Lowstand systems tract

A lowstand systems tract overlies a Type-1 sequence boundary and is produced by rapid relative sea level fall causing incision of the former shelf and the transferral of sedimentation to the basin floor and slope (Fig 2.10B & C). A lowstand systems tract comprises three separate units, a basin-floor (or lowstand) fan, a slope fan and a lowstand wedge.

A *basin-floor fan* is deposited during a time of rapid relative sea level fall and represents sediments bypassed through the shelf and slope and deposited in a submarine fan on the lower slope or basin floor (Fig 2.10b). The top of the fan is a downlap surface, and internal patterns may also contain fan channel and fan lobe facies (Fig 2.2a).

Slope fans are deposited during the late relative sea level fall and early relative sea level rise. Slope fans are characterised by turbidite and debris-flow deposition on the middle or the base of the slope. Deposition can be coeval with the basin-floor fan or with the early portion of the lowstand wedge. The top of the slope is a downlap surface for the lowstand wedge, and internal structures may also contain channel facies (Fig 2.2a).

Lowstand wedges are characterised by incised valley fill on the shelf, onlap onto the slope and downlap onto the previous basin-floor and slope fans. They are deposited during the late relative sea level fall or early rise (Fig 2.10c). The internal structure of a lowstand wedge is progradational, with the top surface representing the top of the lowstand systems tract with a marine-flooding surface termed a transgressive surface (Fig 2.2a).

Transgressive systems tract

A transgressive systems tract is deposited during rapid sea level rise and are characterised by retrogradational parasequence sets (Fig 2.10d). These sets back-step onto the basin margin, with strong onlap onto the sequence boundary in the landward direction and downlap onto the transgressive surface in the basinward direction.

As the rate of relative sea level rise slows, and the rate of addition of new space decreases, the sets of parasequences change from being retrogradational to aggradational. The surface at which this occurs is termed the maximum flooding surface and marks the top of the transgressive systems tract (Fig 2.2a).

Condensed sections occur in the distal regions of the basin during periods of transgression as sediments are trapped on the retrograding shelf (Fig 2.2a).

Highstand systems tract

Highstand systems tracts form after maximum flooding as relative sea level rise slows and aggradational parasequences are succeeded by progradational parasequences with clinoform geometries (Fig 2.10a & e). Highstand systems tract parasequences onlap onto the sequence boundary in a landward direction and downlap onto the previous transgressive and lowstand systems tracts in a basinward direction. Condensed sections

also occur during the early stages of a highstand systems tract before major progradation occurs (Loutit et al., 1988). Initially, as new space is added, rivers will aggrade with a vertical stacking pattern, eventually evolving into lateral stacking patterns as a equilibrium profile is reached. A highstand systems tract is bounded at the top by a Type-1 or Type-2 sequence boundary and at the bottom by a prominent downlap surface. Internal patterns are progradational (Fig 2.2a).

Shelf-margin systems tract

When relative sea level fall is gradual, sedimentation may shift basinward in a series of weakly progradational to aggradational parasequence sets (Fig 2.10f). The sets onlap onto the sequence boundary in the landward direction and downlap onto the sequence boundary in the basinward direction. The base of a shelf-margin systems tract is a Type-2 sequence boundary (Fig 2.2a).

2.1.6 Seismic stratigraphy interpretation procedure

Vail (1987) recommends a seven step seismic stratigraphy interpretation procedure:

1—seismic sequence stratigraphy
2—well-log sequence analysis
3—synthetic, well-to-seismic ties
4—seismic facies analysis
5—interpretation of depositional environment and lithofacies
6—forward seismic modelling
7—final interpretation

Given data constraints some of the above steps are not fully treated in this study.

Vail (1987, p.5) continues to describe the methodology for interpreting depositional sequences and systems tracts on seismic sections by identifying discontinuties on the basis of reflection terminations:

- Look for places where two reflectors converge, as where reflectors converge there will be reflection terminations.
- Mark the reflection terminations with arrows.
- Draw in the discontinuity surface between the onlapping and downlapping reflections above and the truncating and toplapping reflectors below. If discontinuity becomes conformable follow its position across the section by reflection correlation.
- The recommended colour code system for tracing reflection patterns and surfaces of discontinuity are (Table 2.2):

Type of pattern/surface	Colour	Black & white lines
Reflection patterns	red	thin
Reflection terminations	red	thick
Downlap surface	green	dashed
Trangressive surface	blue	dotted

TABLE 2.2: Recommended seismic sequence stratigraphy interpretation colour code (Vail, 1987).

- Identify the type of discontinuity:
    - regional onlap above and truncation below is probably a sequence boundary
    - regional downlap indicates a downlap surface

Given the paucity of well-log information in the study area, well-log sequence analysis and synthetic well-to-seismic ties are of only limited scope. Analysis is restricted to depth/velocity studies.

Also unfortunately, the quality of some of the seismic information in the study area is poor, hampering the ability to fully integrate the above seismic sequence interpretation into an analysis scenario using the systems tract models. In these cases seismic facies analysis and interpretation of depositional environments provides valuable information even though it cannot be fully integrated (for example, see Beggs, 1990; Stagg et al., 1992).

Forward seismic modelling is not carried out in this study.

As discussed above the integrated final interpretation of a seismic sections is only a subdivision of the integral approach to the basin analysis methodology.

2.2 Geohistory Analysis

2.2.0 Overview

Geohistory analysis is the integration of a number of quantitative stratigraphic techniques to display the geological history of an exploration well or section. Lithostratigraphic, biostratigraphic and paleobathymetric information are combined to provide the data for routines that compute decompacted sediment thickness and tectonic movement as a function of time. The results can then be interpreted to reveal sedimentation rates and episodes of thermal uplift and/or subsidence through time. The term *'geohistory analysis'* was introduced by Van Hinte (1978), and the concepts and applications have since developed to the point that it is now a standard tool in sedimentary basin analysis. Of particular importance is the thermal history and associated hydrocarbon maturity modelling (Waples, 1980; Falvey & Deighton, 1982; Guidish et al., 1985; Tissot et al., 1987; Waples et al., 1992). Numerous geohistory application examples are available in the literature, both in New Zealand (e.g. Hayward, 1987; Hayward & Wood, 1989; Cook et al., 1990; Hayward, 1990) and internationally (e.g. Thorne & Watts, 1989; Moussavi-Harami & Brenner, 1992; Tang & Lerche, 1992)

Geohistory analysis aims at compiling a subsidence curve (total and tectonic) and the burial history of stratigraphic units through time (Fig 2.12). One way to conceptualise such diagrams is that they represent the stratigraphic units present at a reference location, backwards through time. Three corrections to the present stratigraphy are needed for the process of generating a geohistory plot (Allen & Allen, 1990):

1 *Decompaction*: present-day compacted thicknesses must be corrected to account for the progressive loss of porosity with depth of burial.

2 *Paleobathymetry*: the water depth at the time of deposition determines its position relative to present sea level.

3 *Eustatic changes*: changes in the paleo sea level relative to that of the present need to be considered.

The calculations involved in these corrections can readily be done manually, but this approach can be time consuming. In this study a computer program has been developed to quickly do the necessary calculations and facilitate ease of use through 'user-friendly' interfaces and graphic visualisation. The program is largely based on GEO_HIST, a VAX/VMS computer program developed by Ray Wood (Wood, 1989) of the Geophysics Division of the Department of Scientific and Industrial Research (now the Crown

Research Institute of Geological and Nuclear Sciences) and based on the decompaction technique of Falvey & Deighton (1982).

2.2.1 Decompaction theory

The decompaction technique of Falvey and Deighton (1982) is based on the concept that each sedimentary unit has a skeletal thickness, the 'ultimate' burial thickness of the unit when porosity equals zero and no further compaction can occur. This can be computed from:

$$Z_{SK} = \int_{Z_1}^{Z_2} (1-\phi(Z))\, dZ \qquad (2.1)$$

where

Z_{SK}	is the skeletal thickness
$Z_2 - Z_1$	is the unit thickness
$\phi(Z)$	is the porosity function with depth.

The skeletal thickness remains constant throughout burial. The decrease in unit thickness can then be calculated if the function $\phi(Z)$ is known for that unit. There are a number of options for modelling the porosity of a sediment with depth. Sclater and Christie (1980) assumed a general exponential function, and Baldwin and Butler (1985) argue for the concept of 'solidity' rather than porosity in their relationship calculations. These models assume 'bulk' properties of the sediment being compacted (or decompacted) and lump together the complex processes of physical compaction and diagenesis, which are often time dependent also. Schmoker & Gautier (1989) present a case using time-temperature exposure as a measure of porosity decrease rather than depth. This approach has the implication that sediments may compact over time forming a second-stage, passively formed basin. The behaviour of compacting clay minerals is also more complex than the simple porosity-depth functions suggest, and is modelled by Audet & Fowler (1992).

Falvey & Middleton (1981, *in* Allen & Allen, 1990) argued that the exponential porosity-depth relationship does not fit shallower depth data very well, and they derived the alternative general porosity-depth relationship used in this study:

$$\frac{1}{\phi(Z)} = \frac{1}{\phi_0} + kZ \qquad (2.2)$$

where

ϕ_0	is the porosity at time of deposition

k is an empirically derived compaction constant
Z is the depth.

This relationship is based on the assumption that an incremental change in porosity is proportional to the change of load and the ratio of void space to skeletal volume (Falvey & Deighton, 1982). With equations (2.1) and (2.2), the skeletal volume can be calculated as:

$$Z_{SK} = (Z_2 - Z_1) - \frac{1}{k} \ln \left[\frac{\frac{1}{\phi_o} + k.Z_2}{\frac{1}{\phi_o} + k.Z_1} \right] \qquad (2.3)$$

Using the terminology Z_3 as the depth to the top of the unit at an earlier time, the bottom depth of the unit, Z_4, can be calculated by iteration from a rearrangement of equation (2.3):

$$Z_4 - \frac{1}{k} \ln \left[\frac{1}{\phi_o} + k.Z_4 \right] = Z_{SK} + Z_3 - \frac{1}{k} \ln \left[\frac{1}{\phi_o} + k.Z_3 \right] \qquad (2.4)$$

The amount of compaction calculated by the above formulas is a function of original porosity (ϕ_o), compaction constant (k), layer thickness and depth of burial. The first two values can be taken from 'standard' constants in the literature, as shown in Table 2.2.

LITHOLOGY	ORIGINAL POROSITY (ϕ_o)	COMPACTION CONSTANT (k)
sandstone[1]	0.40	1.20
siltstone[1]	0.53	2.18
mudstone (shale)[1]	0.70	2.43
overpressured shale[2]	0.45	1.15
limestone (marl)[3]	0.74	1.30
volcanic[2]	0.10	0.00

TABLE 2.3: Porosity and compaction constants of various 'typical' lithologic units.
[1] Falvey & Deighton (1982); [2] Wood (1989); [3] Schmoker & Halley (1982)

It should be noted that the parameters used are empirically derived from data that may not be valid in the setting being analysed. For example the parameters for limestone are derived from tropical carbonates in South Florida, and thus may not accurately reflect the

compaction behaviour of temperate carbonates in New Zealand. Note that volcanics are assumed to have little original porosity and to be uncompactable.

2.2.2 Paleobathymetric and eustatic corrections

Paleobathymetric corrections, or the estimation of water depths are an essential part of establishing the burial history of a stratigraphic unit, yet it is difficult to establish with great accuracy. Paleobathymetric information comes from a number of sources, in particular (Allen & Allen, 1990):

- benthic foraminifera, and less importantly
- sedimentary facies and
- distinctive geochemical signatures.

Some organisms inhabit a particular depth range, and can be used to obtain a direct depth estimate. However, most paleodepth estimates are indirectly obtained. Qualitative estimates can be derived from a comparison with modern species assemblages and by recognition of ecological trends of benthonic and planktonic foraminifera through time. Quantitative methods can also be used to obtain estimates, using ratios of, for example, plankton/benthos, arenaceous/calcereous foraminifers, per cent radiolarins or ostrocods, species dominance and diversity or morphological characteristics. These techniques allow interpretations of environmental factors such as chemical environment (salinity, pH, oxygen and CO_2 contents, nutrient availability), the physical environment (temperature, light, energy level, type of substrate, turbidity) and biological environment. As much information as possible is needed to produce a reliable depth estimate (Allen & Allen, 1990, p.271).

Sedimentary and geochemical data are far less reliable indicators of paleobathymetric data, and generally used only to confirm paleontological observations. Some sedimentary structures, such as wave ripple marks, are restricted to particular depth ranges (<200 m), however general sedimentary facies reflect supply and process and not particularly diagnostic of depth. If identified, the gradients of flood plain slopes may be used to estimate heights above sea level (Homewood et al., 1986, p.207). Geochemical data is restricted to estimates of the carbonate compensation depth (CCD), which can be derived from microfossil studies. Some mineral species such as glaucony and phosphates may also provide water depth information.

Eustatic corrections for global sea level fluctuations can be included after the decompaction process. Bearing in mind the uncertainties and debate surrounding the 'Vail' global sea level curve (Vail, Mitchum & Thompson, 1977; Haq et al., 1987), Allen & Allen (1990) recommend using only the first-order cycles (most likely due to volume changes in ocean ridge systems) and those confidently linked to glaciations/deglaciations be included.

Concern at the possible masking of tectonic information by an uncertain or arbitrarily selected sea level is expressed by Hegarty et al. (1988), but conclude a strong tectonic signal will be unperturbed by sea level corrections of moderate amplitude. The amplitude of sea level fluctuation remains the key question in the use of the relative sea level in this type of application.

2.2.3 Backstripping and tectonic subsidence calculations

Basin evolution is a dynamic process driven by tectonic processes which in turn are a result of the behaviour of the lithosphere. Basin subsidence due to the loading effect of the sedimentary column can be calculated and thus the amount of subsidence due to 'other' tectonic processes (such as thermal cooling, lithospheric thinning or loading) can be estimated. This process is termed *backstripping*, introduced by Watts & Ryan (1976). Numerous examples of backstripping applications exist in the literature, in particular, the Atlantic margin (Steckler & Watts, 1978), the North Sea (Thorne & Watts, 1989), and North American basins (Bond & Kominz, 1984; Heidlauf et al., 1986). Two main assumptions are made in this technique: (1) that the subsidence due to loading occurs rapidly in comparison to other processes and; (2) that the lithosphere fully compensates loading in local (Airy) isostatic equilibrium (Wood, 1989). The second assumption is probably the most open to debate, especially in a foreland basin setting, but further knowledge of the supporting lithosphere is required to calculate the 'true' lithospheric compensation value (see Allen & Allen, 1990, p.272). The loading effect of the water column can also be included or ignored in the following calculations.

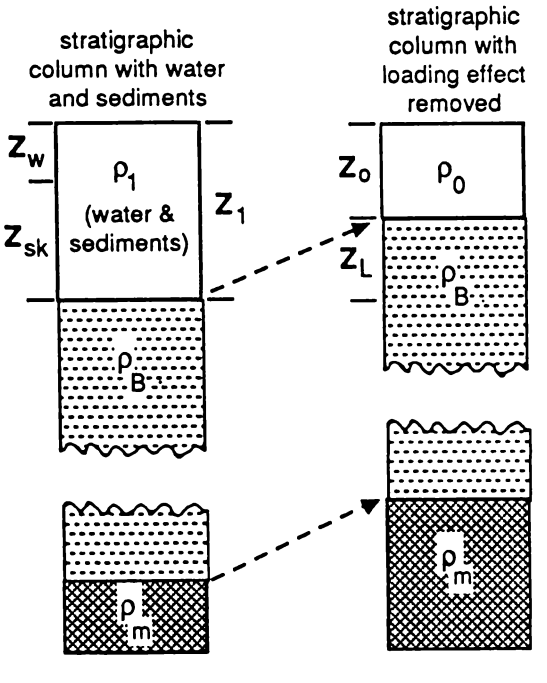

FIGURE 2.11: Diagram illustrating local isostatic equilibrium (from Steckler & Watts, 1978; Wood, 1989)

Figure 2.11 illustrates the concept of local isostatic equilibrium used to calculate the tectonic curve, where:

Z_1 is the observed or backstripped thickness of water and sediments and is the total of:

Z_W, water thickness, and;

Z_{SK}, skeletal thickness.

Z_1 is also equal to the total of:

Z_L, subsidence due to loading, and;

Z_O, subsidence due to other tectonic processes.

If the column were in equilibrium then Z_O and Z_L would be related by

$$Z_L (\rho_m - \rho_1) = Z_O (\rho_1 - \rho_0) \quad (2.5)$$

where

Z_O is subsidence due to tectonic processes

Z_L is the subsidence due to loading

ρ_m is the average asthenosphere density (3.3 Mg/m^3)

ρ_0 is the density of the displaced material, either 0.0 or 1.0 Mg/m^3

ρ_1 is the density of the basin fill (sediment and water).

The total depth to basement Z_1 is the sum of Z_O and Z_L, therefore

$$Z_O = Z_1 \left[\frac{\rho_m - \rho_1}{\rho_m - \rho_0} \right] \quad (2.6)$$

The average or effective density of the water/sediment column (ρ_1) is derived from the relationship (Wood, 1989):

$$\rho_1 = \frac{(Z_W \times \rho_W) + (Z_{SK} \times \rho_S)}{Z_1} \quad (2.7)$$

where

Z_W is the thickness of the water, including the porosity of the sediments

Z_{SK} is the skeletal thickness of the sediments

ρ_W is the density of the water (1.0 Mg/m^3)

ρ_S is the 'average' density of the sediment grains (2.7 Mg/m^3)

and

$Z_1 = Z_W + Z_{SK}$, is the total of the sediment/water column as in Figure 2.12.

The calculated bulk density of the sedimentary column is an important factor in assessing its loading effect. An alternative process for deriving the bulk density by calculating the mean porosity of a layer, using lithologic density 'standards' to find the bulk density of a layer, and then calculating the weighted total of all the layers to find the total bulk

density is given by Steckler & Watts (1978). Tests indicate that results of this method do not significantly differ from those of Wood (1989), and rather than add another area of 'fuzzy' lithologic standards, the technique has not been used in this study.

2.2.4 Computer Programming

The computer application, GeoHist+, was developed for this study largely based on the GEO_HIST program of Ray Wood (Wood, 1989) and interface concepts in similar applications like *Subside!*™ (Wilkerson & Hsui, 1989). The program was originally developed in QBASIC™ on an IBM-PC compatible computer, and then transferred and rewritten for a Macintosh Plus computer using the Lightspeed Pascal™ programming language. GeoHist+ makes full use of the Macintosh 'GUI' (Graphics User Interface) environment of mouse driven windows, menus and dialog boxes. The listings of the program are given in the appendices of this volume.

The program functions with the following steps:

- Information from a well-log or section (seismic or outcrop) is entered. Information for each entered unit comprises:
    - Name of the unit
    - Depth to top of unit
    - Depth to base of the unit
    - Age of the base of the unit
    - Paleodepth of deposition of the unit
    - Lithology of the unit

  In GeoHist+ a unit may be described as a mixture of lithologies, e.g. 30% sand, 10% mud, 40% limestone and 20% volcanic. The full list of possible lithologies is given in Table 2.2. The resulting lithologic parameters (k and ϕ_0) of the unit are calculated automatically as a weighted average of each of the components.

- The entered data can be edited, saved to a text file or restored from a text file. The text file may also be edited independently of the GeoHist+ application.

- The data is processed according to the theory given above. The data is checked for irregularities, and units are then 'removed' from the top of the sedimentary column one by one. At each 'stage' the remaining units are decompacted and adjusted for paleobathymetry and eustacy. The amount of tectonic subsidence at each stage is also calculated.

- The decompacted data set can then be saved or viewed as a text file.

- The decompacted information can also be visually displayed on the screen (see Figure 2.12), or plotted to a graphics plotter.

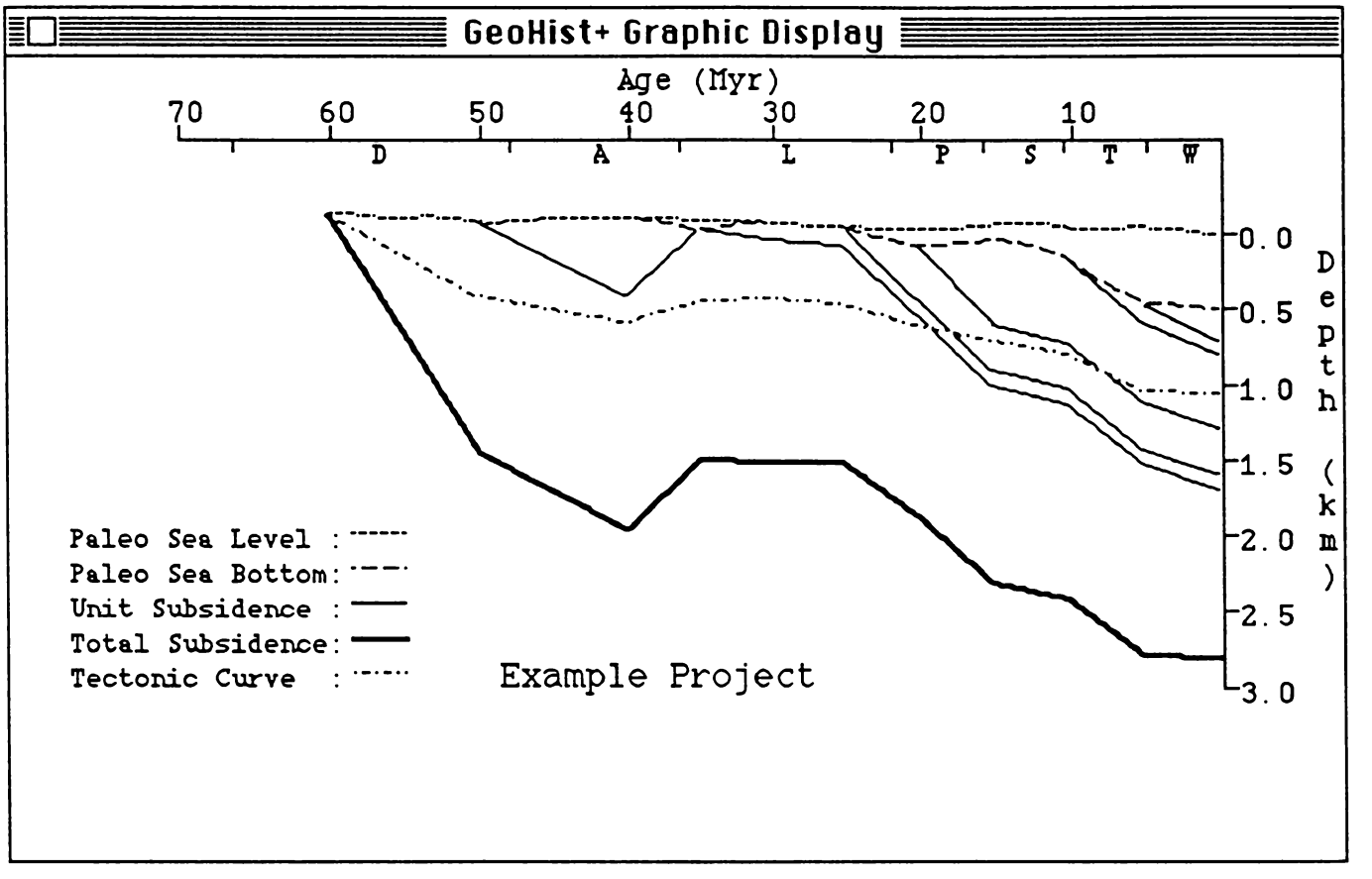

FIGURE 2.12: Example of the graphical display output of GeoHist+.

Computed values in GeoHist+ are corrected for paleo sea levels adapted from the long-term curves of Haq *et al.* (1987). The sea level values are contained in a text file called *Paleosealevel.data* which accompanies the GeoHist+ application. The option of altering the paleo sea level data can be easily exercised with this arrangement. Currently, the maximum sea level is 167 m in the mid Cretaceous. Values for paleo sea-level from the mid Jurassic to the present have been included and a constant sea level of +91 m is assumed for older data.

Stratal unconformities in the form of non-deposition hiatuses or erosion events may be modelled in GeoHist+. To simulate a hiatus, the depth to base is entered as equal to the depth to top (i.e. zero thickness) for the appropriate timespan. To simulate an erosional event a depth to base that is less than the depth to top (i.e. a 'negative' thickness) is

entered. The program checks that a sufficient thickness of sediments are deposited before they are eroded.

One consequence of the Falvey and Middleton (1981, in Falvey & Deighton, 1982) porosity-depth relationship is that there is a limit to the amount of sediment that can be eroded. The limit is

$$\frac{1}{\phi_0 \times k} \text{ km} \qquad \textbf{(2.8)}$$

The actual limits for each lithology are (Wood, 1989):

Sand	2083 m
Siltstone	866 m
Mudstone	588 m
Limestone	1040 m
Overpressured shale	1932 m
Volcanics	unlimited

The program will check the entered data before processing for erosion events that exceed these limits.

Subsidence driven by the effect of the water column is also included in sediment load driven subsidence in the GeoHist+ calculations of the tectonic curve.

2.3 Geodynamical Modelling

2.3.0 Overview

Geohistory analysis is the quantitative analysis of subsidence rates through time derived from the observed data of well-logs, or seismic or outcrop sections. The tectonic subsidence calculations derived from observed data can be compared with geodynamic models in order to possibly obtain information about the nature and geologic history of the supporting lithosphere.

Subsidence models attempt to represent the tectonic processes occurring during and after a rifting event causing lithospheric stretching and resultant subsidence. A number of models have been used in various tectonic situations with varying degrees of complexity. Flexural models simulate the flexure response of the lithosphere to sediment and/or thrust loads, again various models exist with varying degrees of complexity and application. Both type of model are discussed below.

2.3.1 Subsidence modelling

Various models have been used for the subsidence of sedimentary basins and rifted continental margins resulting from thermal changes and compensation mechanisms. McKenzie (1978) proposed a simple model for the development and evolution of sedimentary basins, assuming the crustal and lithospheric extension to be the same (*uniform stretching*) (Fig. 2.13). A number of modifications have been made to the McKenzie model, including non-uniform extension (Royden & Keen, 1980; Hellinger & Sclater, 1983) and variable extension with time (Jarvis & McKenzie, 1980; Cochran, 1983). Given the lack of detailed geologic data required to support the more complex models, the simplest thermal model (McKenzie, 1978) will used in this study. The same approach is used by Wang & Stein (1992) for subsidence analysis in the Gulf of Papua, a similar tectonic setting to the South Westland study area.

The McKenzie model (1978) assumes 'instantaneous' and uniform stretching of the lithosphere and crust with passive upwelling of hot asthenosphere to maintain the isostatic equilibrium. Although an instantaneous rifting event is a mathematical assumption, Jarvis & McKenzie (1980) found that as long as rifting times were less than 20 Myr in duration, the uniform extension model was a very reasonable approximation. The lithosphere is isostatically compensated throughout extension, and radioactive heat sources are ignored.

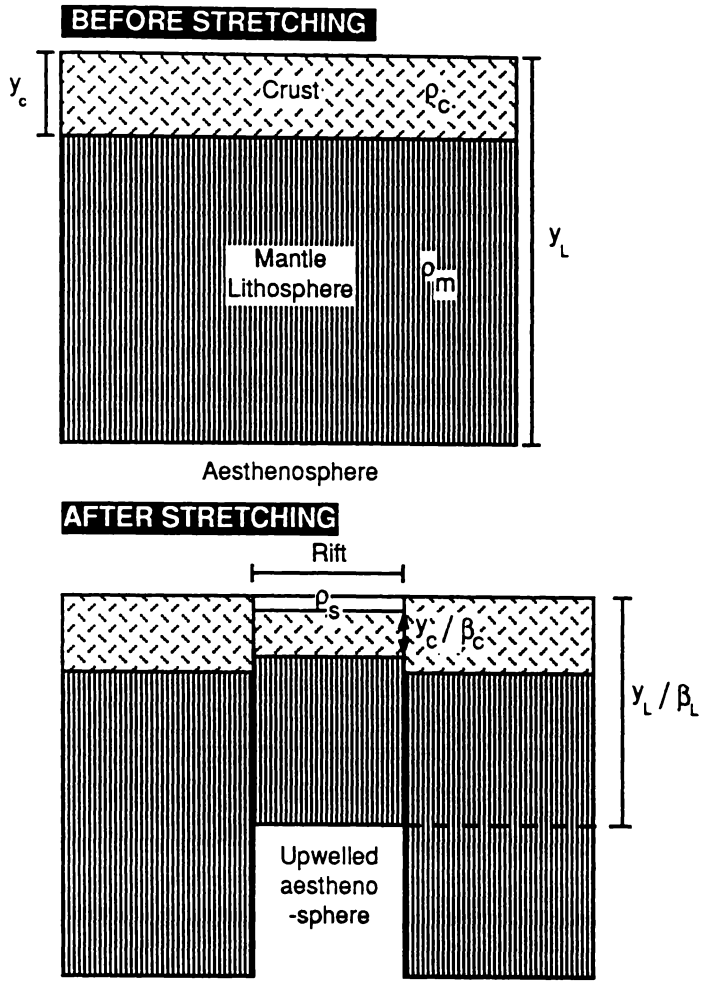

FIGURE 2.13: Schematic diagram of notation and fundamental precepts of the uniform stretching model. The crustal and lithospheric stretch factors are β_c and β_L. For uniform stretching $\beta_c = \beta_L$. (From Allen & Allen, 1990, Fig. 3.9).

The total subsidence in an extensional basin is composed of two components (Fig. 2.14):

- initial fault controlled subsidence which is dependent on the initial thickness of the crust and the the amount of stretching β;
- subsequent thermal subsidence caused by the cooling of the upwelled asthenosphere, and which is dependent on the amount of stretching only.

The subsidence resulting from initial fault controlled, mechanical stretching can be obtained as

$$y_S = \frac{y_L \left\{ (\rho_m - \rho_c) \frac{y_C}{y_L} \left(1 - \alpha_v \frac{T_m}{2} \frac{y_C}{y_L} \right) - \frac{\alpha_v T_m \rho_m}{2} \right\} \left(1 - \frac{1}{\beta} \right)}{\rho_m (1 - \alpha_v T_m) - \rho_s} \qquad (2.9)$$

where

β is the stretch factor

y_L is the initial thickness of the lithosphere

y_c is the initial thickness of the crust

ρ_m is the density of the mantle

ρ_c is the density of the crust

ρ_s is the average bulk density of sediment or water filling the rift

α_v is the thermal expansion coefficient of both crust and mantle

T_m is the temperature of the asthenosphere

y_S is positive for subsidence, negative for uplift. Commonly used literature values can be used when the actual parameters are poorly known (Parsons & Sclater; Allen & Allen, 1990):

y_L = 125 km

ρ_m = 3330 kg m^{-3}

ρ_c = 2800 kg m^{-3}

ρ_w = 1000 kg m^{-3} (fresh water)
= 1030 kg m^{-3} (marine water)

α_v = 3.28 10^{-5} $°C^{-1}$

T_m = 1333 °C

Subsidence caused by thermal contraction is approximated by:

$$S(t) \sim E_0 \frac{\beta}{\pi} \sin \frac{\pi}{\beta} (1 - e^{-t/\tau}) \qquad \textbf{(2.10)}$$

where τ is the thermal time constant of the lithosphere:

$$\tau = \frac{y_L^2}{\pi^2 \kappa} \qquad \textbf{(2.11)}$$

where κ is the thermal diffusivity of the lithosphere (= 10^{-6} $m^2 s^{-1}$). E_0 is given by

$$E_0 = \frac{4\, y_L\, \rho_m\, \alpha_v\, T_m}{\pi^2\, (\rho_m - \rho_s)} \qquad \textbf{(2.12)}$$

The rate of thermal subsidence decreases exponentially with time (Figure 2.14). Model subsidence curves for various values of the stretching factor β, using known values for crustal and lithospheric thickness (y_c and y_L) can be compared with observed tectonic subsidence values through time (derived from geohistory analysis) to obtain an estimate of the amount of stretching that occurred during the initial rifting event.

2.3.2 Flexural modelling

The flexural response of the oceanic and continental lithosphere can be described mathematically in a mechanical model by a number of methods, again with varying degrees of assumptions and complexity. The wavelength and amplitude of the flexural deformation have important thermal and geological implications (Stern, 1990). Three morphological elements (load, basin and forebulge) are a constant theme in flexural modelling (Fig. 2.15).

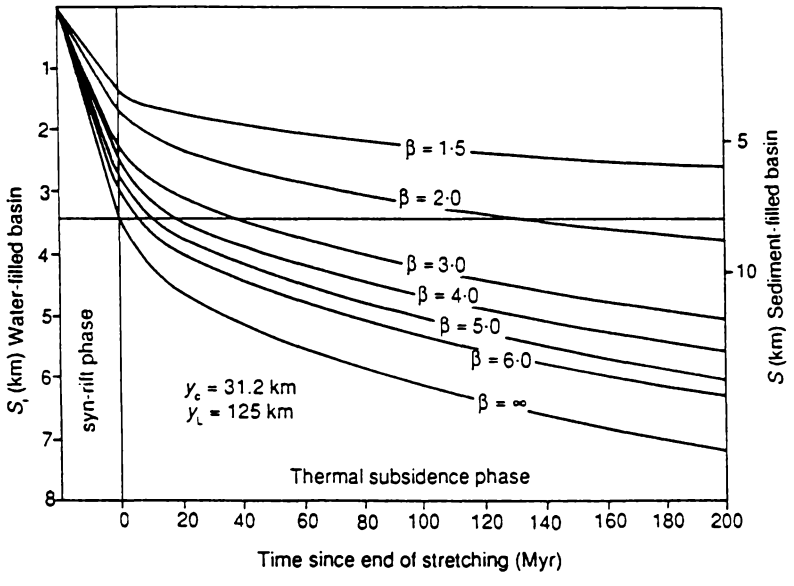

FIGURE 2.14: The subsidence change through time for various values of the stretch factor, β, obtained from equation (2.10). The rate of thermal subsidence decrease exponentially with time. Curves shown refer to a lithosphere of initial thickness 125 km and an initial crustal thickness of 31.2 km (after Dewey, 1982, p.387; Allen & Allen, 1990, p.59).

The general flexural equation for a loaded and flexed plate is

$$D\frac{d^4\omega}{dx^4} + P\frac{d^2\omega}{dx^2} + (\rho_m - \rho_s)g\omega = q_a(x) \qquad (2.13)$$

where

D is the flexural rigidity of the plate

P is the horizontal forces acting on the plate

x is the horizontal scale

ω is the deflection of the plate

$q_a(x)$ is the applied vertical load on the plate

ρ_m is the density of the mantle

ρ_s is the bulk density of the basin sediment fill

g is the gravitational acceleration constant (9.8 m s^{-2})

The flexural rigidity is a function of the *elastic thickness* and other rheological properties of the flexed lithosphere:

$$D = \frac{Eh^3}{12(1 - v^2)} \qquad (2.14)$$

where

E	is Young's modulus	(literature standard = 70 GPa)
h	is the equivalent elastic thickness of the lithosphere	
v	is Poisson's ratio	(literature standard = 0.25)

The elastic thickness is a numerical result derived from the various assumptions about the force system and mechanical properties of the plate, and is intrinsically related to the flexural rigidity of the plate (equation **(2.14)**).

Applying two boundary conditions to the general flexural equation **(2.13)**:

1 Applied load is at the end of the plate, thus the applied vertical load, $q_a(x) = 0$, since the applied load is zero except at the location of the load ($x = 0$).

2 assuming no horizontal forces are applied, $P = 0$

the general equation becomes

$$D\frac{d^4\omega}{dx^4} + (\rho_m - \rho_s)g\omega = 0 \qquad (2.15)$$

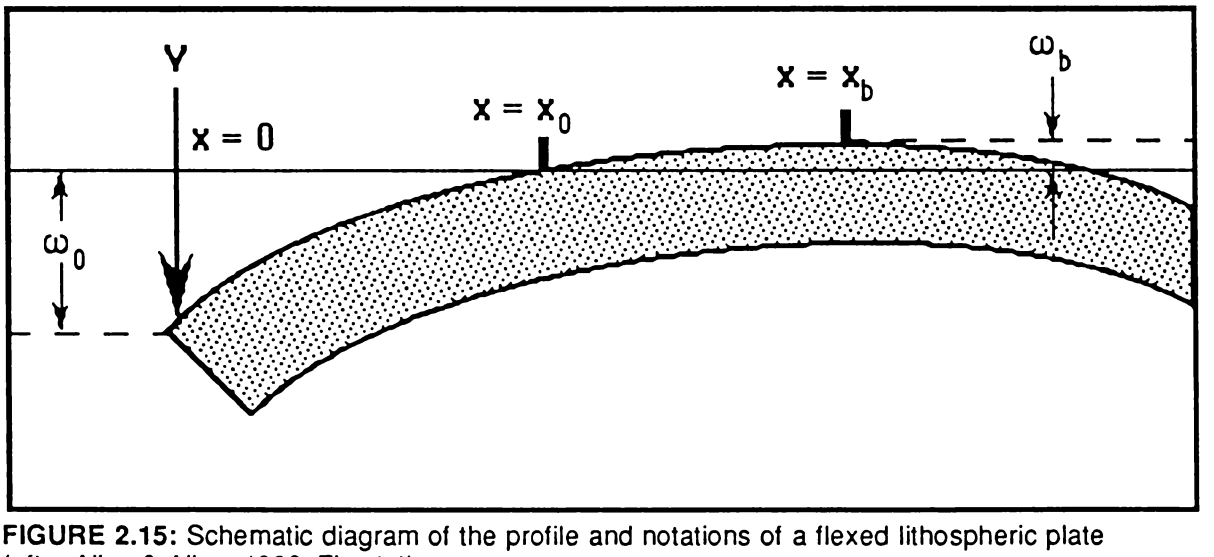

FIGURE 2.15: Schematic diagram of the profile and notations of a flexed lithospheric plate (after Allen & Allen, 1990, Fig. 4.4).

Equation **(2.15)** is ideally limited to modelling the geometry of deflection in oceanic lithosphere. Ignoring the fundamental complexities of continental lithosphere and

assuming elastic behaviour, the equation can be loosely applied in continental flexural situations (Allen & Allen, 1990). Karner et al., (1983) also noted that the with simple thermo-elastic models there was a apparent consistency between oceanic and continental lithospheric rigidities, suggesting that both have similar mechanical properties.

The general solution for a fourth order differential is accomplished by breaking it into exponential, sine and cosine components. Constants are determined according to the boundary conditions (Turcotte & Schubert, 1982, pp.125–126) and α is the *flexural parameter* (Walcott, 1970) given by

$$\alpha = \left\{ \frac{4D}{g\,(\rho_m - \rho_s)} \right\}^{1/4} \qquad (2.16)$$

Following solution of equation (2.15), a number of useful and simple expressions can be made about the geometry of the deflection. Assuming an unbroken lithosphere model and if the maximum deflection (ω_0 at x=0) is known, the profile of the deflection obeys (Fig. 2.15)

$$\omega = \omega_0 e^{-x/\alpha} (\cos x/\alpha + \sin x/\alpha) \qquad (2.17)$$

Alternatively the maximum deflection may also be calculated as

$$\omega_0 = \frac{V_0 \alpha^3}{8D} \qquad (2.18)$$

where V_0 is the line emplaced end load at $x = 0$. The half width of the depression (x_0) can be found at the point where the deflection is zero ($\omega = 0$), equation (2.17) becomes:

$$x_0 = \frac{3\pi\alpha}{4} \qquad (2.19)$$

The distance from the line load to the highest part of the forebulge can be found as:

$$x_b = \pi\alpha \qquad (2.20)$$

If the half width of the depression and/or the distance of the forebulge are already known from other information (e.g. seismic sections), then equations (2.19) and/or (2.20), may be used to calculate the flexural parameter (α), which in turn can be used in equation (2.16) to calculate the flexural rigidity (D) or even the line load (V) in equation (2.18).

The height of the forebulge above the datum of zero deflection is

$$\omega_b = -\omega_0 e^{-\pi} = -0.0432\,\omega_0 \qquad (2.21)$$

If the lithosphere under a line load is broken, such as may be the case in rift zones and obduction or subduction zones, then the boundary conditions need to be modified (Walcott, 1970). For the same load and elastic thickness, the broken plate model is modelled as a semi-infinite elastic plate, and predicts twice the maximum deflection of an unbroken plate model (Turcotte & Schubert, 1982). If the maximum deflection is known, the deflection profile for a broken plate is given by

$$\omega = \omega_0 e^{-x/\alpha} \cos x/\alpha \qquad (2.22)$$

or alternatively the maximum deflection can be found as

$$\omega_0 = \frac{V_0 \alpha^3}{4D} \qquad (2.23)$$

The half width of the basin is given by

$$x_0 = \frac{\pi\alpha}{2} \qquad (2.24)$$

showing that the basin is narrower for the case of a broken plate. The distance to the crest of the forebulge is given by

$$x_b = \frac{3\pi\alpha}{4} \qquad (2.25)$$

showing that narrower forebulges are characteristic of broken plates. The deflection at the forebulge is given by

$$\omega_b = \omega_0 e^{-3\pi/4} \cos 3\pi/4 = -0.0670\ \omega_0 \qquad (2.26)$$

indicating a larger forebulge amplitude for a broken plate.

It is possible to match the theoretical deflection to the observed depth of basement in a region of continental lithospheric flexure such as the Appalachians (Fig. 2.15; Turcotte & Schubert, 1982; Allen & Allen, 1990) and the Gulf of Papua (Wang & Stein, 1992). By trial and error with the critical parameters (lithospheric/crustal thickness, stretching factor, half width of basin, height of forebulge, etc.) a 'best-fit' theoretical curve can be matched to the basement shape (Fig. 2.16). However it should be noted, that often due to lack of detailed geologic data the choice of parameters is neither unique or verifiable.

A number of significant interpretations can be made using knowledge of lithospheric flexure. The half-width (or wavelength) of the deflection caused by flexure is a function of the flexural rigidity (and/or equivalent elastic thickness), and is thought to reflect the

effective thermal age of the flexed lithosphere at time of loading (Karner et al., 1983). The effective thermal age is a measure of the time since the last major thermal or metamorphic event effecting the plate before the loading event. Figure 2.17 illustrates an empirical plot relating rigidity to effective thermal age produced by Karner et al. (1983).

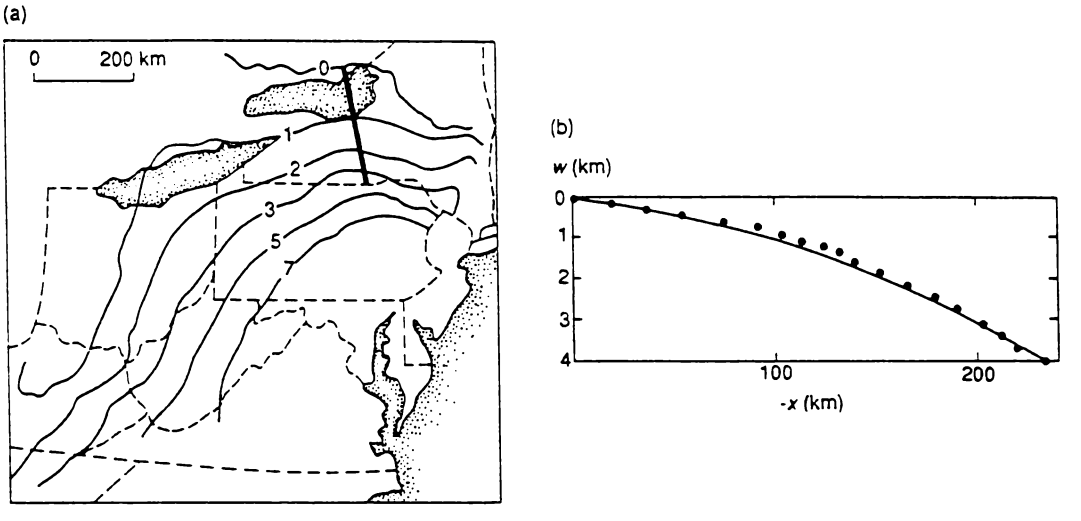

FIGURE 2.16: Example of subsidence model comparison with observation. **(a)** Contours of basement (in km) in the Appalachian foreland basin, based on borehole and seismic reflection data. **(b)** Profile of basement depths from (a), heavy line is the theoretical deflection given by the general flexural equation with half width of basin = 122 km, and height of forebulge = 0.29 km. (Allen & Allen, 1990, Fig. 4.7)

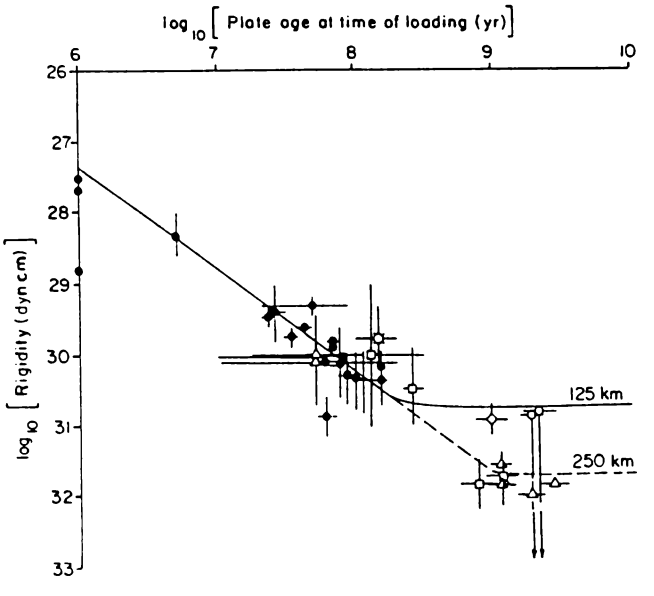

FIGURE 2.17: A log-log plot of effective thermal age at time of loading (both oceanic and continental) versus the effective elastic rigidity (from Karner et al., 1983, Fig.1, note:10^7 dyne cm = 1 Nm)

The assumption that continental lithospheric rigidity is merely a function of the age of the lithosphere was updated by McNutt et al. (1988), who found a correlation between the rigidity (measured by the equivalent elastic thickness) and other parameters such as, age of flexed lithosphere at time of loading, radius of curvature of thrust belts, total length of the thrust segment and dip of the underthrust plate. The main conclusions of McNutt et al.'s (1988) study were:

- no evidence of viscoelastic relaxation (the application of viscoelasticity in foreland basins is further explained in Chapter 3).
- rigidities of some continental lithosphere sections are lower than their age would suggest. Possibly weakened by a decoupling of an elastic plate at some depth, allowing the upper and lower halves to flex independently. Such weakness may also reflect a plate with different rheologies at different depths.
- steep dip is responsible for weakening an otherwise strong plate, as it induces failure of significant sections of the plate by brittle and ductile mechanisms.
- stiff plates always form straight mountain belts, whereas weak plates can form either curved or straight mountain ranges.
- weaker, highly curved plates lack the lateral integrity to form long thrusts.

Another application of elastic flexure modelling is to look for a spatial relationship between major faults and the predicted location of maximum bending stress due to flexure (Stern, 1990). Watts & Talwani (1974) formulate the magnitude of the bending stress in relation to the deflection curve with

$$S = \frac{Eh}{2} \cdot \frac{d^2\omega}{dx^2} \qquad (2.27)$$

where $d^2\omega, dx^2$ is the second derivative of the deflection curve given for a broken and unbroken plate by equations (2.17) and (2.22) respectively. The bending stresses are thus given by

$$S = \frac{Eh}{2} \cdot \frac{2\omega_0}{\alpha^2} e^{-x/\alpha} (\sin x/\alpha - \cos x/\alpha) \qquad (2.28)$$

for an unbroken plate, and

$$S = \frac{Eh}{2} \cdot \frac{2\omega_0}{\alpha^2} e^{-x/\alpha} (\sin x/\alpha) \qquad (2.29)$$

for a broken plate.

If the implied bending stresses exceed the estimates for the maximum stress difference that the lithosphere can sustain (McNutt, 1980), this can be used to predict the location of major faulting systems. Stern (1990) uses such an approach in modelling the location of the Cape Egmont Fault Zone in relation to the bending stresses induced by flexing under the Taranaki Basin.

2.4 Seismic data handling and processing

2.4.0 Overview

There are a number of sources of information regarding the structure and evolution of a sedimentary basin:

- seismic reflection sections
- well-log data
- outcrop observations
- geophysical data (e.g. gravity surveys)

These sources have to be brought together and relevant information integrated to form a comprehensive interpretation of the sedimentary basin under study.

The most complex data handling and processing requirements are often those of the seismic reflection sections, as they frequently represent a vast amount of data. In this study the locations and interpretative data of the 1715 km of seismic reflection sections is 'captured', stored and processed by an engineering relational database management system: **TECHBASE**, running on an IBM-PC compatible computer. This system is exceptionally flexible, allowing the capture, loading, storage, manipulation, reporting and visualisation of data with a variety of TECHBASE application packages (TAPS) which provide specific capabilities required by various engineering disciplines (MINEsoft, 1991). In particular TECHBASE is used in this study to

- store the location of the studied seismic reflection sections.
- construct basemaps with various geographical & geological features.
- store the two-way-travel-time (twt) to the interpreted horizon in each section.
- convert the raw time data to depth using velocity information from well-logs.
- construct and display palinspastic reconstructions along seismic sections, using the methodology of geohistory analysis given above.
- model, contour and display a surface on the various horizons (either twt, implied depth or restored).

The database structures and calculation routines used in these tasks in the TECHBASE package are given in the Appendices of this volume.

2.4.1 TECHBASE routines

The routines used in the processing of the seismic information are summarised in a flow diagram form in Fig 2.18.

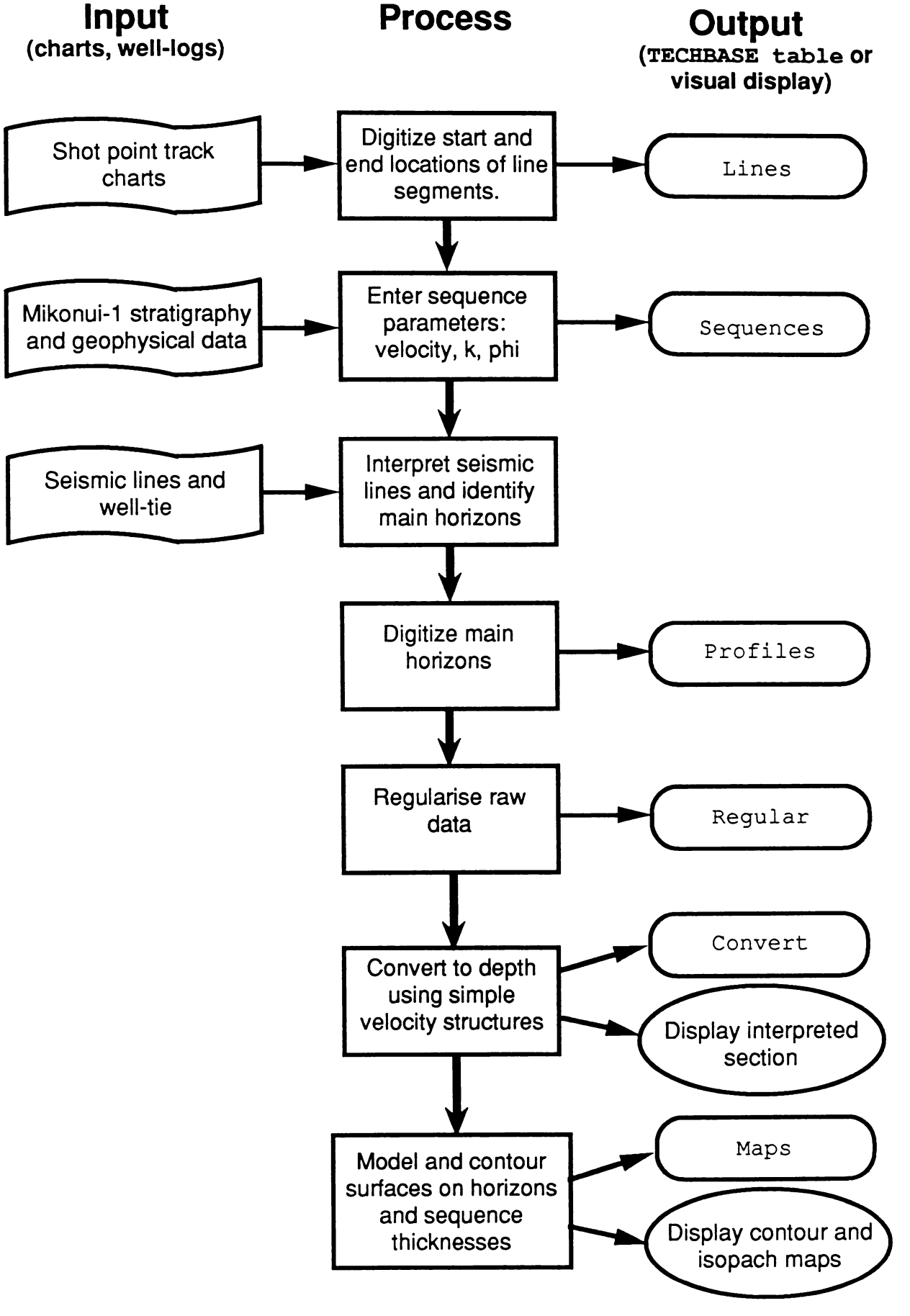

FIGURE 2.18: Flow diagram summarising the procedures undertaken in the processing of information from the seismic lines in this study.

2.4.1.1 *Data capture*

The first step in seismic section processing is to accurately locate the position of the sections in the study area. This is done using charts tracking the location of shot points of the seismic profiles and using the SDIGIT program in the TECHBASE package. Each seismic section is divided into linear segments to avoid too greater drift of shotpoint locations from a linear interpolation between the end points of the line. The end points of each segment are then entered into the database using a digitising tablet. All points are entered using the New Zealand National Grid system coordinates in metres, often converted from latitude and longitude coordinates of the track charts.

The seismic sections are interpreted and significant horizons traced in. These traces are then also digitised using the shotpoints and two way travel time as coordinates. Each line (or line segment) and horizon is uniquely identified. Given the line segment identifier, the database is able to convert shotpoint locations into metric grid coordinates using simple interpolation between the 'known' locations of the end points of the line segment.

2.4.1.2 *Depth conversion*

Before any further processing can occur the raw data for each horizon must be regularised so meaningful unit thickness can be calculated between horizons. The two way travel time to a horizon at each shotpoint is interpolated between known raw data points on either side. Regular points at either end of the seismic section are extrapolated from the slope of the two end points. The regularisation of the raw data is implemented by a small QBASIC routine operated by a TECHBASE project manager.

The conversion of two way travel time to depth in seismic sections is very complex. Here it has been simplified to using interval acoustic velocities of the layers between the identified horizons (Fig 2.19) and is implemented within the TECHBASE database by the use of calculated fields. The interval acoustic velocities are calculated from well-log information and are a function of lithology and porosity. Therefore, velocities tend to increase with depth. The two way travel time for the unit above a particular horizon is calculated and halved to get the interval time for that unit. The interval time is multiplied by the interval velocity of that unit to get the unit thickness in metres. The sum of the thicknesses of all overlying units gives the depth to a horizon.

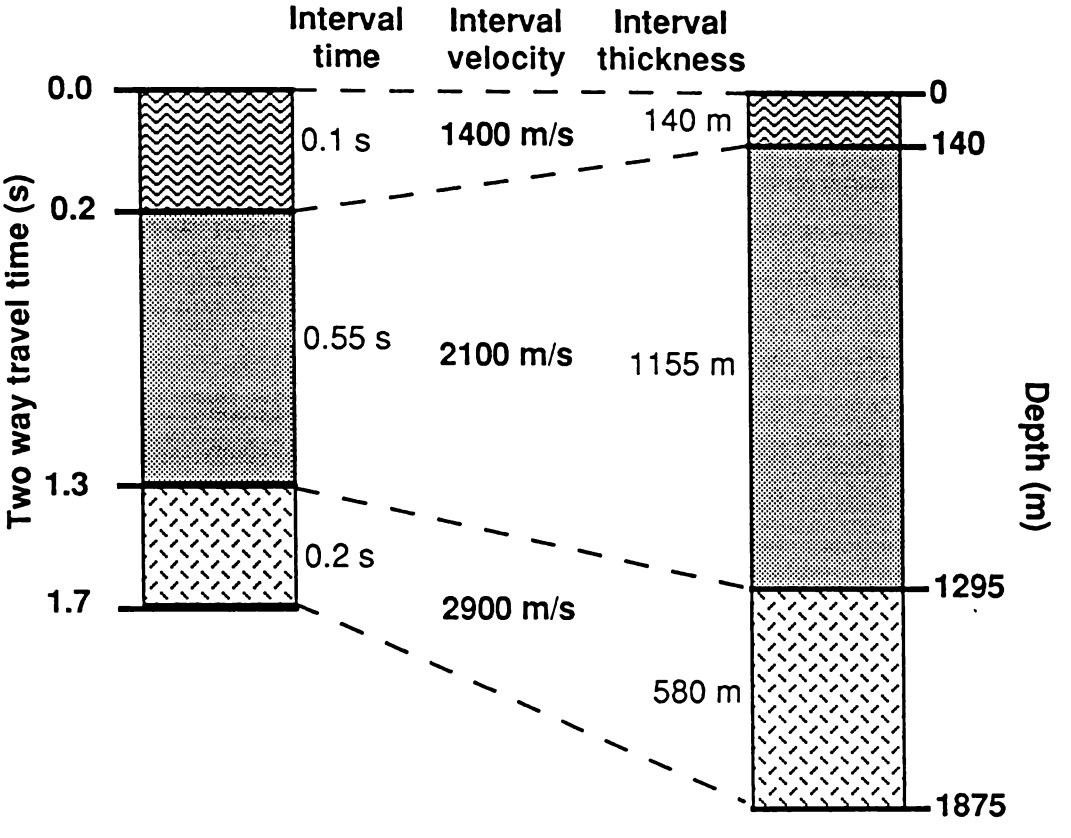

FIGURE 2.19: Principles of simple depth conversion of horizons and unit seismic data measured in two way travel time. Note the interval time is half that of that recorded on a section, as the recorded data is the time it takes for a seismic wave to pass through the unit twice. Only the interval single way travel time is needed.

2.4.1.3 *Backstripping and palinspastic reconstruction*

It is possible to treat each shot point location as a separate sedimentary column and to undertake a backstripping procedure using the principles of geohistory analysis (in particular backstripping) given above. When recombined, these separate columns in effect provide a two dimensional 'reconstruction' (or restoration) of the depth converted seismic section at particular times. Corrections for paleodepth across a section are more difficult to implement, and in this study are simulated by interpolating paleodepth from two depths given at each end. Again, the numerical processing is carried out by a QBASIC routine using the required data extracted from the TECHBASE database.

It is carefully noted that the above process is a gross simplification, ignoring the often detailed methodologies of cross section restoration and balancing (e.g. Dahlstrom, 1969; Hossack, 1979; De Paor, 1988; Marshak & Woodward, 1988; Rowan & Kligfield, 1989; Woodward et al., 1989; Nunns, 1991). Although the area (and hence volume) are conserved during the two dimensional backstripping, the length of horizons between shot points is not. However, provided that a horizon has a dip of less than 25° this modification of length is within a ±10% error range. Faults also pose problems as they are fundamental

indicators of length reduction (reverse faults) or increase (normal faults). The study area largely consists of low angle to sub horizontal deposits with little or no faulting in the offshore region, with no significant signs of deformation within the units. Thus it is considered that further detailed processing to create balanced restored cross sections is not required.

The visualisation of this final product and process steps (e.g. depth converted seismic section) is accomplished by the POSTER application of TECHBASE.

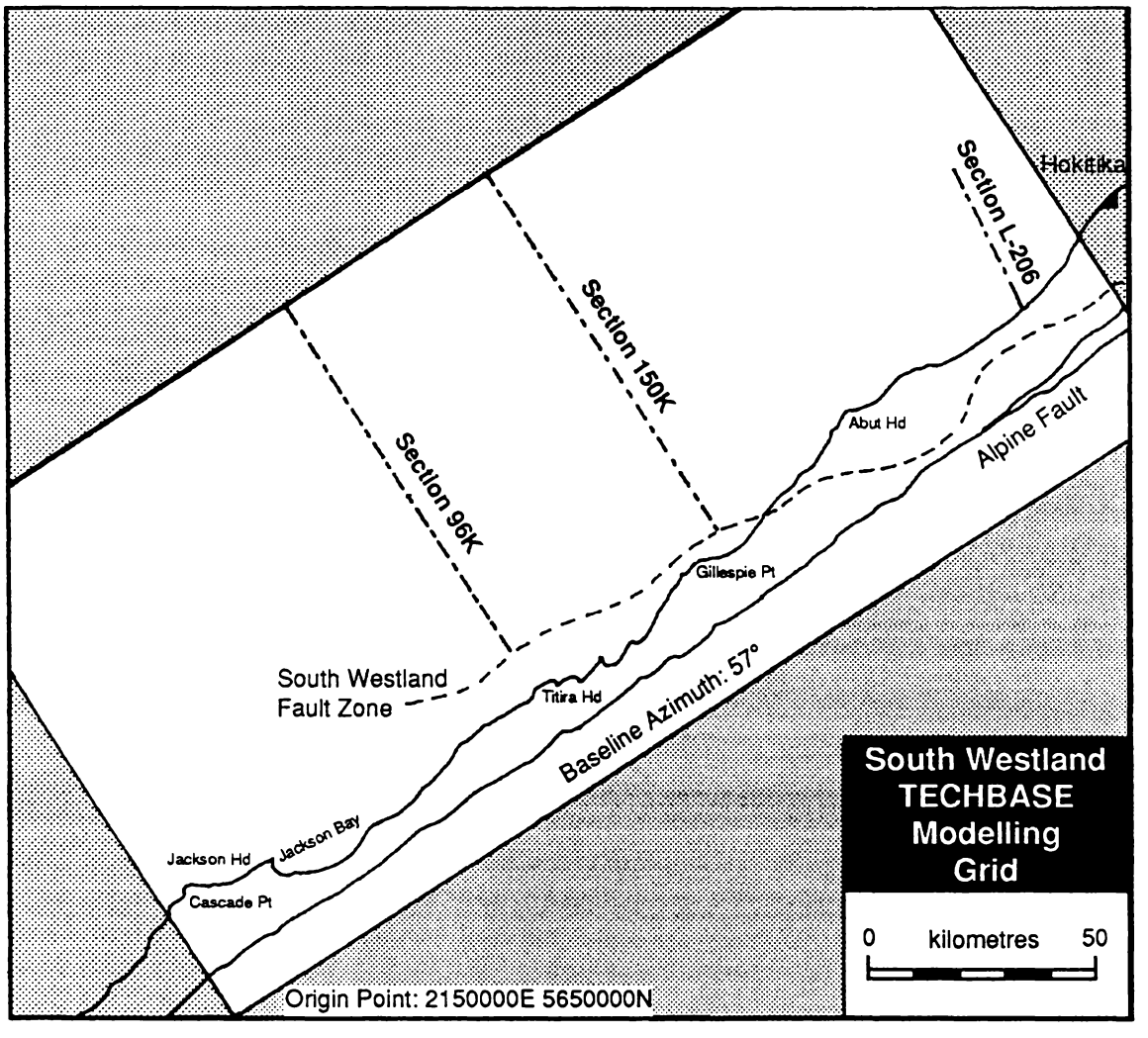

FIGURE 2.20: The TECHBASE modelling grid used in the study of South Westland. Note position of sections extracted for flexural analysis in Chapter 5 and geographic locations discussed in text.

2.4.1.4 *Two dimensional modelling*

Once the data from the individual seismic lines has been entered, it can be modelled across a two dimensional grid to obtain the spatial distribution of a particular variable. In the South Westland database a grid comprising of 2 km square 'cells' was set up. The

dimensions of the grid is 256 km SW-NE by 128 km SW-NE, and is tilted to an azimuth of 57° to lie roughly parallel to the Alpine Fault (Fig. 2.20). The origin of the grid is located at NZMS coordinates 2150000E, 5650000N. The dimensions of the grid were dictated by the algorithms used in the MINQ surface modelling program used to determine the various surfaces mapped in this study. The values of each cell for a particular variable (e.g. basement depth) can be calculated from the inputted seismic data and displayed using contouring and presentation programs (GRIDCONT and POSTER). The entire grid can also be backstripped to obtain tectonic subsidence and decompacted thicknesses by assuming that each cell will behave as an exploration well section.

Chapter 3

Characteristics of Foreland Basins

3.0 Introduction

Foreland basins form as a direct result of the emplacement of a thrust load on a continental margin due to convergent tectonics. Loading causes the lithosphere to flex and create an asymmetric basin, bounded on the cratonic side by a peripheral bulge, with the deepest part of the basin, the proximal foredeep, adjacent to the thrust mass (Fig 3.1; Dickinson, 1974; Beaumont, 1981; Tankard, 1986; Pigram et al., 1989). Foreland basin size is determined by the flexural response of the lithosphere to the loading event and is a function of its rheology and the size of the imposed thrust mass (Stockmal et al., 1986). On a large scale, basin development is controlled principally by the propagation rate of the thrust mass onto the foreland craton which also controls the migration of the peripheral forebulge in front of the thrust front (Tankard, 1986; Sinclair et al., 1991). On a more localised scale stratigraphy is dominantly controlled by a variety of tectonic features (e.g. uplifted thrust fronts and transverse faults) rather than by eustacy as in other sedimentary basin settings (Allen et al., 1986; Swift et al., 1987). Foreland basin deposition is typically characterized by initial accumulation of deep-marine sediments in an early underfilled phase and is followed by the accumulation of shallow-marine to subaerial sediments in a steady-state or overfilled phase (Covey, 1986; Allen & Allen, 1990)

The term 'foreland basin' was formally introduced by Dickinson (1974a), who also proposed two genetic classes (Beaumont, 1981; Allen et al., 1986):

> (1) **peripheral** foreland basins such as the Indo–Gangetic basin, situated against the outer arc of the orogen during continent–continent collision (Fig. 3.1a), and;
>
> (2) **retroarc** foreland basins such as the late Mesozoic–Cenozoic Rocky Mountain basins situated behind a magmatic arc and linked with subduction of the oceanic lithosphere (Fig. 3.1b).

Foreland basins, both modern and ancient, are a common feature around the world. As foreland basins are formed as the result of fold-and-thrust orogenesis, a distribution of such fold-and-thrust belts will generally also display the distribution of foreland basins present on the overthrust craton (Fig 3.2; Rodgers, 1990; 1991).

The classical foreland basin is the North Alpine Foreland Basin (NAFB) of Western Europe. Although there is some debate over the use of the terms 'Molasse' and 'Flysch' to describe sediments in this and other similar basins (Allen et al., 1986), the NAFB remains the classical sedimentological type section for foreland basins. More recently in North America, the Palaeozoic Appalachian foreland basin (Tankard, 1986) and Mesozoic/Cenozoic basins associated with the formation of the Rockie Mountains (e.g.

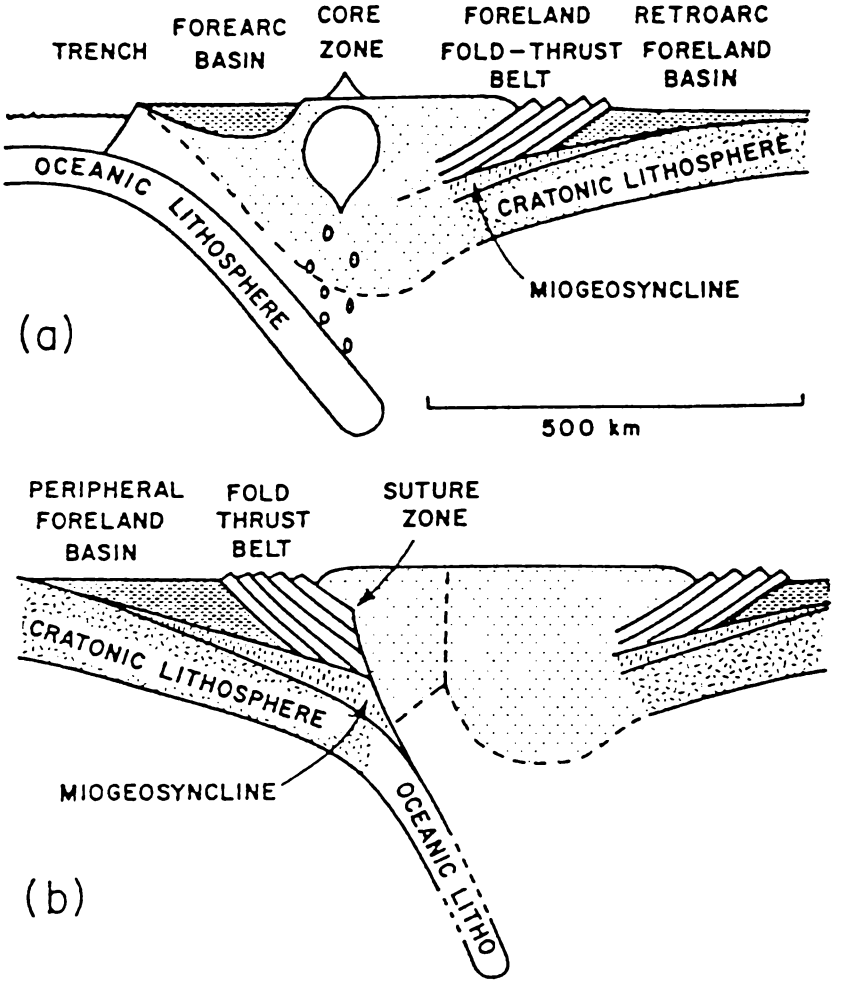

FIGURE 3.1: Systematic illustration of the formation of retroarc and peripheral foreland basins by the flexural bending of cratonic lithosphere. Note that in this example the foreland basin sediments are unconformably deposited over an Atlantic type margin; **(a)** retroarc basin formed next to a Cordilleran-type orogen; **(b)** peripheral basin formed as the result of continental collision. (From Beaumont, 1981)

Beaumont, 1981; Cross, 1986; Cant & Stockmal, 1989) have been intensively investigated, particularly in the use of models to simulate the development of these basins (e.g Stockmal et al., 1986).

As stated by Molnar & Lyon-Caen (1988) the association in both space and time of foredeep basins with neighbouring ranges is inescapable and virtually ensures an origin that couples them. Not only are foreland basins valuable windows into the development of collisional orogens, but many of the major oil fields are found in foreland basin settings, e.g. the Persian Gulf basins (Dickinson, 1974b), the oil fields of the eastern and southeastern United States (Oliver, 1986) and smaller fields such as Taranaki Basin, New Zealand (Stern & Davey, 1990).

FIGURE 3.2: Generalised world-wide distribution of foreland basins. Red indicates Mesozoic/Cenozoic structures; blue indicates Paleozoic structures. European foreland basins: ① Betic; ② Ebro; ③ Aquitaine; ④ North Alpine; ⑤ Appenninic basins; ⑥ Carpathian. (Modified from Rodgers, 1991)

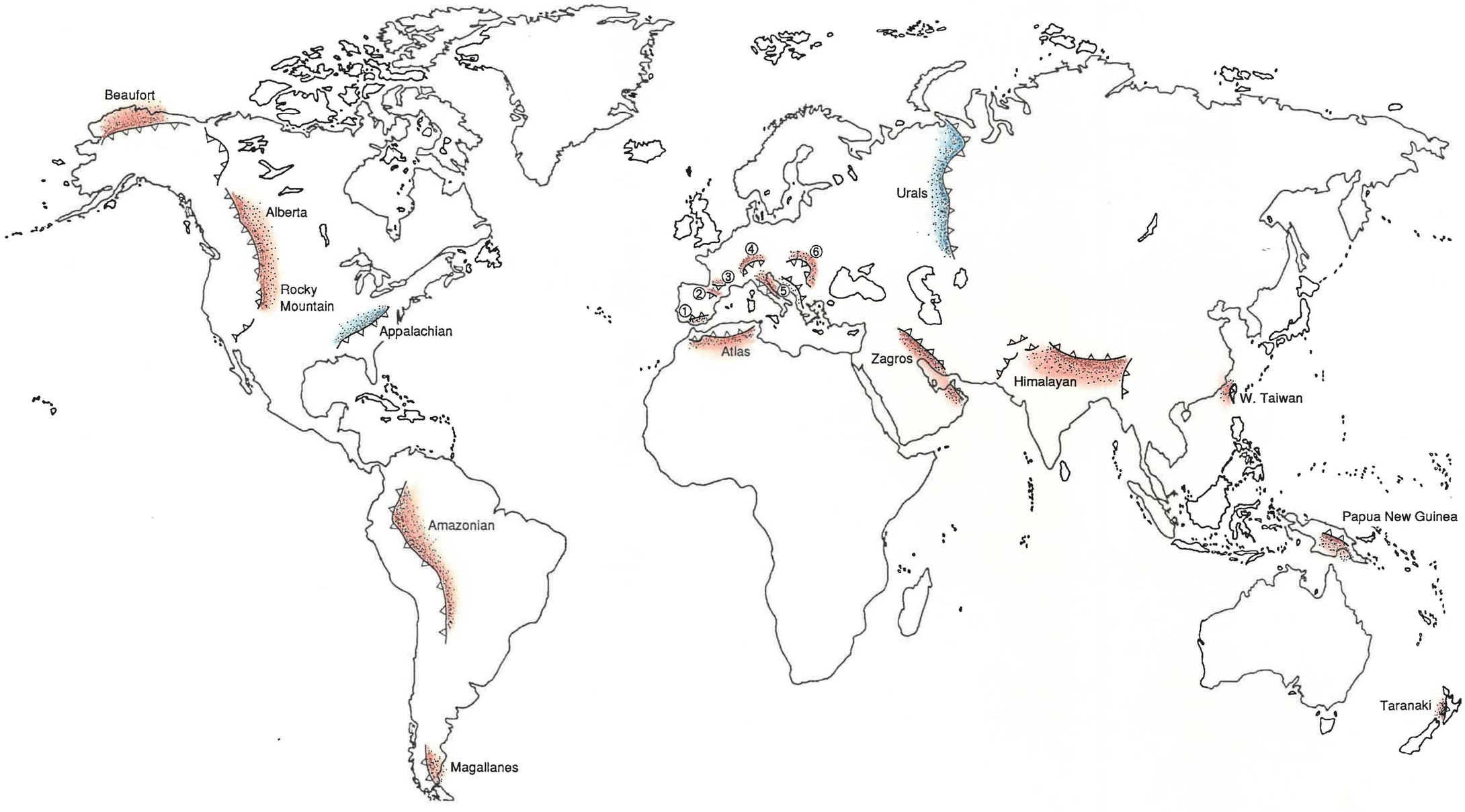

This chapter will outline the lithospheric mechanics, structural controls and deposition styles of foreland basins. An extensive review of current knowledge about foreland basins is included with numerous case studies and examples.

3.1 Geophysical characteristics

3.1.1 Lithospheric behaviour

There has been extensive investigation of the rheological behaviour of the lithosphere supporting a variety of sedimentary basins (e.g. Watts, Karner & Steckler, 1982). Foreland basins were often thought too complex for study in this regard, but recent investigations in this field have contributed to the overall knowledge of lithospheric behaviour.

The supporting lithosphere of a foreland basin can be modelled as a thin, elastic or viscoelastic plate (Fowler, 1990, p.382). In an elastic model the flexural response is a simple function of the emplaced load and rigidity of the lithosphere (Fig. 3.3a). In comparison, a viscoelastic lithosphere also has a similar initial flexure, but the lithosphere relaxes with time (Fig. 3.3b). Both models have been used to explain the features of some foreland basins. For instance, Jordan (1981) used an elastic lithosphere to model the foreland basin in the Rockies, western U.S.A., while Beaumont (1981) used a viscoelastic lithosphere to account for the features of the Alberta basin, Canada.

Kusznir & Karner (1985) emphasised the importance of lithospheric composition and thermal structure in determining its response to loading. An important factor is the thickness of the plate being flexed because this will control the large scale geometry of the foreland basin formed. Generally the characteristic flexural wavelength λ is proportional to the 3/4 power of the thickness of the plate. Thin plates will give rise to narrow, but deep foredeep basins and thick plates will support a wide, but shallow basin (Molnar & Lyon-Caen, 1988).

The rheological characteristics of the lithosphere are determined by the geological events that occur before collision and flexure. Commonly, foreland basins are superimposed on previously thinned continental margins. There are numerous examples and documentation for overthrust passive margins in such diverse locations as the Carboniferous Arkoma basin, south-central U.S.A. (Houseknecht, 1986); the evolution of the Helvetic passive margin of the Alpine Orogen, central Europe (Homewood, Allen & Williams, 1986; Pfiffner, 1986); the deposition of the western Taiwan foreland over the mainland China passive margin (Covey, 1986); and the Neogene evolution of the New Guinea foreland basin over the northern continental margin of Australia (Pigram et al.,

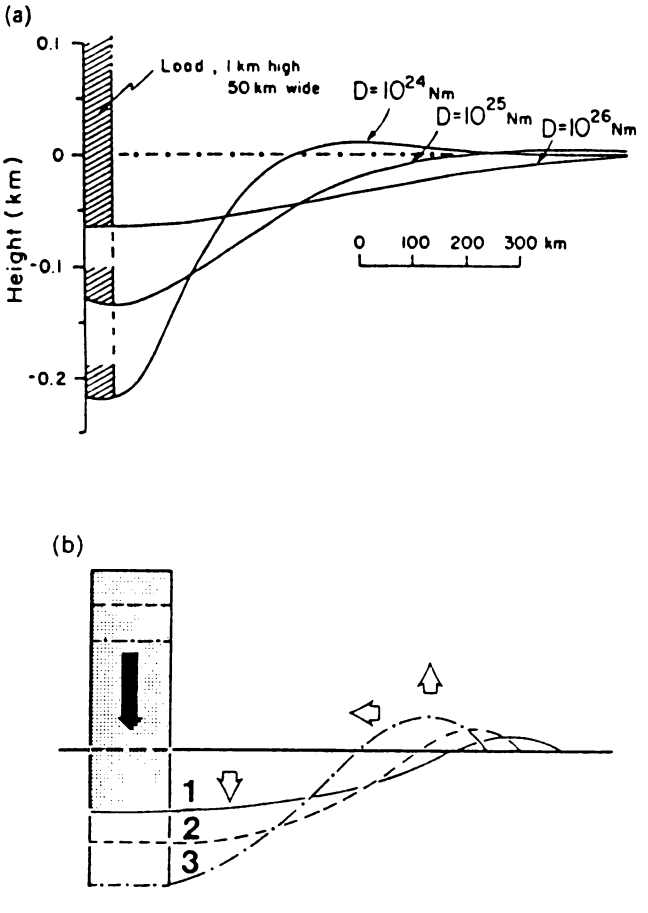

FIGURE 3.3: (a): Cross sections of sedimentary basins formed on an elastic lithosphere due to a 1 km high, 50 km wide two-dimensional load. Load and sediment density are 2.4 × 10^3 kg m^{-3}. The three curves show the difference in basin cross sections for lithosphere with flexural rigidity *D*, of 10^{24}, 10^{25} and 10^{26} Nm. (From Beaumont, 1981; Fowler, 1990) **(b):** Deformation of the surface of a viscoelastic lithosphere by a surface load. The initial deformation is the same for an elastic lithosphere (a). However with time the viscoelastic lithosphere allows the stress to relax; so the deformation evolves to curves 2 and 3. If the load is left in place, the final stage would be local isostatic equilibrium. (From Fowler, 1990)

1989; Abers & Lyon-Caen, 1990; Audley-Charles, 1991; Hill, 1991). Such overthrust rifted passive margins scenarios were modelled by Stockmal, Beaumont & Boutilier (1986).

Foreland basins can also develop over lithosphere other than passive margins. Biddle, Uliana et al. (1986) and Wilson (1991) describe the evolution of a back-arc setting to a foreland basin in the Paleozoic Magallanes basin in southern South America. From this it can be seen that foreland basins vary greatly in the nature of the supporting lithosphere which is a result of previous geological events. Thus care needs to be taken in using broad classifications for describing the variety of foreland basins that occur.

3.1.2 Gravity anomalies

Bouguer anomalies over orogenic belts and associated foreland basins typically show a major gravity 'low' generally displaced towards the foreland from the greatest

topographic relief (Fig 3.4). In some cases an associated gravity 'high' displaced toward the overriding plate is also seen (Karner & Watts, 1983; Allen et al., 1986). This gravity field can be interpreted in terms of lithospheric flexure with the basin sediment mass contributing to the negative Bouguer anomaly (Karner & Watts, 1983).

Often theoretical calculations have shown a discrepancy between the dimensions of the foreland basin and the topographic loads. Karner and Watts (1983) postulated the existence of hidden or subsurface loads, such as density variations in the lithosphere, as an extra driving force for foreland flexure and subsidence. Stockmal et al. (1986) felt that if the foreland plate had previously been extended (as is often the case with overthrusted passive margins) and deep bathymetric conditions existed before collision, then the development of thick overthrust wedges would make the existence of subsurface hidden loads unnecessary.

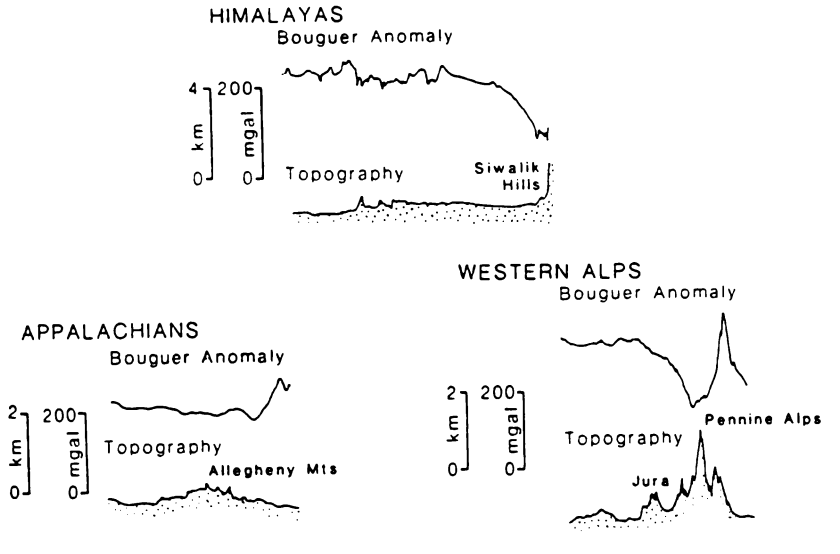

FIGURE 3.4: Gravity profiles across Himalayas, Appalachians and Western Alps, after Karner & Watts (1983). The Alps and Appalachians both show a large asymmetrical negative Bouguer anomaly coupled with a symmetrical positive Bouguer anomaly. The Himalayas lack the gravity 'high'. (From Allen et al., 1986)

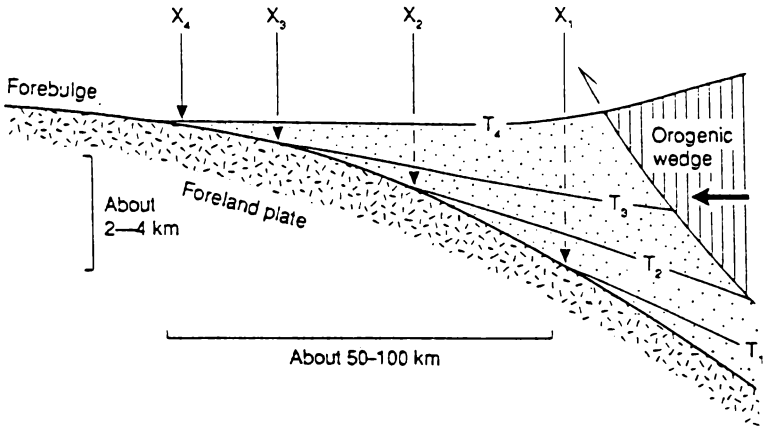

FIGURE 3.5: Diagrammatic illustration of foreland basin stratigraphic pattern of onlap onto the foreland plate. x_1 to x_4 show the successive positions of pinch-outs corresponding to the chronostratigraphic lines t_1 to t_4. (From Allen & Allen, 1990, p.148)

3.2 Structural Control and Stratigraphy

3.2.1 Large scale geometry

On a large scale, foreland basin stratigraphy typically consists of wedge shaped units, thick near the thrust front and pinching out onto the foreland craton. This is a function of increasing subsidence toward the orogenic load. As the orogenic load is inherently mobile, stratigraphic units will tend to be laterally translated ahead of the thrust front. This causes the migration of depocentres and 'feather-edges', producing a characteristic onlap pattern of younger stratigraphic units onto the foreland (Fig 3.5).

Generally there appears to be a strong relationship between load mobility and depocentre migration in foreland basins. In the Molasse basin of western Switzerland, depocentres and pinch-outs of stratigraphic units migrated onto the European craton during the Oligocene-Miocene, corresponding to the main phase of the Alpine orogenesis. Detailed palinspastic restorations allowed the fault tip propagation and shortening rates to be estimated, illustrating a close correspondence between rates of depocentre and pinch-out migration and thrust-related shortening (Homewood, Allen and Williams, 1986).

The flexural or peripheral forebulge in front of the orogenic load migrates coevally with thrust front propagation. The passage of the peripheral forebulge can have a significant stratigraphic effect on basin sediments, as illustrated in a number of examples. Tankard (1986) illustrates the unconformities that formed in the Carboniferous Appalachian foreland basin due to forebulge migration. Sinclair et al. (1991) use a detailed elastic lithospheric model to demonstrate that formation of the prominent Burdigalian (22 Ma)

unconformity in the sediments of the North Alpine Foreland Basin of eastern Switzerland formedas a result of forebulge migration.

The exact details of the evolution of foreland basin stratigraphy with regard to depocentre and pinch-out migration are again dependent on lithospheric behaviour, and in particular whether the foreland plate acts in an elastic or viscoelastic manner. As the orogenic belt moves cratonward, it may be expected that it will load progressively stronger elastic lithosphere (i.e. lithosphere with decreasing passive margin stretching effects). This may result in the foreland basin becoming shallower and wider as the pinch-out migration rate exceeds the thrust-front propagation rate. Conversely, the pinch-out migration rate may slow relative to the mountain front, or the forebulge retreats toward the thrust front, resulting in a narrower basin. Tankard (1986) interprets such an offlapping pattern as a result of stress relaxation in a viscoelastic lithosphere (see Fig 3.3b). Other authors, for example Flemings & Jordan (1989) and Sinclair et al. (1991), have explained how such an effect can be produced by the thickening of the adjacent orogenic wedge loading an elastic plate. In particular Sinclair et al. (1991) used a diffusion equation to model the thrusting, erosion and subsequent sediment loading of the North Alpine foreland basin and concluded that all movement of the forebulge could be simulated by varying the rate of thrust belt propagation and wedge thickening. It was not even necessary to vary the flexural rigidity of the European lithosphere.

Swift et al. (1987) studied the depositional sequences of the Upper Cretaceous Mesaverde Group in Utah and developed a sequence architecture model of shelf sediment progradation in a foreland basin that formed in conjunction with the Late Cretaceous Sevier Orogeny in the western U.S.A. (see Fig 3.6). Although this model may only apply in detail to the area studied, it does clearly illustrate the differences between foreland basin sequences and those of passive margins (Table 3.1).

	Passive Margins (Vail Model)	Foreland Basins (Swift Model)
Dominant Variable Assumed by Investigators	Eustacy	Subsidence
Zone of Most Rapid Shelf Subsidence	Seaward margin	Landward margin
Bounding Surfaces	Subaerial erosional surface, transgressive surface, downlap surface	Downlap surface (= offshore marine erosion surface)
Sequence Components	Early regressive deposits (low stand delta), Estuarine valley fills, transgressive (onlapping) deposits, late regressive (downlapping) deposits	Transgressive deposits (toward load margin, minor) Regressive deposits

TABLE 3.1: Comparison of Depositional sequences between Passive Margins and foreland basins. (From Swift et al., 1987)

3.2.2 Foreland basin structures

As the foreland basin evolves and the thrust load moves further onto the craton, it is inevitable that the sediments of the foredeep itself will become involved in deformation. The extent of this deformation is controlled by a number of factors such as thrust tip propagation, presence of subsurface easy-slip horizons underlying the basin, and the angle of convergence.

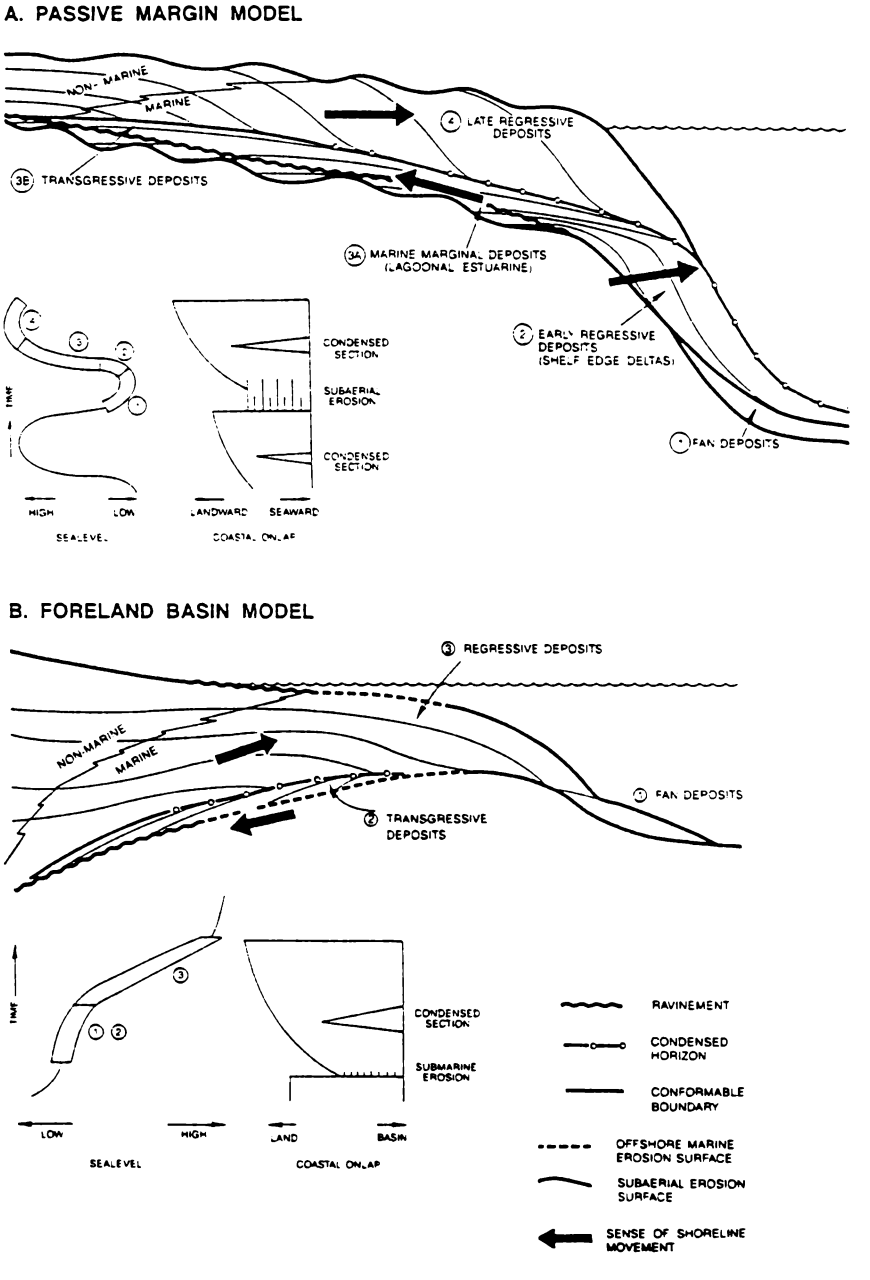

FIG 3.6: Comparison of sequence architecture on passive margins with sequence architecture in the Cretaceous Western interior. **(a)** Passive margin model based on the Vail seismic sequence stratigraphy models. **(b)** Foreland Basin model based on the Utah study area. (From Swift et al. ,1987)

From these, a variety of foreland basin structural styles may develop, with two particular common styles (Allen et al., 1986). A basin actively accumulating sediments in front of the thrust system can be described as a toe-trough or foredeep *sensu stricto* (Fig. 3.7a).

Where deformation has progressed under the basin so that it rests on moving thrust sheets it is termed a thrust-sheet-top or piggy-back basin (Ori & Friend, 1984) (Fig 3.7d). Such an example of the evolution of a thrust-top basin from a foredeep trough can be seen in the Hellenide thrust front of Western Greece (Clews, 1989). Homewood et al. (1986) describe the Molasse basin of Switzerland as containing both styles; the eastern section of the basin shows depocentre migration in front of the thrust belt. In comparison the western and central sections of the basin, a thick sequence of Triassic salt in the subsurface has made the décollement of the strata underlying the basin possible with the subsequent formation of a piggy-back basin. The two styles of basin may even be coupled with synchronised depositional events, such as in the Apenninic chain (Lucchi, 1986) where foredeep basins ahead of the thrust front are coupled with piggy-back basins on top of the thrust sheets. Lucchi (1986) also attempts to schematize the variety of foreland geometries (Fig 3.7).

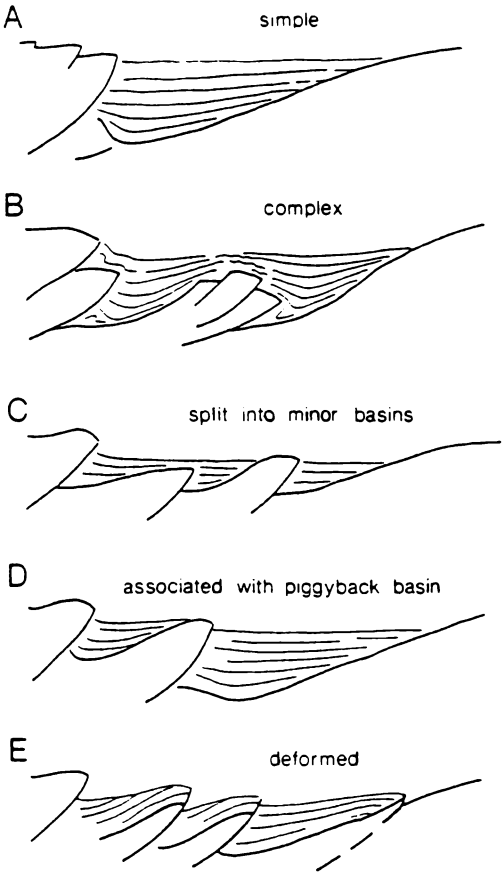

FIGURE 3.7: Systematic diagrams illustrating different foredeep profiles as suggested by seismic records. (From Lucchi, 1986)

3.2.3 Tectonic controls

Tectonism is a major factor in sediment dispersal in any sedimentary basin. Allen et al. (1986) summarise the tectonic sedimentation controls and resultant depositional patterns found in foreland basins:

- uplifted thrust fronts;
- transverse faults, and;
- inversion of previous structures.

Uplifted thrust fronts may act as barriers to basinward sediment transport rather than provide sediment sources. This is clearly seen in the southern Pyrennes where large fluvial systems developed at structural lows in the uplifted basin margin, and smaller alluvial fans formed alongside the higher parts of the thrust front (Hirst & Nichols, 1986; Nichols, 1989; Zoetemeijer et al., 1990). In a subaqueous environment, the steepening of submarine slopes caused by the shortening of the orogenic wedge may encourage the inception of slides, slumps and other gravity flows (Allen et al., 1986). The tectonic mechanisms of uplift within the orogenic belt have also been studied as a contributing factor in the provenance of sediments, particularly distinguishable coarser deposits. Schmitt & Steidtmann (1990) discussed the exhumation and erosion of older units in interior ramp-supported uplifts. In this structure, an older, inactive thrust sheet is part of the upper plate of a younger, active thrust and is transported over a ramp in the younger thrust, thus uplifting it and establishing it as a sediment source area of particularly coarse 'syntectonic' detritus. Further details of the provenance of foreland basin sediments will be discussed below.

Transverse faults cutting across the thrust system and/or foreland basin can have a noted effect on localised sediment deposition. Striking obliquely to the thrust faults, a transverse fault may form a sediment conduit into the foreland basin. Massari, Grandesso et al. (1986) show a good example in the Venetian basin, north Italy (Fig 3.8) where a structural depression through a rising thrust sheet is created by transtensile motion on transverse faults. This then acted as a local connection between the piggy-back basin behind the thrust front and its associated foredeep in front. The evolution of the Venetian basin is also notable for the oblique convergence of the crustal blocks involved. It is regarded that the oblique convergence was accommodated by wrenching along a set of conjugate strike-slip faults (Massari et al., 1986, p.163)—thus forming the structures that act as sediment conduits.

Within the foreland basin itself, transverse faults may be responsible for the prominent localised variations of sediment thicknesses within the basin. Lucchi (1986) and

Homewood et al. (1986) both discuss the influence of these features in controlling sediment distribution in the Appeninic and Molasse foreland basins respectively. DeCelles (1986) describes the diversity of sedimentological and stratigraphic features that have formed as a result of the 'tectonic partitioning' by intra-foreland structures and plutonism in the Lower Cretaceous Kootenai Formation of the Sevier foreland basin in southwestern Montana. A similar theme of tectonic partitioning being a factor in sediment (particularly sand) deposition in a non-marine foredeep is also discussed for the Amazonian foreland basin, South America (DeCelles & Hertel, 1989).

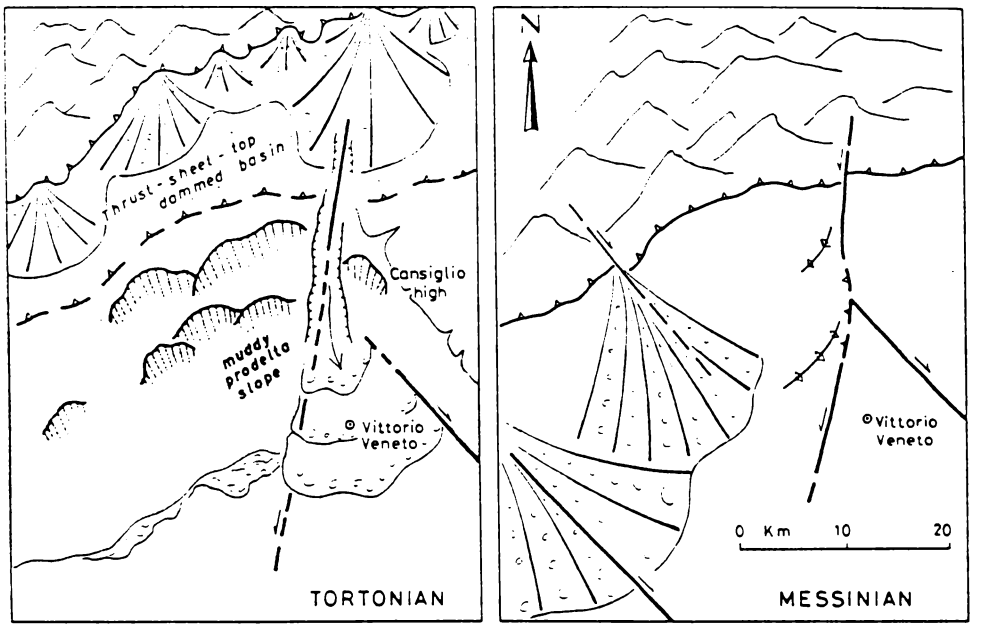

FIGURE 3.8: Sedimentary model for the Vittorio Venato area, Venetian Basin, north Italy in Tortonian (11.2–6.5 Ma) and Messinian time (6.5–5.3 Ma) This model illustrates the local importance of transverse fault-controlled depressions acting as sediment conduits, in this example linking a piggy-back basin and foredeep basin. The structural depression formed as a result of transtensile movement along a conjugate couple of transverse faults. Subsequent Messianian deformation resulted in the gradual occulusion of this preferential pathway (From Massari et al., 1986)

The inversion or rejuvenation of pre-existing extensional faults in a compressional foreland basin setting is as yet a poorly documented field. One difficulty is determining the boundary between 'typical' inversion tectonics and the 'fold-and-thrust' tectonics within an orogenic belt (de Graciansky et al., 1989, p.101). The mild inversion of the Valensole foreland 'molasse' basin on the margin of the Western Alps, France, shows inverted structures that compare well with those observed in 'traditional' north European inverted basins, such as in the North Sea (de Graciansky et al., 1989). Butler (1989) discusses the influence of pre-existing extensional basin structure on thrust system evolution in the Western Alps, Europe. He draws the conclusion that although pre-existing normal faults may be reactivated as reverse thrust faults, not all reverse thrust faults are necessarily

reactivated normal faults. The nature of pre-exisiting basin structures may strongly influence the style of thrust deformation, e.g. the ease of cover/basement detachment and thrust front steepness, and thus indirectly affect the evolution of the foreland basin. Butler also briefly comments on the possibility of normal fault reactivation in response to uplift on the 'outer flexural high' or forebulge. This is another example of how the pre-existing structure of the supporting lithosphere will have a marked influence on the nature of lithospheric flexure.

3.3 Sedimentology

In an idealised foreland basin sequence, the oldest deposits are commonly dominated by fine-grained, often turbiditic sediments which were deposited over the cratonic passive margin classical 'miogeosyncline' sediments. As the thrust load encroaches upon the craton and the foreland basin evolves, the sediments tend to become shallow-water or continental coarser classical 'Molasse' sediments.

Allen & Allen (1990) give a lucid illustration of a typical foreland basin megasequence from the North Alpine Foreland Basin (NAFB):

> ⑦ **Upper Freshwater Molasse**, the final choking of the NAFB by coarse continental clastics.
>
> ⑥ **Upper Marine Molasse**, representing shallow marine and estuarine depositional systems.
>
> ⑤ **Lower Freshwater Molasse**, the first fluviatile and lacustrine deposits of NAFB.
>
> ④ **Lower Marine Molasse**, the transition from shelf to shoreline sedimentation.
>
> ③ **North Helvetic** units representing turbiditic depositional systems shed from the active orogenic wedge.
>
> ② **Nummulitic limestones** and **Globigerina shales** representing foreland drowning.
>
> ① **Basal unconformity** due to regional uplift of the foreland lithosphere.

In summary, this stratigraphic section is comprised of a basal foreland collapse sequence (①), followed by two shallowing-upwards megasequences (③–⑤ and ⑥–⑦). Cant & Stockmal (1989) provide a useful summary of an idealised foreland basin sequence using the Alberta Basin as a model in terms with terrane accretion that has wide application in the interpretation of other foreland basin megasequences (Fig 3.9). In this model as the allocthonous overthrust wedge is loaded upon the earlier passive margin a forebulge migrates ahead of the thrust front. As the predominantly shallow-water passive margin or miogeosynclinal sediments are uplifted over this bulge a basal unconformity is cut (Fig. 3.9a, NAFB stratigraphic unit ①). The topography created by the overthrust wedge is

largely submarine at this stage due to the depth of water over the continental slope and the downwarping of the supporting and possibly previously weakened lithosphere. Combined with the flexural bulge having only a low amplitude of usually less than 350 m, little sediment is shed into the rapidly deepening foreland basin. Thus deep-water conditions prevail as in Fig 3.9b. In the classical Alpine foredeep, this corresponds to the Flysch, the syndeformational turbidite facies (NAFB stratigraphic units ②–③). As the collision continues, accretion and tectonic thickening of the overthrust wedge creates significant topography above sea level, resulting in an increased sedimentation rate and filling the foredeep to sea level and above (Fig 3.9c).

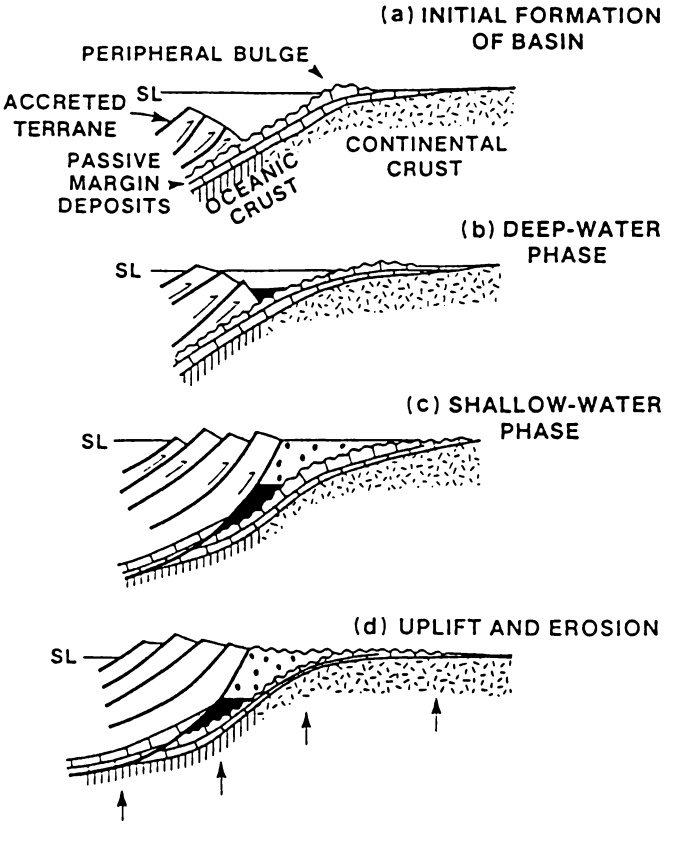

FIG. 3.9: Idealized model of terrane accretion and adjacent foreland basin development. Figure is schematic and not to scale. Forebulge amplitude greatly exaggerated for clarity. **(a)** Initial accretion onto the continental slope cause depression of the passive margin and migration of a flexural bulge. As passive margin sediments are uplifted across this bulge a basal unconformity is cut. Little sediment is shed into the basin due to low elevation of possible source areas. **(b)** Low sedimentation rates combined with rapid flexural subsidence results in early deep-water conditions in the basin. **(c)** Continued thrusting causes topographic uplift and subsequent high rates of sedimentation and the foredeep fills to or above sea level with shallow-water molasse. **(d)** With cessation of thrusting, erosion across the orogen reduces the lithospheric load and the basin 'rebounds' with epeirogenic uplift causing an upper regional unconformity. (From Cant & Stockmal, 1989)

This stage corresponds to the classical Molasse, the syn- to post-deformational shallow-marine to non-marine sediment facies (NAFB stratigraphic units ④–⑤ and again at ⑥–⑦). The final stage in the idealised terrane accretion/foreland basin evolution is shown in Fig. 3.9d. As convergence ceases, the thrusting and loading of the foreland plate also ceases. In the viscoelastic model of the lithosphere, the peripheral bulge retreats as bending stresses relax. The orogenic belt is eroded and the load diminishes, resulting in a regional uplift or 'rebound'. This causes the formation of a regional unconformity at the top of the foredeep megasequence.

The deep to shallow progression of foredeep sediments can also be described in terms of amount of basin fill. The early deep-marine dominated phase may also be described as the *underfilled* stage of the foreland basin. As a mountain belt grows, it can reach a steady state where rapid erosion counterbalances the uplift and the basin is *overfilled* by detritus. Covey (1986) described such an evolution in the Plio–Pliestocene western Taiwan foreland basin, and also demonstrated excess sediment may be removed by fluvial and/or shallow marine processes to maintain a *steady-state* basin profile. In some cases prograding sediments may even overwhelm the peripheral bulge as in the Appalachians (Tankard, 1986; Allen & Allen, 1990, p.155) or in the Sevier foreland basin where sediment input outran the creation of accommodation space in the subsiding basin (Swift et al., 1987).

As well as having significant stratigraphic effects the migration and possible retreat of the peripheral forebulge can also be seen in sedimentological evidence. One Paleozoic example is in the Oslo region of Norway, here a slowly migrating peripheral bulge in front of an early Silurian foreland basin was a major control, along with eustatic sea-level changes, on the bathymetry of deposited sediments and associated palaeocommunities (Baarli, 1990). In the Carboniferous Appalachians, the initial migration of the forebulge had sufficient amplitude to allow the subaerial formation of karst features in the uplifted passive margin sediments (Tankard, 1986; Allen & Allen, 1990).

Retroarc foreland basins such as the western North American foreland basins and a series of basins east of the Andes (e.g. the Magallanes basin of southern Argentina) do not fundamentally differ from the peripheral foreland basins. Their primary distinguishing characteristic is that have often evolved from areas of back-arc spreading, and the sediment fill composition reflects the large amounts of plutonic and volcanic rocks in the loading orogenic belt (Allen & Allen, 1990, p.250)

3.4 Subsidence History

The subsidence histories of foreland basins is not as well documented as those of other sedimentary basins where typically initial rapid fault-controlled subsidence is followed by gradually decreasing subsidence due to thermal cooling and sediment loading. Jordan (1981) studied the Idaho–Wyoming foreland basin and Beaumont (1981) modelled the Alberta foreland basin, Canada. Kominz & Bond (1986) analysed the Denver, Green River and Alberta basins to develop a thermal model of foreland basin subsidence.

The results from these and other studies indicate that foreland basins have some distinct subsidence characteristics as well as similarities with other sedimentary basins styles. Kominz & Bond (1986) concluded that the apparent viscosity of the lithosphere and thus magnitude of subsidence diminishes with distance from the load (the orogen). They also summarized the relatively gradual onset followed by increasing foreland basin subsidence giving a convex-up accelerating subsidence curve (Fig. 3.10a). This feature was further illustrated by Cross (1986) for the Hoback Basin of Montana (Fig. 3.10b). However, the rapid subsidence of the central Utah portion of the Sevier fold and thrust belt (Fig. 3.10c; Cross, 1986) indicates that this is not a universal feature of foreland basin subsidence.

Allen et al. (1986) compared the decompacted subsidence curves from the north Alpine Molasse basins with extensional fault-controlled subsidence curves from the North Sea. They found that there was an order of magnitude difference in subsidence rates between the two styles of basin formation. Further analysis suggested that some foreland basins may be confused with the initial extensional subsidence of highly attenuated continental lithosphere, but not with the longer period of thermal contraction that follows in an extensional regime.

3.5 Petrography

Sandstone framework mineralogy primarily reflects tectonic setting and provenance terranes (Schwab, 1986). In this context, numerous studies have been done to identify and petrographically describe the sedimentological suites of foreland basins in comparison to similar data in other depositional settings (e.g. Dickinson & Suczek, 1979; Dickinson et al., 1983). Consolidating on previous studies, Schwab (1986) discussed four main aspects of the sedimentary 'signatures' of foreland basin assemblages:

- The compositional distinctiveness of sand-sized detritus;
- Provenance mineral suite variations;
- Bulk chemical composition, and;
- Sediment accumulation rate.

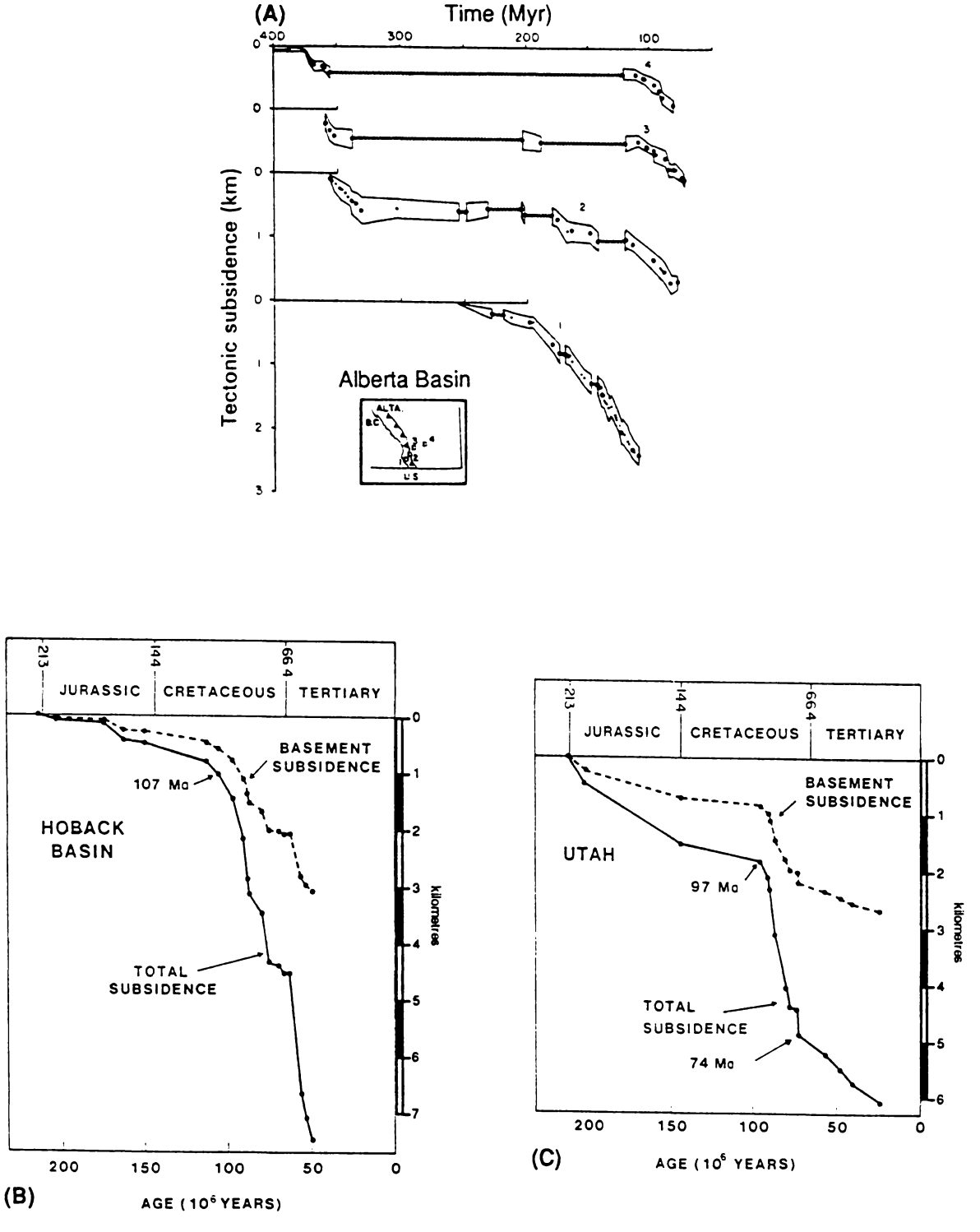

FIGURE 3.10: Tectonic subsidence curves from three foreland basins of North America. **(a)** Alberta Basin (From Kominz & Bond, 1986); **(b)** Hoback Basin and; **(c)** Utah (From Cross, 1986)

Source terranes can be grouped into three fundamental provenance types of *Continental block, Magmatic arc* and *Recycled orogen* (Fig 3.8; Dickinson & Suczek, 1979). Foreland basin sand detritus almost invariable fall within the Recycled orogen provenance with

sediment sources mainly uplifted and deformed sedimentary and metasedimentary rocks. Due to the variety of convergent tectonic settings, the Recycled orogen provenance can be further divided into a variety of sediment sources. These variations include (Dickinson, 1984, *in* Schwab, 1986):

(I) *Backarc thrustbelt sources* — the classical provenance for foreland basins — composed predominantly of continental sedimentary and metasedimenatry strata located immediately adjacent to the overridden foreland basin. These sands exhibit low feldspar and volcanic rock fragment percentages while being richer in quartz and sedimentary rock fragments.

(II) *Uplifted supracrustal sources* provide sand that varies in composition reflecting the nature of the source, e.g. chert-rich subduction complexes floored by oceanic crust.

(III) *Intercontinental collision orogens* or 'suture belts' are typically composed of uplifted and juxtaposed continental and oceanic sediments that are commonly drained by longitudional dispersal systems that deposit sediments into remnant ocean basins. Some sediments may also be shed into flanking peripheral foreland basins.

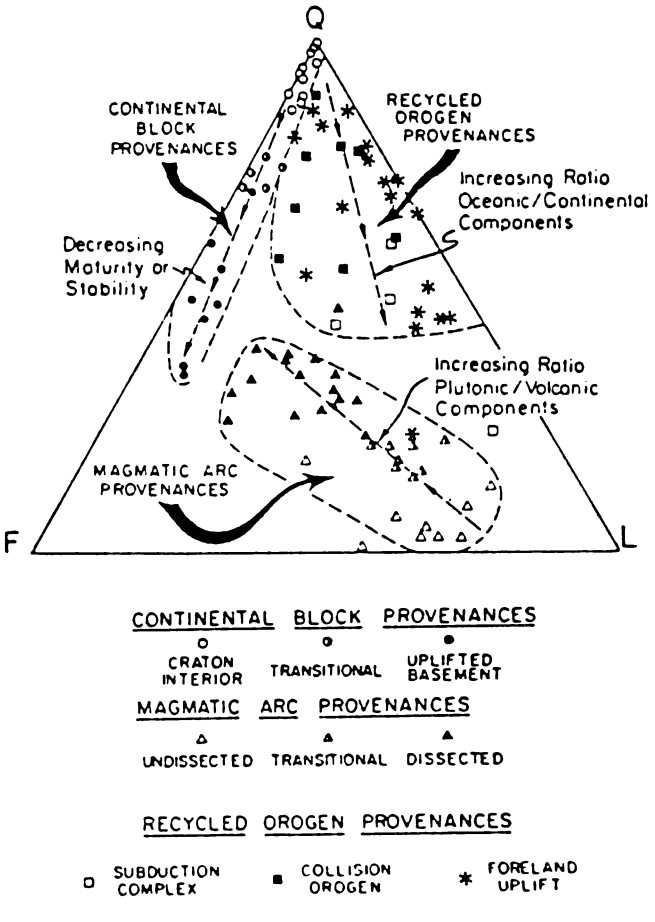

FIGURE 3.11: Triangular QFL (Quartz, Feldspar, Lithics) showing the three main provenance area fields (From Dickinson & Suzcek, 1979)

The provenance analysis of sands from rivers in the eastern Peruvian and Bolivian portions of the Amazonian Foreland Basin support the Recycled Orogen provenance model of Dickinson & Suzcek (1979) (DeCelles & Hertel, 1989)

Generally it can be seen that although the mineralogy framework of foreland basin sediments falls within the broad grouping of Recycled orogen, more detailed information reveals a great variety of sedimentary provenance within orogens. Schwab (1986) examined the detrital sandstone modes of a variety of foreland basins (Appalachian, Western Wyoming and French/Italian Alps) to broadly describe the provenance evolution of those basins. Such an analysis indicates a crude shift from initial continental block sources to recycled orogen sources. Attempts to refine this mineralogy technique to reveal greater details of provenance variations in the sedimentary record have failed to accurately indicate such events (Schwab, 1986).

Schwab (1986) briefly comments on the bulk chemistry of foreland basins as curiously most closely resembling the bulk chemistry of ancient eugeosynclines with moderately high amounts of SiO_2. Finally, the 'average' sediment accumulation rate calculated from a number of sampled foreland basins reveals that those rates were among the highest for all sedimentary basin types at 0.186 m/1000 yr with foredeep flysch sedimentation rates reaching up to 0.927 m/1000 yr. (Schwab, 1986).

3.6 Discussion

Foreland basins are a distinctive sedimentary basin type, formed as a flexural response of a continental lithospheric plate to an overthrust emplaced load. The details of the flexural response is dependant on the thickness, rheology and thermal composition of the lithosphere. These characteristics are in turn determined by geological events that occurred prior to the collisional event. Foreland basins occur both in peripheral and retro-arc settings (Fig 3.1). Geophysically, foreland basins may have a distinctive gravity signature with a displaced gravity 'low' toward the foreland (Fig 3.4).

On a large scale the geometry of a foreland basin is an elongate wedge-shaped basin with the sequences thickest nearest the thrust front thinning out onto the peripheral bulge on the foreland. The stratigraphy of foreland basins is dominated by the mobility and size of the orogenic load. The initial loading of the foreland results in the outward migration of the peripheral bulge which cuts a prominent unconformity in the pre-existing passive margin or miogeosynclinal sediments. The initial rapid subsidence of the foredeep causes an underfilled phase of deep-marine sediments in the basin, typically turbiditic 'Flysch' deposits. As the thrust load moves cratonward and thickens the sediments progress

upward to shallow marine or even subaerial environments as the basin reaches an overfilled or steady state with 'Molasse' deposits (Fig 3.9)

Within the foreland basin structures are dominated by tectonism with such features as uplift thrust fronts and transverse faults controlling localised deposition (e.g. Fig 3.8). Overall deformation of the basin and the resulting distribution of depocentres is a function of thrust tip propagation rates, presence of easy-slip subsurface horizons and angle of convergence. The formation of piggy-back or thrust top basins above thrust sheets is a notable deformation phenomena in foreland basins (Fig 3.7).

The subsidence histories of foreland basins are distinctive for rapid, accelerating exponential growth curves that are only comparable to subsidence in highly attenuated rift situations.

The provenance studies of foreland basin sediments provide a useful, but broad guide to the origin and evolution of the basin sediment fill. Due to their tectonic setting, the sediments of foreland basins generally fall within the Recycled Orogen provenance of Dickinson & Suzcek (1979). Further analysis has revealed that sediment accumulation rates within foreland basins are among the highest of all sedimentary basin types.

Finally, the evidence from previous studies in South Westland resembles some of the stratigraphic and sedimentological characteristics of foreland basins discussed above, strongly suggesting the existence of a retro-arc foreland basin with an inverted southeastern margin in southern Westland.

Chapter 4

Application and Observations of Basin Analysis in South Westland

4.0 Introduction

The basin analysis techniques described in Chapter 2 are applied to the South Westland study area in this chapter. A number of data sources are available for the basin analysis procedures. Predominant among these is 1715 km of seismic reflection profiles. However the accurate interpretation of these lines is dependent upon information from the three petroleum exploration wells in the area, and in particular the more recent offshore well at Mikonui-1, which has been analysed in greater detail than the earlier onshore wells at Harihari-1 and Waiho-1.

This chapter will first look at the stratigraphy of the exploration wells and analyse this information through geohistory analysis. A link will then be made between the well data and seismic data with the use of a synthetic seismogram in Mikonui-1. Observations from the seismic data will be described in detail relating to mapped seismic horizons, faults and other features seen. Finally data from the exploration wells and seismic sections will be examined in a geodynamic modelling framework.

4.1 Well stratigraphy

4.1.1 Well locations

Three petroleum exploration wells have been drilled in the study area to follow up promising leads in seismic, geophysical and geological data. The location of these wells and other details are illustrated and listed below:

Name:	Harihari-1
Operator:	New Zealand Petroleum Co. Ltd.
Year:	1971
Petroleum Report:	PR 528
NZMS Grid Coords.:	2303985E, 5785272N
Longitude:	43° 06' 45.6" S
Latitude:	170° 28' 19.3" E
Elevation:	31 m
Total Depth:	2528 m
Status:	Dry and abandoned.

Name:	Waiho-1
Operator:	New Zealand Petroleum Co. Ltd.
Year:	1972
Petroleum Report:	PR 529
NZMS Grid Coords.:	2269887E, 5762903N
Longitude:	43° 18' 16.68" S
Latitude:	170° 02' 23.27" E
Elevation:	3 m
Total Depth:	3750 m
Status:	Dry and abandoned.

Name:	Mikonui-1
Operator:	Diamond Shamrock Oil Co. (NZ) Ltd.
Year:	1981
Petroleum Report:	PR 836
NZMS Grid Coords.:	2276160.3E, 5831701.6N
Longitude:	42° 41' 16.05" S
Latitude:	170° 08' 45.85" E
Elevation:	181 m (below sea level)
Total Depth:	1846 m
Status:	Dry and abandoned.

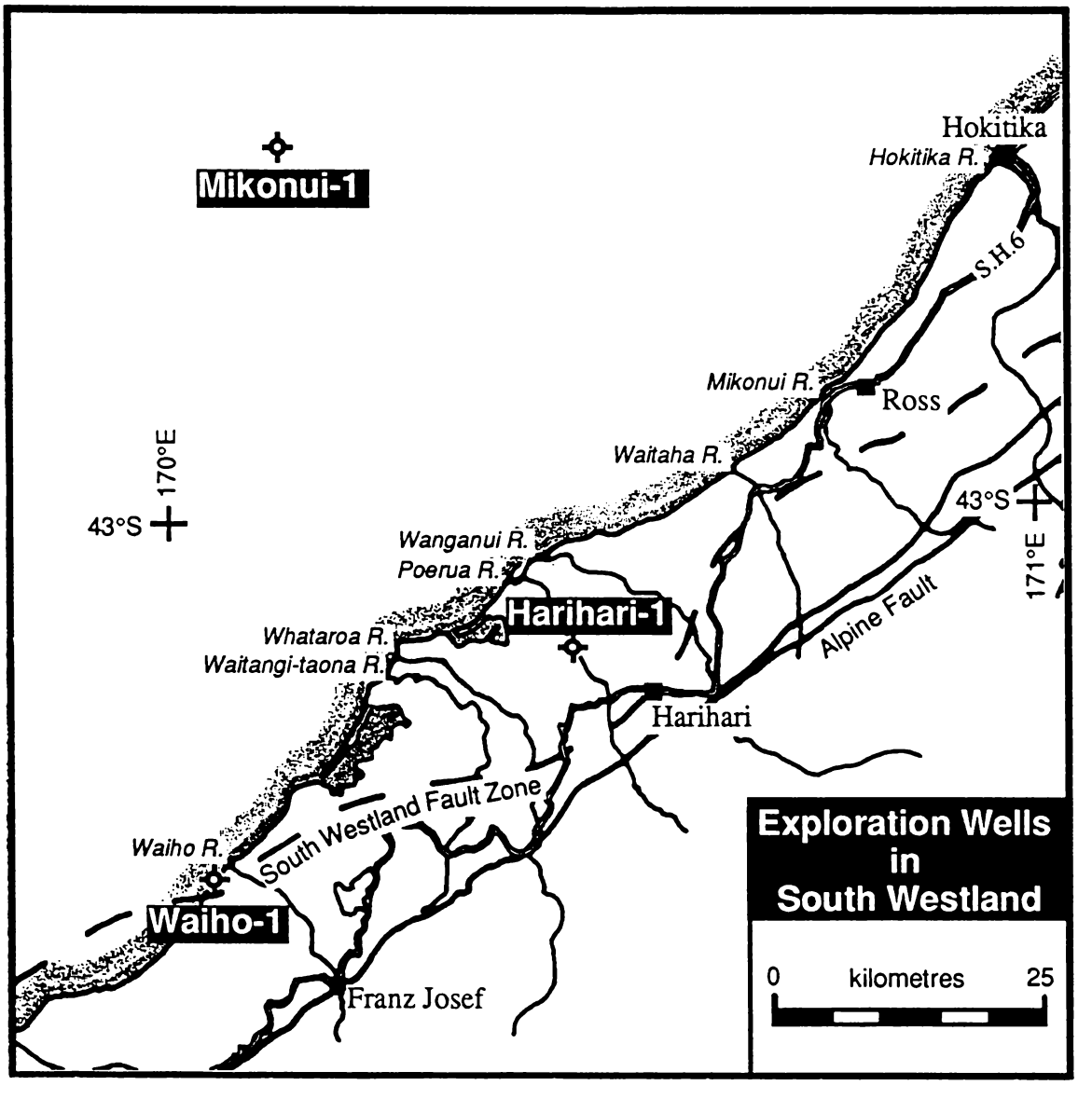

FIGURE 4.1: Location of exploration wells in South Westland.

Two of these wells (Harihari-1 and Waiho-1) were drilled onshore to investigate a thick Tertiary sequence closing against a major sub-surface fault delineated from land seismic surveys. The third, Mikonui-1, was drilled offshore to investigate coal measures pinching out against a basement high. All three exploration wells in the study have been subject to

varying intensities of geophysical survey methods, e.g. dip-meter, resistivity, gamma ray-neutron, etc. However, the records of the two earlier wells (Harihari-1 and Waiho-1) appear undetailed in presentation.

4.1.2 Lithostratigraphy and biostratigraphy

The lithostratigraphy of the three wells is generally quite detailed in its well-site descriptions, and some limited lab analysis of core samples has been undertaken. Broadly speaking, all three wells are dominated by mudstone deposits, with varying amounts of coarser material, underlain by a basal limestone and thin coal measures unit. Reconnaissance biostratigraphic control with foraminifera and basement rock reports were undertaken by the New Zealand Geological Survey. The biostratigraphy has been used to constrain ages and depositional paleodepths of the sediments. These reports are included in the open file Petroleum Records and their records have been briefly checked with contemporary micropaleontology literature (e.g. Hornibrook et al., 1989). No significant changes (e.g. ages/depths) in the report conclusions have been required.

A regional correlation of the three wells is shown in Figure 4.2.

4.1.2.1 *Mikonui-1*

Mikonui-1 is the only exploration well in the offshore region of the South Westland basin drilled by Diamond Shamrock Oil Company (1981). As such it contains vital information about the lithostratigraphy and biostratigraphy of the basin. Dip meter measurements confirmed seismic predictions of low-dip regional trends. Extensive airgun surveying of the well was undertaken. The results of this are discussed and analysed below in Section 4.1.4.

The drilled section can be divided into six parts:

(1) **1841–1810** metres. *A basement complex with thin detrital zone.*
Basement rocks are tentatively identified as quartz-mica schists correlated with the Early Paleozoic Greenland Group. Overlying the basement was a rubble zone of reworked or highly weathered schists approximately 9 m in thickness.

(2) **1810–1675** metres. *Paleogene "Coal Measures"*
Deposited upon the basement complex are the Mata through Eocene (80.0–42.5 Ma) "Coal Measures". The Coal Measures consist of unconsolidated sands with minor traces of coal grading upwards to claystones. Biostratigraphic analysis suggests that the Kaiatan and Runangan stages are absent, as well as a basal section of the Landon Series (42 Ma–34? Ma).
Depositional environment: Marginal marine to non-marine. 0–20 m.

(3) **1675–1640** metres. *Oligocene limestone.*

Limestone is described as soft micritic to firm cryptocrystalline. Biostratigraphy indicates an Whaingaroan to Waitakian age (32 – 22 Ma), with the Duntroonian not being identified. The limestone is tentatively correlated to the regionally extensive Cobden Limestone to the north, and the Awarua Limestone to the south.

Depositional environment: Outer shelf to upper bathyal depths. 200–500 m.

(4) **1640–1510** metres. *Southland Series mudstone.*

Unconformably overlying the limestone are Miocene-Pliocene blue-grey claystones with interbedded thin sand lenses near the base of the interval. Biostratigraphy indicates that the Southland series (16.5 Ma–10.5 Ma) is largely present, but this is bounded above and below by significant hiatuses. Below, no evidence is seen for the presence of the Altonian and Otaian stages (Pareora Series, 22.0–16.5 Ma). Above, a key taxon (*Bolvinita*) for the Tongaporutuan Stage (10.5–6.0 Ma) is absent. This absence suggests a hiatus of at least the mid to late Tongaporutuan and early Kapitean.

Depositional environment: Benthic taxa indicate deep water deposition (500–1000 m).

(5) **1510–340** metres. *Late Taranaki and Wanganui Series sediments.*

Deposited upon the Southland Series mudstones are more blue-grey claystones, tentatively correlated with the Blue Bottom Group, followed by bioclastics with minor slits and clays. Biostratigraphy appears to indicate continuous deposition from the upper Kapitean through Wanganui Series (5.0 Ma onwards). The bioclastics near the top of the recovered section were determined to be of Castlecliffian age (1.2 Ma–0.4 Ma). No returns were recovered from the upper 165 m as drill cuttings went directly to the seafloor.

Depositional environment: Open marine conditions at outer shelf to bathyal depths (200–500 m). A mixture of deep and shallow water Mollusca in the top bioclastic section suggests an alternation of water depth through this time interval.

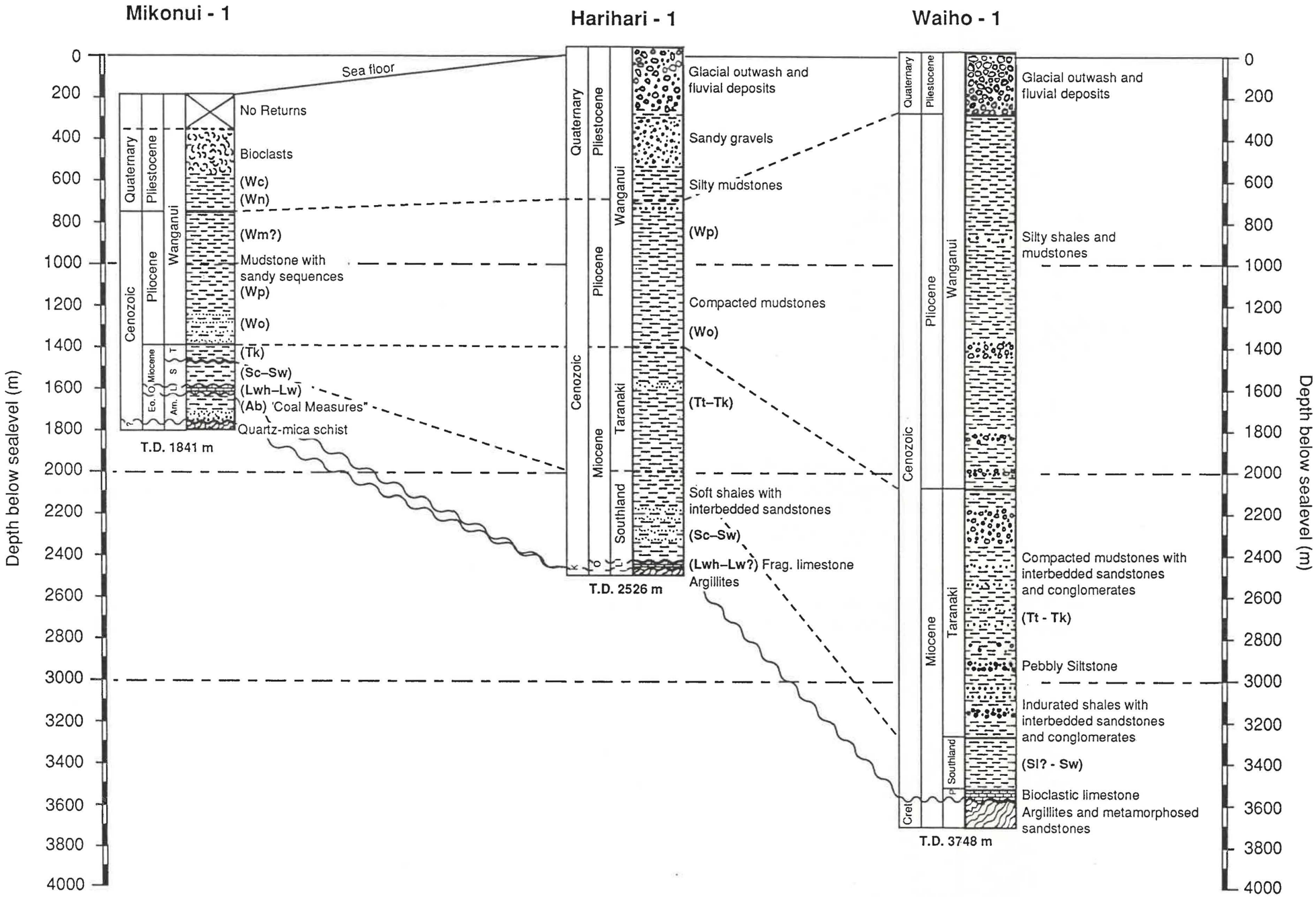

FIGURE 4.2: Lithostratigraphy, chronostratigraphy and regional correlation of Mikonui-1, Harihari-1 and Waiho-1 (After Diamond Shamrock Oil Company, 1981, PR 836, Enclosure 6)

GeoHist+, University of Waikato, Department of Earth Sciences
0:54, Friday, 31 July, 1992.

Project: Mikonui-1
GeoHist+ INPUT SUMMARY.
Water depth or elevation : 158.00m

	Thickness of Unit (m)	Age of Unit base (My)	Lithology % SS	ZS	MS	OP	LS	VO	KK	ø	Paleodepth of Unit (m)	Plot Layer
1:	312.0	0.9	0.0	0.0	0.0	0.0	100.0	0.0	1.30	0.74	158.0	Y
2:	150.0	1.2	0.0	0.0	100.0	0.0	0.0	0.0	2.43	0.70	200.0	Y
3:	420.0	3.1	0.0	0.0	100.0	0.0	0.0	0.0	2.43	0.70	200.0	Y
4:	75.0	3.6	0.0	0.0	100.0	0.0	0.0	0.0	2.43	0.70	200.0	Y
5:	315.0	5.0	10.0	0.0	90.0	0.0	0.0	0.0	2.31	0.67	200.0	Y
6:	75.0	6.0	5.0	0.0	95.0	0.0	0.0	0.0	2.37	0.69	200.0	Y
7:	0.0	10.0	100.0	0.0	0.0	0.0	0.0	0.0	1.20	0.40	300.0	N
8:	80.0	12.0	0.0	0.0	100.0	0.0	0.0	0.0	2.43	0.70	300.0	Y
9:	50.0	16.5	2.0	0.0	96.0	0.0	2.0	0.0	2.38	0.69	300.0	Y
10:	0.0	22.0	100.0	0.0	0.0	0.0	0.0	0.0	1.20	0.40	300.0	N
11:	35.0	36.5	0.0	0.0	0.0	0.0	100.0	0.0	1.30	0.74	150.0	Y
12:	20.0	42.5	5.0	95.0	0.0	0.0	0.0	0.0	2.13	0.52	50.0	Y
13:	60.0	50.0	5.0	95.0	0.0	0.0	0.0	0.0	2.13	0.52	10.0	Y
14:	80.0	60.0	100.0	0.0	0.0	0.0	0.0	0.0	1.20	0.40	0.0	Y

GeoHist+ BACKSTRIPPING SUMMARY.

	Time (Myr) 0.0	0.9	1.2	3.1	3.6	5.0	6.0	10.0	12.0	16.5	22.0	36.5	42.5	50.0	Zsk	Sed. Rate (m/My)
Water Depth (m).....	158.0	158.0	200.0	200.0	200.0	200.0	200.0	300.0	300.0	300.0	300.0	150.0	50.0	10.0		
1: Recent Bioclasts	312.0														110.1	346.7
2: Early Castlecliffian	149.0	214.0													86.6	715.1
3: Wn & Wm	419.0	471.0	555.0												281.5	292.2
4: Waipipian	75.0	79.0	83.0	145.0											54.5	290.9
5: Opotian	314.0	327.0	338.0	422.0	476.0										237.3	340.3
6: Late Kapitean	75.0	77.0	78.0	89.0	93.0	151.0									58.6	151.1
7: Tk/Tt Hiatus	0.0	0.0	0.0	0.0	0.0	0.0	0.0								0.0	0.0
8: Waiauan	80.0	82.0	83.0	92.0	96.0	129.0	165.0	165.0							63.3	82.6
9: Lillburnian & Clifdenian	49.0	51.0	52.0	57.0	58.0	73.0	82.0	82.0	109.0						39.8	24.4
10: Pl & Po Hiatus	0.0	0.0	0.0	0.0	0.0	0.0	0.0	0.0	0.0	0.0					0.0	0.0
11: Landon	34.0	36.0	37.0	41.0	42.0	53.0	58.0	58.0	69.0	84.0	84.0				24.4	5.8
12: Arnold Series	19.0	20.0	20.0	21.0	22.0	25.0	26.0	26.0	28.0	30.0	30.0	33.0			16.1	5.5
13: Late Dannevirke	59.0	61.0	61.0	65.0	66.0	73.0	77.0	77.0	82.0	87.0	87.0	93.0	96.0		48.5	12.9
14: Mata?-E.Dannevirke	80.0	81.0	81.0	85.0	86.0	90.0	92.0	92.0	94.0	96.0	96.0	98.0	99.0	101.0	62.1	10.2
Total Depth (m).....	1830.0	1660.5	1593.6	1221.4	1142.4	796.8	701.9	801.9	684.4	598.7	598.7	374.9	245.6	111.8		
Density (Mg/m3).....	2.01	2.00	1.95	1.84	1.82	1.67	1.62	1.54	1.47	1.43	1.43	1.57	1.77	1.94	Initial depth:	
Tectonic Sub. (m).....	717.7	644.6	638.6	503.4	474.4	348.2	313.2	381.9	304.7	291.9	306.4	97.5	15.7	-42.1	-149.0	

TABLE 4.1: Geohistory analysis input data and output results for Mikonui-1

GeoHist+, University of Waikato, Department of Earth Sciences
0:49, Friday, 31 July, 1992.

Project: Harihari-1

GeoHist+ INPUT SUMMARY.
Water depth or elevation : -31.00m

	Thickness of Unit (m)	Age of Unit base (My)	Lithology % SS	ZS	MS	OP	LS	VO	KK	ø	Paleodepth of Unit (m)	Plot Layer
1:	279.0	0.2	100.0	0.0	0.0	0.0	0.0	0.0	1.20	0.40	0.0	Y
2:	33.0	0.5	0.0	0.0	100.0	0.0	0.0	0.0	2.43	0.70	50.0	Y
3:	240.0	1.5	100.0	0.0	0.0	0.0	0.0	0.0	1.20	0.40	10.0	Y
4:	138.0	2.0	0.0	5.0	95.0	0.0	0.0	0.0	2.42	0.69	50.0	Y
5:	12.0	3.1	100.0	0.0	0.0	0.0	0.0	0.0	1.20	0.40	10.0	Y
6:	658.0	5.0	0.0	0.0	100.0	0.0	0.0	0.0	2.43	0.70	50.0	Y
7:	141.0	6.0	0.0	0.0	100.0	0.0	0.0	0.0	2.43	0.70	100.0	Y
8:	180.0	10.5	1.0	1.0	98.0	0.0	0.0	0.0	2.42	0.70	150.0	Y
9:	790.0	16.5	2.0	2.0	96.0	0.0	0.0	0.0	2.40	0.69	200.0	Y
10:	37.0	30.0	0.0	0.0	0.0	0.0	100.0	0.0	1.30	0.74	50.0	Y

GeoHist+ BACKSTRIPPING SUMMARY.

	Time (Myr) 0.0	0.2	0.5	1.5	2.0	3.1	5.0	6.0	10.5	16.5	Zsk	Sed. Rate (m/My)
Water Depth (m).....	-31.0	0.0	50.0	10.0	50.0	10.0	50.0	100.0	150.0	200.0		
1: One	279.0										174.3	1395.0
2: Two	33.0	53.0									17.6	177.6
3: Three	239.0	254.0	257.0								160.4	257.5
4: Four	138.0	157.0	163.0	221.0							91.1	442.6
5: Five	12.0	12.0	12.0	13.0	13.0						8.4	12.7
6: Six	657.0	695.0	704.0	756.0	851.0	858.0					488.4	452.1
7: Seven	141.0	144.0	145.0	149.0	153.0	153.0	265.0				112.2	265.6
8: Eight	179.0	183.0	184.0	188.0	192.0	192.0	252.0	327.0			145.9	72.7
9: Nine	790.0	800.0	802.0	812.0	821.0	822.0	914.0	962.0	1098.0		666.3	183.0
10: Ten	36.0	37.0	37.0	38.0	38.0	38.0	41.0	42.0	44.0	98.0	28.9	7.3
Total Depth (m).....	2477.0	2339.0	2358.2	2189.8	2121.5	2076.5	1524.5	1432.2	1293.1	298.6		
Density (Mg/m3).....	2.30	2.25	2.23	2.20	2.16	2.18	2.06	2.00	1.91	1.16	Initial depth:	
Tectonic Sub. (m)...	750.9	741.9	760.5	712.8	705.6	668.1	525.4	519.9	489.6	145.7	-27.0	

TABLE 4.2: Geohistory analysis input data and output results for Harihari-1

GeoHist+, University of Waikato, Department of Earth Sciences
0:58, Friday, 31 July, 1992.

Project: Waiho-1

GeoHist+ INPUT SUMMARY.
Water depth or elevation : 0.00m

	Thickness of Unit (m)	Age of Unit base (My)	Lithology % SS	ZS	MS	OP	LS	VO	KK	ø	Paleodepth of Unit (m)	Plot Layer
1:	242.0	1.5	100.0	0.0	0.0	0.0	0.0	0.0	1.20	0.40	0.0	Y
2:	368.0	3.1	0.0	10.0	90.0	0.0	0.0	0.0	2.40	0.68	50.0	Y
3:	490.0	3.6	0.0	10.0	90.0	0.0	0.0	0.0	2.40	0.68	75.0	Y
4:	1000.0	5.0	10.0	0.0	90.0	0.0	0.0	0.0	2.31	0.67	100.0	Y
5:	65.0	5.2	0.0	0.0	100.0	0.0	0.0	0.0	2.43	0.70	150.0	Y
6:	155.0	5.4	100.0	0.0	0.0	0.0	0.0	0.0	1.20	0.40	0.0	Y
7:	1005.0	10.5	15.0	5.0	80.0	0.0	0.0	0.0	2.23	0.65	100.0	Y
8:	289.0	15.0	0.0	0.0	90.0	0.0	10.0	0.0	2.32	0.70	150.0	Y
9:	0.0	16.5	100.0	0.0	0.0	0.0	0.0	0.0	1.20	0.40	150.0	N
10:	16.0	19.0	0.0	0.0	0.0	0.0	100.0	0.0	1.30	0.74	50.0	Y

GeoHist+ BACKSTRIPPING SUMMARY.

	Time (Myr) 0.0	1.5	3.1	3.6	5.0	5.2	5.4	10.5	15.0	16.5	Zsk	Sed. Rate (m/My)
Water Depth (m).....	0.0	0.0	50.0	75.0	100.0	150.0	0.0	100.0	150.0	150.0		
1: One	241.0										150.4	161.3
2: Two	368.0	447.0									218.5	279.8
3: Three	490.0	514.0	652.0								349.5	1304.6
4: Four	999.0	1015.0	1062.0	1275.0							803.8	911.4
5: Five	65.0	65.0	66.0	70.0	146.0						55.2	734.6
6: Six	154.0	156.0	158.0	164.0	194.0	202.0					125.1	1011.9
7: Seven	1004.0	1010.0	1023.0	1050.0	1226.0	1272.0	1363.0				876.1	267.3
8: Eight	289.0	289.0	292.0	297.0	316.0	319.0	323.0	525.0			258.4	116.8
9: Nine (unconf)	0.0	0.0	0.0	0.0	0.0	0.0	0.0	0.0	0.0		0.0	0.0
10: Ten	16.0	16.0	16.0	16.0	18.0	18.0	18.0	25.0	48.0	48.0	13.4	19.2
Total Depth (m).....	3630.0	3516.0	3322.4	2949.8	2003.1	1962.7	1705.8	651.6	198.1	198.1		
Density (Mg/m3).....	2.33	2.31	2.27	2.23	2.13	2.10	2.14	1.71	1.11	1.11	Initial depth:	
Tectonic Sub. (m)...	1061.6	1040.1	1000.9	919.2	665.9	666.4	551.9	260.6	65.2	83.7	19.0	

TABLE 4.3: Geohistory analysis input data and output results for Waiho-1

4.1.2.2 *Harihari-1*

Harihari-1 was the first exploration well drilled in the study area by New Zealand Petroleum Co. Ltd. (1971). Its stratigraphy is dominated by a largely homogeneous sequence of mudstones compacting to soft shales at depth overlying a limestone sitting on basement rock.

The drilled section can be divided into four parts:

(1) 2526–2508 metres: *Pre-Cenozoic basement complex.*
Basement consists of steeply dipping grey-green phyllite or low-grade schist derived from argillites of inferred Greenland Group. This is overlain by a thin layer (approx. 5 m) of sandstone and siltstone, inferred as a residual weathered zone.

(2) 2508–2473 metres: *Basal Limestone*
The upper part of the limestone consists of a tan coloured, very silty, moderately argillaceous extremely fine grained limestone with traces of pyrite and abundant glauconite, which grades into a slightly argillaceous fine to very fine calcarenite with a cement of sparry calcite and extremely fine carbonate material. The calcarenite consists of fragments of bioclastic origin with probable bryozoan and foram remains. Biostratigraphy in this section is hampered by the dense nature of the samples, and the age is uncertain ranging from the Kaiatan to Altonian. However this limestone is again correlated with the Cobden Limestone.
Depositional environment: The key taxon *Amphistegina* indicates an inner to mid-shelf locus of deposition (30–100 m).

(3) 2473–280 metres: *Marine Cenozoic section*
The base of this unit comprises silty shales with thin interbeds of sandstone and siltstone. At 2380 m this grades upwards into soft shales to 1860 m. Above this a monotonous section of mudstone with slight decreases in compaction at 1647 m and 1467 m continues through to 702 m. A thin sandy interval at 690–702 m consisting of well rounded and unconsolidated coarse sand with chert grains. Biostratigraphy indicates that this thin interval is near the Pliocene-Pliestocene boundary. Above this is a sandy gravel near the top of the sequence (313–552 m). The sandy gravel differs from the surface section with darker metamorphics and ultrabasic fragments.
Biostratigraphy would again indicate the absence of Pareora Series sediments. The Southland Series is well represented as well as the Taranaki Series with the

appearance of the Tongaporutuan indicators. The top of Miocene is around 1375 m in depth. Higher in the section Opoitian through to Mangapanian Stage (Pliocene) and younger indicators are seen.

Depositional environment: The Taranaki and Southland Series appear to be the deepest part of the section with outer shelf to slope depths (300–1000 m). The remainder of the sequence is placed in a mid to outer shelf environment (100–300 m).

(4) 280–0 (31 m.s.l) metres: *Glacial outwash and fluvial deposits*

Unconsolidated very coarse sand to fine and pebble gravels with some boulders. Composition is mainly metamorphic with minor igneous.

Depositional environment: Given the fluvial nature of the sediments, these deposits are probably largely non-marine.

4.1.2.3 *Waiho-1*

Waiho-1 is the deepest of the three exploration wells and was drilled by New Zealand Petroleum Co. Ltd. (1972). Lithostratigraphy is again dominated by mudstone, but frequent sandstone and conglomerate units are also seen. The drilling of Waiho-1 also demonstrated that prominent reflectors seen on associated seismic lines were due to the presence of conglomerates in a mudstone background, rather than the 'reefal buildups' of McNaughton & Gibson (1970).

The drilled section can be divided into four parts:

(1) 3748–3629 metres: *Basement complex*

The basement rock is described as a light grey to grey phyllitic slate composed of quartz, white mica and pale green chlorite. The rock is tentatively classed as belonging to the Greenland Group. Low dips of 10° or less were recorded. Above the basement is a complex sequence of siliceous sandstones.

(2) 3629–3613 metres: *Basal Limestone*

The bottom half of the limestone interval is dominantly a white, bioclastic limestone from 3618 to 3629 m, consisting of foraminiferal remains. Above this is a transitional brown-grey argillaceous limestone.

Reconnaissance biostratigraphy suggests that this unit is Altonian in age (19.0 – 16.5 Ma), although this is unusual in comparison to the other basal limestones which belong to the Landon Series (36.5 – 24.0 Ma). Nathan et al., (1986) interpret this limestone has equivalent to the Awarua Limestone of South Westland, of Oligocene age.

Depositional environment: The basal limestone is interpreted as being 'indicative of shallow water deposition' (30–100 m).

(3) **3613–3324** metres: *Middle Miocene*

Moderately hard shales overlie and grade into the basal limestone. The shales are generally slightly calcareous and slightly to moderately silty. Interbedded thin siltstones and sandstones are also present but all coarser clastic content decreases markedly below 3355 m.

Biostratigraphy indicates an age of Lillburnian to Waiauan (15.0–10.5 Ma), and also suggests that there is no evidence for pre Lillburnian (i.e. Clifdenian) in the siltstone overlying the limestone.

Depositional environment: Outer shelf or deeper. (300–1000 m)

(4) **3324–2107** metres: *Upper Miocene*

This section consists of numerous massive conglomerates and conglomeratic coarse and very coarse sandstones. The intervening mudstones present exhibit a gradual increase in compaction until around 2530 m where shales are present.

Biostratigraphic ages are between the Tongaporutuan and Kapitean (10.5–5.0 Ma). No indications of hiatuses are noted, although this may be confused by the numerous conglomeratic sequences seen.

Depositional environment: Deep water benthics are noted in the siltstones in this unit (300-1000). The top conglomeratic unit (2165–2318 m) has little or no fauna and may be non-marine. Deep water benthics are noted near the top of another conglomerate at 3100 m, but this may be due to contamination down the hole.

(5) **2107–242** metres: *Pliocene*

Soft silty mudstones dominate this section. A conglomerate and several gravel intervals are present. A core at 1900 m revealed the presence of shale clasts. A micropaleontological determination of these clasts indicates an Oligocene age. Weathered schist pebbles are noted at around 1200 m.

Biostratigraphic ages range from Opoitian at the base through to Mangapanian or higher at the top of the unit (5.0 Ma onwards). Recycled specimens derived from Arnold to lower Landon Series are also noted.

Depositional environment: Deep water at the base of the unit decreases to mid shelf depths (100 m) higher in the section with some indication of a gradual deepening again near the top.

(6) **242–0** (3 m.s.l.) metres: *Glacial outwash and fluvial deposits*

Gravels, boulders and sand occur at the top of the drilled section with a thin basal very fossiliferous gravel section being present, the fossil content mainly

fragmentary and well worn heavy shelled pelycepod remains. The entire unit is of inferred Pliestocene to Recent age.

Depositional environment: Given the fluvial nature of the sediments, these deposits are probably largely non-marine to marginal marine.

4.1.3 Geohistory analysis

Geohistory analysis was conducted on all three exploration wells based on stratigraphic data from their respective well reports using the GeoHist+ program discussed in Chapter 2. These data and the resulting decompacted thicknesses through time are given in Tables 4.1, 4.2 and 4.3. The geohistory plots for each well are illustrated in Figures 4.3, 4.4, 4.5.

All three wells show rapid subsidence since around 10 Ma. This is particularly emphasised in Mikonui-1 where a long-term gradual subsidence since around 60 Ma is seen. This long term gradual subsidence is analysed in terms of post-rift thermal contraction below in Section 4.3. The two onshore wells do not illustrate an early-stage long-term gradual subsidence as their sedimentary records begin at a later time than that of Mikonui-1. The fluctuations of sea level appear to become increasingly insignificant beside the thick sedimentary deposits seen in the wells—over 3500 m in Waiho-1. The tectonic subsidence calculated in the wells is further discussed in Chapter 5.

4.1.4 Synthetic seismogram

As discussed above, the geophysical data reported for the two earlier wells in the completion reports is poor. In particular, the vital time-depth curves for relating a time on a seismic profile with a depth (and hence a known lithology) in the exploration wells seem to be generalised at best. The geophysical surveys in the more recent Mikonui-1 well were more intensive and better documented. The open-file Petroleum Record 836 contains a wealth of information submitted by Diamond Shamrock, the operators of Mikonui-1. Of specific importance is the Geophysical Airgun Report that provides detailed information about the velocity structure of the well stratigraphy. This report contains information relating two-way travel time with depth, thus allowing direct comparison of seismic profiles passing through the well-site (PS-19 and PS-21) and well stratigraphy. The interval velocity of a unit can also be calculated, and this in turn can be used to generate synthetic seismograms by calculating the acoustic impedence between 'measured' intervals.

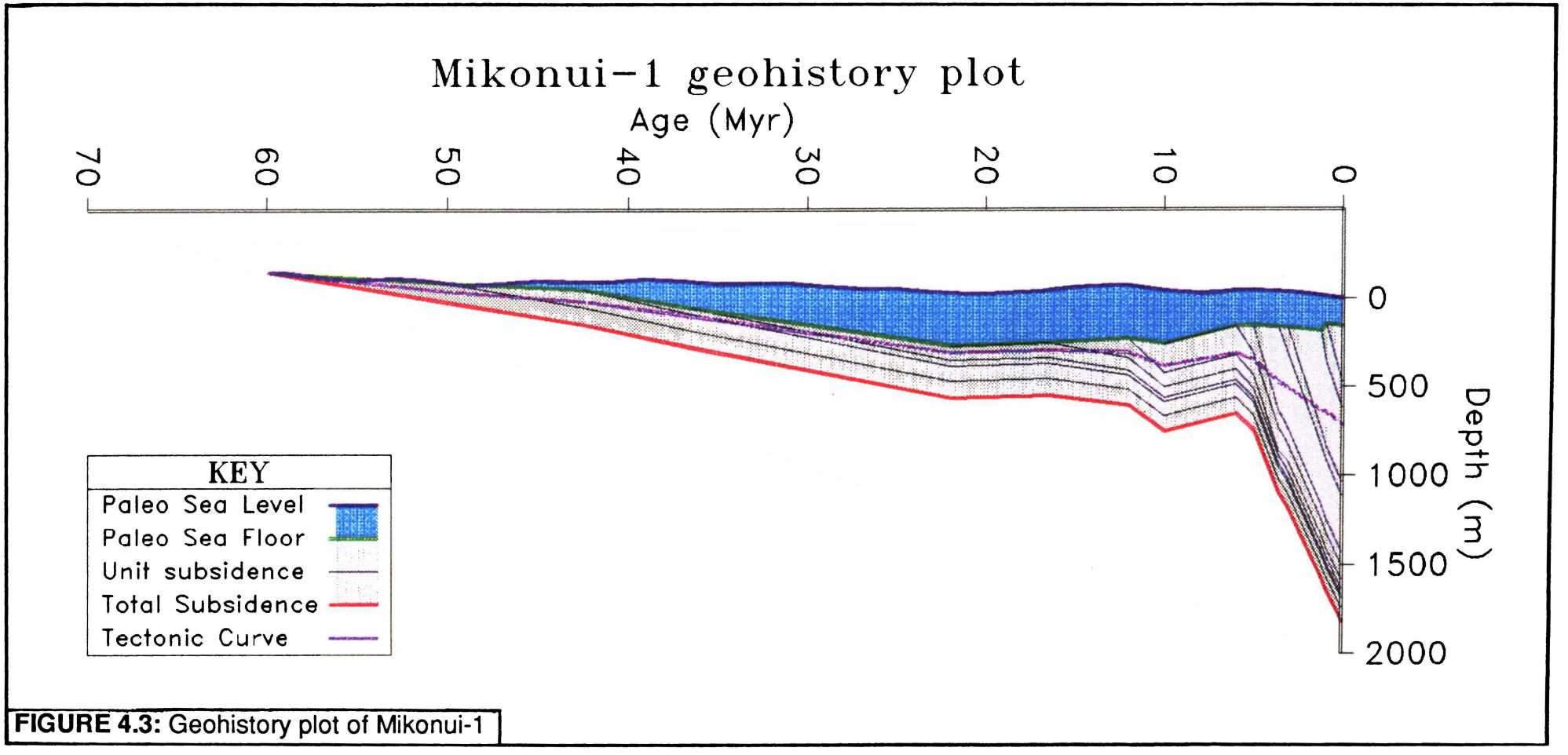

FIGURE 4.3: Geohistory plot of Mikonui-1

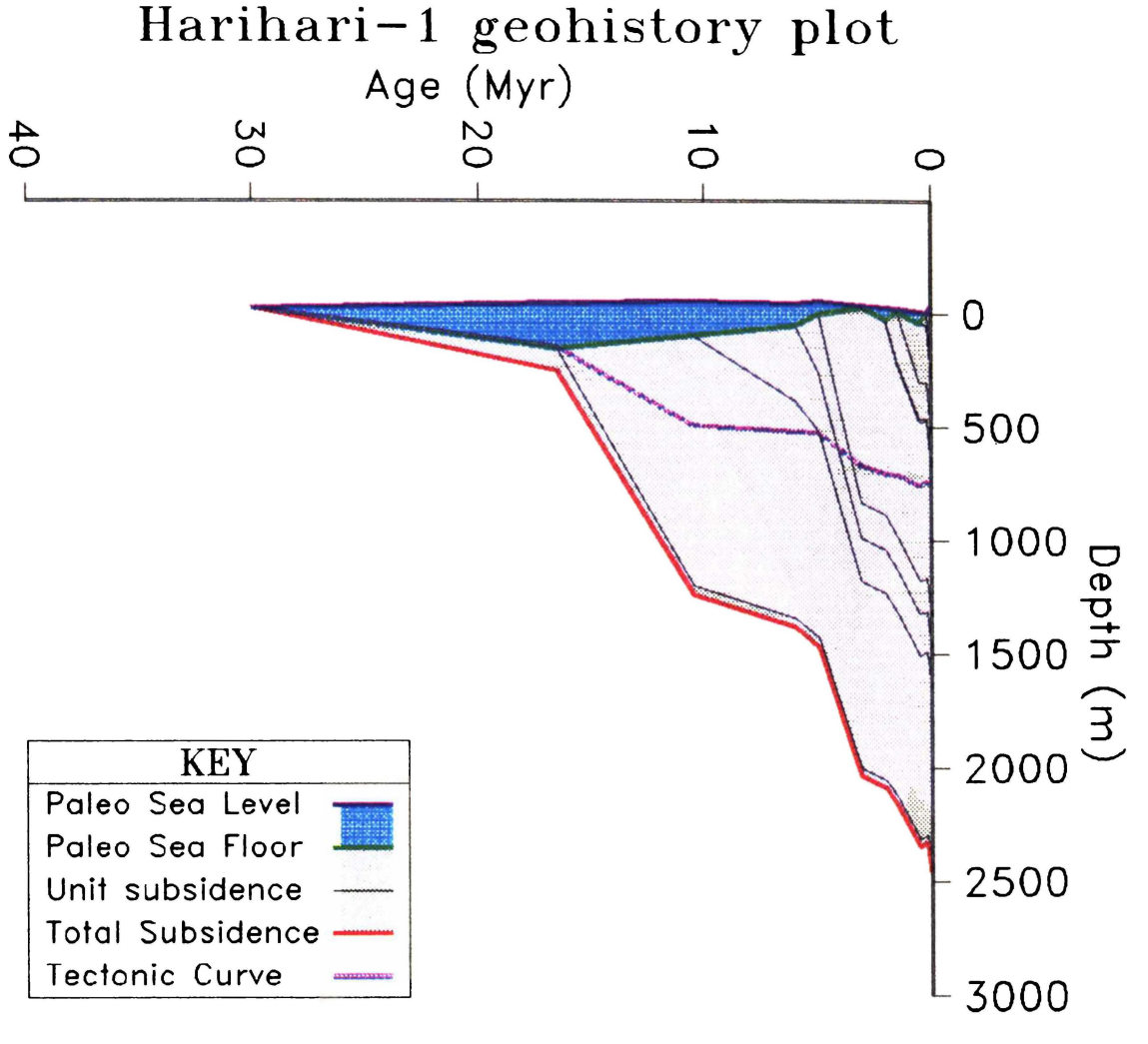

FIGURE 4.4: Geohistory plot of Harihari-1

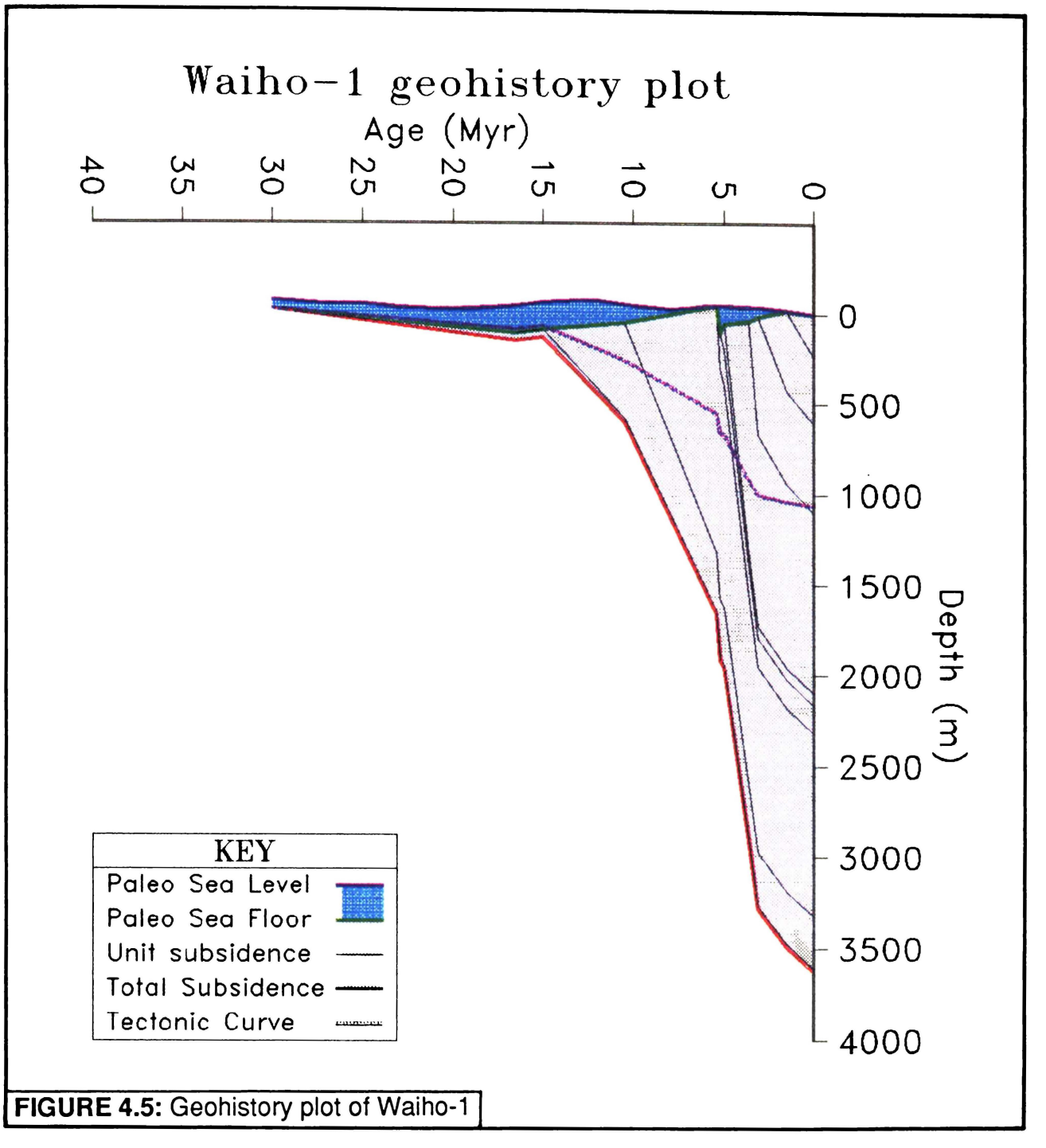

FIGURE 4.5: Geohistory plot of Waiho-1

Using the interval velocity data from the Mikonui-1 report a synthetic seismogram was generated using SYN 2©, a PC-compatiable application[1]. The results of this analysis can be seen in Figure 4.6.

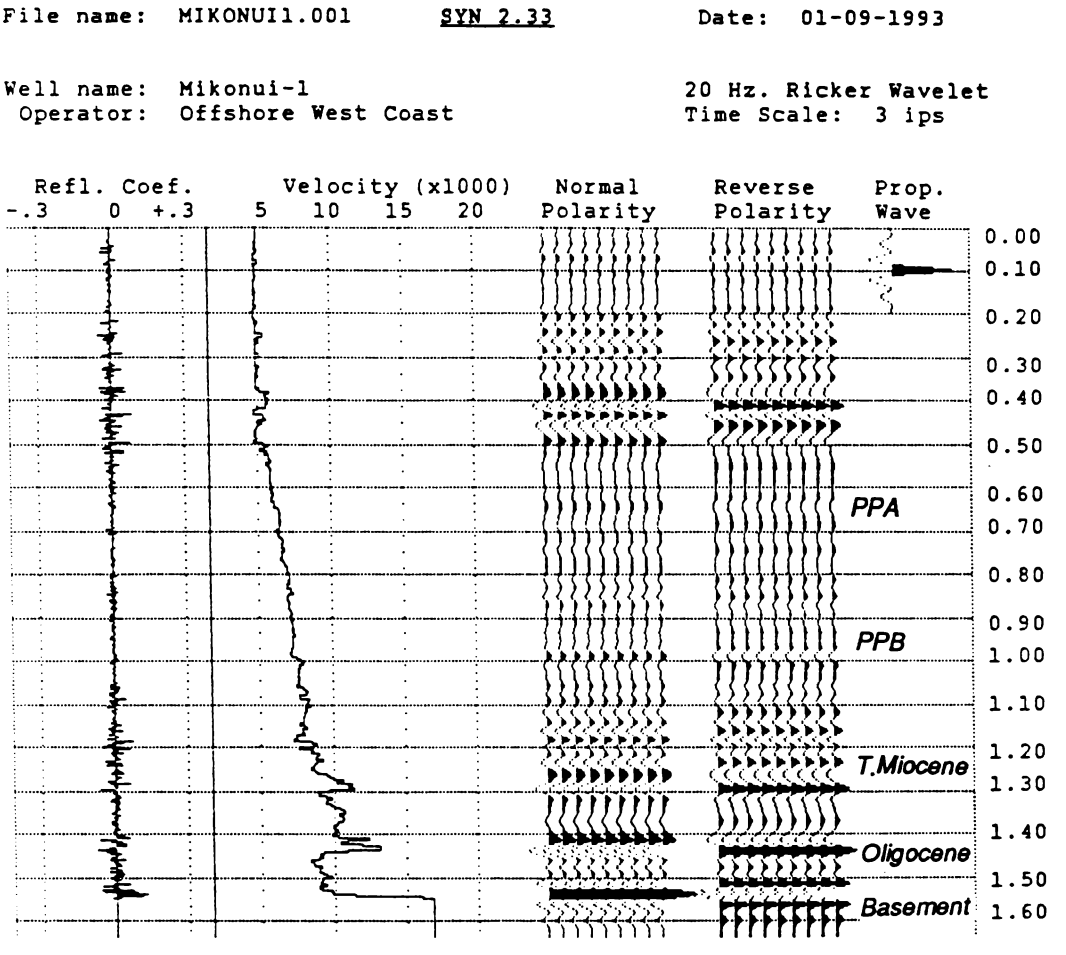

FIGURE 4.6: Synthetic seismogram generated for velocity data from Mikonui-1. Note that velocity data is in feet/second.

In Fig 4.6, prominent reflectors are seen in the upper third of the column, presumably a result of bioclastic layers. In the middle third, no prominent reflectors are seen due to the largely homogeneous nature of the mudstone found in this section. In the lower third, reflectors again become conspicuous as sandstone layers increase in frequency toward the limestone (strong reflector at around 1.4 s), coal measures (weak reflectors) and basement (very strong reflector at 1.55 s). When compared to the seismic lines at the Mikonui-1 well-site the seismogram contains some good correlations.

[1] **SYN 2** is © Jeffrey D. Prouty, 242 Pheasant Drive, Healdsburg, CA 95448, U.S.A. It is a *shareware* program obtained from the Computer Oriented Geological Society, P.O. Box 1317, Denver, CO 80201-1317, U.S.A., via the COGS directory at the anonymous FTP site, csn.org, [128.138.213.21].

4.2 Seismic stratigraphy

4.2.1 Location of seismic lines

Numerous seismic reflection profiling surveys of the South Westland basin have been undertaken in the search for potential petroleum resources. Copies of the seismic lines have been gathered by the New Zealand Geological Survey (now the Institute of Geological and Nuclear Sciences Ltd.) in the Open-file Petroleum Reports. These reports are the source of the seismic profiles used in this study. Not all the gathered information has been used here, but the data used attempts to give a broad regional spread. The Open-file Petroleum Reports used in this study are listed in Table 4.4. Further detail about individual lines in given in Appendix A of this study.

PR	Year	Operator	Line series
400	1968	Esso Exploration	EZD–
523	1971	N.Z. Petroleum	L–, OS–
548	1967	Shell B.P.	M–
575	1971	Magellan Petrol.	W–
614	1973	Australian Gulf	NZ–
629	1974	N.Z. Petroleum	PS–

TABLE 4.4: List of Open-file Petroleum Reports and associated Line series titles used in this study (see Figure 4.7).

This study uses a total of 1715 km of seismic lines, of which 104 km is onshore. The location of the seismic lines is illustrated in Figure 4.7. The seismic coverage is generally broad, but is concentrated offshore the Waiho-1 drill-site. The southwestern corner is sparsely covered by NZ– series lines. The exploration drill-sites are well tied to seismic lines for correlation purposes. Lines PS-19 and PS-21 intersect at Mikonui-1, and OS-3 passes through Harihari-1. Waiho-1 is offset by around 2000 m from the ends of OS-8 and L-212.

The quality of recorded seismic reflection profiles used in this study vary greatly. Earlier lines are often of poor quality and/or reproduction. Indeed, the M– series lines were of such a low standard of reproduction that their use was limited to some correlation of closely spaced tie lines. Any interpretation beyond this would have been entirely arbitrary. It is fortunate in this regard that some of the mapped reflectors (as described below) are frequently prominently displayed, particularly in the basement sequence. This prominence is probably due to a marked increase in acoustic velocity and hence reflection coefficient in the lower layers.

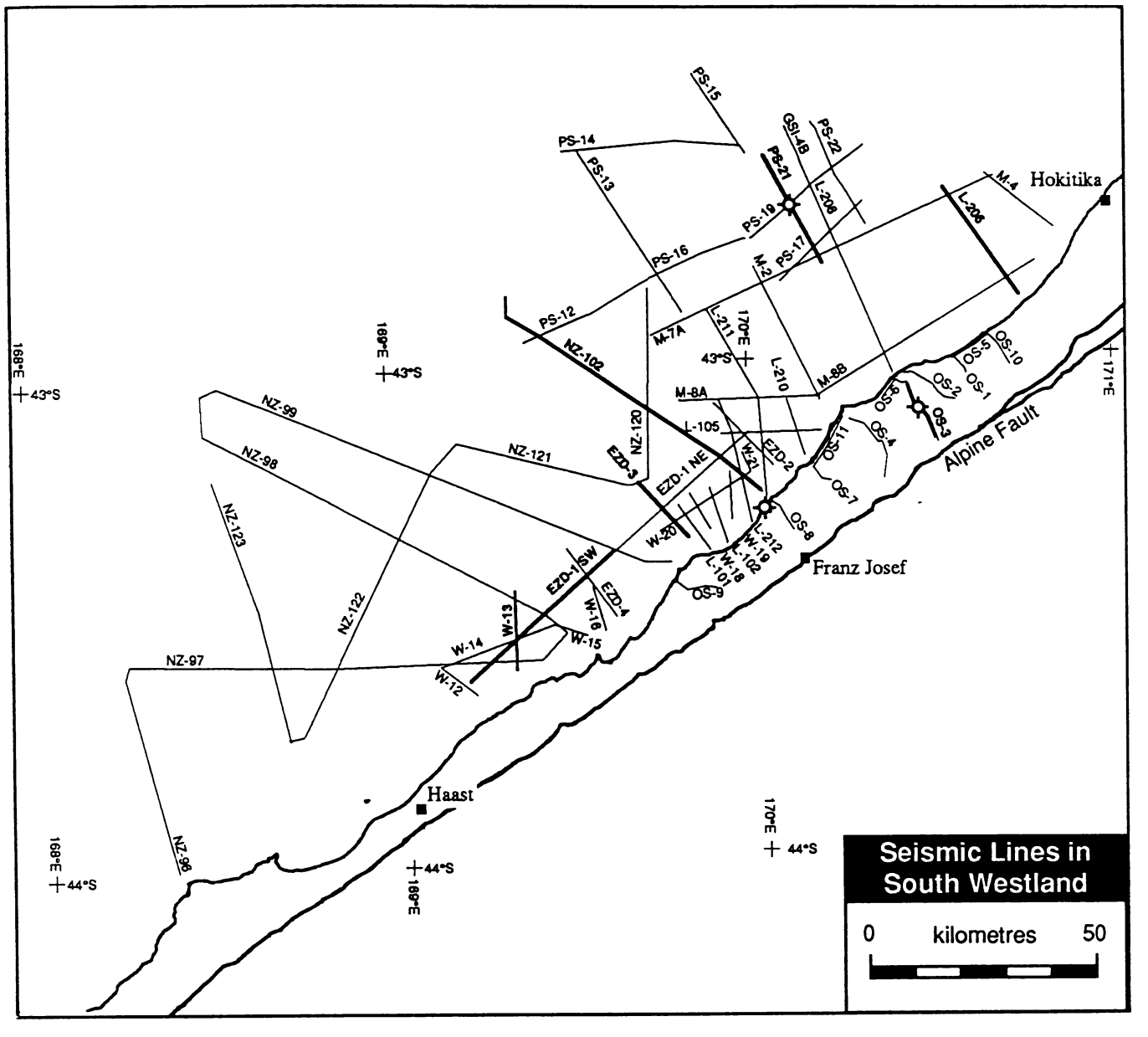

FIGURE 4.7: Diagram illustrating the location of the seismic reflection profiles used in this study. Line titles use the Line series abbreviations in Table 4.4. Bold lines indicate seismic reflection profiles used as 'typical' examples and illustrated in text.

Once the seismic lines have been interpreted the data is captured using the TECHBASE system (see Chapter 2 and Appendices for further explanation). The data can then be modelled to observe depths to horizons and thicknesses of sequences in a designated study area. The following isopach and contour maps are an example of that process.

4.2.2 Seismic sequence analysis

The application of the principles of seismic stratigraphy as discussed in Chapter 2 is limited by the poor resolution seen in a number of the seismic profiles examined. A number of lines show large scale sequences, particularly prograding foreset beds, but within these,

bordering on the edge of resolution are smaller order structures tentatively interpreted as low stand wedges and fans. A wealth of seismic stratigraphic information exists in the study area awaiting better resolution surveying. The importance of identifying and classifying reflector terminations remains an important method in gaining information about the stratigraphy and structure of the basin.

4.2.3 Seismic horizons and sequences

After a reconnaissance analysis of the seismic lines, a number of features were interpreted. A simplified diagram of the mapped horizons and sequences is illustrated in Fig. 4.8. The basal twin reflectors of the basement and basal Oligocene limestone are very prominent in seismic profiles, and thus easily lend themselves to interpretation and mapping. Above this the top Miocene was correlated from Mikonui-1 and although often difficult to trace, this horizon was mapped across the study area. Two prominent horizons were noted in the thick Pliocene-Pliestocene sequence. Both appear to be erosional surfaces subsequently overlain by sediments associated with a variety of transgressive and regressive events. The bottom horizon, named the Plio-Pliestocene Unconformity B (PPB) is loosely correlated with the Waipipian–Mangapanian boundary (3.1 Ma) in Mikonui-1. The PPB appears to be regionally extensive. The higher Plio-Pliestocene Unconformity A (PPA) appears to be of limited extent, but forms a very prominent arcuate horizon. This horizon is loosely correlated with the Nukumaruan–Castlecliffian boundary (1.2 Ma). Unfortunately the PPA horizon often occurs at the height of the first multiple 'ghost' of the seafloor in the seismic displays. This limits the interpretation of the horizon and overlying reflector associations and structures. Finally the seafloor horizon completes the list of mapped horizons and sequences.

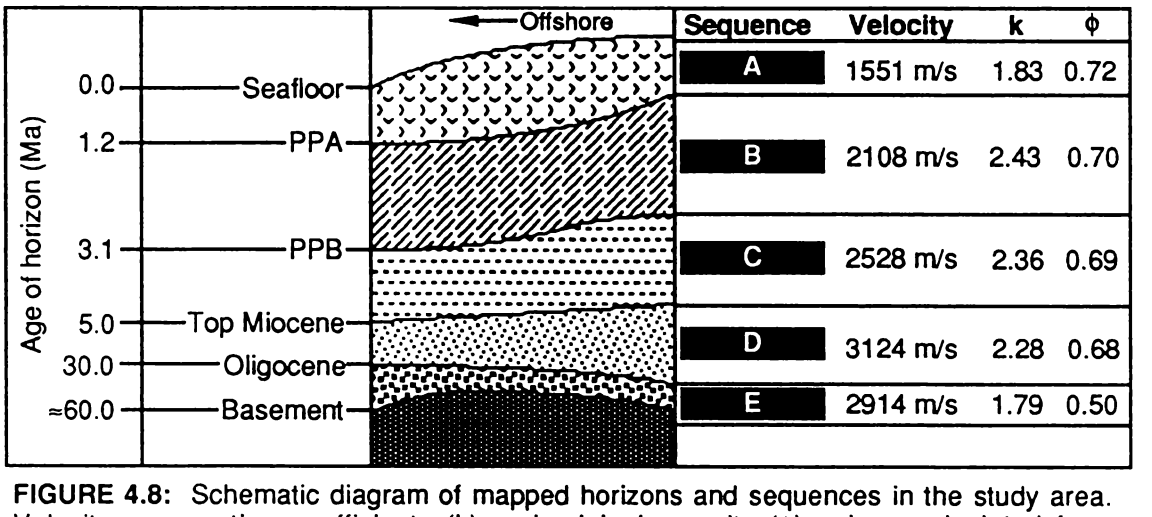

FIGURE 4.8: Schematic diagram of mapped horizons and sequences in the study area. Velocity, compaction coefficients (k) and original porosity (ϕ) values calculated from geophysical and lithologic data in Mikonui-1.

The geophysical parameters of the mapped sequences, e.g. acoustic velocity, compaction coefficients and original porosity, to be used in later backstripping and decompaction exercises were calculated from data in the Mikonui-1 well (Diamond Shamrock, 1981).

4.2.3.1 *Basement*

The basement horizon is generally very prominent, in close association with the Oligocene horizon, although may occasionally become unclear underneath it. The basement horizon is often distinguished by its rugged appearance on seismic profiles and has frequent small dips and breaks (e.g. PS-21, Fig. 4.14). No coherent reflectors are seen below it.

The present basement structure, as illustrated in Fig. 4.16 clearly shows the plunging of the basement toward the southeastern margin of the basin to a depth of up to 4 km. Also seen on the contour map is the basement high upon which Mikonui-1 was drilled. The high appears to continue along strike to the southwest. The basement dips away to the northwest on the other side of these basement highs. The nature of the basement structure is further investigated using geodynamical modelling in Chapter 5.

4.2.3.2 *Sequence E*

Type sections:
Sequence E is a broad, thin sheet-like body. The Oligocene limestone is frequently seen directly overlying basement (e.g. Waiho-1 and Harihari-1). This is also seen in the closely paired nature of the seismic Oligocene and basement horizons, suggesting an absence of this sequence over much of the basin. The sequence thickens offshore and is therefore best represented in the distal sections of NZ-102 (Fig. 4.12), L-206 (Fig. 4.11) and PS-21 (Fig. 4.14).

Well stratigraphy:
Sequence E was the target of the Mikonui-1 exploration well. At Mikonui-1 the sequence lies between 1650 m and 1841 m (total depth) below sea level, and consists of sandstones with occasional coal traces grading upward into mudstones. The sequence is not seen in the onshore wells.

Upper boundary:
The upper boundary of Sequence E is the Oligocene horizon dated at around 30 Ma, but also represents a hiatus through the late Arnold Series (42.0–36.5 Ma). Some truncation of reflectors is seen in distal sections (e.g. NZ-102, Fig. 4.12) as the Oligocene horizon dips to the southeast.

Lower boundary:

The lower boundary of Sequence E is the basement horizon, dated as a Late Cretaceous surface. Distal reflectors in the thicker part of the sequence onlap against the basement surface (e.g. PS-21, Fig. 4.14; L-206, Fig. 4.11).

Internal configurations:

The thinness of this sequence is often below seismic resolution, thus making interpretation of any internal structures impossible. However, where resolution allows in the thicker parts of the sequence (e.g. NZ-102, Fig. 4.12; PS-21, Fig. 4.14), the reflectors seen are generally of moderate to high amplitude and continuity. The internal configuration appears to be generally flat lying and concordant, with reflectors truncating against the upper or lower boundaries.

External form:

Sequence E is generally a thin sheet-like unit over the entire study area, thickening noticeably offshore (Fig. 4.17). It onlaps onto the basement to the northwest of the basement high, and generally thins to absence to the southeast of the high. Locally the sequence may also fill shallow depressions in the basement relief (e.g. NZ-102, Fig. 4.12).

4.2.3.3 *Oligocene Horizon*

The Oligocene horizon is often the most prominent of all the seismic horizons mapped in the study area. Its prominence is due to a sharp acoustic velocity change between the post-Oligocene muds and shales, the Oligocene bioclastic limestone the horizon represents, and where present, the Late Cretaceous–Eocene sediments below. From well stratigraphy the limestone is very thin and thus the resolution of the seismic lines probably correspond to the thickness of the limestone unit. The strongly reflective horizon is closely associated with the basement horizon, sometimes even masking the prominence of that horizon.

The Oligocene horizon is a smooth, gently undulating and continuous horizon, gently dipping to the southeast. In well correlations the Oligocene limestone (variously the Awarua Limestone or Cobden Limestone is dated between the Waitakian and Whaingaroan (≈36.5–22.0 Ma). An 'average' age of 30 Ma has been adopted for the purposes of description. The horizon also represents a significant hiatus through the Pareora to early Southland Series (22.0–≈15.0 Ma). Evidence of this hiatus may be seen in the regional onlap of reflectors onto the Oligocene Horizon. Another hiatus, present below the Oligocene Horizon during the Arnold Series (42.5–36.5 Ma) is suggested by biostratigraphy from the wells. Seismic evidence of this hiatus is possibly represented by reflector truncation below the horizon.

4.2.3.4 *Sequence D*

Type sections:

Sequence D is a fairly uniform sheet of sediment overlying the Oligocene horizon. It occurs throughout the basement and is seen in all seismic lines, although detailed structure is best seen in sections EZD-3 (Fig. 4.10) and L-206 (Fig. 4.11).

Well stratigraphy:

The stratigraphy of this sequence in Mikonui-1 is again dominated by mudstone between the depths of 1400 m and 1650 m below sea level. Interbedded sandstones and conglomerates become a prominent feature of this sequence in Waiho-1, further towards the basin margin.

Upper boundary:

The upper boundary of Sequence D is the Top Miocene Horizon dated at 5 Ma. Reflectors are generally concordant with this horizon, although some truncation is suggested in L-206 (Fig. 4.11) and other lines.

Lower boundary:

The lower boundary of Sequence D is the Oligocene Horizon dated at around 30 Ma, but also representing a significant hiatus through the Pareora Series up to around 15 Ma. Section L-206 (Fig. 4.11) show a significant amount of onlapping onto this horizon from the southeast. This baselap probably grades toward downlap seen in the southeastern ends of NZ-102 (Fig. 4.12) and EZD-3 (Fig. 4.10).

Internal configurations:

The internal configuration of Sequence D comprises low amplitude reflectors and continuity in proximal sections grading and thinning distally to concordant and continuous reflectors. None of the prominent prograding features of higher sequences can be recognised. L-206 (Fig. 4.11) displays a few prominent reflectors in a low amplitude background toward the southeast, that have an undulose nature. Hummocky reflectors are also seen in NZ-102 (Fig. 4.12).

External form:

Sequence D has a broad sheet-like form. The sequence appears to thicken to the northwest in some sections (e.g. NZ-102, Fig. 4.12), but this may be the result of being less compacted by overlying sediments than closer to the modern shoreline. The sequence mainly thickens toward the coastline as seen in sections NZ-102 and L-206 (Fig. 4.11). The interpreted thickening of this sequence is responsible for the prominent bulls-eye seen in the eastern corner of the Sequence D isopach map (Figure 4.18).

4.2.3.5 *Top Miocene Horizon*

The Top Miocene Horizon was originally mapped as a chronostratigraphic guideline, correlating with the 5 Ma Miocene-Pliocene boundary at a depth of around 1225 m below the seafloor in Mikonui-1. However the horizon also displays some seismic stratigraphic features. The horizon is occasionally associated with proximal downlap (EZD-3, Fig. 4.10) and distal onlap (PS-21, Fig. 4.14), with some truncation of reflectors underneath suggested in some sections (L-206, Fig. 4.11) It is the most difficult horizon to trace through the region due to the low amplitude and incoherent nature of the seismic facies it often passes through. The horizon is associated with a group of prominent reflectors in the the synthetic seismogram (Fig. 4.6). This correlates well with some sections where the Top Miocene Horizon occurs among a group of prominent reflectors (e.g. EZD-1, Fig. 4.9)

Generally the horizon dips toward the southeast (PS-21, Fig. 4.14; EZD-3, Fig. 4.10), but it also appears to rise toward the coast in some sections (L-206, Fig. 4.11; NZ-102, Fig. 4.12).

4.2.3.6 *Sequence C*

Type sections:

The internal structure of Sequence C is relatively complex, especially in proximal areas. The complexities of this sequence are well illustrated in section EZD-3 (Fig. 4.10) in particular, with other features highlighted in sections L-206 (Fig. 4.11) and NZ-102 (Fig. 4.12).

Well stratigraphy:

The stratigraphy of this sequence in Mikonui-1 is dominantly mudstone with sandy sequences, between the depths of 1080 m and 1400 m below sea level, with the frequency and coarseness of the sandy sequences increasing shoreward. Exotic blocks and reworked foraminifera from the Arnold and Landon Series are found within sediments of early Opoitian age in Waiho-1.

Upper boundary:

The upper boundary of this sequence is the PPB horizon, dated at near 3.1 Ma. The reflectors are generally concordant with this horizon, although truncation has been noted (e.g. L-206).

Lower boundary:

The lower boundary of this sequence is the Top Miocene horizon, dated at 5 Ma. In EZD-3 (Fig. 4.10), the lower boundary has been interpreted to run below the prominent wedge with distinct downlapping occurring . However the horizon could be alternatively interpreted as being continuous with the top of the wedge rather than the base. Some

onlapping onto the bottom horizon is also seen in EZD-3 and in the southeast of Mikonui-1 in section PS-21 (Fig. 4.14). Elsewhere reflectors are mostly concordant with this horizon.

Internal configuration:
Internally the reflectors have moderate continuity and relatively high amplitude. Some areas have a generally chaotic appearance (e.g. EZD-3, Fig. 4.10). In more distal sections (e.g. PS-21, Fig. 4.14) the reflectors are generally more continuous and weakly hummocky. The amplitude and continuity of reflectors can vary laterally as seen in L-206 (Fig. 4.11) where a mixture of strong laterally continuous and weak chaotic reflectors occur. McNaughton & Gibson (1970), interpreted such configurations as reef and atoll structures. The logging of numerous horizons of sandstones and conglomerates in a mudstone background in the onshore exploration wells has been sited as a more plausible reason for these structures (Nathan et al., 1986). A number of reflectors terminate internally against each other as this sequence thins to the northwest.

The internal configuration is generally concordant, weakly undulose through to chaotic in structure. In proximal sections the internal configuration can be divided into two distinct groups. At the top are the weakly undulose through to chaotic reflectors, while the base has a prominent wedge of reflectors. This structure is well seen in EZD-3 (Fig. 4.10), but is also laterally continuous, and is clearly seen in other lines running perpendicular to the coastline. This group of reflectors has a particularly strong top boundary, with internal reflectors dipping to the northwest, downlapping onto a weakly continuous horizon at the base. The internal configuration of the wedge varies along strike in other lines. In EZD-2, to the north, the wedge is thinner and occurs stratigraphically higher in relation to EZD-3 with another group of concordant reflectors underneath it. Reflectors are generally concordant and gently dipping, but the prominence of the top reflector has decreased, replaced by a prominent and continuous basal reflector. To the south, in EZD-4, the wedge becomes difficult to recognise as reflectors become more rugged and apparently deformed.

A possible low stand fan is identified in L-206 (Fig. 4.11), suggesting that the complex depositional history of the sequence extends into distal areas also.

External form:
Basically, Sequence C forms a large wedge of sediment, thickest against the southeastern margin of the basin at over 1500 m, and thinning to the northwest (Figure 4.19).

4.2.3.7 *PPB Horizon*

The PPB Horizon is the more regionally extensive and prominent of the two mapped unconformities in the Plio-Pliestocene sedimentary sequence. It is best displayed in sections perpendicular to the coastline such as L-206 (Fig. 4.11). The horizon is commonly

found in close association with a number of high amplitude, undulose and generally discontinuous horizons. Together these horizons form a group that appears to dip to the northwest in a series of shallow steps (L-206, Fig. 4.11) or twisted rope-like appearance (EZD-3, Fig. 4.10). Horizons above are generally downlapping to concordant, those below are mostly concordant with truncation suggested on some lines.

The correlation of this horizon with the Mikonui-1 well is near the Waipipian–Mangapanian biostratigraphic boundary at around 3.1 Ma at a depth of about 900 m below the seafloor. On the synthetic seismogram a reflector of moderate amplitude is seen near this point (Figure 4.6).

4.2.3.8 *Sequence B*

Type sections:
Sequence B is weakly lensoidal through to wedge shaped in cross-section, rapidly thickening toward the coastline. The structure of Sequence B is relatively complex, especially in proximal near shore areas, and is best illustrated in seismic sections EZD-3 (Fig. 4.10) and NZ-102 (Fig. 4.12).

Well stratigraphy:
The stratigraphy of the sequence in Mikonui-1 is dominantly mudstone with sandy sequences between the depths of 730 m and 1080 m below sea level. The frequency and coarseness of the sandy sequences appears to increase toward shore in the Harihari-1 and Waiho-1 exploration wells.

Upper boundary:
The upper boundary of this sequence is the PPA horizon, dated at near 1.2 Ma. The reflectors are generally concordant with this horizon.

Lower boundary:
The lower boundary is the PPB horizon correlated with the Mangapanian–Waipipian biostratigraphic boundary at around 3.1 Ma. The reflectors of Sequence B generally thin and downlap onto this horizon.

Internal configuration:
Internally the reflectors have high continuity and relatively high amplitude and display a number of the features associated with a prograding complex. This is particularly well seen in seismic profiles such as EZD-3 (Fig. 4.10) where very distinct complex sigmoid-oblique reflection patterns can be seen, complete with topset and foreset segments In more distal sections (e.g. PS-21, Fig. 4.14) these horizons tend to thin out and may downlap against the lower horizon as a bottomset segment. It is interesting to note that at the

distal margin in PS-21 some horizons bear a strong resemblance to the PPA horizon above them, although these horizons appear to be only locally significant.

The complexity of this sequence is revealed on detailed inspection of line EZD-3 (Fig. 4.10). The prograding complex exhibits a range of structures and numerous possible seismic sequence boundaries as defined by reflector terminations. This complexity is reinforced by the reflector configurations seen in EZD-1 (Fig. 4.9) and NZ-102 (Fig. 4.12) which run parallel and perpendicular to the coastline respectively. In EZD-3, the evolution of the sequence through time can be seen where the sequence can be broadly divided into two parts. The basal part of the sequence does not show the prograding configurations of the upper section. The reflectors are generally parallel, but undulose, thinning toward the northwest. Prograding clinoforms become increasingly prominent higher in the sequence, suggesting the basal sequence is the bottomset segment of an earlier prograding sequence now closer to the shore The distal bottomset segments seen in PS-21 (Fig. 4.14) also display a hummocky and discontinuous nature. The prograding foresets display significant structure with some reflectors often truncated, and others laterally continuous as truncating surfaces. Unfortunately the resolution of the seismic profiles limits further investigation of these features, but a complex depositional history is inferred.

External form:

Sequence B is broadly lensoidal and elongate along the coast (Fig. 4.20), a form typical of prograding clinoforms. The thickest part of the sequence (around 1200 m) is closer to shore than that of Sequence A (Fig. 4.21). Figure 4.20 suggests that the sequence occurs in a number of distinct lobes, again a feature typical of a prograding facies.

4.2.3.9 *PPA Horizon*

The Plio-Pliestocene Unconformity A Horizon is unusual as it is only significantly seen in seismic profiles. In typical sections perpendicular to the coastline (e.g. PS-21, Fig. 4.14), the horizon is a prominent arcuate reflector with a dip increasing in steepness toward the coastline. In the Mikonui-1 exploration well the correlation of the horizon with the stratigraphy of the well, at 550 m below the seafloor, does not reveal any significant changes in lithology or density to explain the prominence of the horizon. Neither is it seen in the synthetic seismogram (Figure 4.6). The horizon occurs just below the biostratigraphic Nukumaruan–Castlecliffian boundary, dated at around 1.2 Ma. There is some weak onlap at the proximal end of the horizon, with the distal margin showing weak downlap. This reflector association, along with the prominent arcuate shape would suggest that the horizon is an erosional feature, or at least represents the boundary between two differing depositional regimes. It is interesting to note that in distal sections,

such as PS-21, some horizons near the top of Sequence B also display the prominent arcuate reflection configuration of Horizon PPA.

4.2.3.10 *Sequence A*

Type sections:

Sequence A occurs as an areally restricted lenticular body, a typical section is seen in PS-21 which strikes along the narrow axis of the body as illustrated in Fig. 4.21. The sequence is also well displayed in NZ-102 (Fig. 4.12). This sequence may be analogous with the 'Hawera Series' rocks of the late Pliestocene discussed by Norris (1978).

Well stratigraphy:

The well stratigraphy of Sequence A in Mikonui-1 (Fig. 4.2) occurs between the seafloor (182 metres below sea level) and 730 metres below sea level. The sequence consists of unconsolidated mudstones capped by a thick sequence of bioclasts derived from both shallow and deep water. Onshore, the sequence is not recognised in the exploration wells as a mudstone, but is probably represented by the upper sequences of fluvial and glacial deposits with occasional marine macrofossils seen in the upper parts of those wells.

Upper boundary:

The upper boundary of Sequence A is the seafloor, but due to low resolution and interference no clear interaction between the internal reflectors and the seafloor can be seen.

Lower boundary:

The lower boundary (PPA horizon) is a distinctive arcuate reflector with dip decreasing as it moves offshore. The age of the lower boundary is placed just below the Nukumaruan–Castlecliffian boundary in Mikonui-1 at around 1.2 Ma. Some onlap onto the lower boundary is suggested in the shoreward proximal section (PS-21, Fig.4.14; NZ-102, Fig. 4.12), with downlap and/or apparent truncation due to thinning in the distal section (NZ-102, Fig. 4.12).

Internal configuration:

The internal reflector associations and therefore the seismic structures of Sequence A are often difficult to see due to frequent interference from the primary multiple of the seafloor reflector. However, the internal structure has few laterally continuous reflectors and are of generally low amplitude, this contrasts strongly with the strong continuous reflectors immediately below the lower boundary. The amplitude of the internal reflectors appears to vary laterally in other lines, but can be described as generally hummocky/concordant in distal sections through to chaotic in proximal sections.

External form:

This sequence appears to be confined to a lens running along the present shelf break at between 20 km offshore near Paringa and 40 km offshore on the northern shelf bulge

(Fig. 4.21). Sequence A appears to be at it thickest (about 500 m) at or near the modern shelf break. Fig. 4.21 would suggest that there are two distinct lobes in this distribution, but the gap between these may just be the result of not recognising Sequence A in seismic lines between the two lobes. The shoreward margin of the lens is undefined as no clear truncation of the lower boundary with the seafloor could be seen, although both type sections show it approaching the seafloor. The 'Hawera' beds of Norris (1978) thin to an order of 10-20 m nearshore, so the sequence may simply thin to below the resolution of the seismic profiles used in this study. The seaward margin is again difficult to define, with the sequence thinning and downlapping as the seafloor dips down the continental slope onto the Challenger Plateau (NZ-102, Fig. 4.12). In some locations the sequence appears to have been eroded by the canyons cutting the shelf, and some reflectors in the sequence appear to terminate against the modern seafloor. In PS-15 the sequence abruptly terminates against a small scarp possibly cut by the Hokitika Canyon.

4.2.3.11 *Seafloor*

The seafloor horizon appears prominently on most seismic displays, although the overall physiography of the seafloor is better studied using bathymetry charts (Eade, 1972; Carter, 1981). The seafloor is generally flat lying over most of the study area, with a gentle slope offshore to the northwest. However a number of major canyon systems cut across the shelf in South Westland, especially in the southwest. In the northeast the Hokitika Canyon occurs as an extensive system of canyons and branching channels (Eade, 1972; Norris, 1978). In the southwest the major feature is the Cook Canyon which heads within 3 km of the mouth of the Cook River (Norris, 1978). It turns southwesterly about 40 km from shore and thereafter continues roughly southwesterly into the Puysegur Trench immediately offshore of Fiordland. Branching off the southwesterly extension of the Cook Canyon are a number of shorter canyons reaching into the shelf. The Moeraki Canyon heads about 3 km offshore of the mouth of the Moeraki River, and the Haast Canyon heads offshore the Haast River. A complex of three or more intertwining canyons form just off Jackson Head (Carter, 1981).

In the seismic sections, the southwestern canyon complexes are revealed as steep sided scarps. The most southerly line, NZ-96, shows the shelf edge immediately off Cascade Point with the seafloor plunging around 1500 m in the space of 10 km. Nearby NZ– lines cross the Haast and Moeraki Canyons. NZ-98 does not appear to cross any significant canyons, even though it lies south of the Cook River. Bathymetry would suggest the Cook Canyon becomes broad and flat in the area northwest of Paringa River. The upper reaches of the Cook Canyon are seen crossing the middle of EZD-1. Lines W-14 and W-12 clearly

show the upper reaches of the Moeraki Canyon. In the northeast the PS– lines often show the transition from the shelf into the Hokitika Canyon.

Another notable topographic feature of the shelf is a seaward bulge of the shelf offshore from Ross and immediately south of the Hokitika Canyon. Other studies (e.g. Norris, 1978) have revealed the general form of the canyons, but they await further detailed study, especially in regard to currents and sediments moving through them. Norris (1978) speculates that the Hokitika Canyon may have formed as a result of the combined actions of land streams (Hokitika, Mikonui and Waitaha), or southward drifting littoral currents being deflected seaward by the shelf bulge during a sea level low stand.

4.2.3.12 *Summary of seismic facies*

Using the nomenclature of Sangree & Widmier (1979) the attributes of the sequences are summarised below in Table 4.5:

Sequence	Proximal facies	Distal facies	External form
A	C? – On / C	C? – Dwn / C	Lens
B	C – Dwn / Ob/Sig	C – Dwn / P	Lens
C	C/Er? – Dwn / Ch	C/Er? – On / W	Wedge
D	C/Er? – On / P		Sheet
E	Er – On / P		Sheet

TABLE 4.5: Summary of seismic facies observed in the mapped sequences. Nomenclature after Sangree & Widmier (1979):

upper boundary – lower boundary / internal configuration

C=concordant; Ch=Chaotic; Dwn=Downlap; Er= Erosional truncation; Ob/Sig=Oblique/Sigmoidal progradation; On=Onlap; P=parallel; W=wavy;
see Section 2.1.4.3 for further explanation.

4.2.4 Faulting

The offshore basin exhibits a marked lack of significant faulting, although some of the steeper features in the rugged basement reflector may be or have been fault controlled. The main faulting feature seen in the study area is the poorly understood South Westland Fault Zone.

McNaughton & Gibson (1970) used the Magellan data to identify the presence of an offshore basin separated from coastal outcrops by a large fault zone running parallel to the coastline. Norris (1978) discussed possible links between the South Westland Fault Zone and other faults further north, in particular the Cape Foulwind Fault which also runs parallel to the coast in northern Westland. Nathan et al. (1986) noted that the fault zone marks a distinct break between an apparently continuous offshore sequence and an onshore sequence cut by unconformities during the early Cretaceous and late Miocene, suggesting that the block immediately east of the South Westland Fault Zone has been intermittently uplifted during deposition.

The seismic expression of the fault is indicated by a sharp break in the continuity of reflectors, especially the otherwise prominent basal reflectors. An illustration of this can be seen in seismic line W-13 (Fig. 4.15). Here the prominent basal reflectors between 2.5 and 2.8 twt appear to abruptly end toward the southeastern end of the profile. Reflectors associated with the Top Miocene between 1.8 and 2.0 twt also appear to be truncated at this point. Higher reflectors appear to rise up and over the fault zone, although due to near-surface noise, this interpretation is not clear. The fault appears to be uplifted to the east. The dip direction or angle is not clear from any the seismic profiles that it cuts and further study may be necessary to ascertain this. However given the oblique strike-slip compressive nature of the region the fault zone would be unlikely to be a normally faulted extensional feature. To the east of the fault there are no coherent and laterally continuous reflectors, except for the possible presence of weak diffraction patterns. The lack of reflectors is an indication of either a homogeneous sediment, a strongly deformed zone and/or 'basement' rock (see section 2.1.5.1). The sudden appearance of a homogeneous sediment in a basin dominated by mixed sand and mud deposits is unlikely, and the no reflector zone probably represents an uplifted and probably deformed basement block. Deformation of this zone may be linked to the sheared strata and possible thrust structures seen immediately onshore in the Paringa section (Adams, 1987).

The zone may continue southwards, and faults have been mapped onshore in the Jackson Head area. The coastward end of seismic lines NZ-96, NZ-122 and NZ-123 all show signs of reflector termination similar to the W-13 section (Fig. 4.15). Apparent truncation may also be a result of interference from the rugged seafloor topography found in the southern end of the study area. To ease contouring and mapping difficulties the uplifted block has been continued seaward in the southern corner of the modelled area.

In the north, interference in otherwise prominent basal reflectors is seen in line L-102. Also the top of the uplifted block appears to lie lower in the section with older reflectors around the Top Miocene rising from the basin onto the block. Further north the fault comes

onshore near Waiho-1. The nearby seismic line OS-8 displays weak reflectors in higher levels, but no clear basal reflectors. This may indicate that this line sits entirely on top of the eastern uplifted block. In which case it is interesting to note that higher reflectors appear to have a shallow dip to the northwest.

Other onshore seismic lines in the Abut Head area all display prominent, mostly flat lying and continuous basal reflectors that tie well with nearby offshore reflectors. OS-10 again displays an apparent truncation of basal reflectors, suggesting that the South Westland Fault in the Abut Head area bends inland towards the Alpine Fault in a wide U-bend. Another subsurface fault, possibly a reverse fault, in the basal reflectors is seen in this U-bend on lines OS-2 and OS-3 (Fig. 4.13) immediately northwest of Harihari-1 effectively uplifting the block the well is located in. Further north the South Westland Fault may merge with the Hohonu Fault. The location of the fault in the Abut Head/Harihari area would also seem to closely correspond to the inferred boundary of outcropping Paleozoic basement rocks (Warren, 1967; Nathan et al., 1986).

There is a gap of around 900 metres between the shoreward ends of line L-208 and OS-3A near the mouth of the Poerua River. The ends match well with respect to twt depth of the basal reflectors suggesting that no significant near coastal fault occurs in the area and the main zone of deformation exists inland with the continuation of the South Westland Fault Zone. Further north, in L-206 (Fig. 4.11), a near coast fault may account for the sudden thickening of older sequences. Such a fault may be the southern continuation of the Cape Foulwind Fault as postulated by Norris (1978).

In summary, the South Westland Fault Zone is uplifted to the southeast and is seen in seismic reflection profiles by the abrupt truncation of otherwise clearly prominent and continuous reflectors. The uplifted block displays no coherent and continuous reflectors suggesting that it is a deformed basement unit. Surface geology generally describes undifferentiated Greenland Group rocks, in which Adams (1987) postulated localised depocentres. The uplifted block appears to dip toward the north as older reflectors are seen rising from the basin and onto the block. The bounding South Westland Fault Zone evidently comes onshore near Waiho-1 and bends inland toward the Alpine Fault in the vicinity of Harihari.

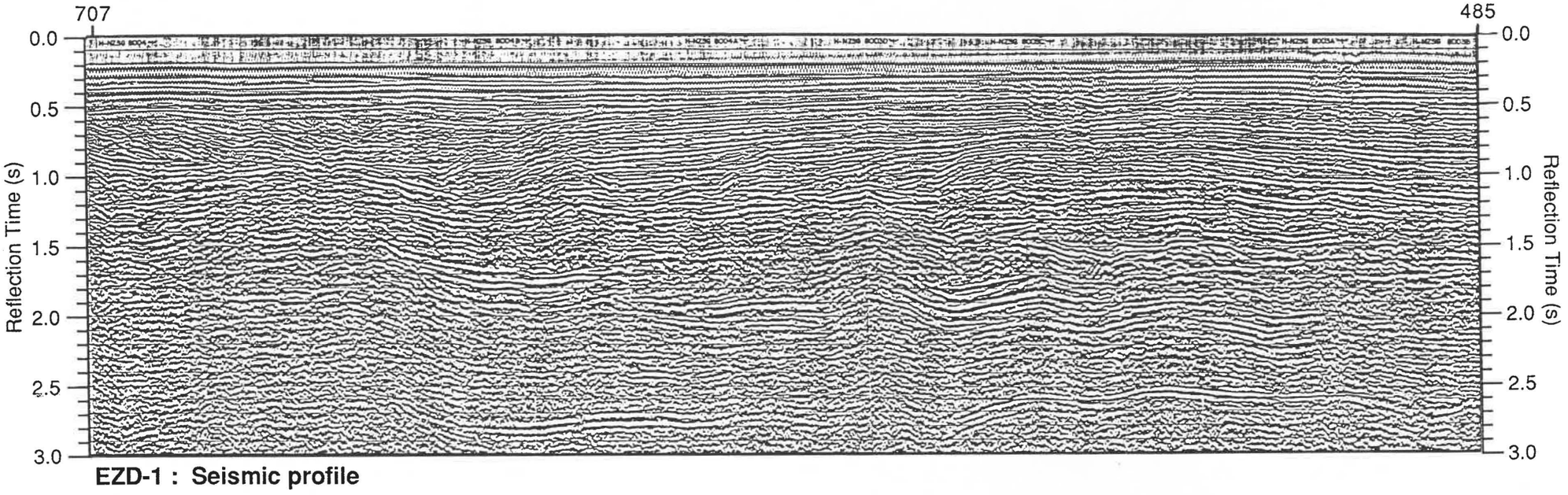

FIGURE 4.9: EZD-1 seismic profile and interpretation.

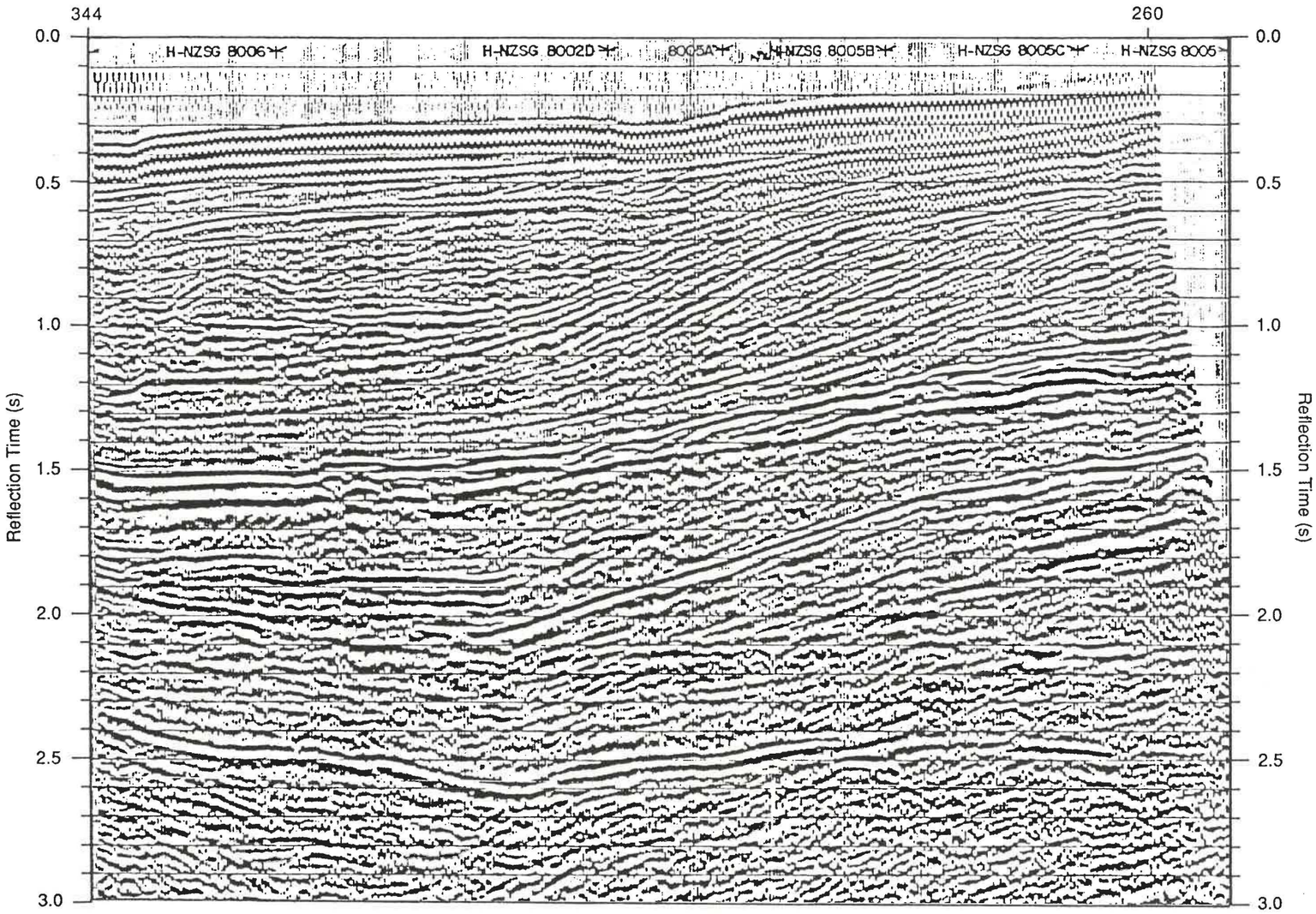

EZD-3 : Seismic Profile

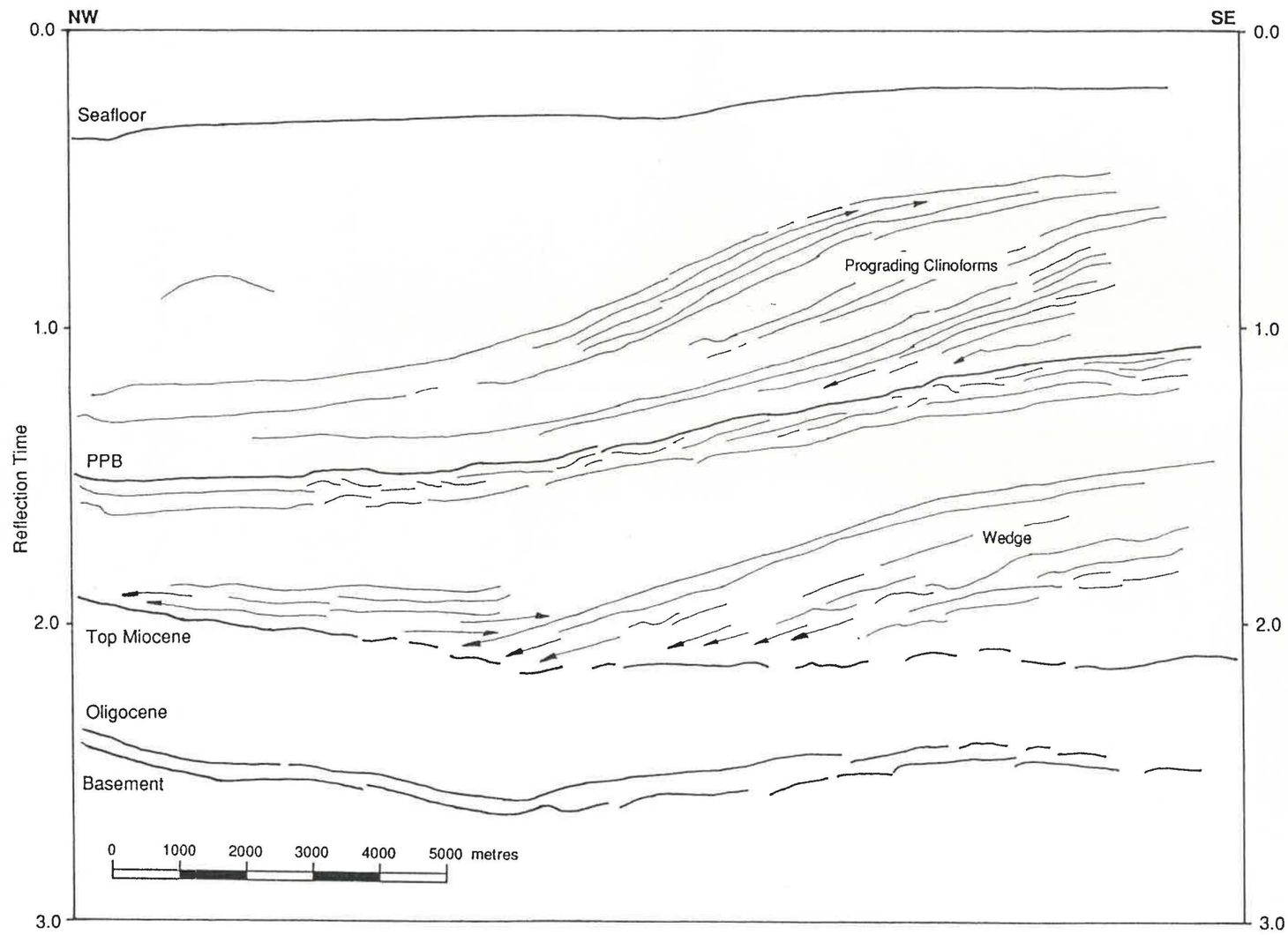

EZD-3 : Interpretation

FIGURE 4.10: EZD-3 seismic profile and interpretation.

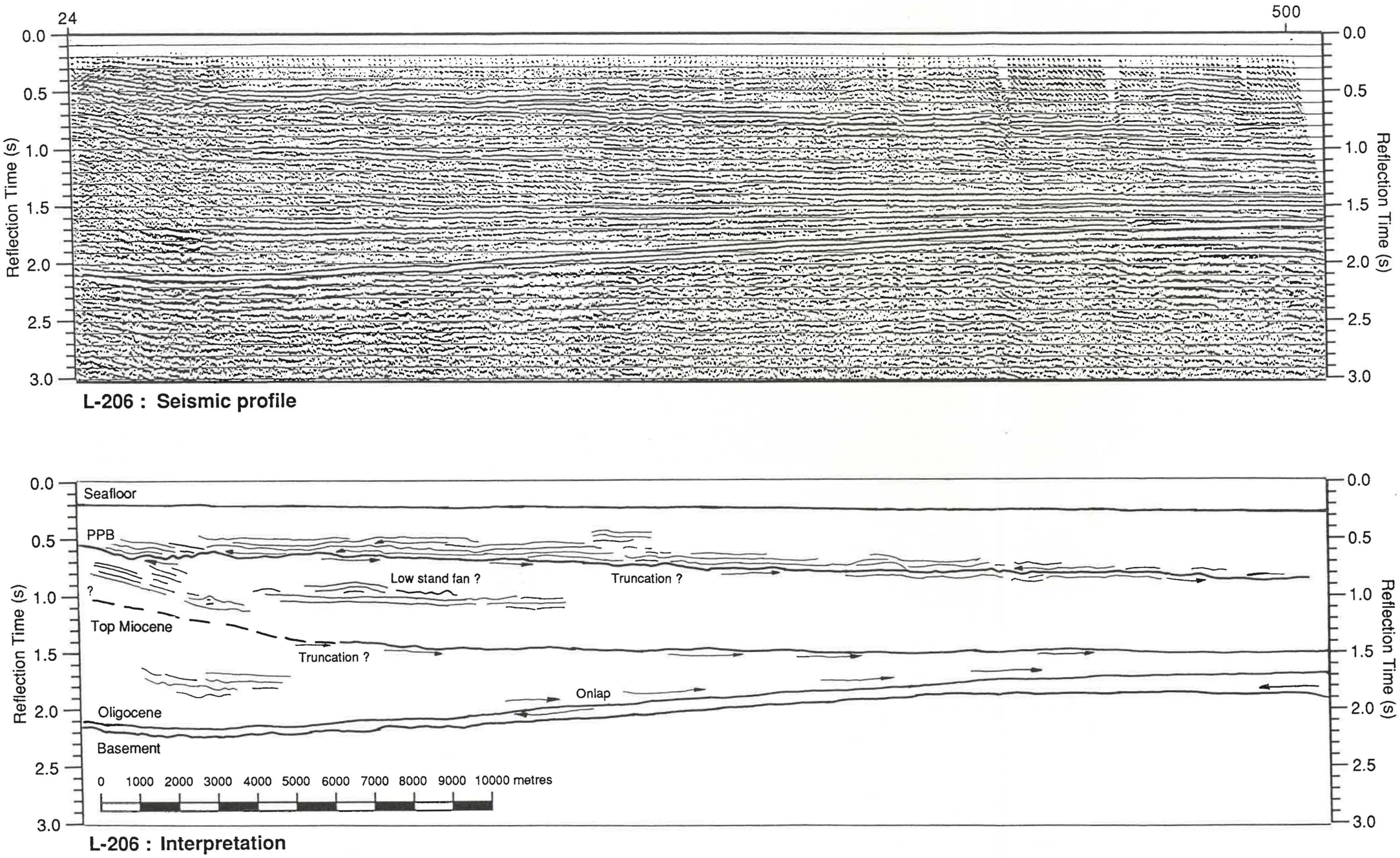

FIGURE 4.11: L-206 seismic profile and interpretation.

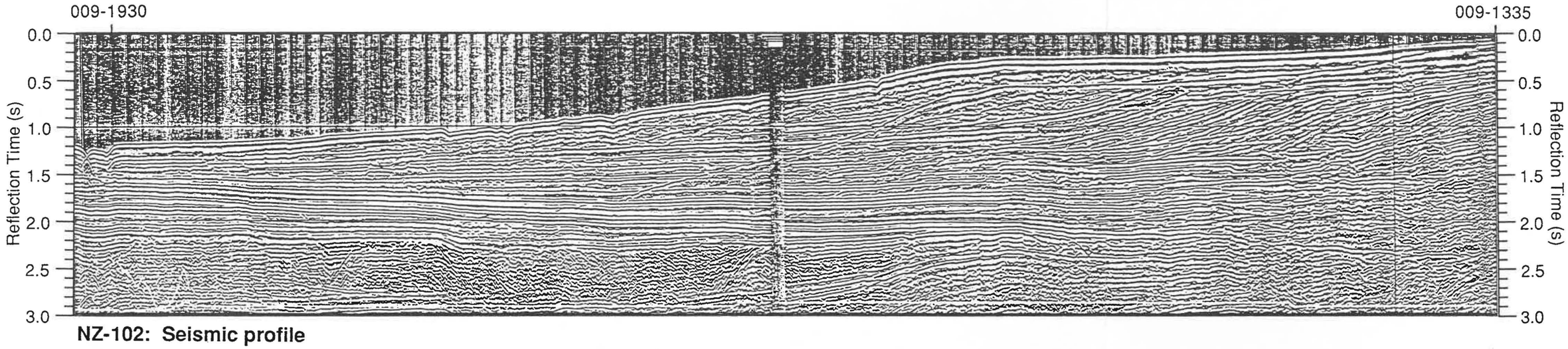

NZ-102: Seismic profile

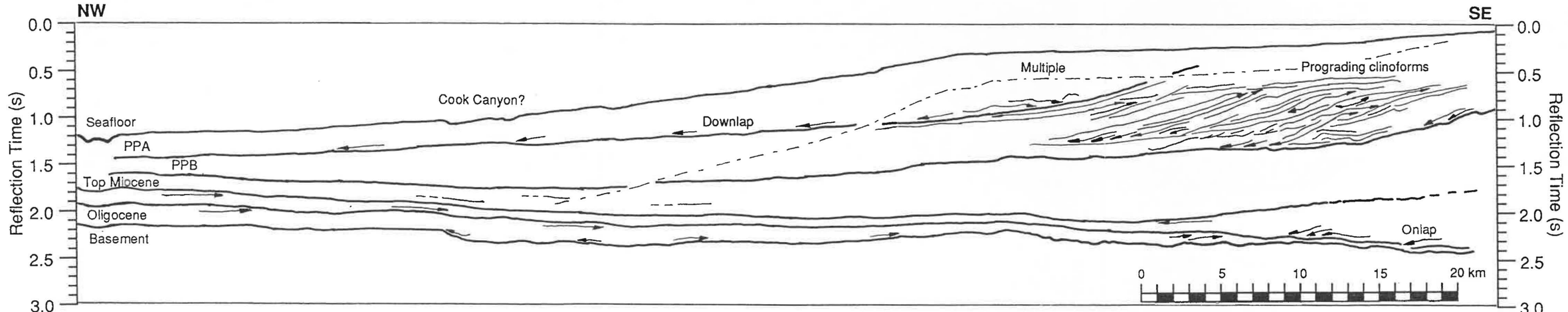

NZ-102: Interpretation

FIGURE 4.12: NZ-102 seismic profile and interpretation.

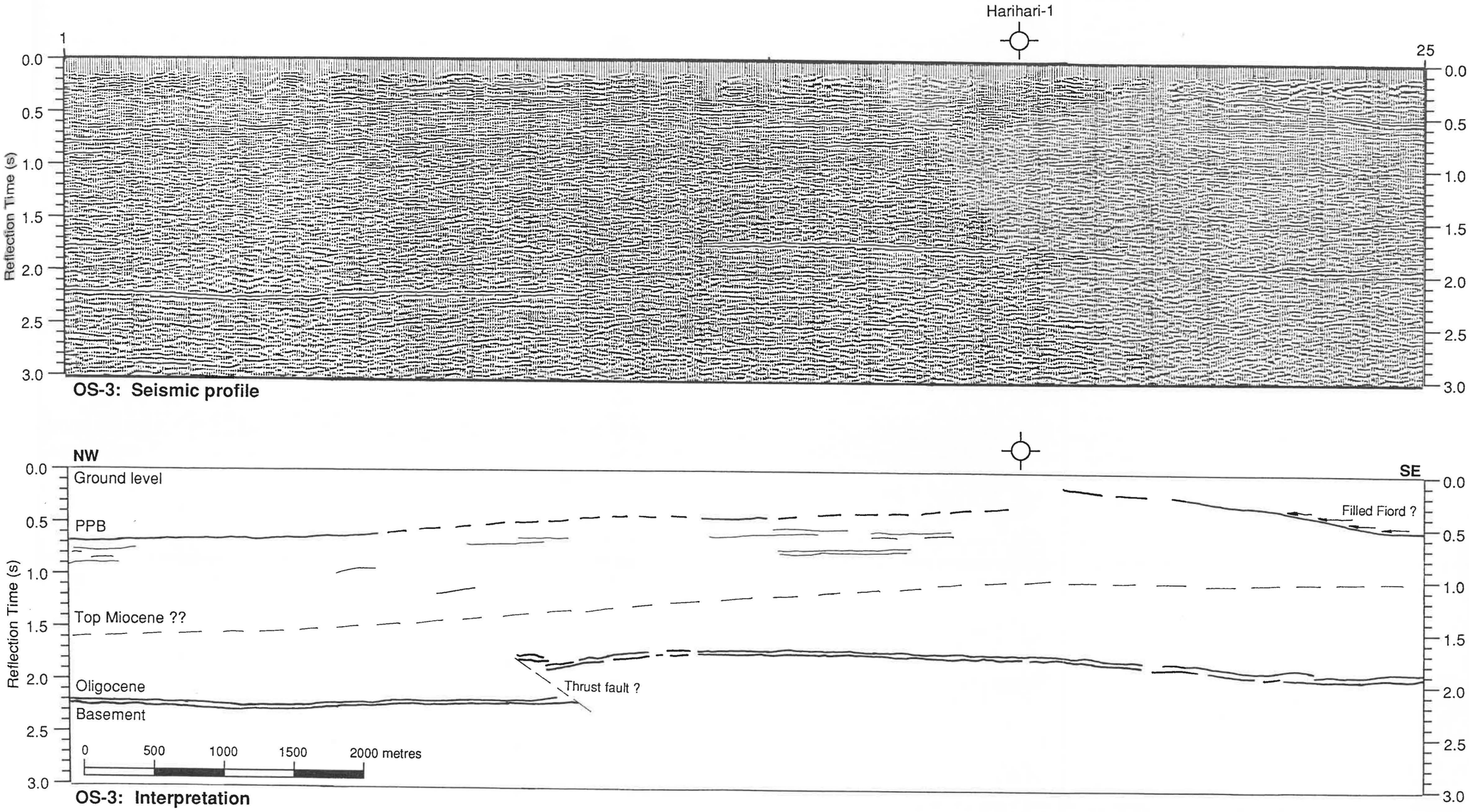

FIGURE 4.13: OS-3 seismic profile and interpretation.

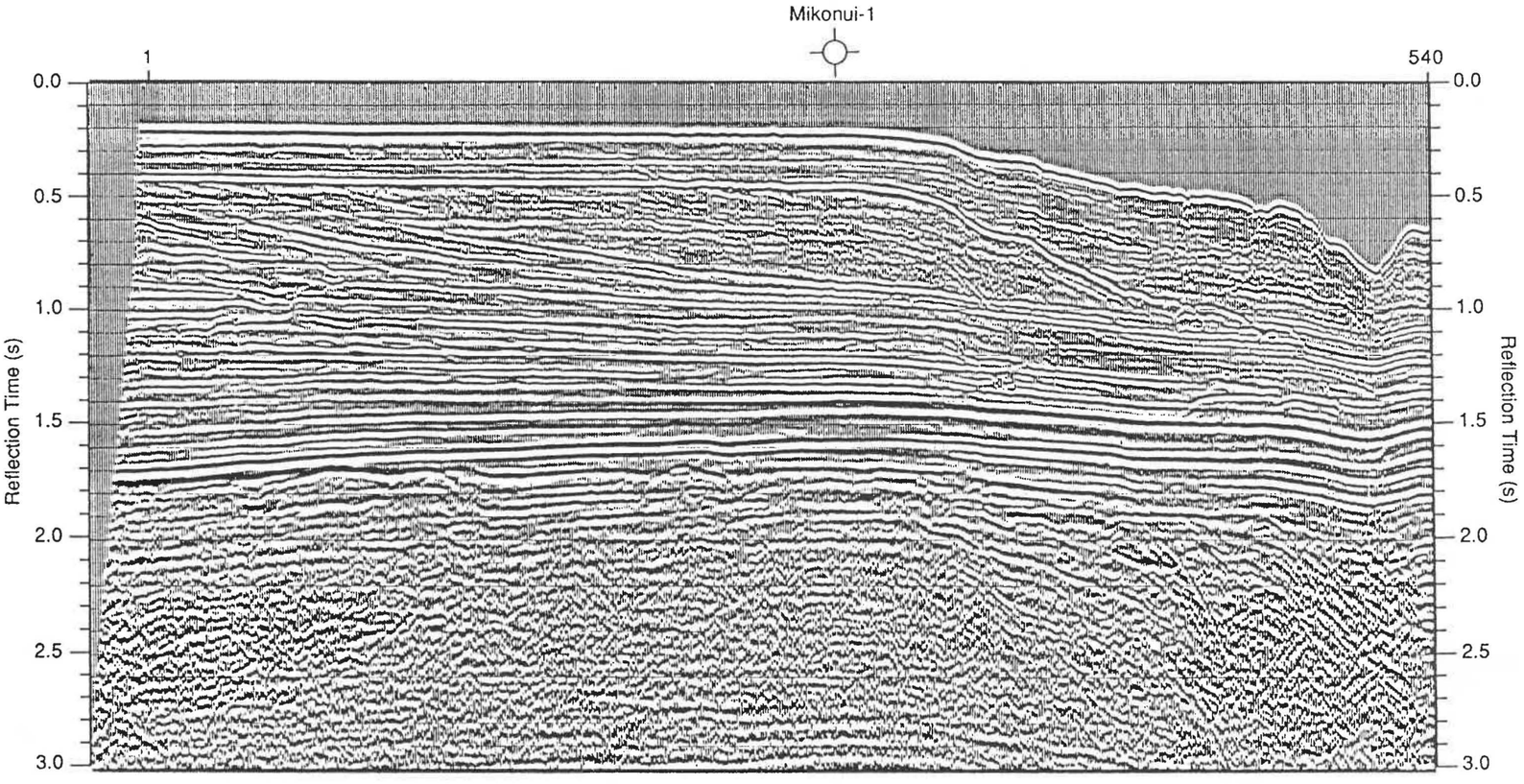

PS-21: Seismic profile

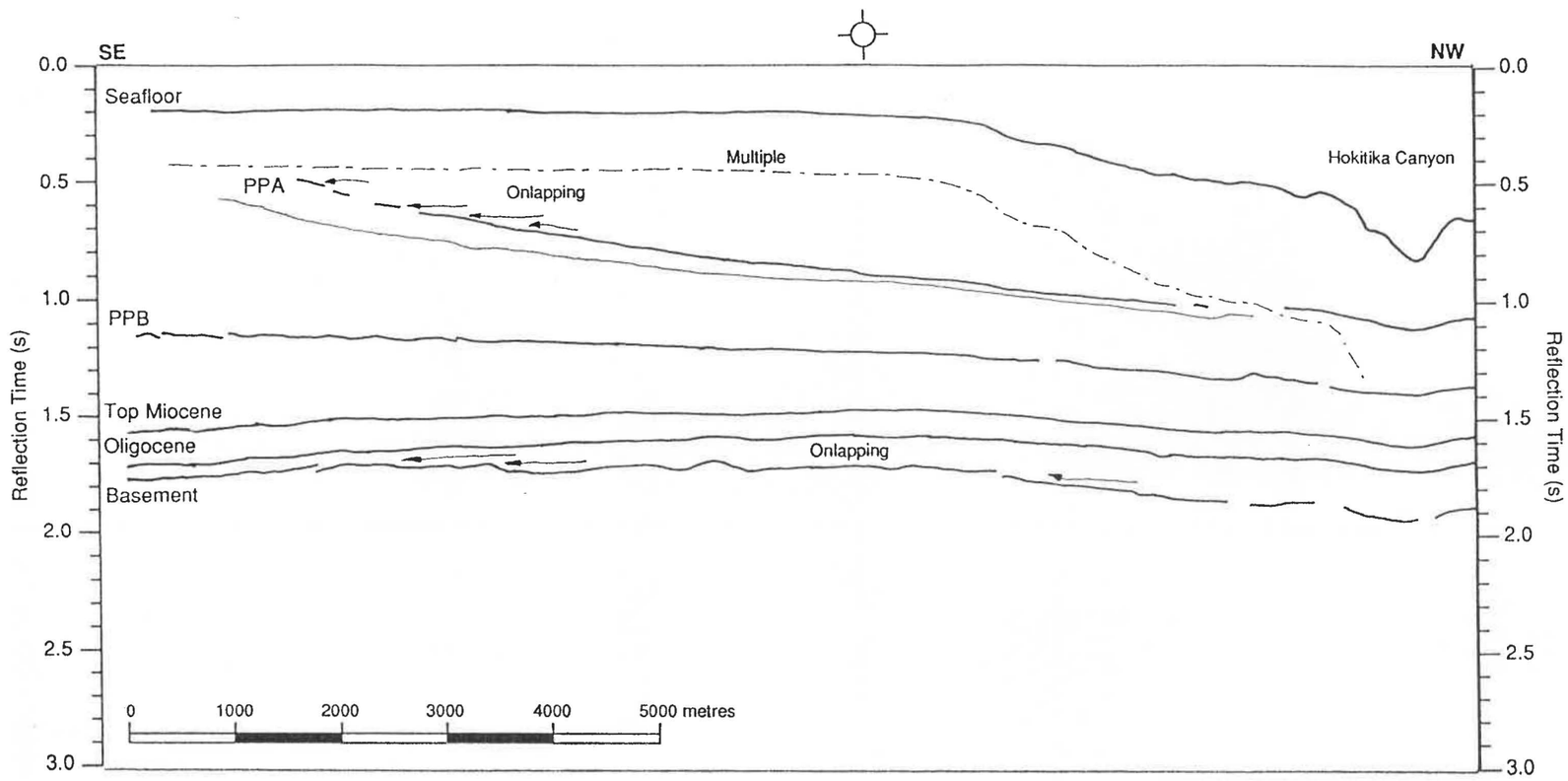

PS-21: Interpretation

FIGURE 4.14: PS-21 seismic profile and interpretation.

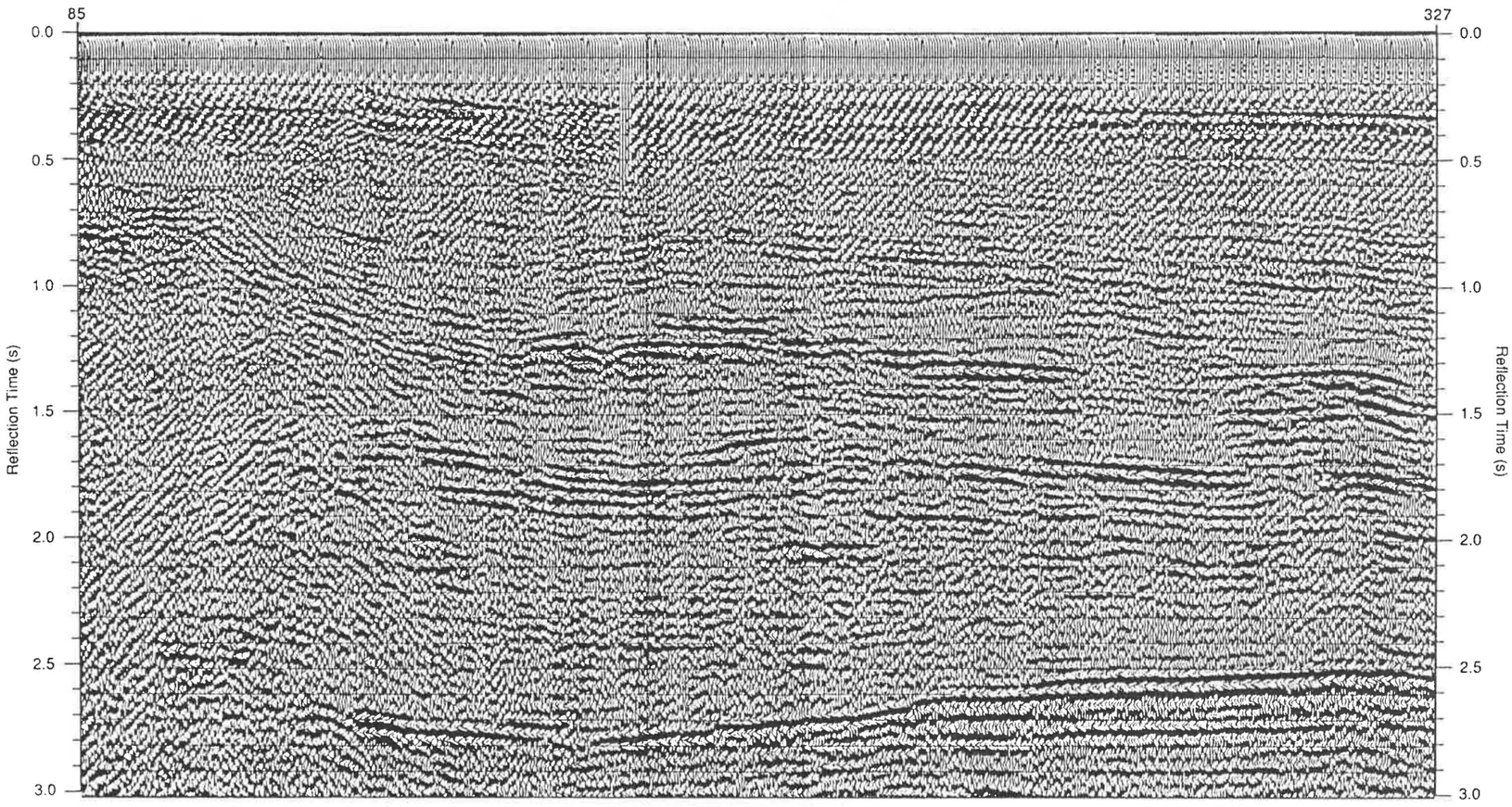

W-13 : Seismic profile

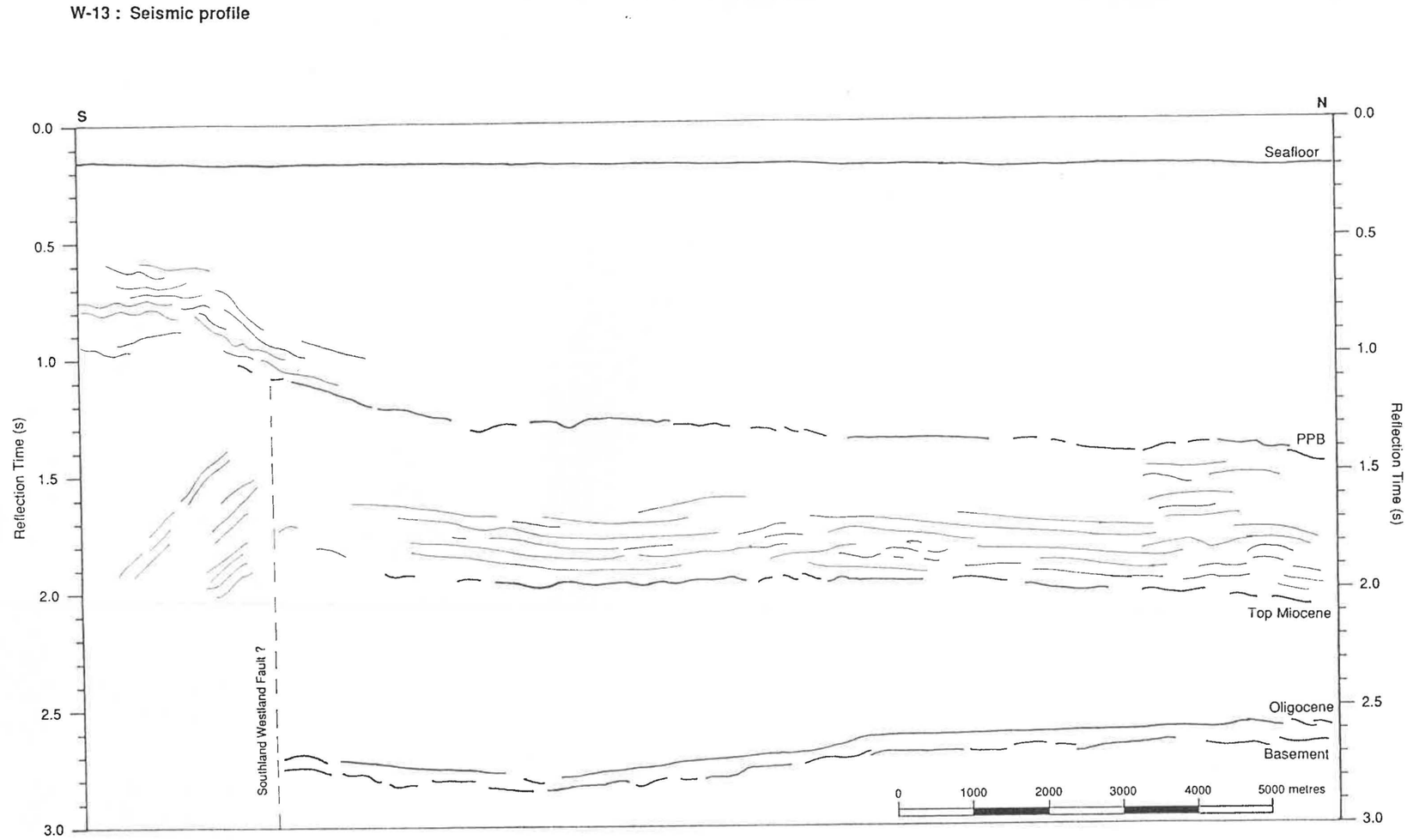

W-13 : Interpretation

FIGURE 4.15: W-13 seismic profile and interpretation.

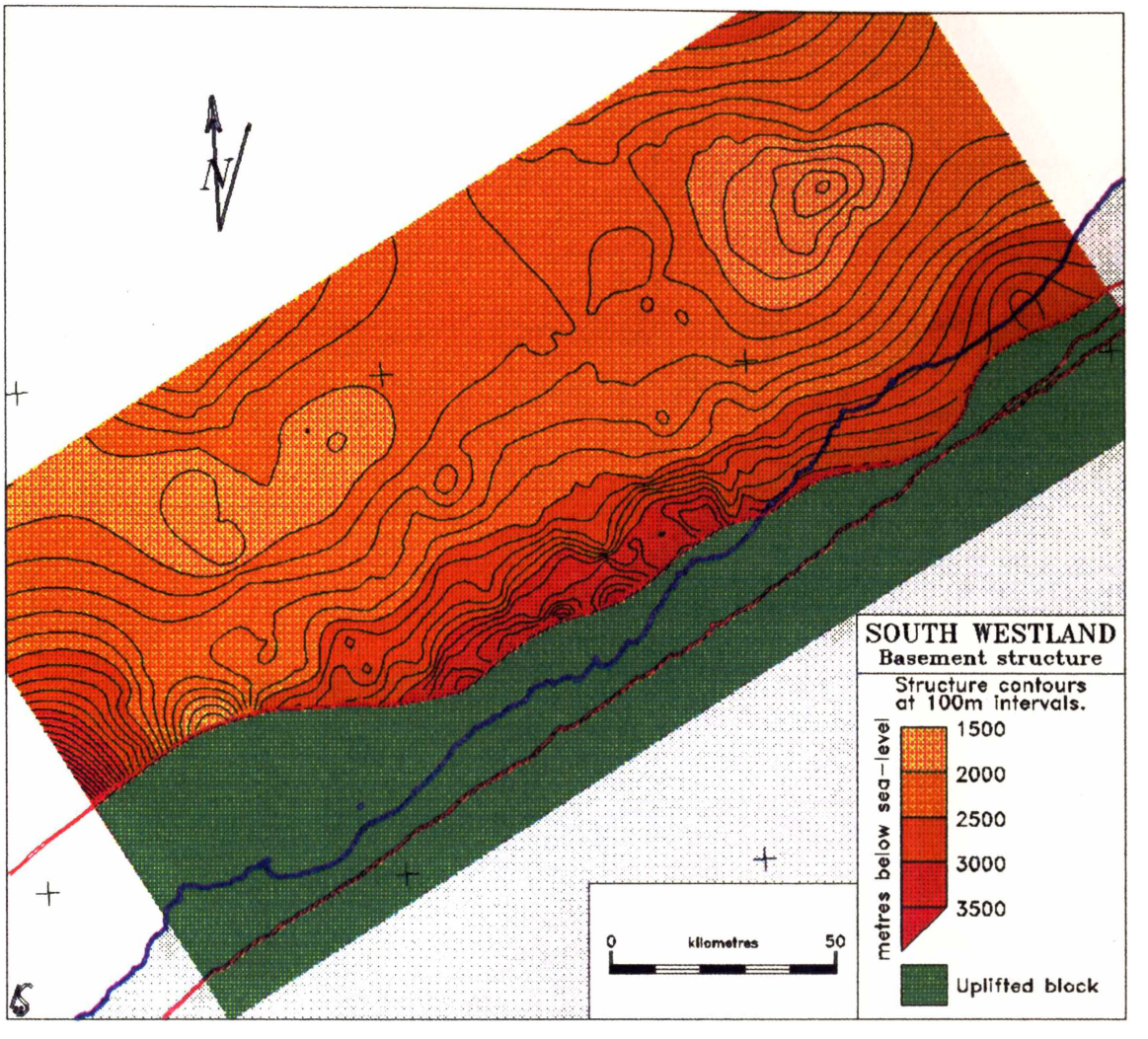

FIGURE 4.16: Basement structure contour map.

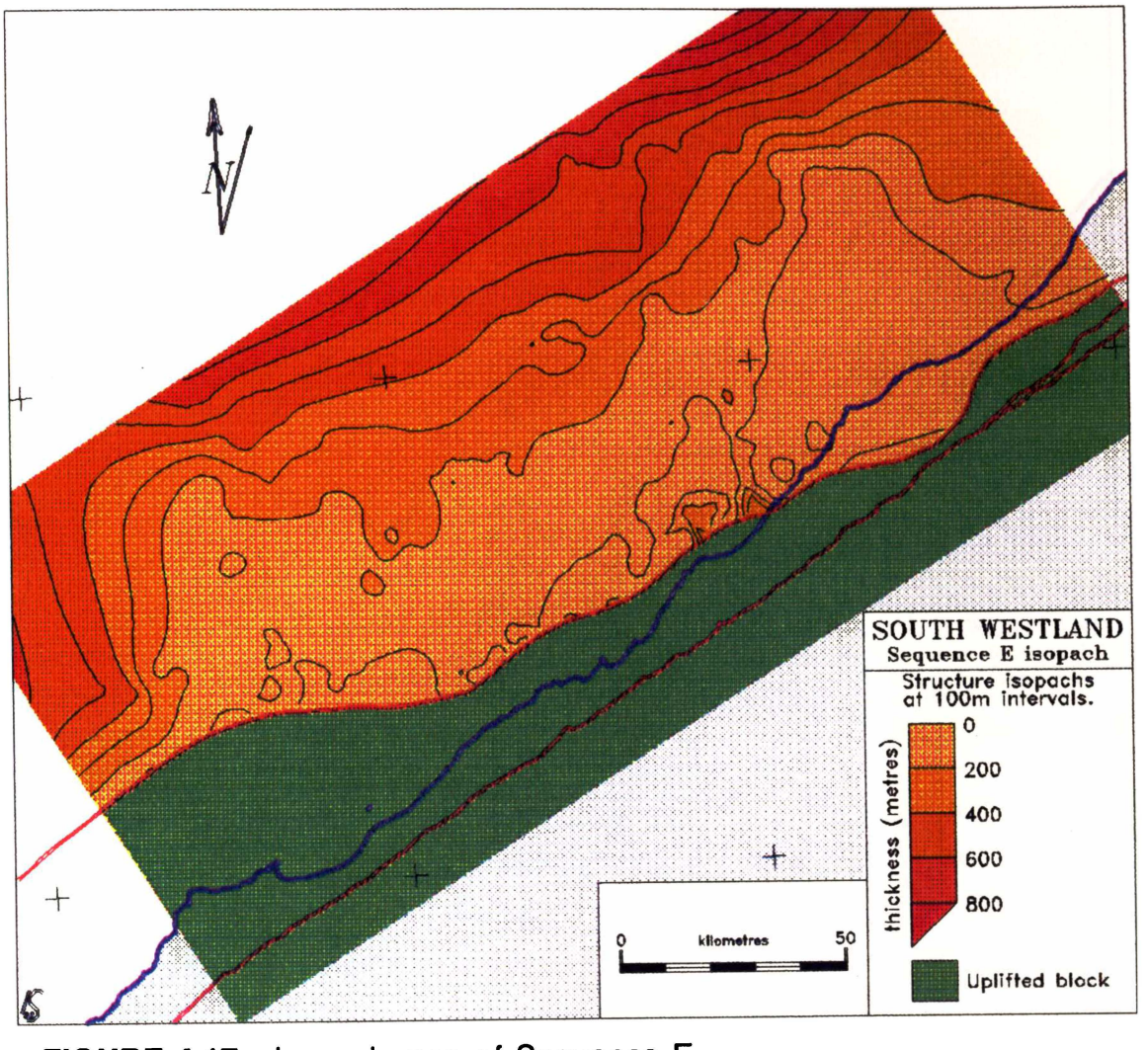

FIGURE 4.17: Isopach map of Sequence E.

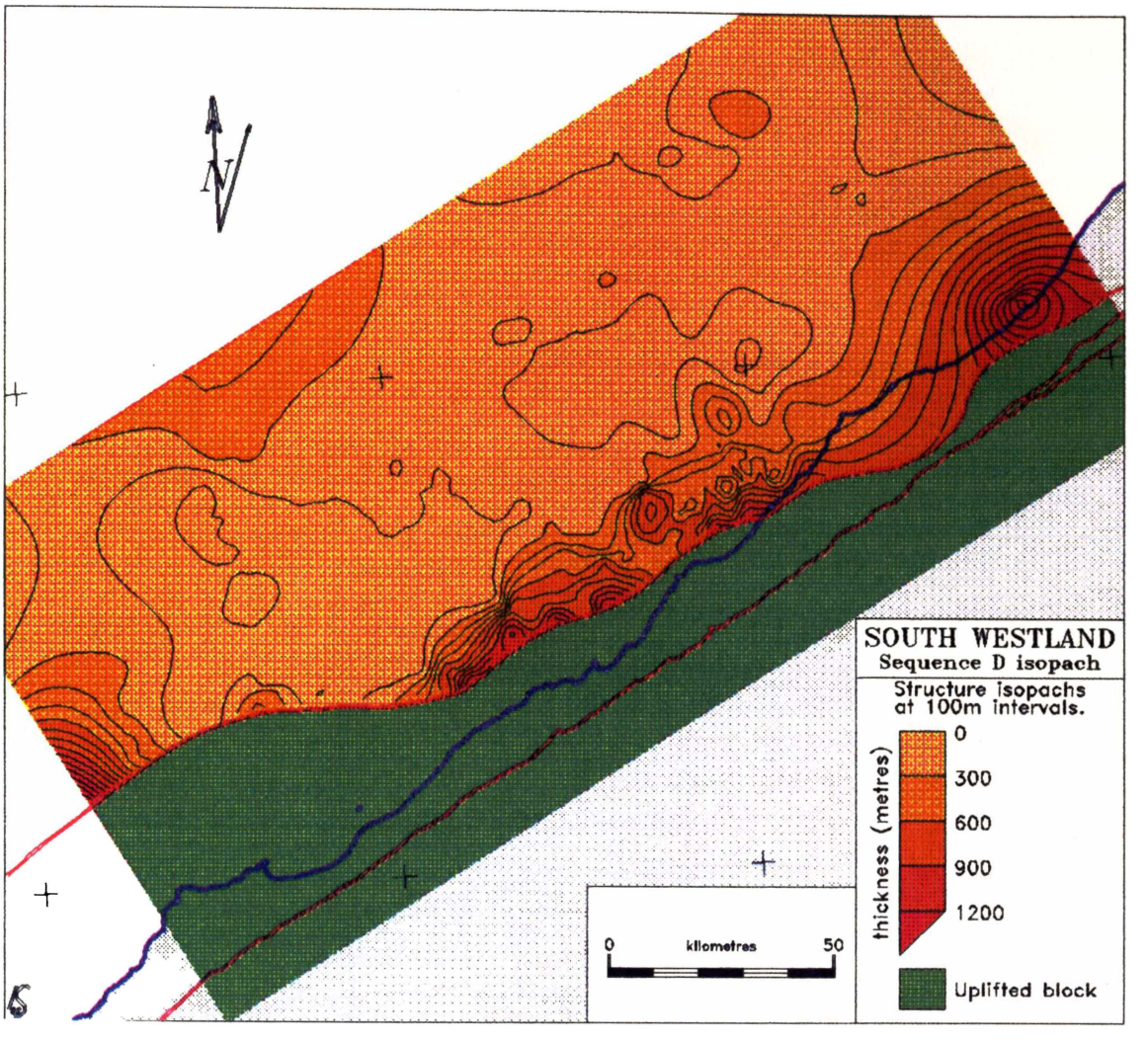

FIGURE 4.18: Isopach map of Sequence D.

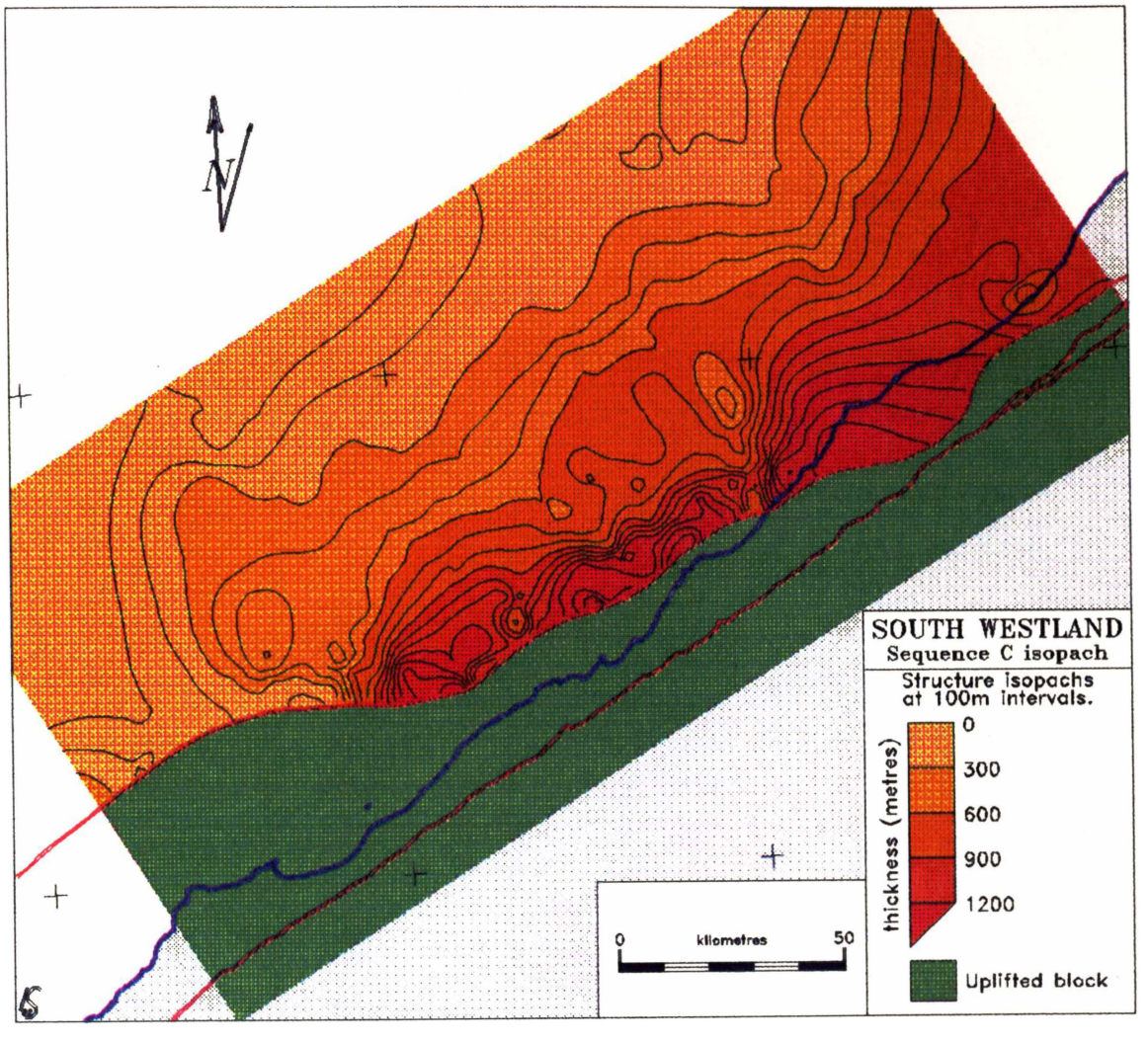

FIGURE 4.19: Isopach map of Sequence C.

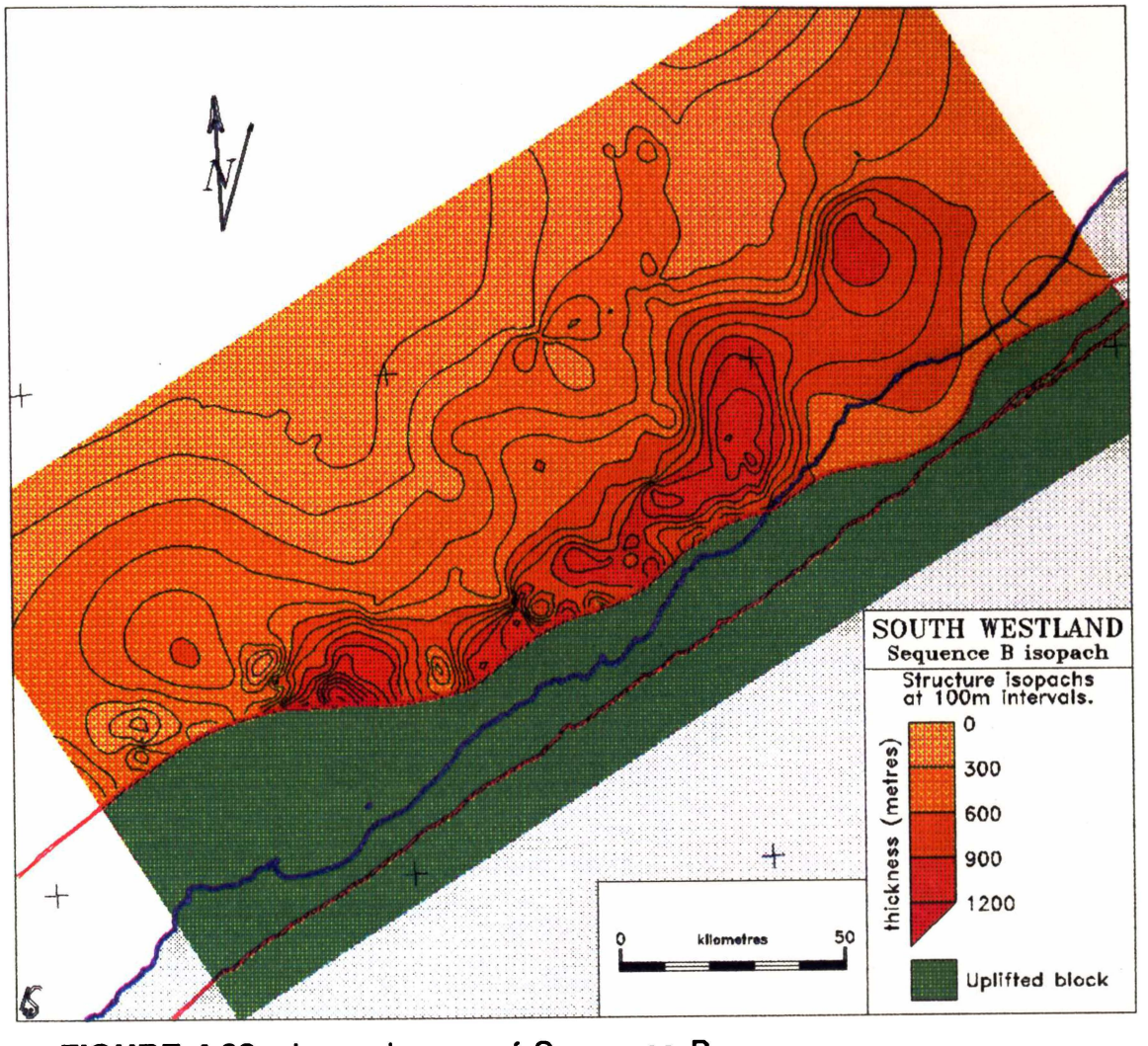

FIGURE 4.20: Isopach map of Sequence B.

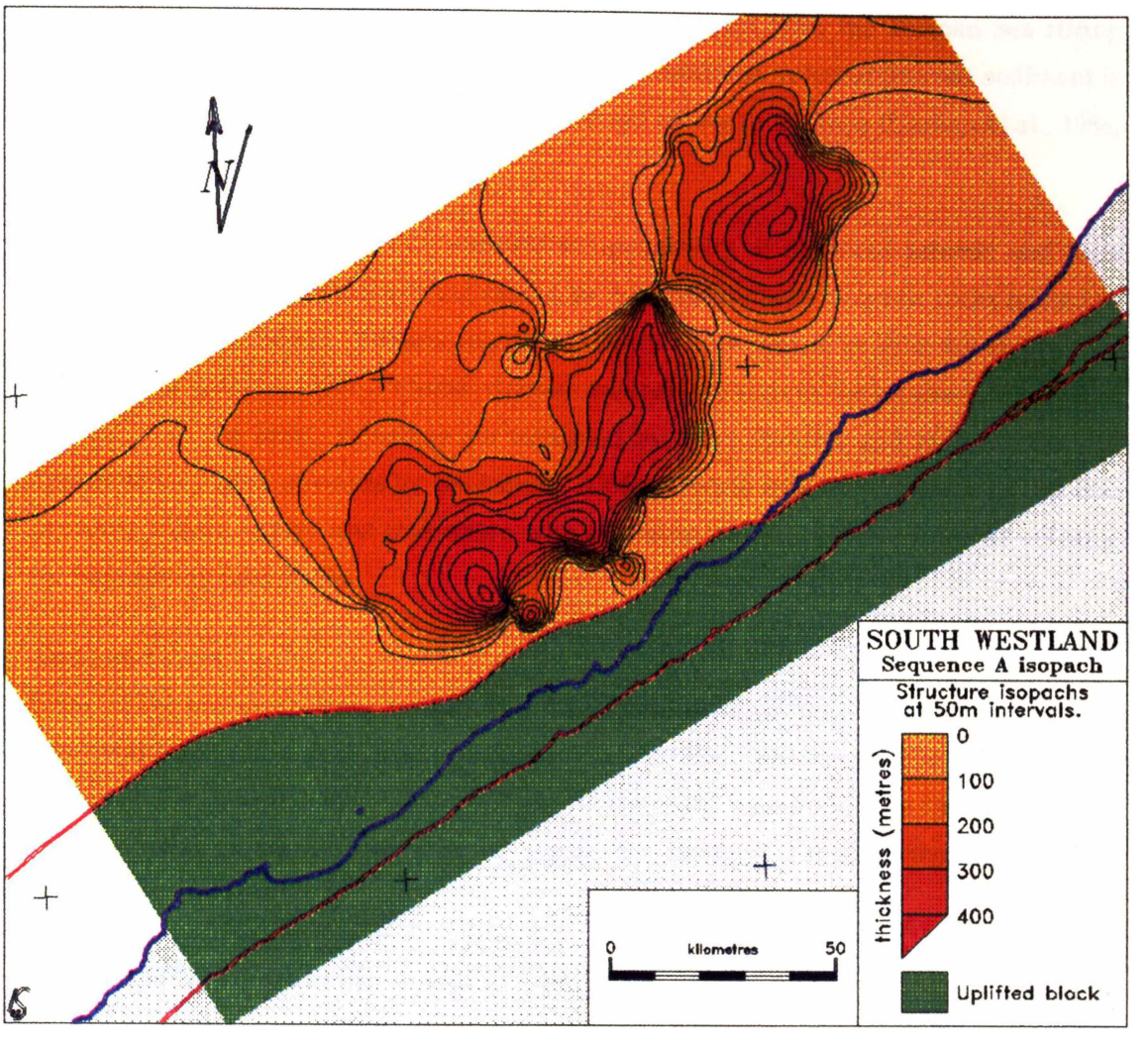

FIGURE 4.21: Isopach map of Sequence A.

4.2.5 Other seismic features

Volcanic intrusions

Two basaltic units have been studied in South Westland. The Arnott Basalt is of Late Cretaceous to Paleocene age and thought to be associated with the Tasman Sea rifting event at that time. The younger Otitia Basalt and associated volcanic derived sediment is of late Eocene age and possibly related to renewed rifting in the area (Nathan et al., 1986; Sewell & Nathan, 1987).

McNaughton and Gibson (1970) outlined the possibility of observed seismic and high amplitude magnetic anomalies being caused by near surface basic volcanic rocks related to the outcrops seen onland. Volcanic intrusions inferred from seismic profiles are mapped by Nathan et al. (Map 8, 1986). Possible volcanic mounds are seen in the southwestern half of line EZD-1. The basal reflectors are truncated by these features and higher reflectors appear to be folded upwards by the feature. Unfortunately seismic resolution in this line prevents a clear outline and interaction with adjoining reflectors of the inferred volcanic intrusion being interpreted.

Onshore basins

Some of the onshore seismic profiles (e.g. OS-3) display a prominent near surface convex downward horizon that defines a wide depression. The reflectors in this depression or basin are undulose and exhibit some onlap onto the lower boundary. The fill is most likely glacial-fluvial outwash as seen at the top of the Harihari-1 well further to the west along the same profile.

4.3 Further geologic observations

4.3.1 Sedimentation volumes and rates

The decompacted volumes of the mapped sedimentary sequences can be calculated using the TECHBASE database and totalling the values for each sequence in each cell. All figures exclude sediments to the east of the South Westland Fault Zone, and thus cover an area of 23464 km^2. Note that due to the areally restricted nature of Sequence A, the rate of deposition given here has probably been underestimated. All rates of deposition compare well with those calculated for the well sections (Tables 4.2, 4.3, 4.4).

These volumes and rates are given in Table 4.6 and graphically illustrated in Fig. 4.15. The younger sequences, A, B, and C have the highest sediment volumes and sedimentation rates, and together account for 65% of the total sedimentary volume. Tippett (1992) estimates that around 120000 km^3 of material has been removed from the Southern Alps

during their uplift. From these estimates it can be said that about a quarter of that amount has been deposited in the South Westland Basin.

Sequence	Decompacted volume (km^3)	Average volume deposition rate (km^3 / Ma)	Average sedimentation rate (m / Ma)
A	2359	1966	84
B	10684	5623	240
C	15233	7617	325
D	10905	1091	46
E	4524	151	6
Total	**43705**		

TABLE 4.6: Estimated decompacted sediment volumes and rates in the South Westland Basin for each mapped sequence.

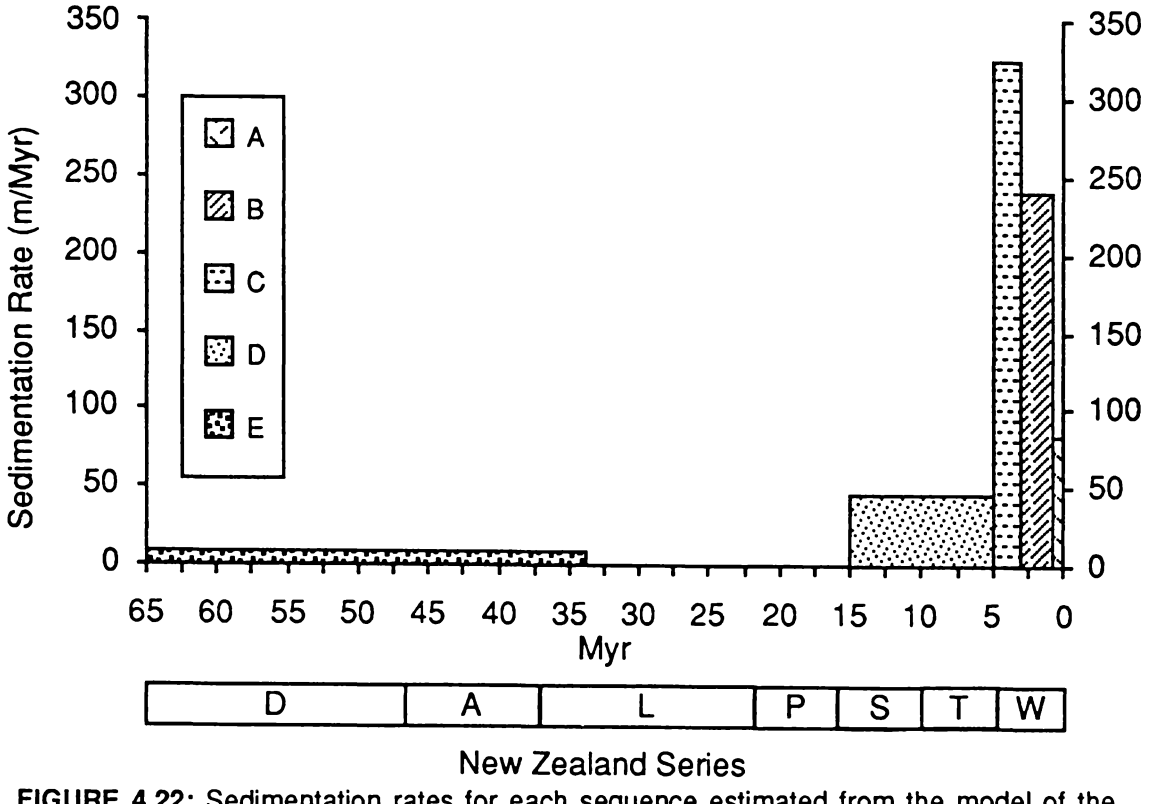

FIGURE 4.22: Sedimentation rates for each sequence estimated from the model of the South Westland Basin.

4.3.2 Petrography

No petrographic analysis were undertaken in this thesis. Instead, petrographic data from other studies (Nathan, 1977, 1978; Adams, 1987) have been incorporated here for further interpretation. Modal analyses (details given in the Appendices) for samples from various Late Cretaceous–Miocene sediments have been used to compile a triangular QFL

diagram for comparative provenence studies (Fig. 4.16). The comparative provence types given by Dickinson & Suczek (1979) are outlined in Section 3.5 and Fig. 3.11.

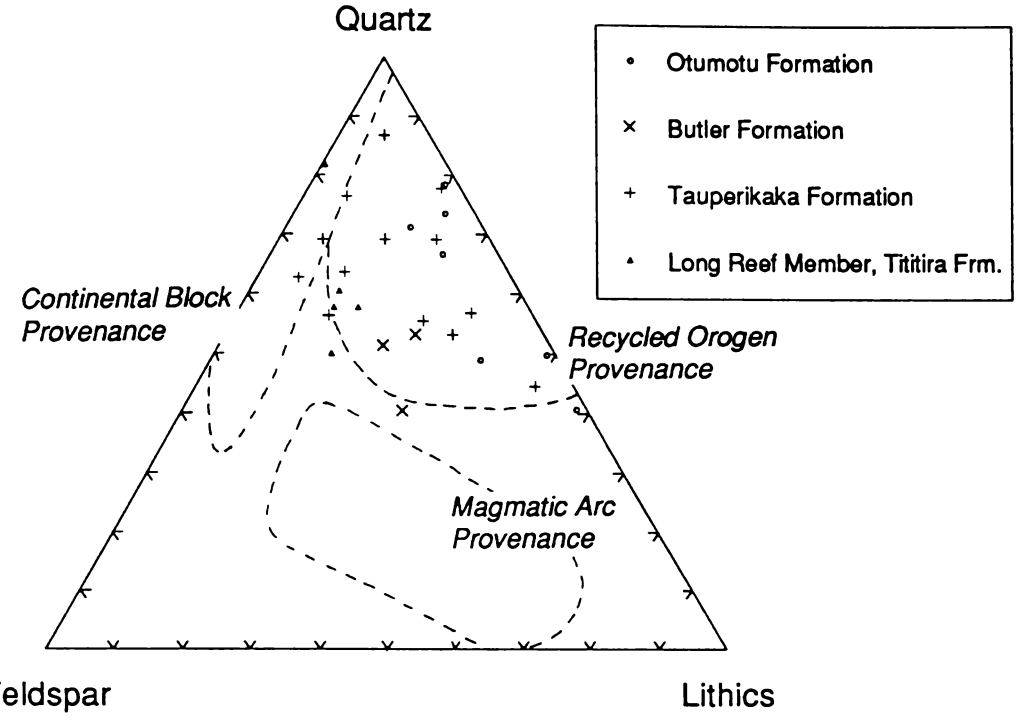

FIGURE 4.23: QFL diagram of Late Cretaceous–Eocene sediments studied in onshore South Westland (data from Nathan, 1977, 1978; Adams, 1987).

4.3.3 Geophysical observations

Completing the broad survey of geologic information in the study of the South Westland Basin is geophysical data from gravity and magnetic studies. A number of gravity and magnetic anomaly maps covering the study area have been compiled (e.g. Woodward, 1975; Davy & Davey, 1985; Rose & Davey, 1985). The gravity anomalies across the study area are fairly complex, dominated by two large negative anomalies. To the southwest is a large regional anomaly of around -900 μN/kg (-90 mgal), believed to be associated with the formation of a root of continental crust underneath the Southern Alps (Allis, 1981, 1986). To the southwest is another regional scale anomaly in the order of -2000 μN/kg (-200 mgal) which is associated with the ocean-continent convergent Puysegur margin, although complicated by inherited tectonic structures in the Fiordland block (Kamp & Hegarty, 1989). The anomaly associated with the Puysegur margin appears to run northeast into the southwestern corner of the study area (Fig. 4.17). To the northeast and around 60 km offshore, a gravity high of +200 μN/kg (+20 mgal) is seen in the vicinity of the Mikonui-1 well and basement high.

Aeromagnetic surveys have been used to delineate a NE-trending belt of high amplitude (100–300 nT) positive magnetic anomalies immediately offshore between the Cook River

and Haast township. This anomaly is correlated with outcrops of Arnott Basalt at Arnott Point, and thought to represent a linear volcanic centre (McNaughton & Gibson, 1970; Nathan, 1977; Sewell & Nathan, 1987). It is interesting to note that the magnetic anomalies appear to be orientated along the 'Coastal Monocline', suggesting that the eruptive centres were structurally controlled (Nathan, 1977).

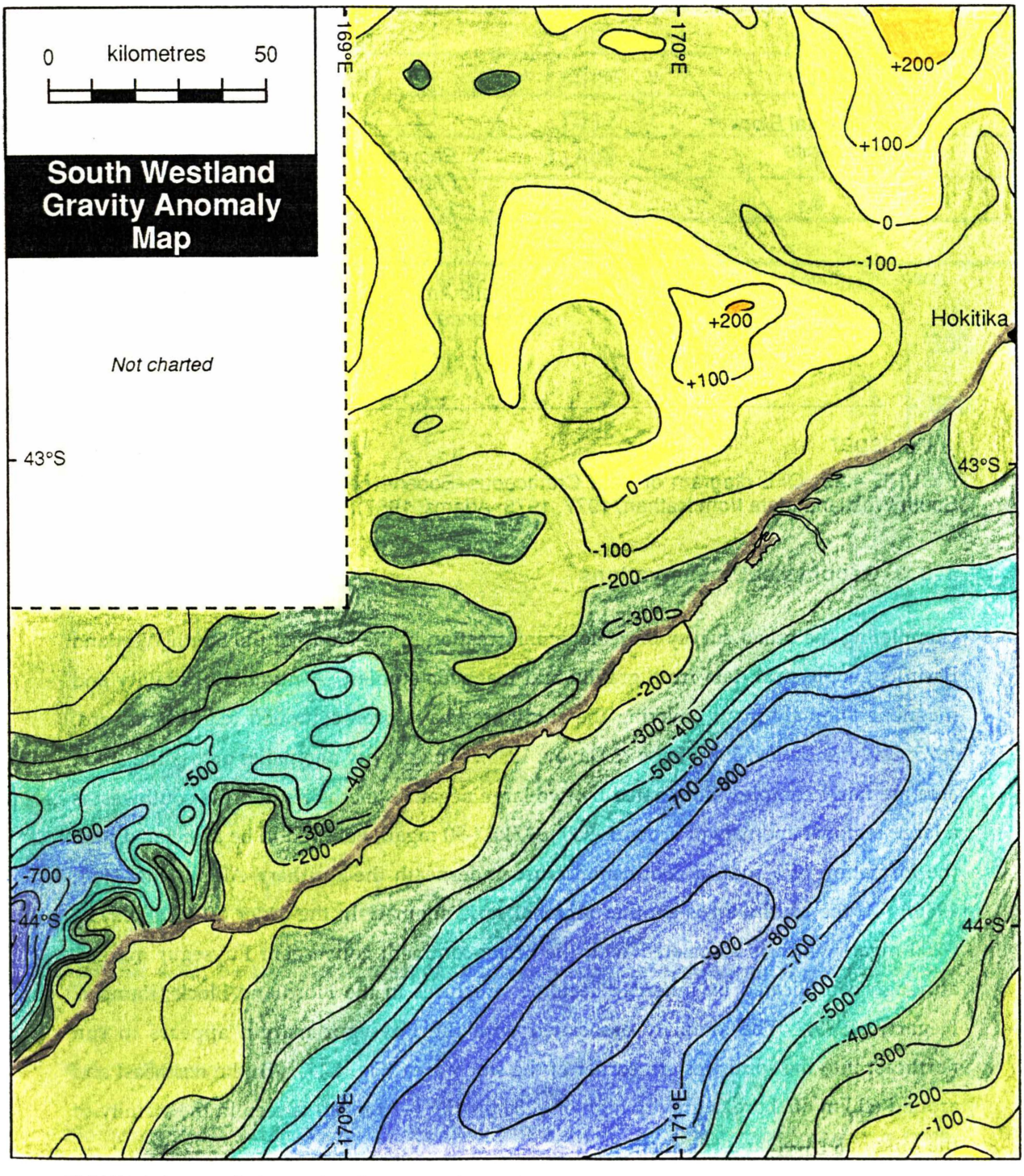

FIGURE 4.17: Schematic diagram of gravity anomalies across the study area and surrounding regions in the South Island. Free Air Anomalies over sea, Bouguer Anomalies over land. Contour units in μN/kg. Note 10 μN/kg = 1 mgal.

Chapter 5

Interpretation and Discussion of Basin Analysis in South Westland

5.0 Introduction

In Chapter 4 the various methodologies of basin analysis were applied to geological, geophysical and industry acquired seismic data from the South Westland Basin. The objective of this chapter is to interpret the observations of Chapter 4, in particular in the terms of features that may be associated with foreland basins.

5.1 Exploration well stratigraphy

The stratigraphy of the three exploration wells drilled in the basin are dominated by thick Miocene–Pliestocene mudstones with occasional interbedded sand and conglomeratic layers (Fig. 4.2). The basement has been correlated with the Greenland Group, overlain, where present, by a thin, possibly marginal marine, coal measures sequence. Above this is a regionally extensive shallow to upper bathyal marine bioclastic limestone. Overlying the limestone unit are the thick mudstone sequences deposited in bathyal through to shelf marine environments. A comparison of the well and outcrop stratigraphy in South Westland with the 'classical' foreland basin sequence from the North Alpine Foreland Basin (NAFB) (Allen & Allen, 1990) is given below in Table 5.1.

From this comparison, a number of similarities and differences are highlighted between South Westland and the classical model. In both basins there is a similar overall sedimentation pattern or megasequence, involving rapid basin subsidence followed by a gradual shallowing upwards of sediment as the basin is filled. However, the successions underlying the Molasse deposits formed in different differing tectonic settings. In the classical model, the inception of a foreland basin was the result of lithospheric loading and associated rapid subsidence. In South Westland, the possible inception of a foreland basin occurred after long term gradual subsidence phase. This difference in early stage basin formation is reflected in the sediments deposited.

The two basins have similar sequences of thick turbiditic deposits derived from active denudation of uplifted crust in the hinterland of the collision zone. In the NAFB these turbidites gradual grade upwards into shallow and marginal marine sedimentation and continental 'Molasse'. In South Westland such deposits are restricted to the uplifted inner margin, although the prograding Foreset beds noted in the seismic sections (see Chapter 4 and interpretation below) may represent the overall shallowing of the basin. The restricted nature of the Molasse equivalent sediments may indicate that the South Westland Basin has not fully evolved to a completely filled basin as in the NAFB.

North Alpine Foreland Basin	South Westland Basin
⑦ **Upper Freshwater Molasse:** the final choking of the NAFB by coarse continental clastics.	⑥ **Recent 'Molasse'** coarse glacial derived clastics with occasional marine fossils. Restricted to uplifted inner margin.
⑥ **Upper Marine Molasse:** represent shallow marine and estuarine depositional systems.	
⑤ **Lower Freshwater Molasse:** first fluviatile and lacustrine deposits of NAFB.	
④ **Lower Marine Molass:** transition from shelf to shoreline sedimentation.	⑤ **Foreset beds*:** the transition from deep marine to shelf depth sedimentation?
③ **North Helvetic:** represent turbiditic depositional systems shed from the active orogenic wedge.	④ **Tititira Formation:** represent turbiditic depositional systems shed from active oblique collisional zone.
② **Nummulitic limestones and Globigerina shales:** represent foreland drowning.	③ **Bioclastic limestone:** represent marine transgression across thermally subsiding continental block.
No equivalent ?	② **Coal Measures:** represent marginal marine conditions in localised rift depressions.
① **Basal unconformity:** due to regional uplift of the foreland lithosphere.	① **Basal unconformity:** due to orogenic uplift of lithosphere and subsequent thermal contraction.

TABLE 5.1: Comparison and interpretation of 'classical' foreland basin megasequences from the North Alpine Foreland Basin (Allen & Allen, 1990) and broad sequences in the South Westland Basin (this study). * Foreset beds are described and interpreted below.

The loss of sediment accommodation potential invokes the evolution of foreland basins from an underfilled stage, through overfilled to a steady-state as described by Covey (1986) for the western Taiwan foreland basin. Similar descriptions can be applied to the NAFB, and the South Westland Basin. The earlier deposits (④ in Table 5.1) represent the underfilled stage of foreland basin evolution where subsidence is faster than the rate of deposition. As the uplift of the Southern Alps continued and increased sediment sources become available, the South Westland Basin has gradually filled, shallowing through a prograding sequence (⑤ in Table 5.1) to Molasse-type deposits presently at the top of the sequence. This overall sequence implies that the basin may have reached or is near a steady state profile where sediment bypasses deposition in the basin. This simple pattern of basin evolution is probably complicated by glacially driven sea level fluctuations during the Pliestocene.

5.2 Seismic stratigraphy

5.2.1 Seismic horizons and sequences

5.2.1.1 *Basement Horizon*

The basement horizon is very prominent in most of the seismic sections. The frequent absence of this reflector near shore may be due to the effects of the South Westland Fault Zone, discussed elsewhere. The basement reflector is often closely associated with the Oligocene horizon. The overall structure of the basement reveals a steep dip toward the present coastline and the inferred location of the South Westland Fault Zone to a depth of up to 4 km. About 60 km offshore is an elongate basement high running parallel with the coast rising to around 1600 m below sea level (Fig. 4.16). The Mikonui-1 exploration well was deliberately sited over this basement high. Hereinafter this notable basement high is entitled the Mikonui High. Westward of the Mikonui High, the basement begins to dip to the west, but seemingly at a shallower angle than to the east. Reconstructions of the plate boundaries during the Late Cretaceous through to the Oligocene (e.g. Walcott, 1984a, 1987) and stratigraphic evidence onshore (Nathan, 1977, 1978; Adams, 1987) suggests that the present basement high was already present at this time, forming a possibly uplifted dome between two obliquely orientated extensional zones (Fig. 1.5). The nature and geometry of this basement structure will be further explored using flexural models of the lithosphere below.

5.2.1.2 *Sequence E : Post rifting marine transgression*

Sequence E is often too thin to display any internal configuration in seismic sections. The sequence thickens offshore toward the west, where seismic reflectors are seen onlapping onto the basement toward the east (e.g. PS-21, Fig. 4.14; L-206, Fig. 4.11). This onlap is an indication of the regional marine transgression across the area after the rifting of the New Zealand continental block from eastern Gondwanaland. The thickening toward the west is probably toward the loci of subsidence along the margins of the Tasman Sea rifting centre, now the present margins of the Challenger Plateau (Fig. 4.17; Fig. 5.3). Onshore, outcrop evidence suggests that, at least locally, Late Cretaceous–Eocene sediments thicken eastward also (Adams, 1987). This may indicate the deposition of sediments on essentially passive margins on either side of a basement high.

5.2.1.3 *Oligocene Horizon : Maximum flooding surface*

The Oligocene horizon represents a time of major change within the basin. Significant hiatuses are noted above and below it in most areas. The horizon itself is the seismic

expression of the regionally extensive Awarua limestone which covers most of the area. The Awarua Limestone has a bioclastic origin with depositional depths varying from inner shelf in the onshore wells to outer shelf–upper bathyal depths in Mikonui-1. The Awarua Limestone, along with numerous other Oligocene limestones in New Zealand is interpreted as marking the height of a marine transgression across continental New Zealand due to thermal subsidence after the rifting of the Tasman Sea. In broad seismic stratigraphic terms, this horizon may be thought of as a maximum flooding surface.

5.2.1.4 *Sequence D : Early turbiditic filling*

A major factor in the interpretation of this sequence is the correlation with sediments onshore. The Tititira Formation consists of a deep-water sequence passing upwards from hemipelagic mudstone through distal and proximal turbidites into a mass-flow conglomerate-sandstone complex (Nathan, 1978). Sequence D has an overall sheet-line form (e.g. EZD-3, Fig.4.10), with possible localised thickenings. Sediment volumes and rates suggest that deposition was slower during Sequence D than in the overlying Sequence C (Table 4.6). This may be due to a lack of an erosional source area and/or sediment starvation in a deep basin. The sequence onlaps onto the Oligocene Horizon toward the basement high (L-206, Fig. 4.11), indicating that it is filling a basin that subsided rapidly sometime after the Oligocene. This subsidence must have been, at least initially, more rapid than the rate of deposition (Sequence D average = 46 m/Ma) to create a basin where Sequence D could infill and gradually onlap toward the basement high in the west.

5.2.1.5 *Top Miocene Horizon : Early uplift event*

Due to the generally low amplitude nature of the reflector, the Top Miocene Horizon only weakly displays some seismic features, mostly in proximal sections associated with the wedge seen in Sequence C (EZD-3, Fig. 4.10). Some truncation against the lower boundary is suggested by distal sections (L-206, Fig. 4.11). The horizon appears to indicate a change in depositional regimes between the sequences above and below it. This horizon may therefore represent a regional erosional event. Indeed, the Tongaporutuan series (Late Miocene) is inferred to be absent from the Mikonui-1 well section (Diamond Shamrock, 1981), although completely present in Harihari-1 and Waiho-1 (Fig. 4.2). This may indicate that erosion was limited to an emergent basement high during the Late Miocene. No significant eustatic sea level fall is noted in the Haq curve (Bally, 1987) at around the 5 Ma point. This seismic structure may be associated with the increased convergence across the Alpine Fault. Geohistory analysis of the exploration wells indicates that the Late Miocene was a time of rapid subsidence, but this does not appear to have caused a significant change in the styles of deposition within the basin.

5.2.1.6 *Sequence C : Further turbidite infilling and reworking*

The interpretation of Sequence C is also closely linked with the interpretation of the Tititira Formation. The formation covers an age range from the Lillburnian through to the Tongaporutuan. Onshore, this formation is bounded above and below by extensive unconformities, which do not appear to continue into the wells at Harihari-1 and Waiho-1. In the exploration wells, the Tititira Formation only represents the lowest part of a continuous upper Cenozoic sequence. Exotic blocks and reworked foraminifera from the Arnold and Landon Series are found within sediments of early Opoitian age in Waiho-1. Nathan (1978) interprets this as a result of rapid uplift and deformation along the 'Coastal Monocline'. The sediments at the base of Sequence C are correlated with well sediments of Opoitian age in Mikonui-1. Thus the prominent wedge that occurs in proximal sections is probably related to the inferred uplift of the 'Coastal Monocline' (EZD-3, Fig. 4.10). It may represent a fan of detritus eroded from the uplifted sediments.

If this is the case, then a number of inferences may be drawn from the nature of the wedge along the basin margin where it occurs. The wedge is deformed in the south, and appears to thin and occur at higher stratigraphic levels further north. This infers that uplift and associated deformation began earlier in the south and migrated northwards. The amount and/or duration of uplift has also decreased northward. This interpretation is inconsistent with the findings of Kamp et al. (1992) which find the inversion of the basin margin beginning in the north and migrating southward.

There are also alternative interpretations for the wedge structure. At first appearance it may resemble a thrust structure. However, the top of the wedge is not a basement surface as numerous coherent reflectors can be seen below it. The wedge may then represent a thin-skinned thrust of older Miocene sediments as purported by Adams (1987), but a repeating sequence of Miocene sediments is not seen in the nearby exploration at Waiho-1 as would be expected if this were the case. Although it cannot be confirmed either way until directly sampled, the wedge is probably not tectonic in origin.

The reflectors above the wedge represent the continuation of moderately rapid deposition into the basin. The reflectors are parallel with the top of the wedge, and the prominence of the wedge may simply be a result of a brief erosional interval that highlighted the reflector at the top of the group. The discontinuous and undulose nature of the reflectors suggests a degree of mixing of the sediments and depositional structures. These may represent the fan and channel systems associated with the deep-water turbidite deposition in the offshore continuation of the Tititira Formation.

5.2.1.7 *Horizon PPB : retrogradational transgression*

This horizon is probably better described as a relatively thin transitional sequence. The stepping upwards and shorewards of the reflectors suggests a retrogradational transgressive systems tract formed during a rapid relative rise of sea level. The prominent reflectors in a background of low-amplitude reflectors may represent a coastal and near shore lithofacies of coarser sands in a background of mudstones above and below. The often undulose nature of the horizon and occasional truncation of underlying reflectors suggest that it is an erosional feature, probably associated with the fall of relative sea level before the transgression.

5.2.1.8 *Sequence B : Foreset beds*

Sequence B contains a seismic stratigraphic record of a complex history of deposition. The basal sections of this unit appear to be generally flat-lying, but undulose, dipping and thinning to the northwest. They grade upwards into increasingly prominent prograding configurations. This suggests that the basal sections are the distal bottomset segments of prograding clinoforms that occur to the southeast (onshore direction) of the seismic profiles. As the sequence continued to prograde outwards the clinoforms began to build over the older bottomset segments. These bottomset reflectors are also notably undulose and discontinuous in nature, as are the younger bottomset segments in the distal sections. These features may represent slumping of the prograding clinoforms and/or distal fans deposited during times of sediment bypassing on the shelf to the southeast. Such seismic features are also evident in the Plio-Pliestocene Giant Foreset Beds in Taranaki Basin (Beggs, 1990).

The topset segments of the prograding clinoforms seen in the section show some reflectors as mostly continuous from foreset to topset, while others are truncated. This variability infers topset strata with a depositional history of alternating aggradation and sediment bypassing within a high energy depositional environment (Mitchum, Vail & Sangree, 1977; Section 2.1.5.1). Such a high energy environment would be found in the near shore, with sediment being supplied in high volumes by rivers. If the modern situation is an analog for this depositional environment, then the rivers carried high volumes of sediment and could rapidly change course during large floods which were frequent. This presumably would have a corresponding effect on the sediment distribution and deposition on the shelf. Eustatic controls on the topset segment depositional environment could also be significant.

5.2.1.9 *Horizon PPA : Change in depositional regimes*

The prominent arcuate shape of this horizon suggests that it represents a significant change in depositional regime between the sediments above and below. Such a change is also suggested by the change in the internal configuration of seismic reflectors across this horizon. The horizon may represent an erosional surface, possibly the top boundary of a sequence overlapped by a rapidly prograding complex. However, the erosional interpretation is inconsistent with the lack of truncated reflectors below the horizon. This infers that no significant erosion occurred at this level. The similarity of this horizon with reflectors immediately below in the top of Sequence B would suggest that it is a depositional feature that marks the rapid transition between depositional environments. The sequence below is generally progradational, while the sequence above has been interpreted as a rapidly deposited and frequently slumped unit.

5.2.1.10 *Sequence A : Eustatically dominated progradational complex*

Some evidence of onlap onto the lower boundary of this unit (Horizon PPA) suggests that at least the lower part of this sequence may be retrogradational. Above the base the reflectors become discontinuous, although this may also reflect interference from the seawater-sediment interface. The lower boundary is dated at near 1.2 Ma, thus the sediment deposited should presumably represent the huge volumes of material eroded off the Southern Alps during that time which includes numerous glacial periods. Presumably the depositional environment would have also been effected by sea level changes associated with glacial periods during the Pliestocene glaciations. The lithology of the sequence comprises unconsolidated mudstones capped with a thick unit of bioclasts derived from both shallow and deep waters. The alternation of depth of deposition may reflect sea level changes during glacial–interglacial cycles. The bioclasts are well preserved, indicating little or no transportation. The presence of such a thick sequence of bioclasts immediately offshore from a zone of high terrestrial deposition suggests that the sediments were actively bypassing the shelf and/or being actively scoured from the area. It may be that the bioclast deposits are confined to the shelf bulge and are the result of ocean currents scouring the seafloor over the bulge. Only further in-situ investigations of the near surface sediments in the area will reveal the extent and nature of the bioclastic deposits.

Sequence A may represent a very rapidly constructed progradational complex. Some sections show onlap in the shoreward section of the lower boundary with either erosional truncation or downlapping in the distal margins of the sequence. This is typical of a prograding configuration (see Section 2.1.5.1, Figure 2.6), but may also occur in lowstand

wedges (Section 2.1.6, Figure 2.10c) if deposition occurs beyond the shelf break. The undulose nature of reflectors in PS-19 may be interpreted as channel structures associated with the progradational complex. Muddy sediments were deposited at outer shelf to upper bathyal depths, with rapid deposition causing frequent collapses of the prograding foresets. This would cause any reflectors to become discontinuous, confusing what was probably an already seismically homogeneous sequence. The bioclasts may indicate the point at which muddy sediments bypassed deposition at the shelf break (e.g. channelled away by the canyon systems) and/or were scoured by strong ocean currents.

5.2.1.11 *Seafloor : Present surface*

The seafloor bathymetric record shows that two broad zones of seafloor physiography in South Westland, roughly divided north and south at the mouth of the Cook River. In the northern sector, the seafloor is generally flat lying with the shelf sloping to the northwest. Directly offshore from Hokitika the extensive Hokitika Canyon marks the northern edge of a shelf bulge.

To the south of the Cook River the seafloor is more rugged, cut by numerous canyons branching off the laterally continuous Cook Canyon as it runs down into the Puysegur Trench off Fiordland. The seismic lines in the southwest cross these canyons and often illustrate how steeply walled they are, suggesting glacial or associated fluvial erosion and/or some form of fault control. Unfortunately the resolution of the seismic lines prevents the determination of any fault structures, although the South Westland Fault Zone may extend through this area. The seafloor in the region awaits further study, especially in concern to the flow of currents and sediments. However, the Cook Canyon system broadly resembles the Hikurangi trough system on the eastern seaboard of the North and South Islands with active canyons reaching into the shelf and close to the modern shoreline. The southwesterly extension of the Cook Canyon is probably better thought of as a northeasterly extension of the Puysegur Trench acting as a sink for sediments derived from the Southern Alps south of the Cook River and channelled into it by a number of canyon systems.

5.2.2 Faulting

Overall, the offshore sediment sequences in the South Westland Basin appear to be remarkably undeformed by faulting, assuming the wedge structure in Sequence C is not a tectonic feature. The only major fault present is the South Westland Fault Zone, marking the southeastern margin of the basin, presumably uplifting the southeastern block. The pre-Miocene horizons are notably truncated by this fault zone, but higher horizons may be continuous onto the block. There is some evidence to suggest that the block dips toward the

north, as older reflectors appear to be continuous onto the block further north. The South Westland Fault Zone appears to come onshore somewhere near, but to the southeast of Waiho-1. Onshore the fault is more easily traced as the boundary of uplifted Paleozoic basement rocks to the southeast. Near Harihari-1 the fault appears to form a large U-shaped bend, with another, much smaller thrust being present within this U-bend. The fault is inferred to continue into the Hohonu Fault further north (Kamp et al., 1992). The most northerly lines in the study area exhibit noticeable thickening toward the coastline, and although not directly seen , these may imply the presence of a southerly extension of the Cape Foulwind Fault as proposed by Norris (1978), this fault being upthrown on its eastern side.

Onshore, numerous faults have been invoked by various workers (Mutch & McKellar, 1964; Nathan, 1977; Adams, 1987) to explain the complex relationships between sedimentary sequences seen in the Paringa area. Adams (1987) went further and described these features as a possible thrust structure, implying that similar structures may be seen offshore. Apart from a possible structure dated at near the Top Miocene in Sequence C, no thrust structures have been recognised. However it may be possible that such structures exist immediately offshore in the small gap in geological coverage between onshore outcrop and offshore seismic lines.

5.2.3 Other seismic features

Onshore basins

Adams (1980) described the river valleys in South Westland as 'overfilled fiords' which were formed by glacial action, and then completely filled by sediment when the glaciers retreated. The features seen in onshore seismic lines (OS-3, Fig. 4.13) exhibit a wide U-shaped depression often associated with a glacial valley. The onlapping of the horizons in the basin are probably the glacial outwash and fluvial deposits infilling the valley left by the retreating glacier.

5.3 Further geological interpretations

5.3.1 Sedimentation rates

The sedimentation rates discussed here are summarised in Table 4.6. The low accumulation rate of Sequence E is reminiscent of rates in cratonic basins (Schwab, 1986). Sequence D resembles the depositional rate on a continental shelf, although biostratigraphy indicates that this sequence was deposited at greater depths than on the shelf and the low rate may be an indication of sediment starvation in a deep basin. 5 million years before present appears to mark a point of rapid transition, with a huge increase in sedimentation rates

than in the previous two sequences. The calculated sedimentation rates for the Sequences B and C are particularly high at 0.240 and 0.325 m/1000 yr respectively. These compare well with the mean accumulation rate for foreland basins of 0.186 m/1000 yr and flysch deposits in foreland basins of 0.345 m/1000 yr (Schwab, 1986). The last three sequences make up the bulk of the total sediment body in the basin and clearly indicate that vast amounts of sediment were deposited comparatively recently in the basin.

Unfortunately, no errors have been calculated for the estimation of sediment volumes, so it is unclear if the difference in rates between the last three sequences, particularly C and B, is statistically valid. The rate of deposition for Sequence A has probably been underestimated due to its restricted area of deposition. Any difference may indicate a reduction of sediment supply and/or accommodation for deposition. A decrease in sediment supply is unlikely as fission track dating evidence indicates that uplift in the Southern Alps continued to increase through the Plio-Pliestocene to the present (Tippett & Kamp, in press). The thick and extensive deposits of Sequence C have probably filled most of the available space in the basin formed after the Oligocene, causing sediment bypassing in the higher sequences, particularly to the north and south within the nearshore zone.

5.3.2 Petrography

The petrography of the onshore sedimentary units, displayed in Fig. 4.16, all dominantly plot within the Recycled Orogen provenance of Dickinson & Suczek (1979; Fig. 3.11). Unfortunately the petrography is not detailed or extensive enough to differentiate between the provenances of a variety of convergent tectonic settings as suggested by Dickinson (1984, in Schwab, 1986). So, although foreland basin detritus invariably plots within the Recycled Orogen provenance, the fact that sediments in the South Westland Basin do also, is not conclusive proof of their deposition in a foreland basin.

5.3.3 Geophysical observations

Karner & Watts (1983) studied the gravity anomaly profiles of three major collisional zones with their associated foreland basins: the Himalayas, Appalachians and Western Alps (Fig. 3.4). All exhibited a gravity low displaced toward the foreland, presumably a result of lower density sediment infilling a flexurally formed basin. An outer gravity high was also noted. The last two examples also displayed gravity highs toward the highest topography. In the South Westland case an outer gravity high (+200 μN/kg; +20 mgal) can be seen to the northwest of the deepest part of the basin, coinciding with the Mikonui basement high (Fig. 4.17). This gravity high appears to be isolated to the area around the Mikonui-1 well-site, even though the basement high continues to the southwest. This may just reflect the less pronounced nature of the basement high further south and/or

interference form the large negative gravity anomaly caused by the ocean-continent collision across the Puysegur margin further to the southwest.

Alternatively, the positive gravity anomaly may be an inherited feature from an earlier tectonic regime. A similar situation is suggested in the western margin of Fiordland (Kamp & Hegarty, 1989). As discussed above, the Mikonui High appears to have been an elevated area since the inception of rifting in the Tasman Sea, and was for some time flanked by rift margins on two sides. Although subsidence is noted in the Mikonui-1 wellsite, it is possible that the high was formed as an uplifted rift shoulder, emphasised by the proximity of two rift margins. The present gravity anomaly structure over this feature may be inherited from this tectonic regime.

A possible corresponding gravity low over the deepest part of the basin is difficult to recognise due to the large regional field associated with the crustal thickening in the Southern Alps (-900 μN/kg; -90 mgal; Allis, 1981). The gravity anomalies associated with the examples of Karner and Watts (1983) are in the order of 200 mgal (2000 μN/kg), seemingly twice the size of the gravity anomaly gradient across South Westland and the Southern Alps. This may reflect the smaller scale of the South Island collision in comparison with the examples used by Karner & Watts (1983), especially in comparison with the Himalayas. Further analysis of the gravity field, not undertaken in this study, would help to delineate the structures responsible for the mapped gravity anomalies.

5.4 Geodynamical modelling

5.4.1 Subsidence modelling

5.4.1.1 *Exploration well subsidence*

The long term tectonic subsidence calculated in the geohistory plot of Mikonui-1 (Fig. 4.3) lends itself to subsidence modelling using the McKenzie model. Mikonui-1 is sited on the continental shelf approximately 50 km offshore. The region was marginal to rifting between eastern Gondwanaland and New Zealand during the Late Cretaceous (see Chapter 1). After the opening of the Tasman Sea about 80 Ma ago, the New Zealand micro-continent drifted away from the active spreading ridges. During this time the thinned lithosphere cooled and gradually subsided. This caused a marine transgression to occur, which is recorded in the Eocene–Oligocene succession. The Late Cretaceous–Oligocene sediments in Mikonui-1 are an example of such a record. When extracted from the geohistory results, the tectonic subsidence can be compared directly to various models of tectonic subsidence driven by thermal contraction after a rifting event, as discussed in Section 2.3.1. The models were calculated using equation 2.10, with a standard lithospheric thickness of 125 km. The results of the modelling for ß-values of 1.20, 1.25 and 1.30 are shown in Fig. 5.1.

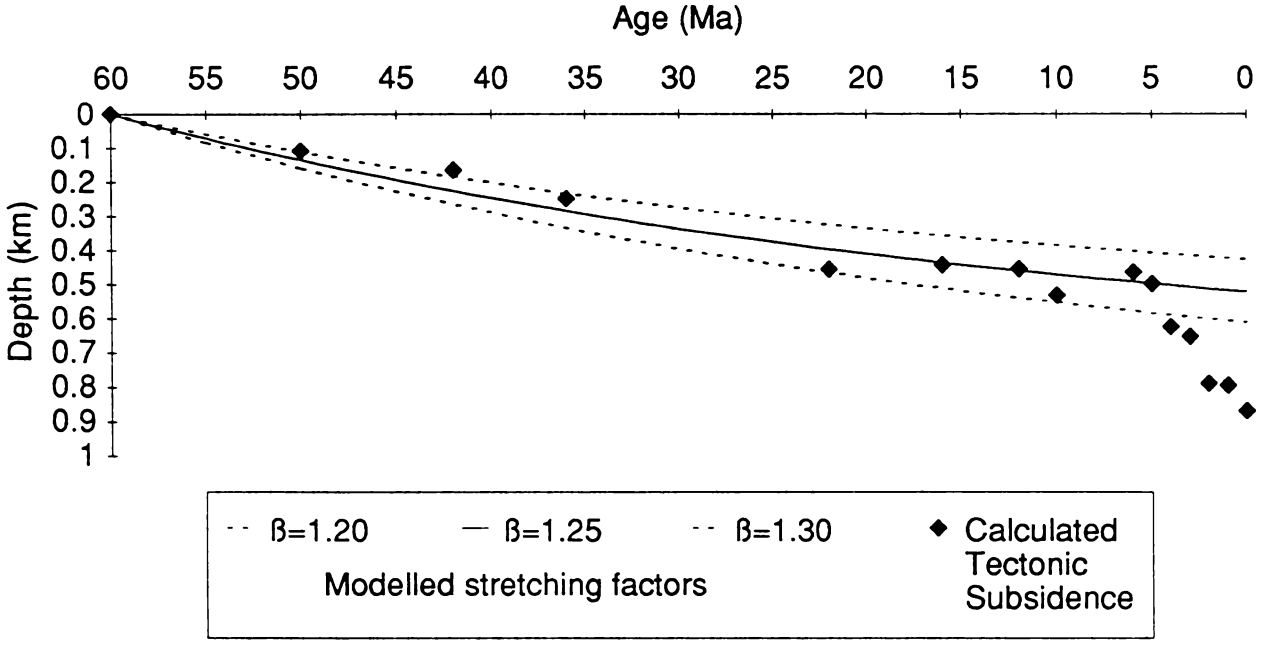

FIGURE 5.1: Plot of calculated tectonic subsidence in Mikonui-1 compared with modelled tectonic subsidence for a lithosphere of original thickness 125 km and stretched by a factor of 1.20, 1.25 and 1.30 at 60 Ma.

For the 60–35 Ma (Paleogene) section of the tectonic curve a visually estimated best-fit line would be ß=1.20. Overall, up to around 5 Ma, the visually estimated best-fit line would appear to be that of ß=1.25. This means the assumed original lithospheric thickness of 125 km was thinned to 100 km.

Of interest is that the tectonic subsidence calculated in Mikonui-1 continues to fit the model quite well even after the inception of the Alpine Fault during the Miocene about 23 Ma. It is not until about 5 Ma, that tectonic subsidence is displaced from the model.

In Harihari-1 and Waiho-1 the Late Cretaceous–Oligocene marine transgressive sediments are absent, so no record exists for comparison with theoretical models. Both onshore wells instead show a rapid overall subsidence from the start of their sedimentary records (Figure 5.B). To model such subsidence using the McKenzie model would require a ß-factor in the order of 10 and larger. Such stretching factors are associated with major rifting evolving into seafloor spreading (Allen & Allen, 1990). This clearly did not happen in South Westland. The area is not or has not recently been subject to volcanic activity, and the seismic profiles do not show the rift structures that would be expected if such an event had occurred. Another driving force for the recent and rapid subsidence in the three wells must be found.

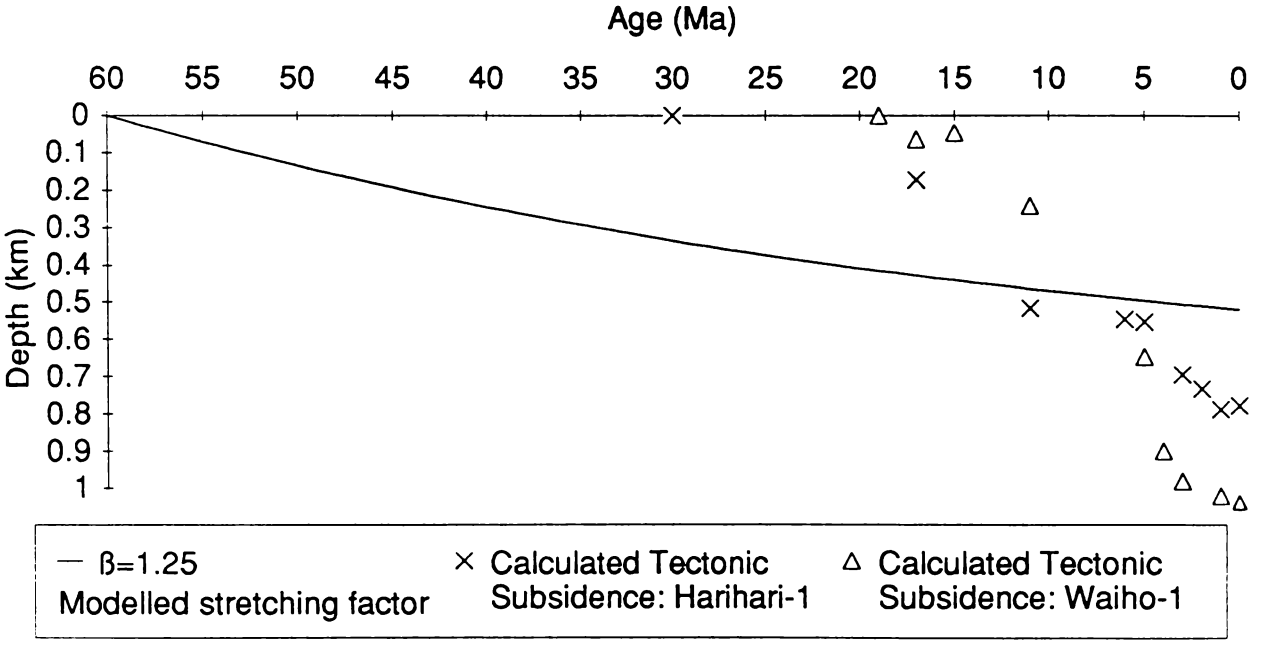

FIGURE 5.2: Plot of calculated tectonic subsidence in Harihari-1 and Waiho-1 compared with modelled tectonic subsidence for a lithosphere of original thickness 125 km and stretched by a factor of 1.25 at 60 Ma.

The overall shape of all three tectonic subsidence curves is similar to those found in foreland basins studied in North America (see Figure 3.10) and Taranaki (Stern, 1991). The early stage exponential-decay curve represents subsidence in rifted margins which develops into an exponential-increase curve that represents the loading and compression in a foreland basin. The small upward kinks at the end of the subsidence curves in the onshore exploration wells represent the uplift of thrust blocks.

If foreland basin formation is assumed to be the explanation, then onset of foreland basin subsidence appears to begin in the onshore wells around 20–15 Ma. Similar subsidence in Mikonui-1 doesn't begin until around 5 Ma, although subsidence appears to accelerate around this time in the onshore wells. This may mean the 'front' of subsidence migrated westward at a rate of around 5 km per million years. Assuming that this rate has continued constantly, the subsidence front would now lie a further 25 km beyond Mikonui-1. However, a cautionary note should be made that without the older sediments in the onshore wells a definite onset of rapid subsidence cannot be exactly defined. Also, both onshore wells occur near a major fault zone. At least a part of their subsidence may be fault controlled, indeed the faulting itself may be associated with the formation of the foreland basin, or subsequent basement inversion and loading (Kamp et al., 1992). At this level it would be impossible to differentiate between the two controls in the sedimentary record. No significant faulting occurs near Mikonui-1, thus the rapid subsidence that has occurred there since 5 Ma may be entirely due to the loading of the Australia Plate, forming a foreland basin in South Westland.

5.4.1.2 *Regional tectonic subsidence*

The tectonic subsidence of the entire South Westland Basin has been calculated by treating each cell in the TECHBASE model as a well section, and thus backstripping it and calculating the tectonic subsidence using the same principles from geohistory analysis. The tectonic subsidence through time effectively gives the evolution of the external tectonic controls on basin formation. The tectonic subsidence was calculated using geohistory techniques at each horizon mapped in the study area and the results are illustrated in Figures 5.3 to 5.7. One of the most difficult parameters to calculate is the paleodepth across the basin at each time interval. As there is only limited information available from the exploration wells and surface outcrops, a simple uniform paleodepth for each time interval has been assumed. It is acknowledged that is oversimplifies the situation, but such problems will remain until further information about the paleodepth conditions in the basin can be obtained. The paleodepths derived from the micropaleontology of each sequence is discussed in Section 4.1.2 and is summarised below in Table 5.2:

Horizon	Age (Ma)	Paleodepth (m)
Seafloor	0	150
PPA	1.2	150
PPB	3.1	300
Top Miocene	5	300
Oligocene	≈30	500

TABLE 5.2: Simplified summary of paleodepths at each time interval represented by the mapped seismic horizons.

The five diagrams clearly show the migration of the depocentre of basin tectonic subsidence from the northwestern side of the study area in the Oligocene, (Fig 5.3) to the south eastern margin from the late Miocene through to the present day (Figs. 5.4 to 5.7). Such depocentre migration would be consistent with the evolution of the basin from a passive margin/post rift setting in the Oligocene through to a possible loading event in the late Miocene and the subsequent rapid subsidence of the southeastern margin of the basin.

5.4.2 Flexural modelling

5.4.2.1 *Flexure*

Flexural modelling in the South Westland Basin can be done using cross-section basement profiles from both actual (and depth converted) seismic profiles and sections derived from the structural model. Three sections have been modelled, one actual line (L-206), and two section from the grid model of the study area at 96 and 150 km from the origin of the model grid, thus they are titled 96K and 150K (Fig. 2.20).

The flexural equations discussed in Chapter 2 model a continuous lithospheric plate to the edge that it is loaded on and/or broken. In South Westland, the South Westland Fault is inferred as the edge of the Australia Plate for flexural modelling purposes for a number of reasons:

- The South Westland Fault has been the site of around 4 km of uplift since the end of the Miocene (Kamp et al., 1992), thus the Australia Plate at that point may be significantly broken ib terms of flexural modelling.
- The uplift of the block to the east of the South Westland Fault would now presumably contribute to the load upon the Australia Plate to the west.
- No seismic lines penerate with enough resolution to delineate the structure of the South Westland Fault and the associated uplifted block, especially the nature and depth of any underthrust lithosphere.

• Although fission track data (Kamp et al., 1992) gives a measurement of depth to basement, this is a paleodepth at a previous time, and unsuitable for use in modelling the present profile.

All three sections, and the basement structural map (Figure 4.16), show the basement dipping toward the modern coastline from a structural high about 60 km offshore from the inferred load point at the South Westland Fault Zone. This is a very short wavelength for such a feature in continental lithosphere. Using the equations discussed in Section 2.3.2 the lithospheric parameters of the Australia Plate underneath the basin can be calculated.

In the instance of an unbroken lithosphere, the flexural parameter is found with equation (2.20):

$$x_b = \pi\alpha$$

$$\Rightarrow \quad \alpha = \frac{60}{\pi}$$

$$\Rightarrow \quad \alpha = 19.10 \text{ km}$$

Using equation (2.16) the flexural rigidity can be calculated:

$$\alpha = \left\{\frac{4D}{g\,(\rho_m - \rho_s)}\right\}^{1/4}$$

$$\Rightarrow \quad D = \frac{\alpha^4\, g\,(\rho_m - \rho_s)}{4}$$

$$\Rightarrow \quad D = \frac{(19.10^4) \times 9.8 \times (3300 - 2350)}{4}$$

$$\Rightarrow \quad D = 3.10 \times 10^{20} \text{ Nm}$$

The effective elastic thickness can then be derived from equation (2.14):

$$D = \frac{Eh^3}{12(1 - v^2)}$$

$$\Rightarrow \quad h = \sqrt[3]{\frac{D\ 12(1 - v^2)}{E}}$$

$$\Rightarrow \quad h = \sqrt[3]{\frac{(3.10 \times 10^{20})\ 12(1 - (0.25)^2)}{70 \times 10^9}}$$

$$\Rightarrow \quad h = 3680 \text{ m}$$

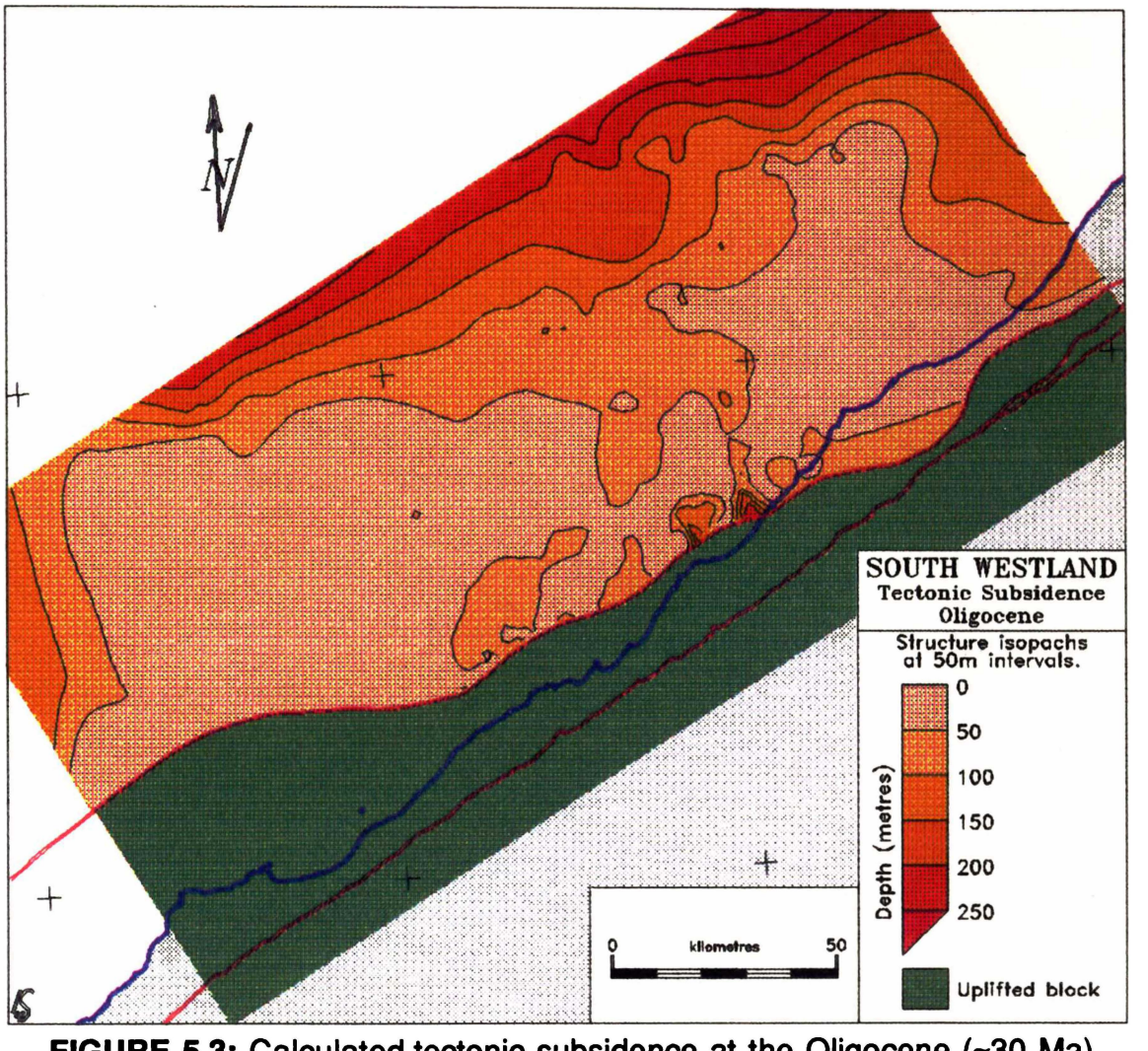

FIGURE 5.3: Calculated tectonic subsidence at the Oligocene (≈30 Ma).

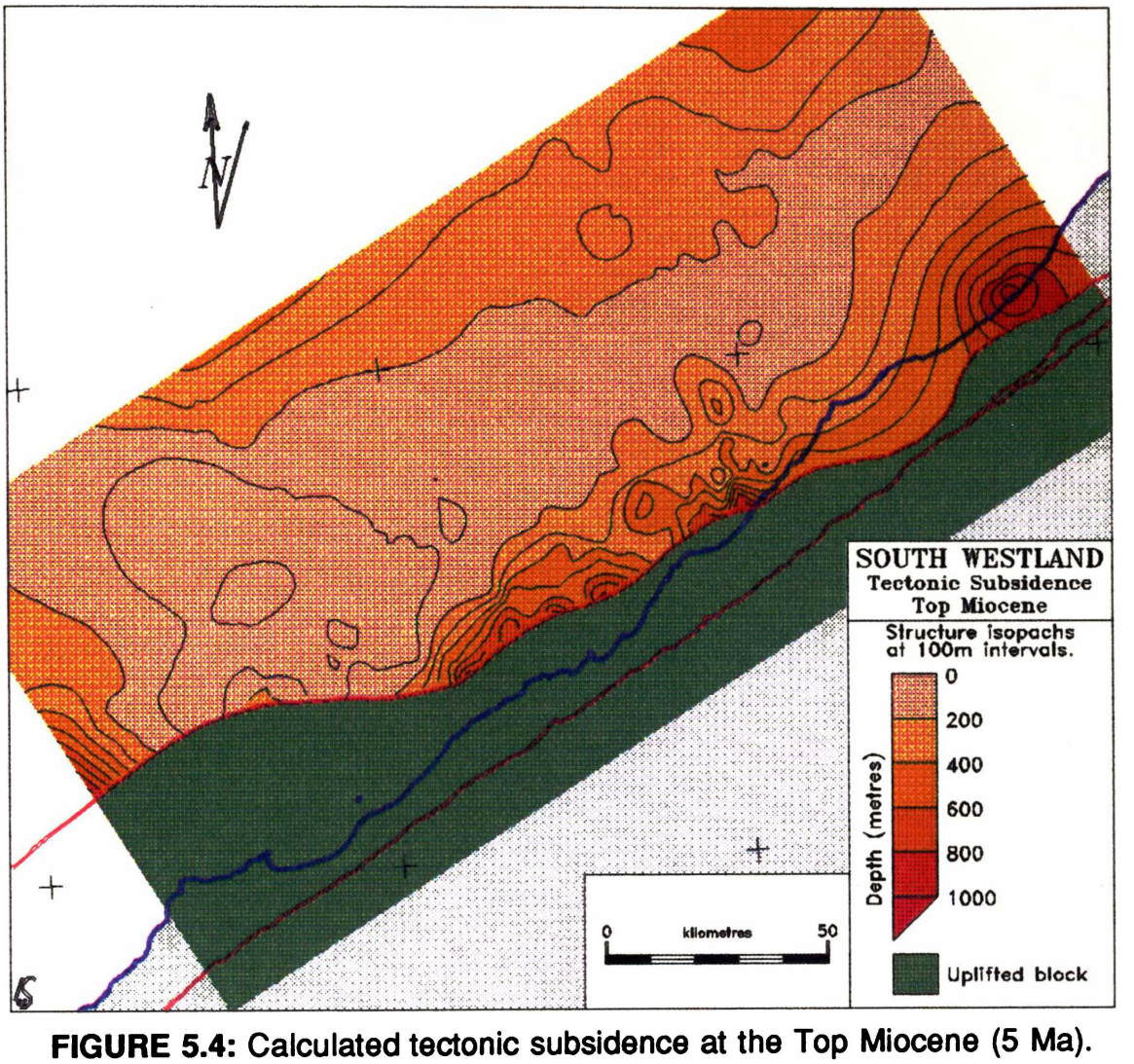

FIGURE 5.4: Calculated tectonic subsidence at the Top Miocene (5 Ma).

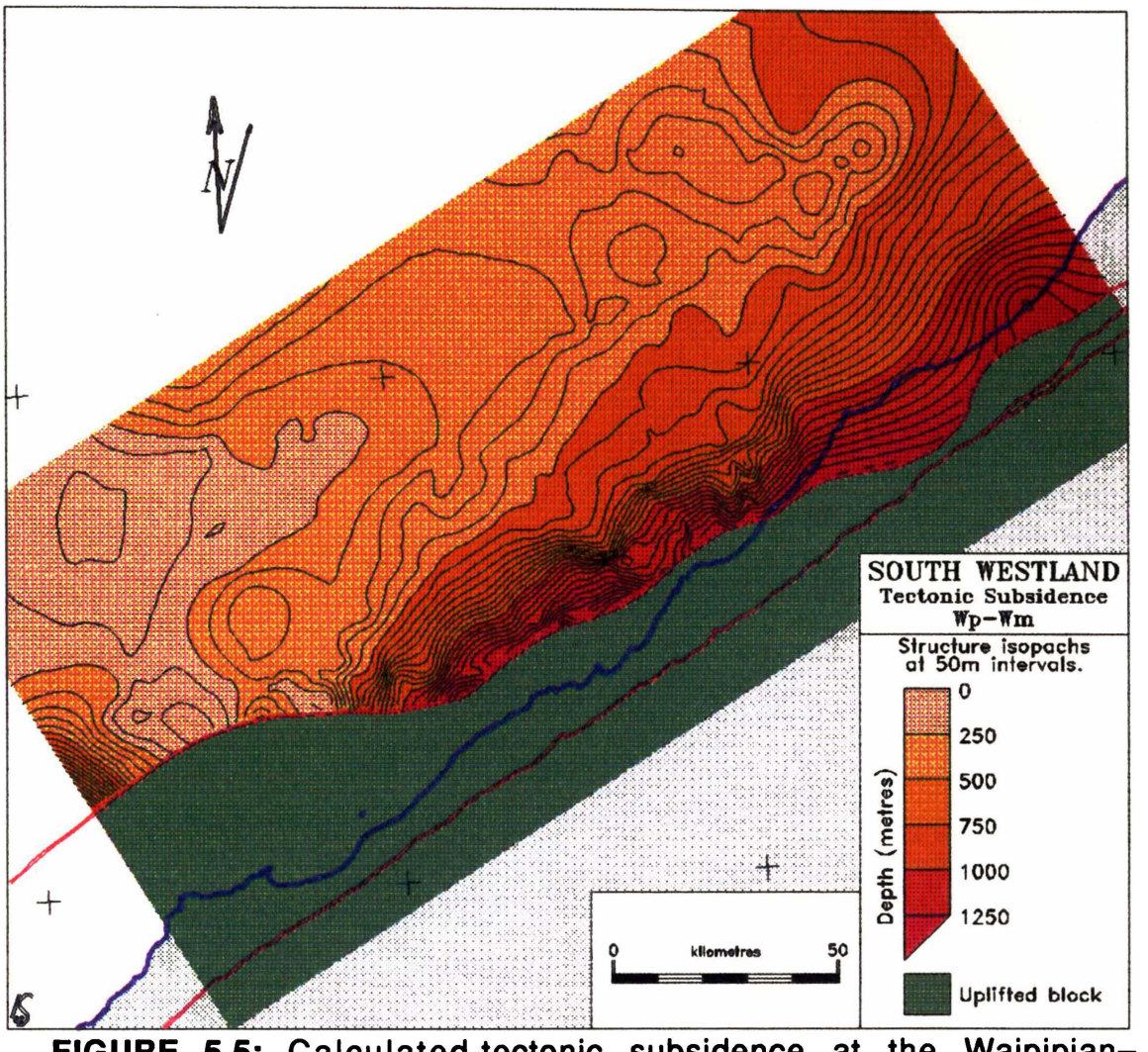

FIGURE 5.5: Calculated tectonic subsidence at the Waipipian–Mangapanian boundary (3.1 Ma).

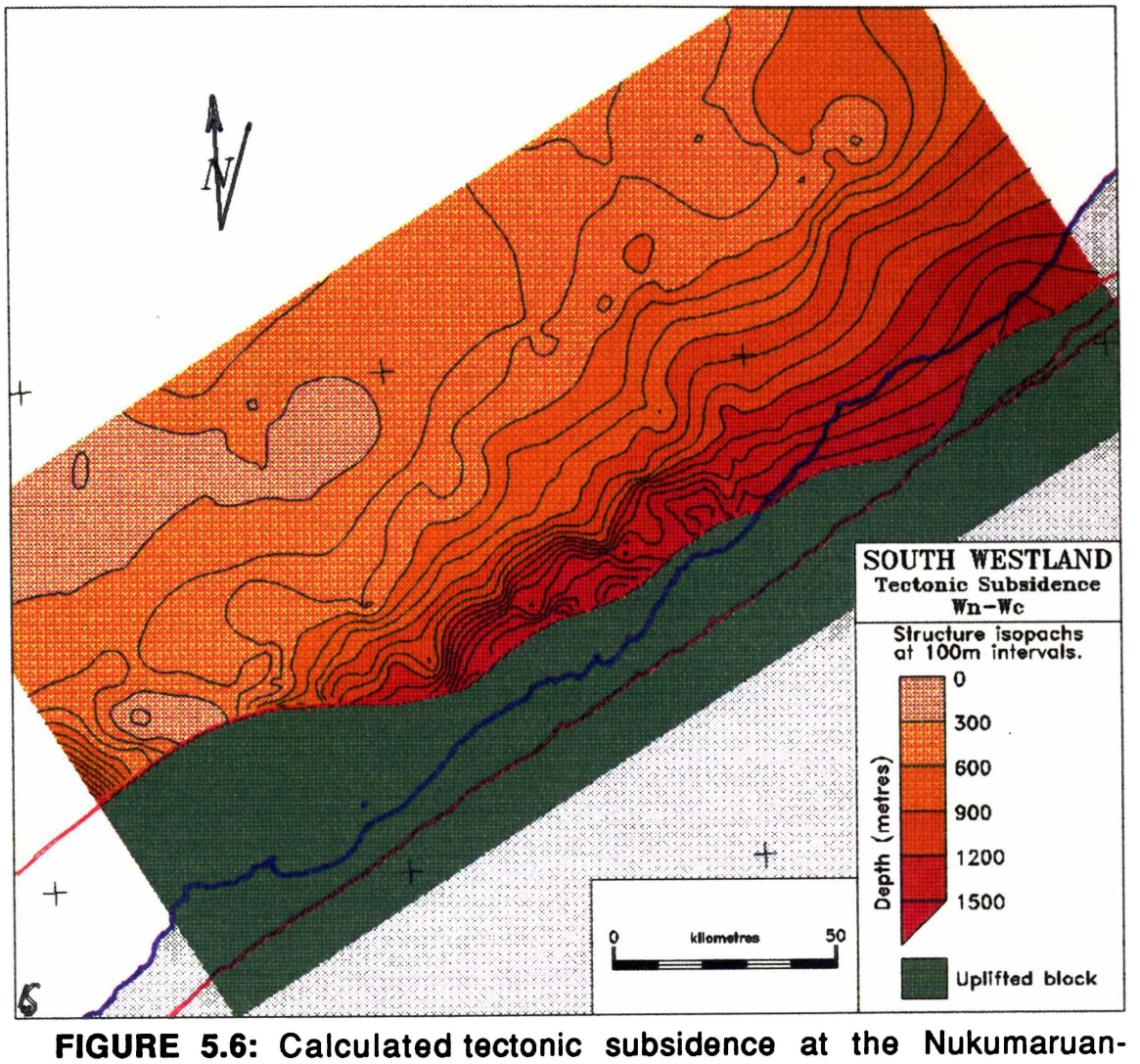

FIGURE 5.6: Calculated tectonic subsidence at the Nukumaruan-Castlecliffian boundary (1.2 Ma).

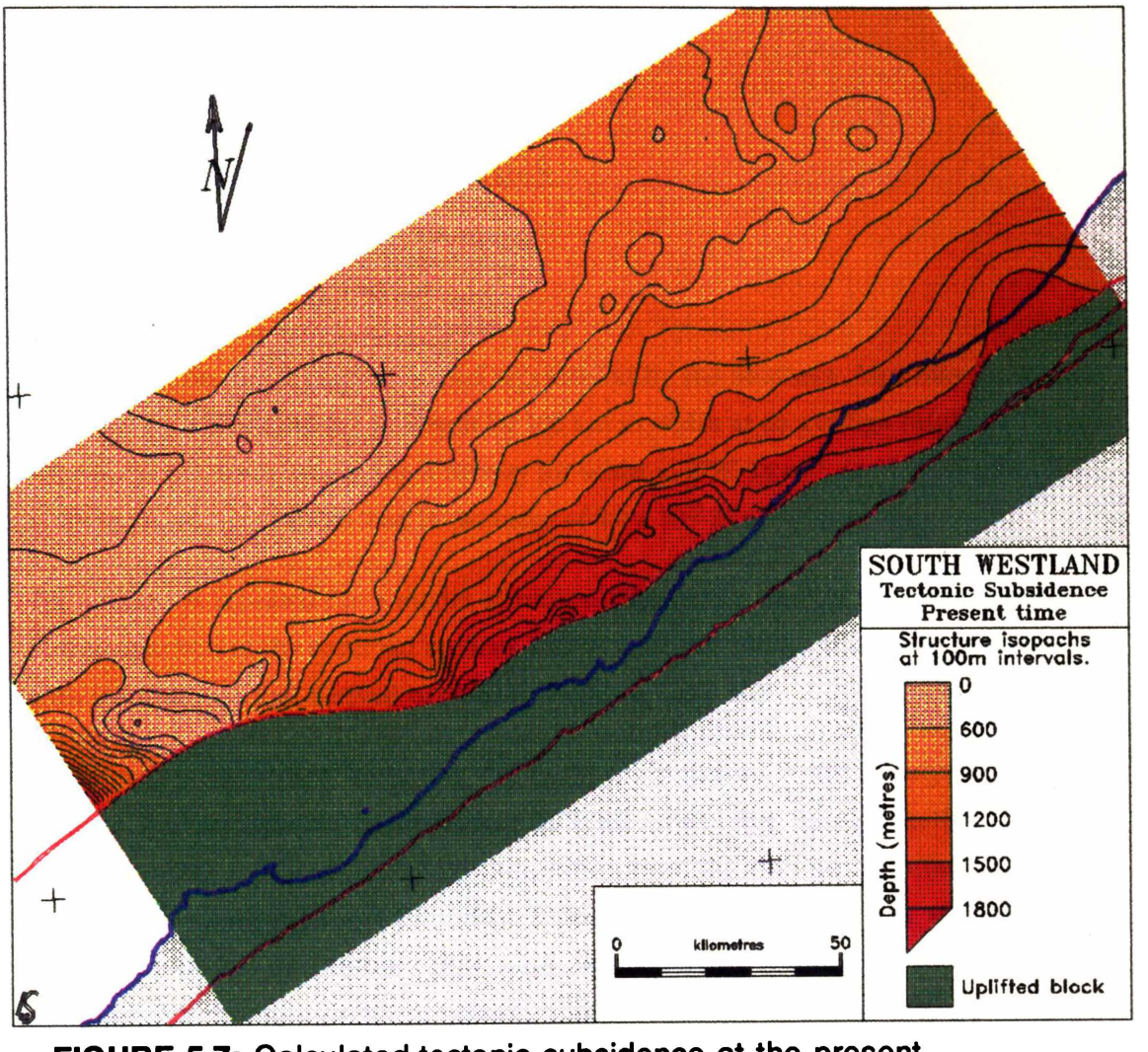

FIGURE 5.7: Calculated tectonic subsidence at the present.

An estimation of the line load (in $N.m^{-1}$) required to produce the flexure can be derived from equation (2.18):

$$\omega_0 = \frac{V_0 \alpha^3}{8D}$$

$$\Rightarrow \quad V_0 = \frac{\omega_0 8D}{\alpha^3}$$

$$\Rightarrow \quad V_0 = \frac{1400 \times 8 \times 3.1 \times 10^{20}}{19100^3}$$

$$\Rightarrow \quad V_0 = 4.98 \times 10^{11} \text{ N.m}^{-1}$$

For comparison, the topographic load represented by the Southern Alps may be roughly modelled by a block 240 km in length by 100 km in width at an average height of 1.25 km (Tippett, pers. com.). Assuming a density for schist at 2730 $kg.m^{-3}$, and a gravity constant of 9.8 $m.s^{-2}$, this gives a line load in the order of 8.0×10^{12} $N.m^{-1}$.

The process is repeated for a model of broken lithosphere using the relevant equations. The comparison of the observed sections and flexural models are illustrated in Figure 5.8, with the observed and derived parameters listed in Table 5.2.

These results show that, assuming the basement structure is completely the result of flexure, the lithosphere of the Australia Plate under the South Westland Basin is extremely weak at 3.10 and 9.79×10^{20} Nm, occurring at the low end of studied lithospheric rigidities (Karner et al., 1983). Holt & Stern (1991) calculated the rigidity of the lithosphere under the Western Platform off Taranaki in the region of 5.6×10^{22}–1.5×10^{23} Nm, roughly two orders of magnitude greater than the calculated values for South Westland.

When the calculated values are plotted on the age versus flexural rigidity graph of Karner et al. (1983; Fig. 2.17), a thermal age of around 1.5–2.0 Ma is suggested. Given that the tectonic subsidence curves suggest that loading probably occurred around 15-10 Ma, the inferred thermal event would have occurred during the Southland Series.

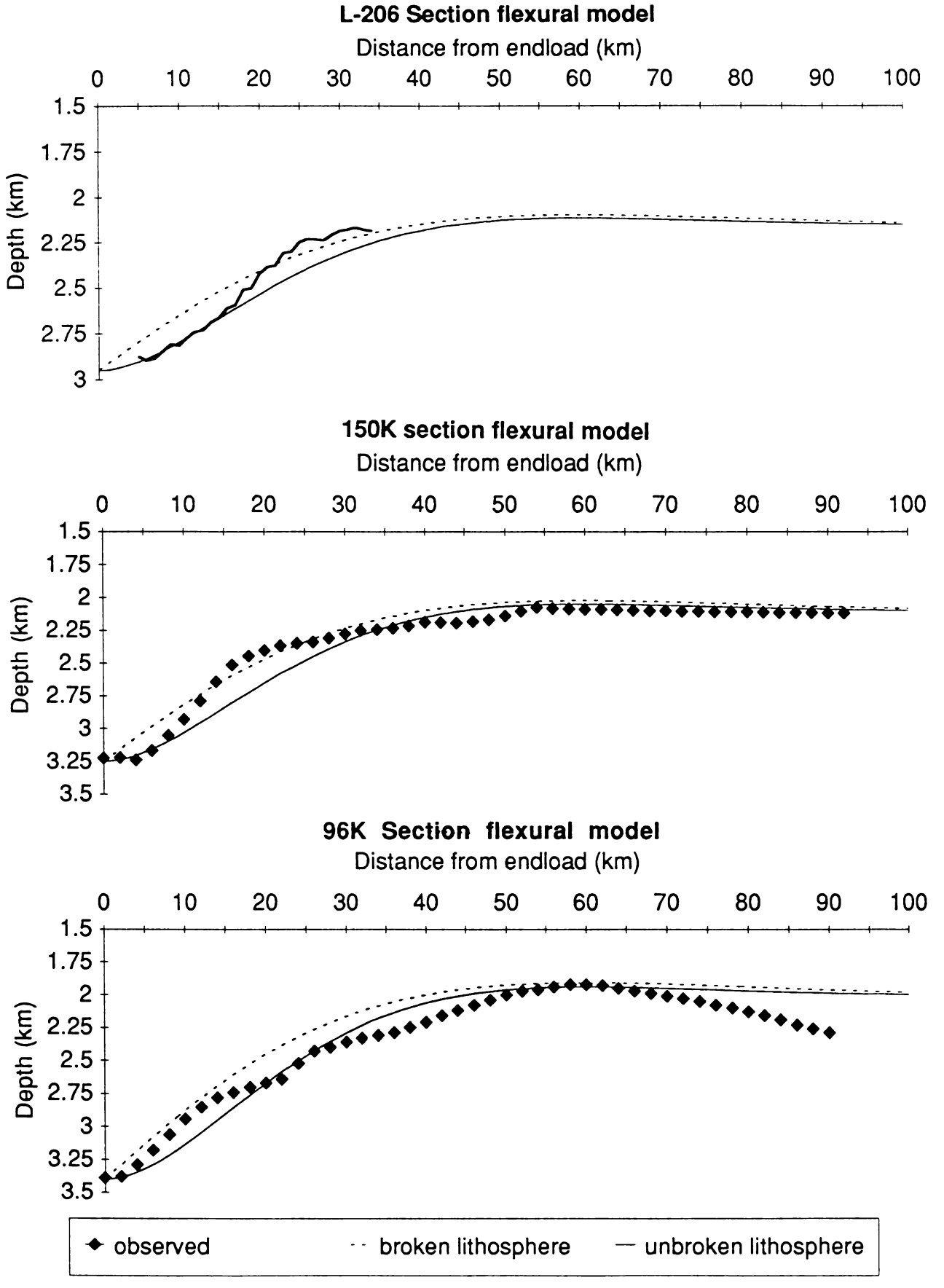

FIGURE 5.8: Flexural models of the 96K, 150K and L206 basement sections. Model curves derived using parameters given in Table 5.3.

Observed parameters:			
Distance to forebulge	x_b	60 km	
Maximum deflection	ω_0	1.40 km	(96K Section)
		1.10 km	(150K Section)
		0.80 km	(L-206 Section)
Calculated Parameters:			
Unbroken Lithosphere			
Flexural parameter	α	19.10 km	
Flexural rigidity	D	3.10×10^{20} Nm	
Elastic thickness	T_e	3.65 km	
Line load	V_0	4.98×10^{11} Nm^{-1}	(96K section)
		3.92×10^{11} Nm^{-1}	(150K section)
		2.85×10^{11} Nm^{-1}	(L-206 section)
Broken Lithosphere			
Flexural parameter	α	25.46 km	
Flexural rigidity	D	9.79×10^{20} Nm	
Elastic thickness	T_e	5.35 km	
Line load	V_0	3.32×10^{11} Nm^{-1}	(96K section)
		2.61×10^{11} Nm^{-1}	(150K section)
		1.90×10^{11} Nm^{-1}	(L-206 section)

TABLE 5.3: Lithospheric parameters observed and calculated in the flexural models.

5.4.2.2 *Bending stress*

Using the bending stress equations (2.28 & 2.29) derived from Watts & Talwani (1974) and the calculated configuration of the lithosphere discussed above, the bending stresses induced by flexure have been calculated. These are displayed in Fig. 5.9. The maximum amount of stress appears to occur at around 20 km from the endload, and increase southwards from section L-206 at around 130 MPa to section 96K at around 210 MPa. These bending stresses are in excess of those that the lithosphere can sustain as outlined by the yield strength envelopes of McNutt (1980) and McNutt et al. (1988). This suggests that some faulting may occur at and/or around the 20 km point from the endload. No obvious structures are noted in the basement or overlying sediments at this point. However, it is interesting to note, that the basement profiles illustrated in Fig. 5.8 all show a 'stepped' geometry, with a step seen at or near the 20 km point. In sections 96K and 150K the stepping may be a side-effect of the contouring algorithm used to create the basement

surface they represent, although the stepping can also be seen in section L-206 which has been taken directly from a depth converted seismic profile. Possible stepping in the basement reflector in the seismic profile of L-206 (Fig. 4.11) is weak. Assuming that the steps are a real feature of the basement surface, what is their origin and their relationship with the bending stresses of the flexed lithosphere?

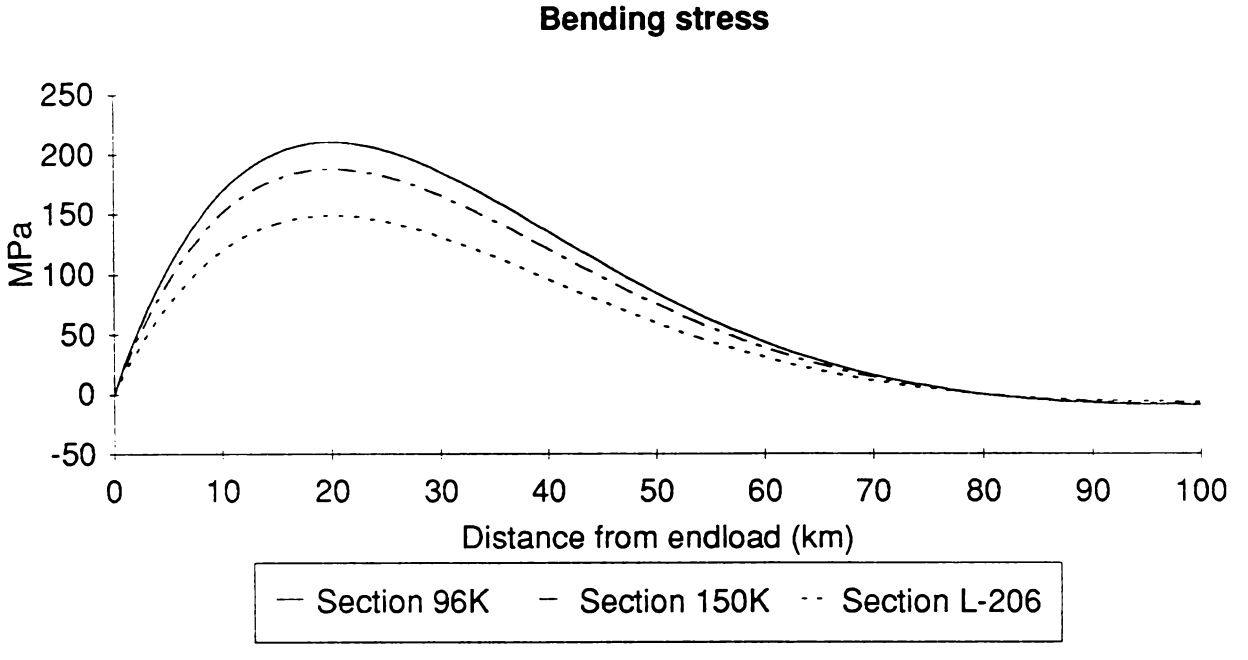

FIGURE 5.9: Bending stress models for broken lithosphere of the 96K, 150K and L206 basement sections. Positive stress is extensional, although does not necessarily imply extensional features in reality. Model curves derived using parameters given in Table 5.3.

5.4.3 Discussion of geodynamical results

5.4.3.1 *Early stage subsidence*

The early stage thermal subsidence seen in Mikonui-1 is typical for passive margins formed after a rifting and drifting event. The estimated amount of lithospheric stretching is in the order of ß=1.25. Such a relatively low stretching factor could be expected for the Mikonui-1 well-site which is about 150–200 km from the margin of the Challenger Plateau, which is underlain by continental crust. Low stretching factors result in the formation of 'sags'—basins experiencing regional subsidence but lacking major extensional faulting (Allen & Allen, 1990). No significant faulting is recognised in the basement underlying the sedimentary sequence at Mikonui-1.

5.4.3.2 *Late stage subsidence*

The late stage rapid subsidence bears many similarities with subsidence curves in foreland basins. However, rapid subsidence is not a characteristic unique to foreland basins alone.

Attempting to model the rapid subsidence in the terms of the McKenzie model would require an unrealistically high ß factor. The geological implications of this would see the presence of rift structures and associated volcanism in the modern basin. These clearly do not occur, thus renewed rifting may be dismissed as a cause of the subsidence. Fault controlled subsidence cannot be as easily dismissed. The two onshore wells are near a major fault zone that bounds the margin of the basin. A directly extensional regime across this fault zone is unlikely as the the nearby Alpine Fault has been to some degree compressional through its existence, especially in the last 10 Myr. The Alpine Fault has also been responsible for a massive displacement of major tectonic units on either side by the means of a strike-slip movement. Although no evidence exists to confirm or deny the fact, the South Westland Fault Zone may also have had and/or have some degree of a strike-slip component in its movement. Basins associated with strike-slip deformation are generally small and complex compared to other basin types (Allen & Allen, 1990).

If this is this the case, then part of the subsidence seen in the three wells from around 15 Ma onwards may be due to strike-slip movement. Some foreland basins, particularly in the European collisional belt, exhibit features associated with strike-slip deformation. For example, the Venetian Basin in northern Italy (Massari et al., 1986) has a number of transpressional faults cutting across the basin, oblique to the strike of the main thrust fault. These faults are responsible for the tectonic control of sediment deformation and deposition within the basin. However, these faults have a distinct surface expression. No synthetic or antithetic faulting associated with strike-slip deformation along the Alpine Fault have been recognised in South Westland. Such structures are generally associated with thin-skinned tectonics in cover sediments, controlled by shallow faults steepening and converging at depth. Apart from possible thrust structures in the Paringa area, no thin-skinned style tectonics are easily recognised in South Westland as presumably the cover rocks that might have contained such structures have been removed by the uplift of the Southern Alps, and the onshore part of South Westland.

5.4.3.3 *Basement flexure models*

The flexural models of the three sections across the basement surface in the South Westland Basin have a peculiar result. If the basement surface is assumed to be entirely derived from the flexure of the Australia Plate, then the geodynamical equations suggest very weak flexural rigidities of the underlying lithosphere. The calculated rigidities are largely dependent on the distance to the forebulge in the basin, which appears to be around 60 km offshore from the South Westland Fault Zone, taken as the site of the endload in the flexural equations. The equations suggest a flexural rigidity in the order of 3.10–9.79 $\times$ 10^{20} Nm for unbroken and broken lithosphere respectively. Given that the

model is assuming that the Pacific plate has been loaded onto the edge of the Australia plate, the broken lithosphere model is probably a better mathematical representation of the physical structure of the collision zone. There are a number of possible explanations for this low lithospheric rigidity, and these option will be explored below.

Initial setting

There are a number of unusual aspects of the geological setting of the South Westland basin that may make the normal assumptions about foreland basin formation invalid and/or inapplicable. The continental crust under the Challenger Plateau is notably thin, possibly around 20 km. This in turn resulted in the region being well below sea level before any loading event at the Alpine Fault could occur. This low profile may have contributed to the rapid nature of the loading event and resulting subsidence. The presumed forebulge has a transitional margin with oceanic crust at the edge of the Challenger Plateau to the southwest. The Puysegur ocean-continent convergence zone represents the southern continuation of the Pacific Plate thrusting over the Australia Plate in the central South Island. The transition between continental and oceanic crust in the South Westland situation may have a weakening effect on the flexed continental lithosphere. It is interesting to note that within 'pure' continental settings that significant lateral variation in flexural rigidity is postulated postulated in the Himalayan collision zone (Lyon-Caen & Molnar, 1985) and the Ebro basin (Zoetemeijer et al., 1990).

Karner and Watts (1983) postulated the existence of hidden or subsurface loads, such as density variations in the lithosphere, as an extra driving force for foreland flexure and subsidence in the Alps and Appalachians (Karner & Watts, 1983). A similar situation exists in the Appennines and Carpathians (Royden & Karner, 1984). Further study of gravity anomalies and basement structure may help to delineate possible subsurface loads.

One fundamental assumption of the general flexural equation is that no horizontal forces act on the flexed lithosphere (Equation 2.15). Given the tremendous rates of uplift and convergence occurring across the Alpine Fault this assumption may not be valid in the South Westland basin. Studies of shear strain rate across the Alpine Fault (Walcott, 1979) suggests that a large part of the strain is accommodated at and immediately southeast of the Alpine Fault. The inferred low rates of strain to the west of the Alpine Fault may be further complicated by the presence of the South Westland Fault Zone. No attempt has been made in this study to relate the strain with possible horizontal stresses acting on the Australia Plate. Recent work in the Appalachians has developed a conceptual framework for linking vertical movements in a foreland basin with intraplate stress fluctuations (Peper et al., 1992). Again, no such analysis in the South Westland basin has been undertaken by this study.

High heat flow

Low lithospheric flexural rigidities are frequently associated with high heat flows through the lithosphere, e.g. Western United States (Turcotte & Schubert, 1982, p.222) and the Ebro Basin, northern Spain (Zoetemeijer et al., 1990). This reflects the weakening effect of elevated temperatures on the mechanical properties of the lithosphere. Zoetemeijer et al. (1990) discuss the correlation of flexural models of the lithosphere below the Ebro basin with laboratory experiments of the dependence of lithospheric yield strength on temperature. They find an elastic thickness of 8 km ($D = 3.2 \times 10^{21}$ Nm), is comparable with the cumulative strength of the yield envelope calculated for a heat flow of 100 $mW.m^{-2}$. An elastic thickness of 30 km ($D = 1.68 \times 10^{23}$ Nm) is consistent with a lithospheric strength profile corresponding to a heat flow between 60 and 80 $mW.m^{-2}$. The high heat flow in the Ebro basin is attributed to the previous formation of an aulacogen immediately to the south of the basin. If the analog is valid in the case of South Westland, then a heat flow of over 100 $mW.m^{-2}$ could be expected. Unfortunately, no direct heat flow measurements in the South Westland basin have been undertaken. A relatively high geothermal gradient, averaging around 35°C/km have been noted in oil exploration wells in other parts of the West Coast Region (Matthews, 1984). The rapid uplift of the Southern Alps has brought high temperature geotherms closer to the surface, with temperatures between 140° and 350°C predicted within 2 km of the surface (Allis et al., 1979). The effect of this heating on the nearby Australia plate is unknown, and the thermal model of Allis et al. (1979) is restricted to a zone 15 ± 10 km from the Alpine Fault.

Viscoelasticity

A possible viscoelastic relaxation of the lithosphere with time after an initial loading event has been used to model the features noted in the Alberta Basin, Canada by Beaumont (1981). Essentially, a viscoelastic lithosphere relaxes with time after the emplacement of a load, causing the basin to become deeper and narrower (Fig. 3.3b). The narrowness of the basin in South Westland may reflect such relaxation. However, relaxation may occur a significant time after the loading event, for example Beaumont (1981) estimated a viscoelastic relaxation time of 27.5 Myr. Also, relaxation presumably occurs after any new loading and thus renewed elastic subsidence has ceased. In both instances the South Westland basin may not comply. Initial loading possibly occurred around 15-10 Ma, and convergence across the Alpine Fault has only increased since then, making any possible long-term tectonic quiescence periods unlikely in which viscoelastic relaxation could occur. Viscoelastic relaxation could also be possibly interpreted from stratigraphic features in the basin, as in the case of the Alberta Basin. However, the stratigraphy of the basin has not been studied in enough detail to provide the evidence for or against such a hypothesis.

Recent formation

The weak rigidity of the lithosphere suggests that it may have formed or at least significantly heated around 2 Myr before the loading event. As discussed above, this would imply a large heating event in the basin occurred during the Southland series sediments. This in turn would suggest either renewed rifting and/or volcanism. No evidence has been recognised for either instance in the sediments of this age (Sequence D). Structures generally associated with rifting, e.g. normal extensional faults, cannot be seen in seismic profiles. Volcanism in the South Westland basin appears limited to around and immediately offshore the Paringa section, and no later than Eocene in age.

Inherited structures

The narrow nature of the basin may be the result of an inherited structure from a previous tectonic regime that has continued to have a significant control on the present geometry of the basin. Two such structures may have existed, and in combination may contribute to the basement profile seen. The Mikonui basement high marks the position of the forebulge of the basin, assuming flexure of the Australia Plate. The basement high appears to have existed since at least the Late Cretaceous where it formed a ridge between two extensional centres that were oblique to each other. Although since overwhelmed by thermal subsidence and outward building of sediments, the basement high appears to have remained in place. As discussed above from the geohistory analysis results, a linear migration of the apparent subsidence front from the onshore wells to Mikonui-1, would suggest that the front would now lie a further 25 km or so beyond the basement high. Together these two notes may suggest that the Mikonui basement high is some sort of structural flaw in the lithosphere, presently acting as a hinge zone for the flexure of the Australia Plate, and not allowing further migration of the forebulge. If this were the case then the entire flexure model of the plate may be invalid.

As discussed above, there is the possibility that some deformation occurred as the result of strike-slip movement along the Alpine Fault before it became significantly convergent. Similar polyhistory basins occur in the European collision zone with complex tectonics causing foreland basins to contain strike-slip structures and vice versa (e.g. Massari et al., 1986). Although no surface record of such deformation is now recognised, it is intuitively unreasonable to assume that around 300 km of lateral movement could occur on the Alpine Fault without some deformation in nearby regions, especially the South Westland Basin which is particularly close. The steps noted in the basement profiles in the flexural models (Fig. 5.8) may be related to such deformation as they appear to mark the point where the basement dips at a steeper angle toward the basin margin. The stepped basement profiles , possibly in combination with a hinge zone along the Mikonui basement

high, may represent an inherited structure from previous tectonic regimes that have contributed to an apparently weak lithosphere.

Crust decoupling

In the review and update of contributing factors to lithospheric rigidity, McNutt et al. (1988) develop a flexure model in which the rigidity of the lithosphere is dependent on the stress associated with flexure. In particular a decoupling zone is placed at half the 'normal' elastic plate thickness, effectively reducing the elastic thickness of the entire plate by 63%. This decoupling zone is associated with the effect of a ductile zone in the lower crust, and become significant when the bending stress induced by the flexing of the plate exceed the yield strength of this zone. As illustrated in Fig. 5.9, the bending stresses associated with the flexure of the Australia Plate are relatively large, exceeding the yield strength of the crust for a considerable depth. Even though these bending stresses may be a function of flexure after decoupling it is probably reasonable to assume that large enough bending stresses may have existed to induce possible decoupling at depth. Assuming that this is the case, then the calculated elastic thickness of the lithosphere for a broken plate model is only 63% of the pre-decoupling thickness. Thus a pre-decoupling elastic thickness would be 8.5 km, giving a lithospheric rigidity of 3.8×10^{21} Nm. This is nearly 4 times greater than the modelled decoupled rigidity at 9.79×10^{20} Nm for South Westland, but still 15 times smaller than values calculated for the Western Platform in the Taranaki Basin (Holt & Stern, 1991).

In summary, the basement profile of the Australia Plate appears to be well matched by a flexural model. However, this flexure implies that the lithosphere is particularly weak. As discussed above there are numerous possible explanations for this feature. It is reasonable to assume that any cause for the low rigidity of the lithosphere may be a combination of these. Only further measurement (e.g. heat flow) and models emcompassing more variables (e.g. oceanic crust transition) will provide better constraints on the rheological/mechanical nature of the lithosphere and its flexural behaviour.

Chapter 6

Summary and Conclusions

6.0 Introduction

It has previously been proposed that the elongate basin immediately offshore in South Westland, South Island, New Zealand, is a foreland basin, formed in response to the loading of the Australia Plate by the Pacific Plate across the obliquely convergent Alpine Fault (Kamp et al., 1992). The objective of this thesis has been to study the South Westland sedimentary basin and test the hypothesis that it is a foreland basin, by basin analysis methods. Basin analysis draws techniques from a number of disciplines within Earth Sciences. The two principle study tools used here have been seismic stratigraphy, using industry seismic reflection data sources, and geodynamical modelling, using data from both the seismic reflections and exploration wells.

Chapter 1 outlined the evidence for the foreland basin hypothesis, and the location, nature and geological setting of the study area. Chapter 2 outlined the broad range of disciplines used collectively in basin analysis for the study and interpretation of information from sedimentary basins. Chapter 3 described the geophysical and lithostratigraphic features associated with foreland basins studied elsewhere in the world. Chapter 4 applied the techniques of basin analysis, in particular the observation of the seismic profiles and exploration wells. Chapter 5 drew interpretations from those observations and used the data in geodynamical models of the basin structure and evolution. This chapter will summary these observations and interpretations in a regional synthesis of basin evolution in South Westland.

6.1 Seismic stratigraphy

Five seismic horizons plus the seafloor/ground surface were identified within the 1715 km of seismic reflection profiles studied in this project. Between these horizons, five sequences were studied in detail and their depositional history interpreted from reflection configurations.

The seismic reflection profiles were interpreted using a general application of the principles of seismic stratigraphy. Most of the profiles were of insufficient quality for further detailed analysis. With well and outcrop stratigraphy and models of plate tectonic reconstructions the depositional environments of each sequence and interrelated horizons have been interpreted. The stratigraphy of the South Westland basin bears some similarity with 'classical' foreland basin stratigraphies, although the pre-foreland basin histories are different. In this framework the mapped horizons and sequences are summarised in Table 6.1.

Horizon	Sequence	Age (Ma)	General form	Depositional Environment	Tectonic Interpretation
Seafloor	----------	0	North: gently sloping shelf South: rugged with canyons	Sediment channelling by canyons?	
	A		Restricted lens	Rapid, slumping. Eustatic control ? Sed. bypassing?	Foreland basin overfill–steady-state?
PPA	----------	1.2	Arcuate reflector. Dipping to NW.	Top of prograding sequence. Marks transition.	
	B		Lensoidal. Prograding facies	Prograding shelf	Foreland basin late stages of underfill–early overfill?
PPB	----------	3.1	Sub-parallel group of reflectors. Dipping to NW.	Trangressive sequence?	
	C		Wedge with generally chaotic internal details	Deep water turbiditic systems	Foreland basin underfill.
T.Miocene	----------	5.0	Weak, generally concordant reflector.	Minor sequence boundary?	
	D		Sheet-like. Internally generally chaotic.	Deep water turbiditic systems	Foreland basin underfill, early starvation?
Oligocene	----------	≈ 30	Prominent reflector Dipping to SE.	Shelf–bathyal limestone	Post-rift marine transgression
	E		Thin sheet. Thickens westward	Marginal marine.	Syn-rift – post-rift marine transgression
Basement	----------	> 60	Prominent reflector Basement high parallel to coast.		Eroded surface.

TABLE 6.1: Simplified summary of horizons and stratigraphy mapped and interpreted in the South Westland Basin.

6.2 Geodynamical modelling

Two principal areas of geodynamical analysis were undertaken in this study using data derived from the South Westland Basin: thermal subsidence and flexural modelling. The long-term gradual subsidence noted in the tectonic curve of Mikonui-1 was well suited for modelling of thermal subsidence of continental lithosphere after a stretching event. The simple McKenzie (1978) stretching model was used for this analysis. By a visual comparison, a modelled thermal subsidence curve following a stretching event of ß=1.25 was found to be the best fit for the tectonic subsidence between 60–10 Ma. Using the McKenzie model to explain the rapid subsidence from 10 Ma onwards is invalid, as ß-factors of around 10 are predicted, normally associated with sea floor spreading centres. Obviously no such features are recognised.

Assuming flexure of the Australia Plate, the basement profiles derived from the seismic profiles were modelled with general flexural equations. The results have shown that the

lithosphere of the Australia Plate is particularly weak with rigidities in a modelled broken lithospheric plate around 9.79×10^{20} Nm (effective elastic thickness = 5.35 km). This is at the low end of observed lithospheric rigidities. A number of explanations for this feature have been discussed. The setting of the basin is unusual. The Australia Plate was already low lying before any possible loading event across the Alpine Fault. The lithosphere also has a transitional zone with oceanic crust nearby at the margins of the Challenger Plateau. The large amount of flexure of the lithosphere may be a result of a mechanical weakness caused by a high heat flow, or recent heating event. No direct heat flow measurement have been undertaken in the basin, and there is no stratigraphic evidence of a comparatively recent heating event in the region. The crust may be decoupled at depth causing a decrease in the effective rigidity of the plate. Even accounting for this possibility the lithosphere still seems to be particularly weak. A number of inherited structures from previous tectonic regimes may have effected the lithosphere, constraining and/or enhancing the response of the lithosphere. A basement high now seemingly acting as a forebulge appears to be inherited from rifting during the Late Cretaceous. Although no evidence is recognised, possible strike-slip deformation associated with the early stages of movement along the Alpine Fault may have effected the lithosphere under the basin and provided an edge to the plate for later loading.

6.3 Synthesis

Using the discussions in Chapter 5 and above, a geological history of the South Westland Basin, in terms of it evolving from a rift margin in the Late Cretaceous through to a comparatively recent foreland basin, can be synthesised. This synthesis is presented below, combining regional paleogeography with total basement subsidence at each mapped time interval.

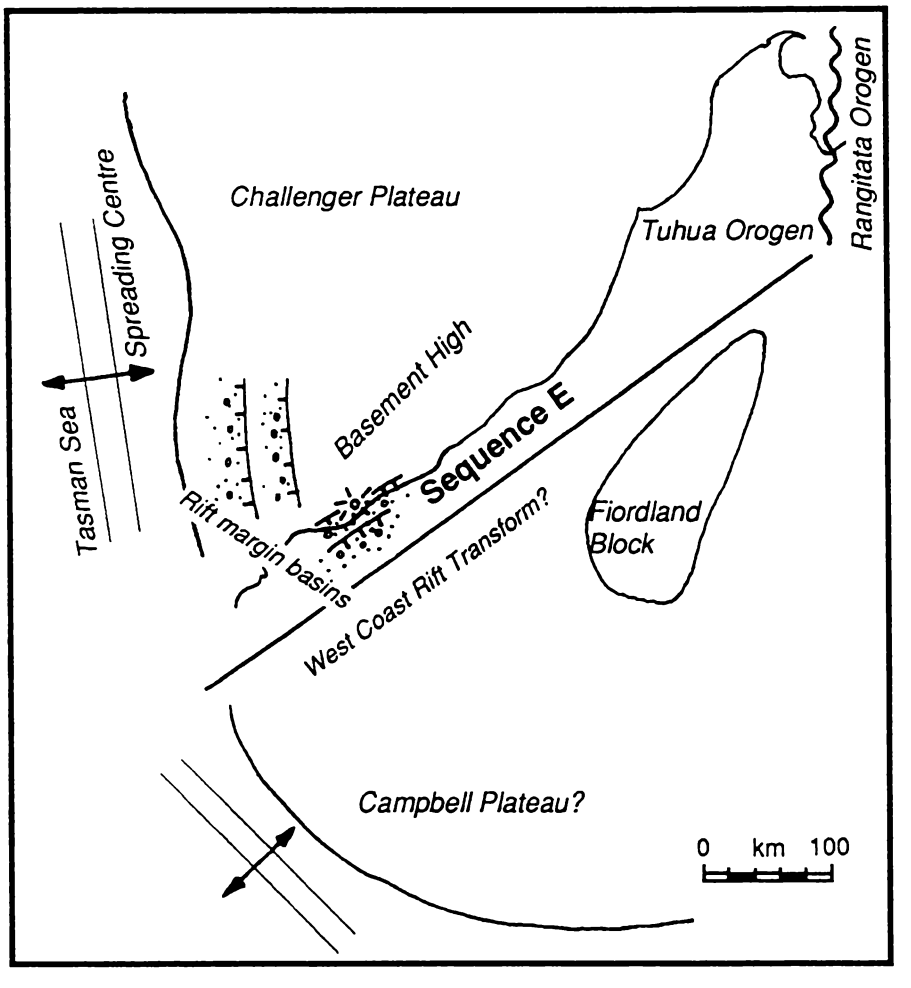

FIGURE 6.1: Paleogeography of Sequence E (Late Cretaceous–Eocene). Note location of a postulated basement high between two rift zones.

6.3.1 Late Cretaceous–Eocene

Deposition in the South Westland Basin began during the Late Cretaceous where localised rift margin basins formed in response to the rifting of the Tasman Sea, and a postulated rift transform zone through the New Zealand continental block (Fig. 6.1, Fig. 6.10A). The sediments are marginal marine and reflect the continuing thermal subsidence of the continental block and subsequent marine transgression. Some rift associated volcanism is

also noted. A basement high (herein titled the Mikonui High) is thought to have formed between the rifting centres (Fig. 6.2) with an overall lithospheric stretching factor of around ß=1.25.

6.3.2 Oligocene

The thermal subsidence induced marine transgression reached its maximum during the Oligocene when a regionally extensive limestone, the Awarua Limestone, was deposited in

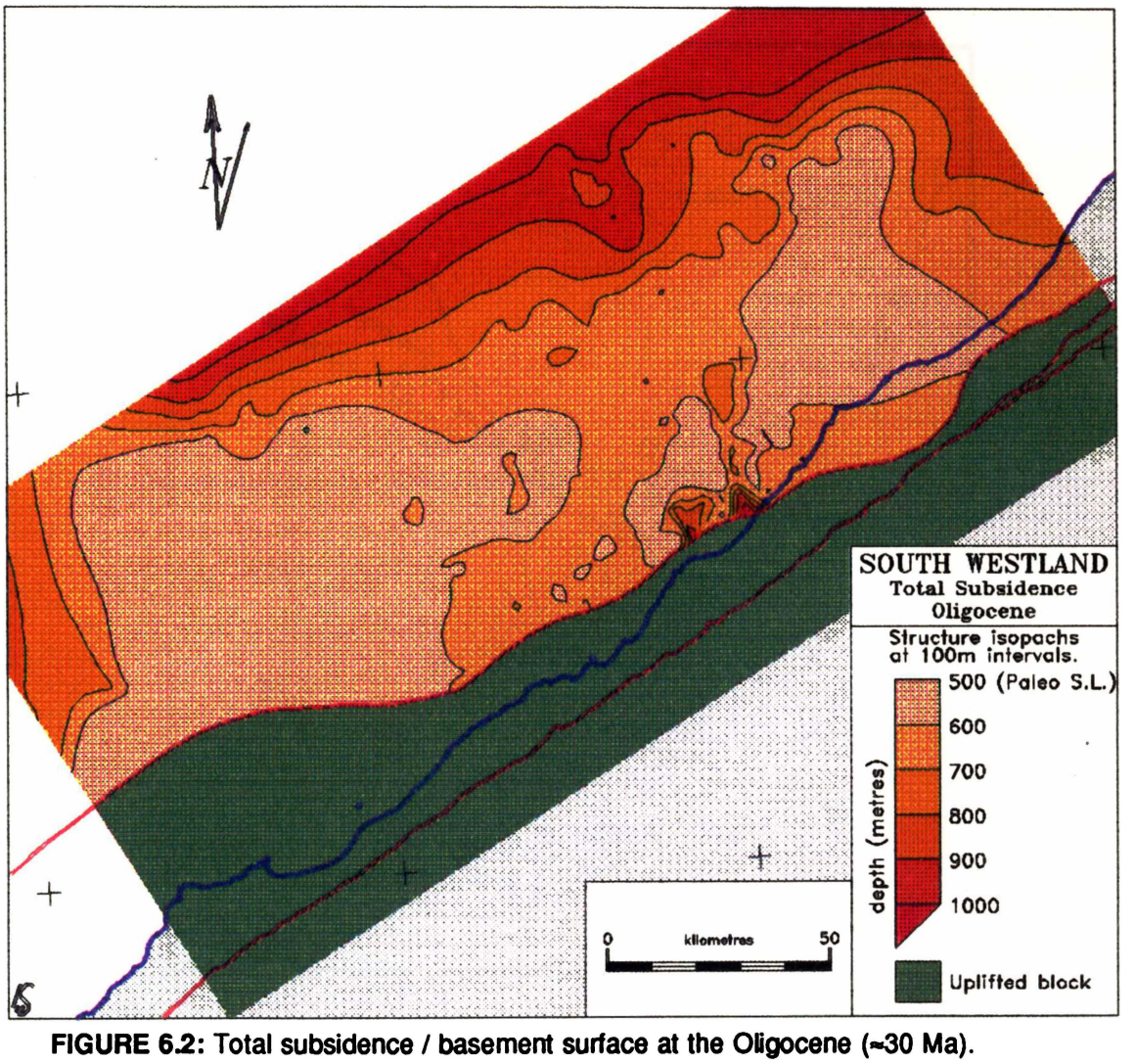

FIGURE 6.2: Total subsidence / basement surface at the Oligocene (≈30 Ma).

a terrigenous sediment starved basin. Subsidence even overwhelmed the Mikonui basement high. The limestone appears to shallow toward the east, suggesting that this margin of the basin was slightly uplifted, possibly in response to nearby spreading in the Emerald Basin (Fig 6.10A).

6.3.3 Miocene

The marine transgression was halted by the inception of the Alpine Fault through the New Zealand block at around 23 Ma. Initially movement was principally strike-slip, causing the prominent displacement of the Fiordland block from its counterpart in Nelson (Fig. 6.3).

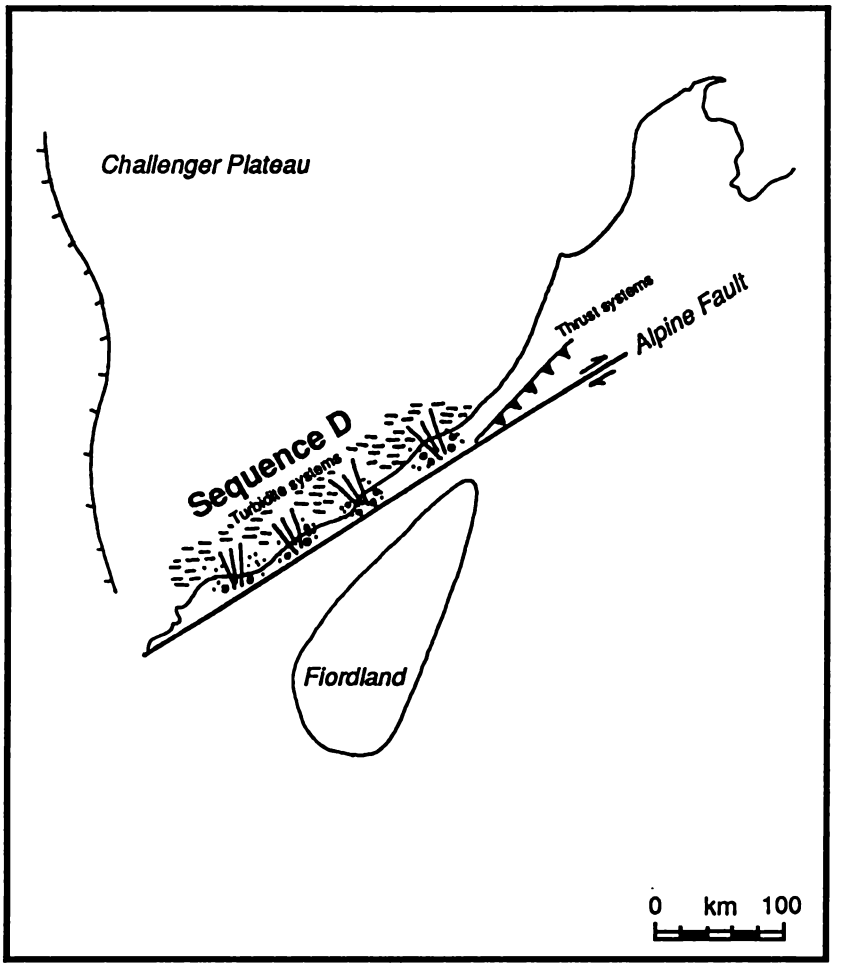

FIGURE 6.3: Paleogeography of the Sequence D (Mid–Late Miocene). Note movement on the Alpine Fault has commenced.

At least some localised form of strike-slip deformation may have occurred (Fig. 6.10B). Rapid subsidence in the South Westland Basin is noted in stratigraphic records and geohistory analyses of the onshore wells at around 15–10 Ma. A deep basin began forming adjacent to the Alpine Fault (Fig. 6.4), and the first, relatively thin, sequence of turbiditic systems were deposited at bathyal depths. The formation of a new basin overwriting the old rift margin basins may have been fault controlled at this point. The 15–10 Ma time

interval is also coincident with increasing convergence across the Alpine Fault, and may indicate the early stages of loading on the Australia Plate and the inception of the foreland basin. Topographic expression and hence sediment supply may have been limited at this stage.

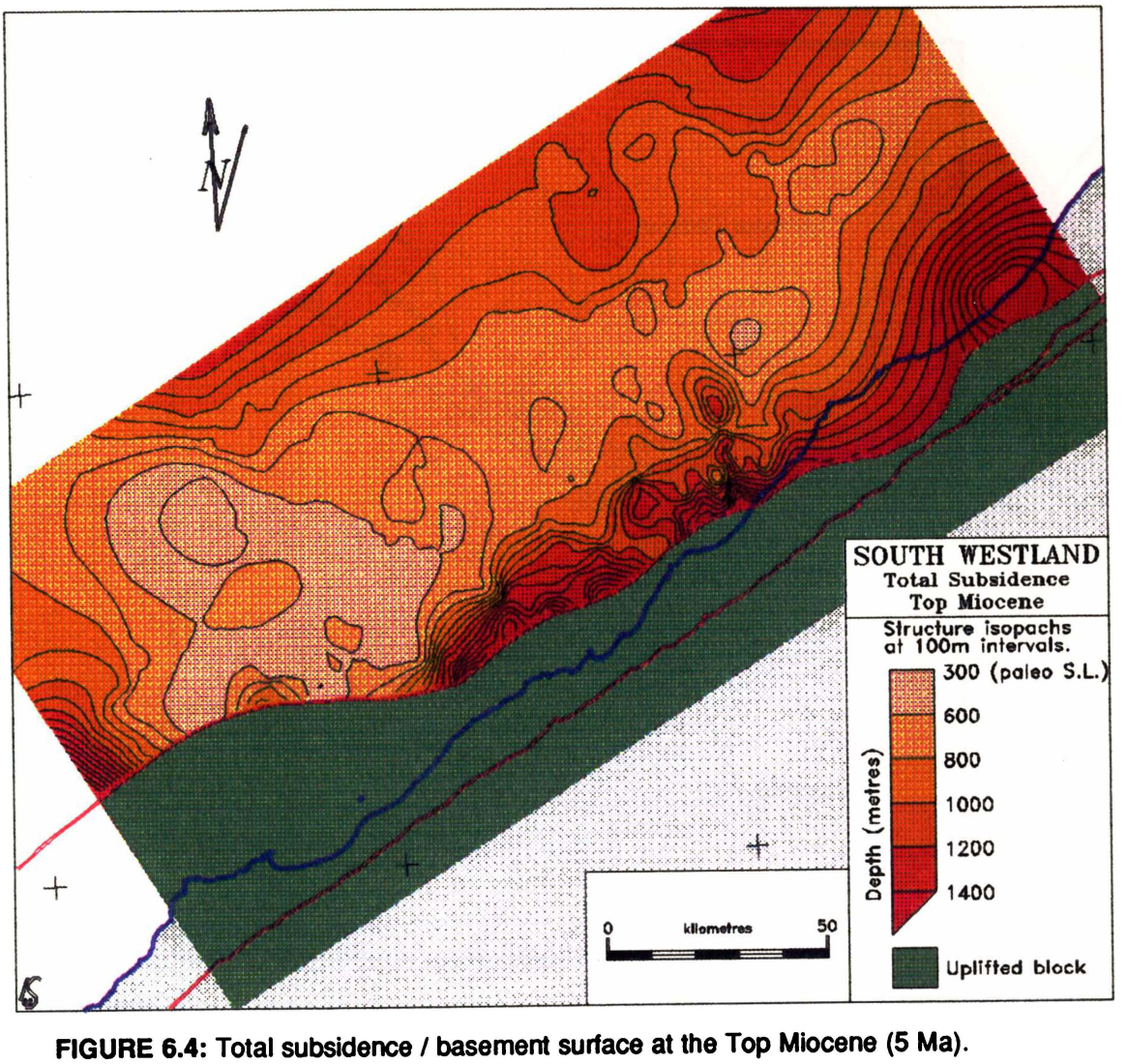

FIGURE 6.4: Total subsidence / basement surface at the Top Miocene (5 Ma).

6.3.4 Early Pliocene–Mid Pliocene (Opoitian–Waipipian Stages)

A major tectonic event appears to have occurred at the Top Miocene around 5 Ma as shown by the tectonic subsidence in the three exploration wells. From other studies this time coincides with accelerating convergence and resulting uplift across the hitherto transform Alpine Fault.. Recycled sediments from older successions have been noted in the Waiho-1 well during the Opoitian (Early Pliocene), and in combination with fission track data,

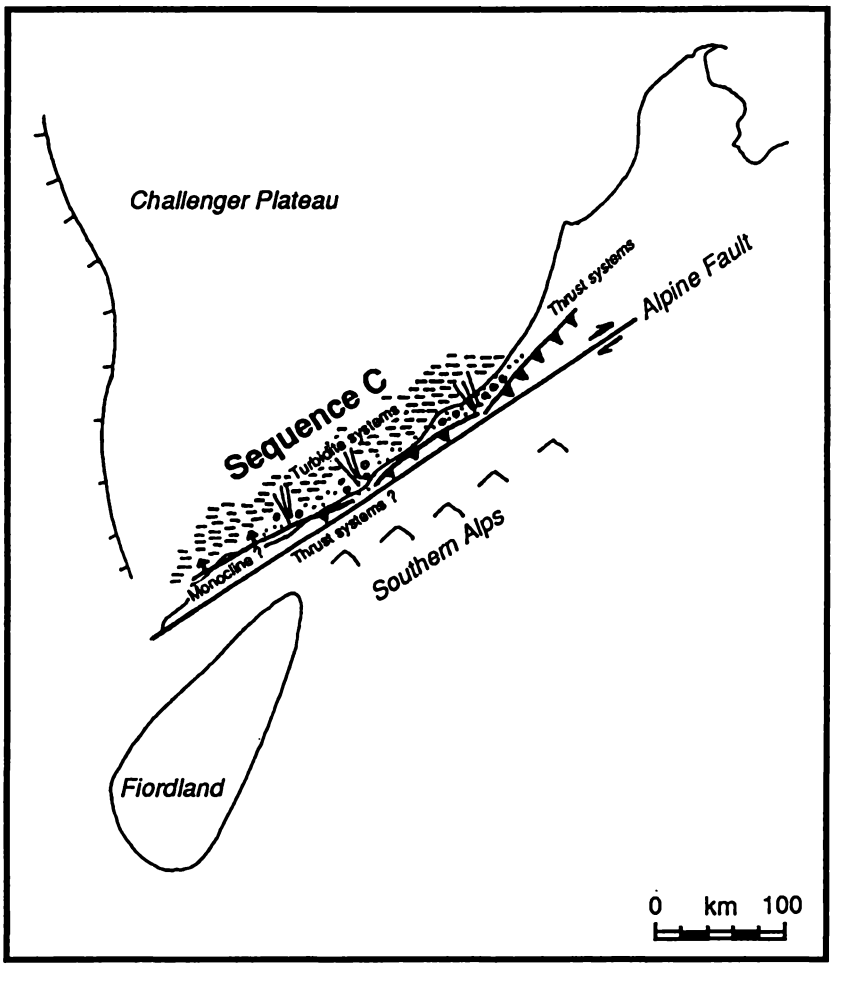

FIGURE 6.5: Paleogeography of Sequence C (Opoitian–Waipipian). Note postulated southward migration of inversion and deformation of the inner margin of the basin.

suggests that the inner basin margin was rapidly uplifted at around 5 Ma (Fig. 6.5; Fig. 6.10C).

This is postulated to have formed the Coastal Monocline, although this may also be alternatively interpreted as a thrust system (Fig. 6.10D). The rapid subsidence phase began in the distal Mikonui-1 well at 5 Ma. This point may mark the inception of uplifting along the South Westland Fault Zone bounding the uplifted inner margin, further

loading the Australia Plate. The sedimentation of the sequence immediately after this point is particularly thick and deposited rapidly at a rate of around 325 m/Myr, consisting of further turbiditic systems (Fig. 6.5; Fig. 6.10C). The sediments of this time interval (Sequence C) thicken to around 1500 m against the uplifted southwestern margin of the basin Such a sediment load would enhance the flexure of the Australia Plate (Fig. 6.6).

The rapid flysch-like sedimentation of this period also reflects the underfilled nature of

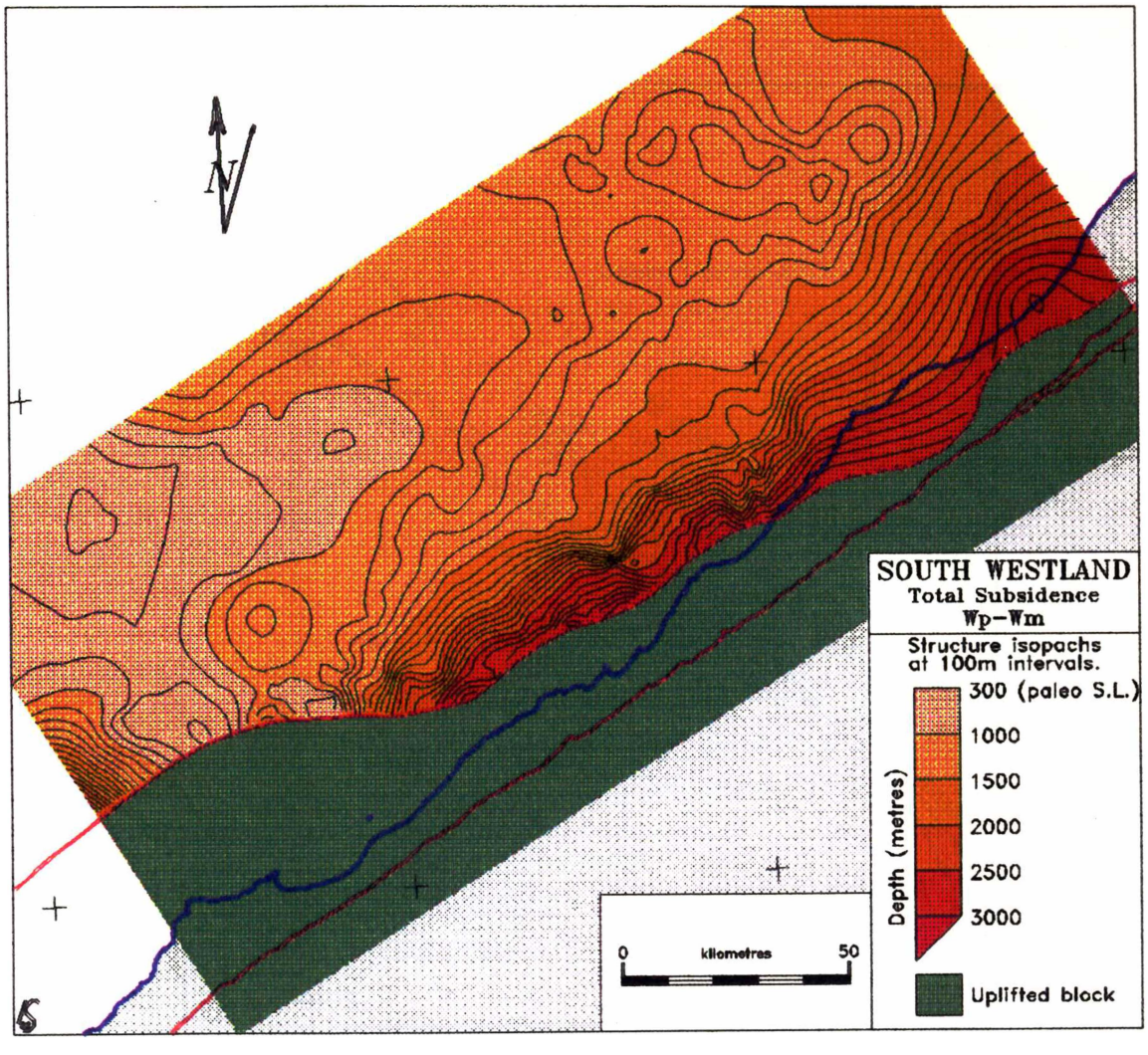

FIGURE 6.6: Total subsidence / basement surface at the Waipipian–Mangapanian boundary (3.1 Ma).

the foreland basin.

6.3.5 Late Pliocene–Early Pliestocene (Mangapanian–Nukumaruan Stages)

After the creation of the foreland basin around 10–15 Ma and the rapid and thick deposition of turbidite systems, the sedimentation in the basin continued to remain high during the mid-Wanganui Series (Late Pliocene–Early Pliestocene), but the character of the depositional regime changed. The sediments of this time interval (Sequence B) are dominantly progradational, exhibiting prominent sigmoid-oblique complex foreset

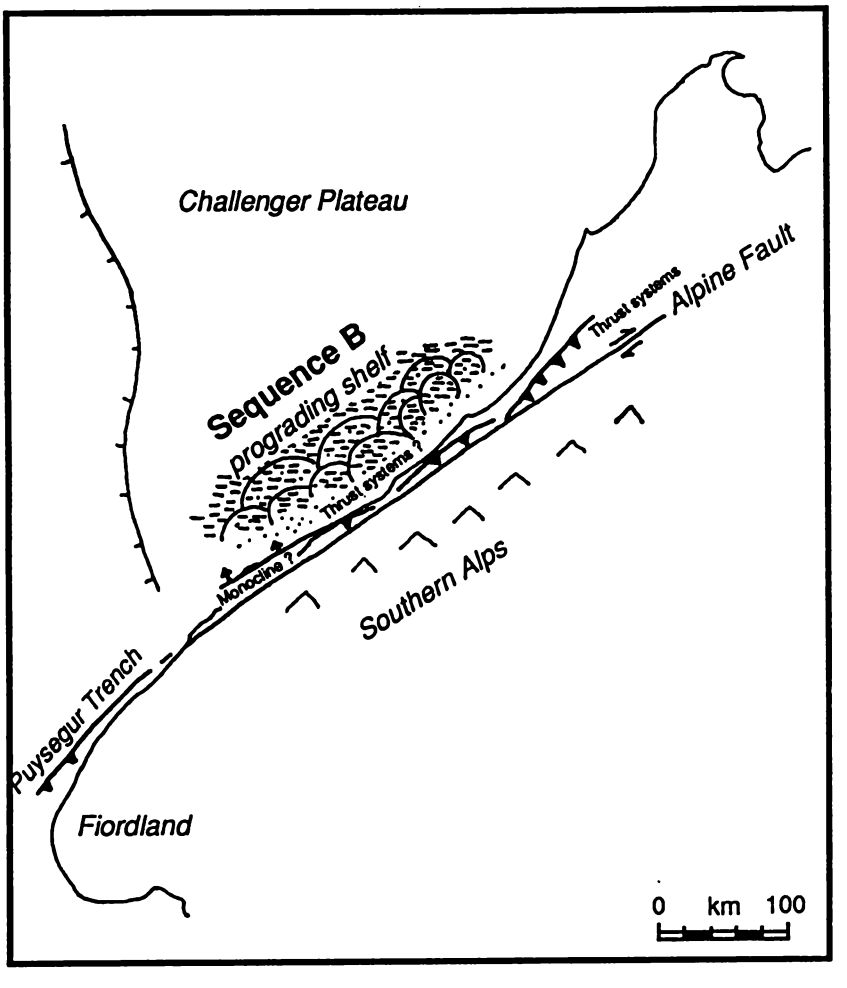

FIGURE 6.7: Paleogeography of Sequence B (Mangapanian–Nukumaruan). Note extensive prograding facies, and increased topography of the uplifting Southern Alps.

patterns. This suggests a measure of stability in the basin, and a shallowing of the depositional depths to around mid shelf depths. The sedimentation rates appear to decrease slightly from the previous period (to around 240 m/Myr), perhaps indicating the early signs of the basin sediments evolving toward an equilibrium profile. The maximum thickness of the sequence deposited during this period is around 1200 m.

In foreland basin terms, the prograding facies may represent the later stages of basin underfill as the basin begins to fill and sediment accommodation potential decreases. Deposition also began to overwhelm the forebulge during this time (Fig 6.7; Fig. 6.10D). The thick sediment fill continued to emphasis the deep flexure basin forming adjacent to the uplifted inner margin (Fig. 6.8).

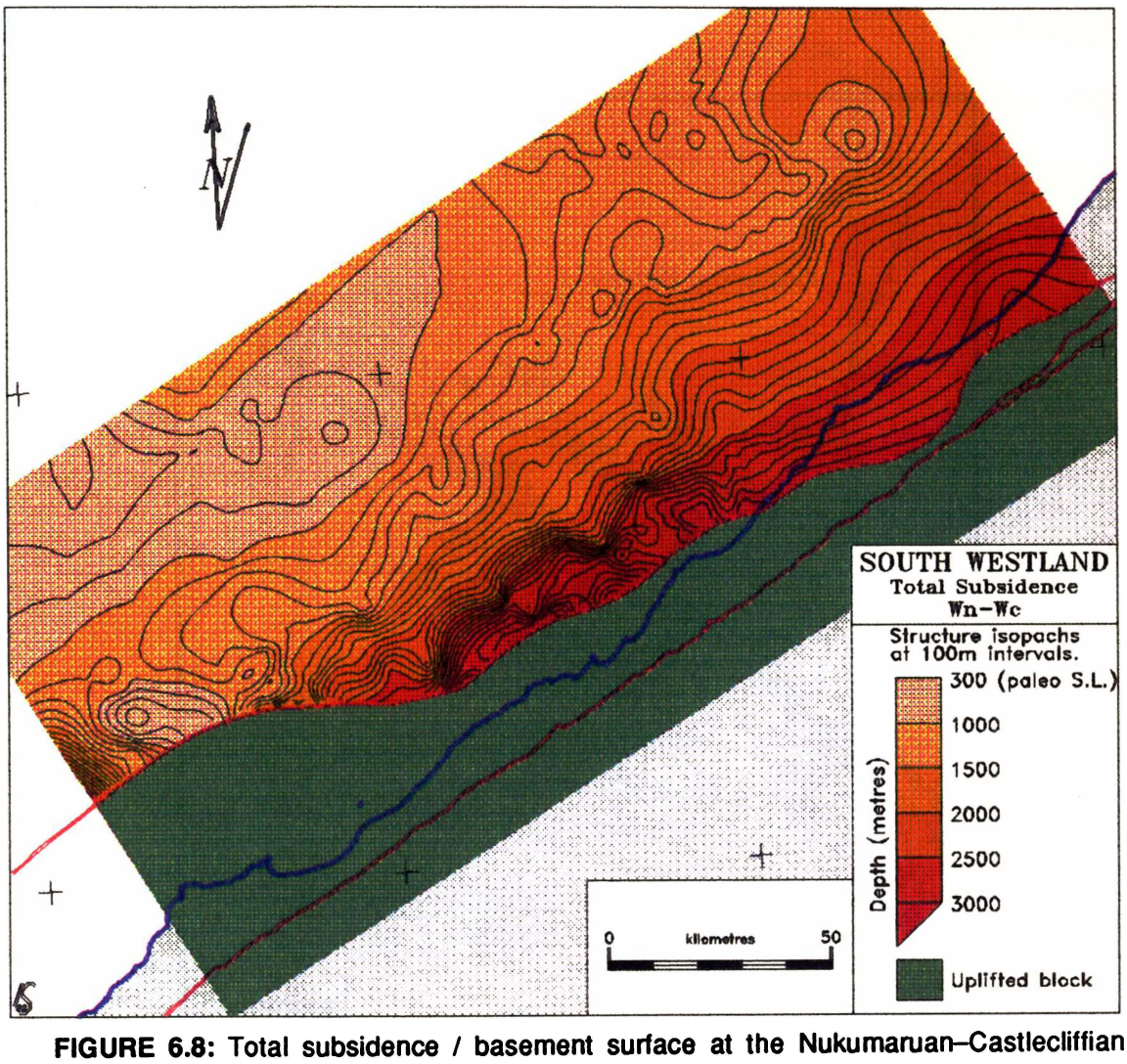

FIGURE 6.8: Total subsidence / basement surface at the Nukumaruan–Castlecliffian boundary (1.2 Ma).

6.3.6 Middle–Late Pliestocene (Castlecliffian–Hawera Series)

Another change in the depositional regime appears to have occurred at the Nukumaruan–Castlecliffian boundary (early Pliestocene). The prograding facies abruptly cease and deposition becomes more restricted to predominantly around the shelf break, with little or no recognisable sedimentation patterns visible. This may reflect rapid deposition and/or

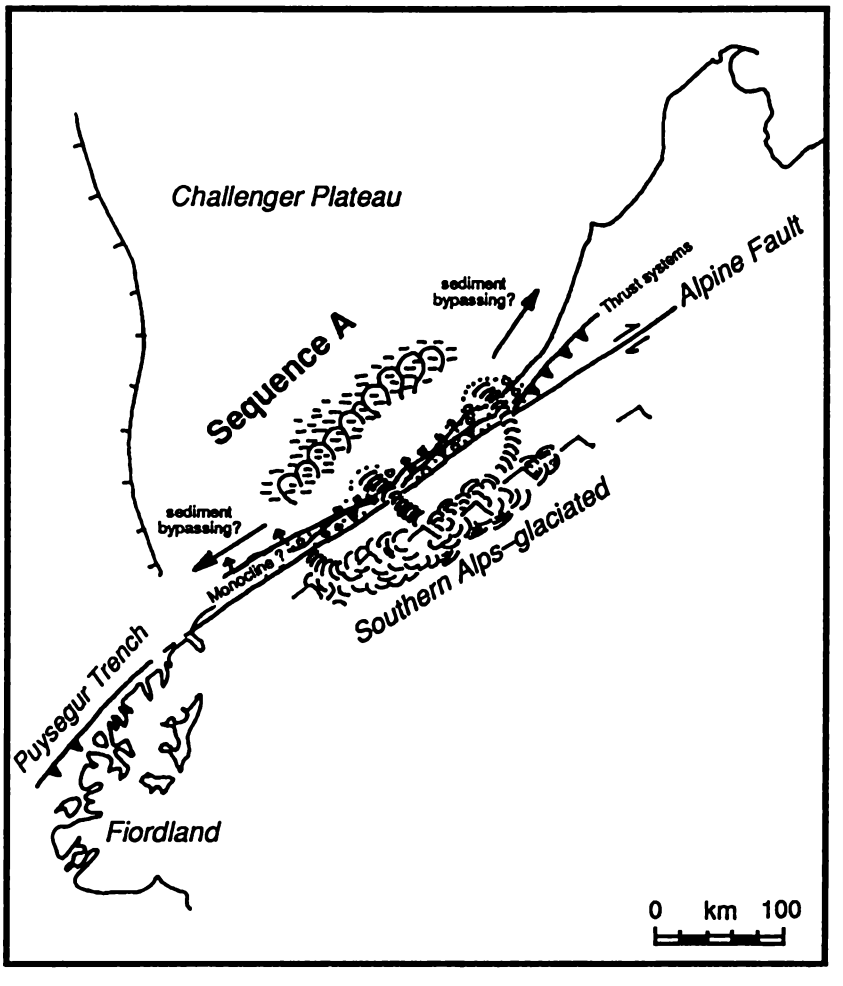

FIGURE 6.9: Paleogeography of Sequence A (Castlecliffian–Hawera). Note areally restricted facies, and glaciation of the Southern Alps.

strong eustatic control during the glacial cycles of the Pliestocene.

Bioclasts in a predominantly terrigenous depositional environment also suggest a change in sedimentation regimes. In foreland basin terms, the basin may have reached an overfilled state and a steady-state profile began to form with sediment bypassing occurring (Fig. 6.10E). The basement structure of the South Westland basin at present is illustrated in Fig. 4.16.

FIGURE 6.10: Schematic reconstructed cross-sections across the South Westland Basin through time. Basin fill to northwest of the South Westland Fault is extracted from the database at the 96K section. Southeastern structures are largely speculative. Vertical exaggeration 4x.

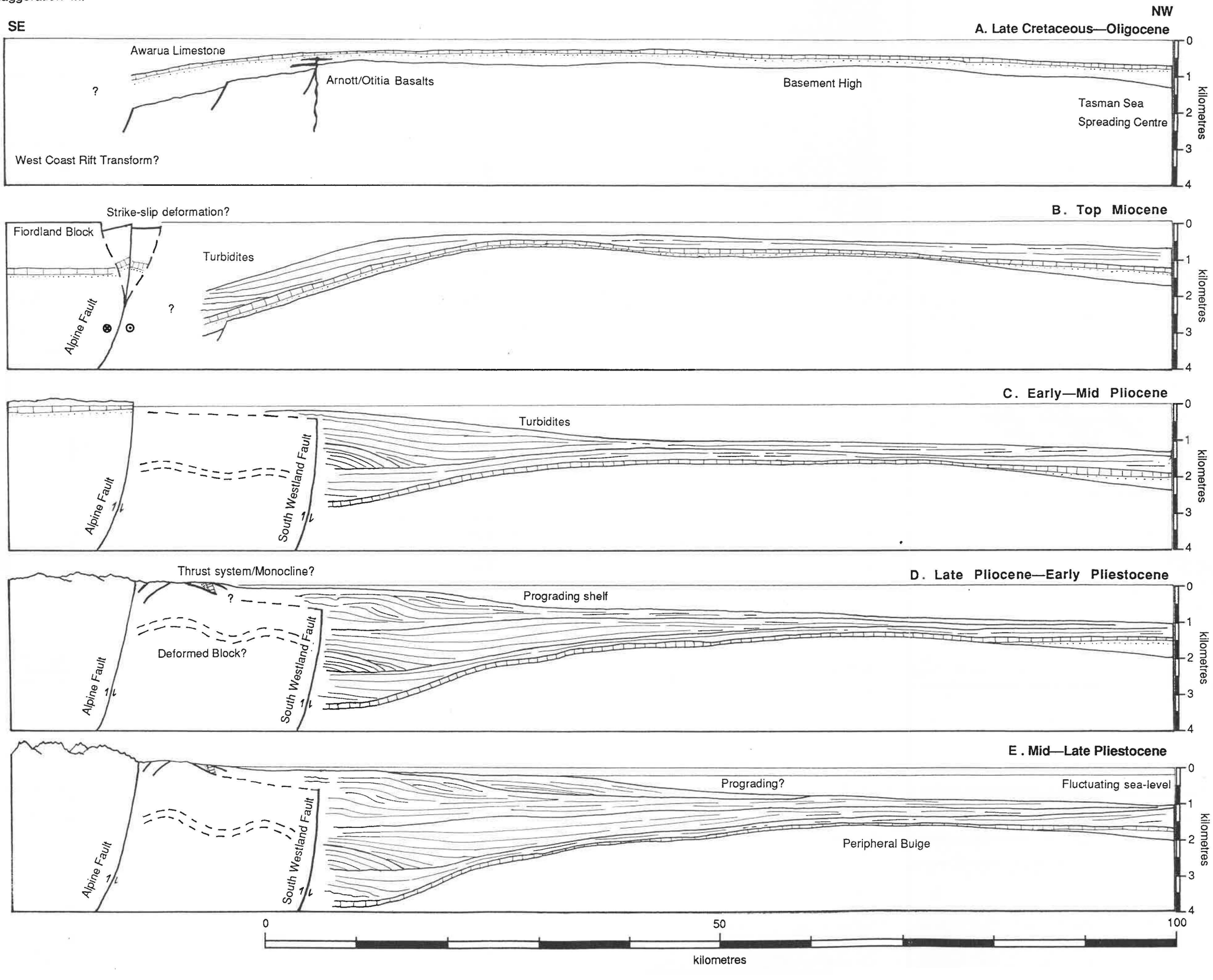

6.4 South Westland—a Foreland Basin?

The hypothesis of this thesis is that the sedimentary basin observed in South Westland is a foreland basin formed as a result of the Australia Plate being loaded by continental convergence across the Alpine Fault during the late Cenozoic. Previous studies (Kamp et al., 1992) combined broad scale evidence of the structure and location of the South Westland basin with fission track data delineating the timing and amount of uplift on the inner margin of the basin in proposing that the basin formed as a foreland basin. This study has undertaken analysis of the industry seismic reflection data and stratigraphic information gathered in the basin, both directly in the nature of the seismic units mapped, and indirectly by modelling the lithospheric subsidence and flexure that these units inferred. The subsidence history of the three exploration wells shows the rapid subsidence curves considered typical of subsidence in a foreland basin. The stratigraphy of both the exploration wells and surface outcrops suggests the rapid filling of an initially deep, underfilled basin, to the early stages of a relatively shallow overfilled basin. This basin fill evolution corresponds well with depositional models of other foreland basins. The basement structure appears to match flexural models reasonably well, albeit describing a very weak lithosphere. These features combined with the broad scale and thermochronological evidence of previous workers would strongly suggest that the basin adjacent to the Southern Alps in South Westland, South Island, New Zealand, is indeed a foreland basin formed by the flexing of the Australia Plate.

As the convergence across the Alpine fault is between two continental plates, the South Westland basin can be described as peripheral foreland basin in the sense of Dickinson (1974a; Fig. 3.1). For comparison, the nearby Taranaki Basin, now termed a foreland basin also, is described as a retroarc foreland basin (Stern & Davey, 1990). Other features associated in the literature with foreland basins, particularly thrust fronts and subdivided depocentres may await further investigation.

6.5 Conclusions

The South Westland Basin is a polyhistory basin. The basin was initially formed on the margins of rifting centres during the Late Cretaceous. After the inception of the Alpine Fault during the Miocene, the basin was probably fault controlled in response to strike-slip movement and deformation. Subsidence may have occurred near the fault zones during this time. The Alpine Fault became increasing convergent over time during the Miocene (15–10 Ma), loading and causing flexure of the Australia Plate. Sedimentation was relatively slow, reflecting the depth of the basin and lack of uplifted source areas. At the end of the Miocene, around 5 Ma, the inner margin of the basin was rapidly uplifted from a depth around 4 km and deformed. In response, the subsidence rate of the Australia Plate

quickened. Sedimentation in the foreland basin became more rapid as source areas were uplifted, passing from an underfilled stage to a recent overfilled stage with possible sediment bypassing.

This multiple history of the basin appears to have a significant effect on the mechanical strength of the Australia Plate, as geodynamical models indicate that the margin of this plate now under the foreland basin is particularly weak at around 9.79×10^{20} Nm (effective elastic thickness = 5.35 km). A number of scenarios explaining the weakness of the lithosphere have been proposed, but until these can be tested by various means, it is reasonable to assume that structures inherited during the complex history of the basin has weakened the lithosphere.

More questions than answers have been revealed by this study. A number of interesting avenues for further research have been noted. The implications of a weak Australia Plate on the models of the collisional zone in the South Island may be of particular importance. Renewed study and possible reinterpretation of the well sections in conjunction with the reprocessing of the seismic profiles may reveal greater detail about the sedimentation history of the basin. More precise models of the flexural response of the Australia Plate could be compiled, accounting for such parameters as the nearby oceanic crust transition and possible horizontal stresses across the Alpine Fault. Further study could also explore the links between the recent mountain building processes in the Southern Alps and corresponding deposition patterns in the South Westland Foreland Basin.

Appendices

Appendix A: Seismic Line details

The details of the seismic lines used in this study are listed below. 58 'complete' lines have been subdivided into 124 line segments to aid the accuracy of shotpoint locations on meandering lines. The location of the lines are illustrated in Figure 4.7.

The *Line_id* titles highlighted in bold type are 'typical' sections illustrated in Chapter 4.

The *PR/encl.* numbers are the Open File Petroleum Reports and enclosure numbers of each seismic reflection profile (see Table 4.4 for further details).

The start shot points are taken from the left hand end of the profile.

Coordinates of the start and end shotpoints of the seismic lines are given in the NZMS metric standard. These coordinates were digitized from track charts in the Open File Petroleum Reports, in particular:

Chart	Line series
523/4	OS-
523/5	M-
575/1	L-, W-
614/1	NZ-
629/1	PS-, GSI-4B

Each set of lines listed below is described by:

Petroleum exploration licence holder
Geophysical exploration contracter
Date of recording (accuracy varies)

Line_id (type sect.)	PR/encl.	Start shot-point	End shot-point	Start east coords.	Start north coords	End east coords.	End north coords	Length (m)

ESSO Standard Oil (Aust)
Western Geophysical
26 Feb - 27 Feb 1968

EZD-1	400/9	708	485	2202810	5723596	2236013	5752979	44338
EZD-1b	400/10	485	440	2236013	5752979	2242644	5758978	8942
EZD-1c	400/10	257	101	2242871	5759170	2266244	5780291	31502
EZD-2	400/11	1	100	2257951	5786447	2271373	5772072	19667
EZD-3	400/12	343	260	2241732	5768260	2252757	5756182	16353
EZD-4	400/13	344	439	2224876	5753535	2236189	5738441	18863

New Zealand Petroleum Co. Ltd.
M.L. Randall Exploration
September 1971

(These lines are marked 'OS-' for OnShore, and are the only seismic lines recorded onshore in the project area)

OS-1	523/7	1	7	2311600	5797294	2312330	5795698	1755
OS-1b	523/7	7	8	2312330	5795698	2312828	5795695	498
OS-1c	523/7	8	10	2312828	5795695	2313073	5795053	686
OS-1d	523/7	10	13	2313073	5795053	2314339	5794326	1460
OS-1e	523/7	13	14	2314339	5794326	2314443	5793601	733
OS-2	523/8	0	5	2300564	5793261	2302689	5793467	2135
OS-2b	523/8	5	19	2302689	5793467	2307553	5790468	5713
OS-2c	523/8	19	23	2307553	5790468	2308061	5789274	1298
OS-2d	523/8	23	29	2308061	5789274	2309551	5788049	1929
OS-2e	523/8	29	34	2309551	5788049	2311699	5787537	2209
OS-3	523/9	1	8	2301380	5791411	2302057	5788740	2755
OS-3b	523/9	8	17	2302057	5788740	2304010	5785341	3920
OS-3c	523/9	17	20	2304010	5785341	2305228	5784976	1271
OS-3d	523/9	20	25	2305228	5784976	2306292	5783545	1784
OS-3A	523/10	7	4	2298609	5791908	2299805	5791176	1403
OS-3Ab	523/10	4	1	2299805	5791176	2301093	5791325	1296
OS-3BB	523/11	1	51	2305870	5784112	2308248	5777913	6639
OS-4	523/12	1	8	2288539	5782973	2291379	5781808	3069
OS-4b	523/12	8	12	2291379	5781808	2292312	5780404	1686
OS-4c	523/12	12	20	2292312	5780404	2294847	5777865	3588
OS-4d	523/12	20	22	2294847	5777865	2295656	5777886	809
OS-4B	523/13	5	30	2295674	5777875	2296828	5774513	3554
OS-4Bb	523/13	30	65	2296828	5774513	2296161	5769704	4855
OS-5	523/14	1	14	2311826	5797356	2315538	5799711	4396
OS-5b	523/14	14	25	2315538	5799711	2318358	5802276	3812
OS-6	523/15	14	1	2295155	5788228	2298495	5792409	5351
OS-7	523/16	1	10	2279153	5772400	2280379	5772093	1264
OS-7b	523/16	10	25	2280379	5772093	2281610	5770562	1965
OS-7c	523/16	25	35	2281610	5770562	2281931	5769327	1276
OS-7d	523/16	35	57	2281931	5769327	2284579	5769089	2658
OS-8	523/17	22	16	2270624	5764325	2272698	5763166	2376
OS-8b	523/17	16	5	2272698	5763166	2274707	5759355	4308
OS-8c	523/17	5	1	2274707	5759355	2275760	5757930	1773
OS-9	523/18	23	17	2250141	5745989	2252109	5744402	2527
OS-9b	523/18	17	5	2252109	5744402	2256928	5745436	4929
OS-9c	523/18	5	1	2256928	5745436	2258456	5744997	1590
OS-10	523/19	64	40	2319148	5802265	2321401	5800003	3192
OS-10b	523/19	40	1	2321401	5800003	2324110	5795499	5256
OS-11	523/20	108	90	2279039	5772109	2280627	5773987	2460
OS-11b	523/20	90	1	2280627	5773987	2286660	5784486	12109

New Zealand Petroleum Co. Ltd.
Geophysical Services Inc.
4-7 November 1974

GSI-4B	523/31	617	781	2277509	5841478	2274276	5848782	7988

New Zealand Petroleum Co. Ltd.
Teledyne
June 1971

L101	523/51	176	-13	2257330	5753461	2250265	5763475	12255
L102	523/53	203	-13	2261092	5755230	2257244	5767438	12800
L105	523/57	3	375	2259849	5779467	2282220	5780282	22385
L206	523/65	25	500	2326502	5811255	2309836	5834886	28916
L208	523/70	7	525	2298185	5793181	2274276	5848782	60523
L210	523/76	514	290	2278450	5774378	2274536	5787187	13394
L211	523/79	590	230	2269901	5765150	2268356	5787550	22453
L211b	523/79	230	-185	2268356	5787550	2256923	5807002	22563
L212	523/85	592	280	2266623	5759272	2262635	5778550	19687
L212b	523/85	280	120	2262635	5778550	2259138	5787470	9581

Bataafse Internationale Petroleum Maatschappij N.V.
?
June 1967

M-2	548/21	1321	1227	2267194	5816847	2275499	5800358	18463
M-2b	548/21	1207	1167	2275531	5800262	2278934	5792549	8430
M-2c	548/21	1372	1399	2279131	5792294	2281710	5787266	5651
M-4	548/23	669	693	2318956	5838209	2322954	5835038	5103
M-4b	548/23	708	721	2322965	5835043	2324797	5833434	2438
M-4c	548/23	719	781	2324964	5833335	2334065	5826103	11625
M-7A	548/26	1662	1787	2244466	5801186	2266738	5811878	24706
M-7Ab	548/26	1802	1844	2266746	5811884	2273908	5815475	8012
M-7Ac	548/26	2077	2322	2274227	5815653	2320589	5837945	51443
M-8A	548/28	1564	1459	2250757	5786888	2271298	5787702	20557
M-8Ab	548/28	1422	1455	2271745	5787657	2277636	5787946	5898
M-8Ac	548/28	1344	1366	2277748	5787993	2282017	5788245	4276
M-8B	548/29	1165	920	2280414	5787838	2320641	5813220	47566
M-8Bb	548/29	909	897	2320658	5813225	2322584	5814418	2265
M-8Bc	548/29	856	815	2322918	5814680	2329805	5818935	8095

Magellan Petroleum N.Z., Ltd
United Geophysical Corp.
1970

W-12U	575/30	145	1	2204455	5720887	2196382	5726998	10126
W-13U	575/32	85	329	2213574	5726899	2213280	5743880	16984
W-14U	575/34	1	381	2196747	5727563	2221386	5736675	26270
W-15U	575/36	1	120	2221685	5736590	2229533	5734379	8153
W-16U	575/38	149	1	2233697	5735745	2230649	5745718	10429
W-18U	575/40	131	3	2257216	5758162	2252803	5765890	8900
W-19U	575/42	37	189	2262227	5760636	2261716	5770796	10173
W-20U	575/44	1	355	2246048	5757541	2266696	5771134	24721
W-21U	575/47	76	1	2266437	5770769	2264402	5775278	4947

Gulfrex
New Zealand Recon
January 1973

(The shot points of these lines are actually displayed in days, hours and minutes. They have been converted here into 'total' minutes.)

NZ-96	614/208	11630	11850	2136669	5680634	2125084	5723964	44852
NZ-96b	614/208	11850	11874	2125084	5723964	2126098	5727124	3318
NZ-97	614/209	11874	12105	2126098	5727124	2173318	5727001	47221
NZ-97b	614/209	12105	12312	2173318	5727001	2219494	5728844	46213
NZ-97c	614/209	12312	12399	2219494	5728844	2224973	5735148	8352
NZ-98	614/210	12399	12434	2224973	5735148	2219809	5738936	6404
NZ-98b	614/210	12434	12880	2219809	5738936	2142652	5778787	86841
NZ-98c	614/210	12880	12939	2142652	5778787	2142265	5787749	8971
NZ-98d	614/211	12939	12960	2142265	5787749	2146194	5789504	4303
NZ-99	614/211	12960	13440	2146194	5789504	2243119	5750671	104415
NZ-99b	614/211	13440	13486	2243119	5750671	2248671	5750849	5556
NZ-102	614/214	13775	13832	2268869	5766448	2259661	5774377	12152
NZ-102b	614/214	13832	14040	2259661	5774377	2223019	5798882	44081
NZ-120	614/234	33283	33381	2243577	5811625	2243478	5769245	42380
NZ-120b	614/234	33381	33408	2243478	5769245	2239695	5767702	4085
NZ-121	614/235	33408	33648	2239695	5767702	2200402	5777019	40383
NZ-121b	614/235	33648	33682	2200402	5777019	2198482	5774783	2947
NZ-122	614/236	33682	33720	2198482	5774783	2194160	5770157	6331
NZ-122b	614/236	33720	33864	2194160	5770157	2184699	5751515	20906
NZ-122c	614/236	34254	34488	2184699	5751515	2165069	5711271	44776
NZ-122d	614/236	34488	34523	2165069	5711271	2162042	5710398	3151
NZ-123	614/237	34523	34710	2162042	5710398	2154162	5741774	32350
NZ-123b	614/237	34710	34860	2154162	5741774	2144758	5768208	28057
NZ-102c	614/214	14040	14091	2223019	5798882	2211833	5805611	13054
NZ-102d	614/214	14091	14130	2211833	5805611	2211725	5809319	3709

New Zealand Petroleum Company
Prakla-Seismos
16 Feb - 19 Feb 1974

PS-12	629/12	164	80	2214844	5799336	2231175	5806539	17850
PS-12b	629/12	80	1	2231175	5806539	2244158	5814351	15152
PS-13	629/13	207	1	2251213	5806768	2227991	5842540	42649
PS-14	629/14	192	70	2224687	5842611	2250140	5845120	25576
PS-14b	629/14	70	1	2250140	5845120	2264621	5844197	14511
PS-15	629/15	112	1	2265759	5841951	2254112	5860304	21736
PS-16	629/16	436	200	2244502	5814615	2255668	5819753	12291
PS-16b	629/16	200	1	2255668	5819753	2265637	5823356	10599
PS-17	629/17	528	1	2273136	5813770	2291768	5831613	25798
PS-19	629/19	644	398	2266817	5823350	2275879	5831013	11867
PS-19b	629/19	398	280	2275879	5831013	2280341	5835500	6328
PS-19c	629/19	280	1	2280341	5835500	2292016	5844378	14667
PS-21	629/21	1	290	2282269	5818065	2275886	5831034	14454
PS-21b	629/21	290	540	2275886	5831034	2270111	5842040	12429
PS-22	629/22	528	400	2292134	5826538	2289053	5832088	6348
PS-22b	629/22	400	260	2289053	5832088	2285343	5837941	6929
PS-22c	629/22	260	40	2285343	5837941	2281447	5848059	10843
PS-22d	629/22	40	1	2281447	5848059	2280328	5849442	1779

Appendix B: TECHBASE database

For the purposes of this study, the TECHBASE package was installed on a Mitac MPC-3060E PC-compatiable computer, using a 386 processor, with 60 Mb hard drive and 1 Mb RAM memory. The digitiser used was a Graphtec KD4600. To aid the handling of the numerous files produced during the processing of seismic lines and data a number of directories within the 'parent' project directory were established:

C:\TBASE\WCOAST
├─ LINEDIGI
│ └→ *'raw' digitised data of the seismic lines.*
├─ MAPSETUP
│ └→ *saved map set ups from SDIGIT.*
├─ PICTURES
│ └→ *metafiles from various sources.*
├─ TECHNIC
│ └→ *TECHNICN and TASK files.*
├─ MACROS
│ └→ *runlogs and associated files.*
├─ POLYGONS
│ └→ *various polygons files used in displays.*
├─ BASIC
│ └→ *Q-BASIC number crunching programs.*
├─ SWLANDTA
└→ *The Database*

This appendix lists the TECHBASE database used in this thesis and a brief explanation of each field and its purpose in the processing of seismic information.

The following listing is based on a TECHBASE print-out. Definitions of the terms used are given below (from the TECHBASE Manual, MINEsoft Ltd., 1990).

Table: A file within a database that contains a set of records, each with a value for a set of related fields.

Field: A variable. Can be considered a "column" in a database table.

TABLE TYPES:

Flat table store lists of discrete data, similar to a spreadsheet layout.

Cell tables provide storage for raw data or models best represented as a two-dimensional array, or grid of records.

Polygon tables provide storage for the boundary points and any attribute information associated with a two-dimensional polygon.

Join tables allow two tables to be combined. Records are related according to a common field in the two tables.

FIELD TYPES:

Text fields contain values made up of a fixed number of printable characters.

Integer fields contain whole-number values

Real fields contain real-number values.

FIELD CLASSES:

Actual fields contain values supplied by the user, and modifiable by the user or TECHBASE programs.

Calculated fields contain values calculated from other fields. Equations are defined using Reverse Polish Notation.

Automatic fields are automatically generated by TECHBASE to uniquely identify records in a table.

A **Key** field defines a record as being unique to the value in the keyed field.

```
DATABASE definition for database = swland
   Title: South Westland, NZ, Foreland Basin modelling KNS June '92
   Created: 1992/06/03;19:58   Modified: 1993/01/10;23:18
With 15 tables and 266 fields

TABLES:
```

```
Lines  is a          FLAT table with  29 fields and   124 records
  Table Keys:
       line_id

  Fields:
       Lines_rec     Lines_nul     *line_id          start_sp
       end_sp        start_east    end_east          end_north
       start_north   +east_diff    +north_diff       +line_length
       +sp_diff      +east_diff2   +north_diff2      +alpha_y
       +alpha_x      title_line    pr_encl           start_day
       start_hour    start_min     end_day           end_hour
       end_min       +miscell      +start_daym       +start_hourm
       +line_lenrnd
```

Lines contains information about the attributes of each of the lines studied.

```
Lines_rec   is an  AUTOMATIC        INTEGER field
       Expected Minimum = 1  Maximum = 1125
       0 bytes stored per value

Lines_nul   is an  AUTOMATIC        INTEGER field
       Expected Minimum = 0  Maximum = 1
       0 bytes stored per value

line_id  is an       ACTUAL         TEXT field
       Length = 12 characters,  LEFT justified.
       12 bytes stored per value
       Identifies the line segment an individual point came from. Keyed.

start_sp  is an      ACTUAL         INTEGER field
       Expected Minimum = *  Maximum = *
       4 bytes stored per value
       The number of the shotpoint on the profile at the start of the line segment.

end_sp is an         ACTUAL         INTEGER field
       Expected Minimum = *  Maximum = *
       4 bytes stored per value
       The number of the shotpoint on the profile at the end of the line segment.

start_east  is an    ACTUAL         REAL field
       Expected Minimum = *  Maximum = *
       8 bytes stored per value. Precision 2
       The NZMS east coordinates of the start point of the line segment.

end_east  is an      ACTUAL         REAL field
       Expected Minimum = *  Maximum = *
       8 bytes stored per value. Precision 2
       The NZMS east coordinates of the end point of the line segment.

end_north   is an    ACTUAL         REAL field
       Expected Minimum = *  Maximum = *
       8 bytes stored per value. Precision 2
       The NZMS north coordinates of the end point of the line segment.
```

```
start_north is an     ACTUAL          REAL field
       Expected Minimum = *  Maximum = *
       8 bytes stored per value. Precision 2
       The NZMS north coordinates of the start point of the line segment.

east_diff   is a  CALCULATED          REAL field
       Expected Minimum = *  Maximum = *
       0 bytes stored per value. Precision 2
       Equation: end_east start_east -
       Calculates the east coordinate difference between the start and end points.

north_diff  is a  CALCULATED          REAL field
       Expected Minimum = *  Maximum = *
       0 bytes stored per value. Precision 2
       Equation: end_north start_north -
       Calculates the north coordinate difference between the start and end points.

line_length is a  CALCULATED          REAL field
       Expected Minimum = *  Maximum = *
       0 bytes stored per value. Precision 2
       Equation: east_diff2 north_diff2 + sqrt
      Calculates the metric length of the line using Pythagoras formula on the east and
      north differences.

sp_diff  is a  CALCULATED             REAL field
       Expected Minimum = *  Maximum = *
       0 bytes stored per value. Precision 2
       Equation: end_sp start_sp - abs
       Calculates the difference in shot points between the start and end of the line.

east_diff2  is a  CALCULATED          REAL field
       Expected Minimum = *  Maximum = *
       0 bytes stored per value. Precision 2
       Equation: start_east end_east - abs 2 ^
       Calculates the square of the east difference for length calculations.

north_diff2 is a  CALCULATED          REAL field
       Expected Minimum = *  Maximum = *
       0 bytes stored per value. Precision 2
       Equation: start_north end_north - abs 2 ^
       Calculates the square of the north difference for length calculations.

alpha_y  is a  CALCULATED             REAL field
       Expected Minimum = *  Maximum = *
       0 bytes stored per value. Precision 2
       Equation: north_diff line_length / asin
       Calculates the angle opposite the north difference of the line.

alpha_x  is a  CALCULATED             REAL field
       Expected Minimum = *  Maximum = *
       0 bytes stored per value. Precision 2
       Equation: east_diff line_length / acos
       Calculates the angle opposite the east difference of the line.

title_line  is an     ACTUAL          INTEGER field
       Expected Minimum = 0  Maximum = 1
       1 bytes stored per value
      Indicates if line is the first of a series of line segments and therefore should bear
      the proper title of that line.
```

```
pr_encl  is an        ACTUAL         TEXT field
       Length = 10 characters,  LEFT justified.
       10 bytes stored per value
```
Contains the Petroleum Report and enclosure number where the line is found.

```
start_day   is an     ACTUAL         INTEGER field
       Expected Minimum = 1  Maximum = *
       4 bytes stored per value
```
Day value at start point of lines using time to number shotpoints.

```
start_hour  is an     ACTUAL         INTEGER field
       Expected Minimum = 0  Maximum = 23
       1 bytes stored per value
```
Hour value at start point of lines using time to number shotpoints.

```
start_min   is an     ACTUAL         INTEGER field
       Expected Minimum = 0  Maximum = 59
       1 bytes stored per value
```
Minute value at start point of lines using time to number shotpoints.

```
end_day  is an        ACTUAL         INTEGER field
       Expected Minimum = 1  Maximum = *
       4 bytes stored per value
```
Day value at start point of lines using time to number shotpoints.

```
end_hour  is an       ACTUAL         INTEGER field
       Expected Minimum = 0  Maximum = 23
       1 bytes stored per value
```
Hour value at end point of lines using time to number shotpoints.

```
end_min  is an        ACTUAL         INTEGER field
       Expected Minimum = 0  Maximum = 59
       1 bytes stored per value
```
Minute value at end point of lines using time to number shotpoints.

```
miscell  is a  CALCULATED            REAL field
       Expected Minimum = *  Maximum = *
       0 bytes stored per value. Precision 6
       Equation: start_daym start_hourm + start_min +

start_daym  is a  CALCULATED         REAL field
       Expected Minimum = *  Maximum = *
       0 bytes stored per value. Precision 6
       Equation: start_day 1440 *

start_hourm is a  CALCULATED         REAL field
       Expected Minimum = *  Maximum = *
       0 bytes stored per value. Precision 6
       Equation: start_hour 60 *

line_lenrnd is a  CALCULATED         INTEGER field
       Expected Minimum = *  Maximum = *
       0 bytes stored per value
       Equation: line_length 49 + 100 / int 100 *
```
Calculated rounding of line to nearest 100 m for display purposes.

```
Profiles  is a        FLAT table with   6 fields and 18762 records
  Table has no Keys

  Fields:
       Profiles_rec  Profiles_nul  shot_point         twt_time
       line_id       horizon_name
```

Profiles contains the 'raw' seismic data that is entered from the digitiser with minimal editing.

```
Profiles_rec is an  AUTOMATIC       INTEGER field
       Expected Minimum = 1  Maximum = 20841
       0 bytes stored per value

Profiles_nul is an  AUTOMATIC       INTEGER field
       Expected Minimum = 0  Maximum = 1
       0 bytes stored per value

shot_point  is an     ACTUAL        REAL field
       Expected Minimum = *  Maximum = *
       8 bytes stored per value. Precision 2
       The shot point value as for an individual digitised point from the line.

twt_time  is an       ACTUAL        REAL field
       Expected Minimum = *  Maximum = *
       8 bytes stored per value. Precision 2
       The two-way travel time as for an individual digitised point from the line

line_id  is an        ACTUAL        TEXT field
       Length = 12 characters,  LEFT justified.
       12 bytes stored per value
      Identifies the line segment an individual point come from. Not keyed.

horizon_name is an    ACTUAL        TEXT field
       Length = 15 characters,  LEFT justified.
       15 bytes stored per value
      The name of the horizon as recorded by the 'marker' value in the digitising
      process.
```

```
Joined is a           JOIN table with   5 fields
       Table 1: Profiles            to Table 2: Lines

  Fields:
       Joined_rec     Joined_nul     +sp_reqlength      +sp_east
       +sp_north
```

Joined is a join table, combining the attributes of the line segments in the Lines table with raw data in the Profiles table via the common field, line_id.

```
Joined_rec  is an  AUTOMATIC        INTEGER field
       Expected Minimum = 1  Maximum = *
       0 bytes stored per value

Joined_nul  is an  AUTOMATIC        INTEGER field
       Expected Minimum = 0  Maximum = 1
       0 bytes stored per value
```

```
sp_reqlength is a  CALCULATED        REAL field
       Expected Minimum = *  Maximum = *
       0 bytes stored per value. Precision 2
       Equation: shot_point start_sp - abs sp_diff / line_length *
```
Finds the metric length along the line from the start point to a given point from the raw data by multiplying the length of the line by the ratio of the raw shotpoint over the shot point difference.

```
sp_east  is a  CALCULATED           REAL field
       Expected Minimum = *  Maximum = *
       0 bytes stored per value. Precision 2
       Equation: alpha_x cos sp_reqlength * start_east +
```
Calculates the east coordinates of the raw shotpoint.

```
sp_north  is a  CALCULATED          REAL field
       Expected Minimum = *  Maximum = *
       0 bytes stored per value. Precision 2
       Equation: alpha_y sin sp_reqlength * start_north +
```
Calculates the north coordinates of the raw shotpoint.

```
Bathymetry  is a      FLAT table with   5 fields and  5498 records
  Table has no Keys

  Fields:
       Bathymetry_rec  Bathymetry_nul  x_bathy         y_bathy
       z_bathy
```

Bathymetry contains the raw bathymetry data digitised from various hydrographic charts.

```
Bathymetry_rec is an  AUTOMATIC     INTEGER field
       Expected Minimum = 1  Maximum = 18134
       0 bytes stored per value

Bathymetry_nul is an  AUTOMATIC     INTEGER field
       Expected Minimum = 0  Maximum = 1
       0 bytes stored per value

x_bathy  is an        ACTUAL        REAL field
       Expected Minimum = *  Maximum = *
       8 bytes stored per value. Precision 2
       x-coordinate (east) of digitised data point.

y_bathy  is an        ACTUAL        REAL field
       Expected Minimum = *  Maximum = *
       8 bytes stored per value. Precision 2
       y-coordinate (north) of digitised data point.

z_bathy  is an        ACTUAL        REAL field
       Expected Minimum = *  Maximum = *
       8 bytes stored per value. Precision 2
       z-coordinate (depth) of digitised data point.
```

```
Sea_Floor   is a      CELL table with   9 fields and 23000 records
  Table attributes:
       Lower-left X coord: 2160000  Column size: 1000  Number: 230
                  Y coord: 5660000  Row size:    1000  Number: 100
       Baseline azimuth:   34.00

  Fields:
       Sea_Floor_rec Sea_Floor_nul Sea_Floor_row      Sea_Floor_col
       Sea_Floor_xc  Sea_Floor_csz Sea_Floor_yc       Sea_Floor_rsz
       seafloor_q
```

Sea_Floor is a cell table that contains the surface of the bathymetry in the study area, as modelled from raw data in the Bathymetry table.

```
Sea_Floor_rec is an  AUTOMATIC      INTEGER field
       Expected Minimum = 1  Maximum = 24000
       0 bytes stored per value

Sea_Floor_nul is an  AUTOMATIC      INTEGER field
       Expected Minimum = 0  Maximum = 1
       0 bytes stored per value

Sea_Floor_row is an  AUTOMATIC      INTEGER field
       Expected Minimum = 1  Maximum = 100
       0 bytes stored per value

Sea_Floor_col is an  AUTOMATIC      INTEGER field
       Expected Minimum = 1  Maximum = 230
       0 bytes stored per value

Sea_Floor_xc is an  AUTOMATIC       REAL field
       Expected Minimum = 2160000  Maximum = 2205980
       0 bytes stored per value. Precision 0

Sea_Floor_csz is an  AUTOMATIC      REAL field
       Expected Minimum = 1000  Maximum = 1000
       0 bytes stored per value. Precision 0

Sea_Floor_yc is an  AUTOMATIC       REAL field
       Expected Minimum = 5660000  Maximum = 5905210
       0 bytes stored per value. Precision 0

Sea_Floor_rsz is an  AUTOMATIC      REAL field
       Expected Minimum = 1000  Maximum = 1000
       0 bytes stored per value. Precision 0

seafloor_q  is an    ACTUAL         REAL field
       Expected Minimum = *  Maximum = *
       8 bytes stored per value. Precision 2
```

The value of the seafloor bathymetry modelled for each cel by MINQ is stored in this field.

```
Polygons  is a  POLYGON table with  18 fields and   664 records

  Fields:
       Polygons_rec   Polygons_nul   Polygons_npt       Polygons_xc
       Polygons_yc    Polygons_are   Polygons_per       Polygons_xmn
       Polygons_ymn   Polygons_xmx   Polygons_ymx       poly_x
       poly_y         poly_owner     poly_style         poly_colour
       poly_type      line_id
```

Polygons contains the polygons used in various parts of processing of the seismic lines and other functions.

```
Polygons_rec is an  AUTOMATIC       INTEGER field
       Expected Minimum = 1  Maximum = 1664
       0 bytes stored per value

Polygons_nul is an  AUTOMATIC       INTEGER field
       Expected Minimum = 0  Maximum = 1
       0 bytes stored per value

Polygons_npt is an  AUTOMATIC       INTEGER field
       Expected Minimum = 1  Maximum = *
       0 bytes stored per value

Polygons_xc is an  AUTOMATIC        REAL field
       Expected Minimum = *  Maximum = *
       0 bytes stored per value. Precision 0

Polygons_yc is an  AUTOMATIC        REAL field
       Expected Minimum = *  Maximum = *
       0 bytes stored per value. Precision 0

Polygons_are is an  AUTOMATIC       REAL field
       Expected Minimum = *  Maximum = *
       0 bytes stored per value. Precision 0

Polygons_per is an  AUTOMATIC       REAL field
       Expected Minimum = *  Maximum = *
       0 bytes stored per value. Precision 0

Polygons_xmn is an  AUTOMATIC       REAL field
       Expected Minimum = *  Maximum = *
       0 bytes stored per value. Precision 0

Polygons_ymn is an  AUTOMATIC       REAL field
       Expected Minimum = *  Maximum = *
       0 bytes stored per value. Precision 0

Polygons_xmx is an  AUTOMATIC       REAL field
       Expected Minimum = *  Maximum = *
       0 bytes stored per value. Precision 0

Polygons_ymx is an  AUTOMATIC       REAL field
       Expected Minimum = *  Maximum = *
       0 bytes stored per value. Precision 0

poly_x is an          ACTUAL        REAL field
       Expected Minimum = *  Maximum = *
       8 bytes stored per value. Precision 2
       This field nominally contains the x-coordinate of a polygon for loading purposes.
```

```
poly_y is an          ACTUAL          REAL field
       Expected Minimum = *  Maximum = *
       8 bytes stored per value. Precision 2
```
This field nominally contains the y-coordinate of a polygon for loading purposes.

```
poly_owner  is an     ACTUAL          TEXT field
       Length = 35 characters,  LEFT justified.
       35 bytes stored per value
```
Text field used for describing 'owner' of line, e.g. PS-21_seafloor.

```
poly_style  is an     ACTUAL          INTEGER field
       Expected Minimum = *  Maximum = *
       4 bytes stored per value
```
Style attribute of polygon, e.g. solid, wide, fill, hollow, etc.

```
poly_colour is an     ACTUAL          INTEGER field
       Expected Minimum = *  Maximum = *
       4 bytes stored per value
```
Colour attribute of polygon, e.g. red, black, brown etc.

```
poly_type   is an     ACTUAL          INTEGER field
       Expected Minimum = *  Maximum = *
       4 bytes stored per value
```
This field contains the 'code' of each polygon, expressing its purpose, e.g.:
1: cartographic, polygons for basemaps, coastlines, roads etc.
2: seismic lines, polygons of the actual location of the digitised seismic lines.
3: raw horizons, polygons of the digitized raw horizons for display if needed.
4: regularised horizons, polygons of the horizons once regularised at each shot point, for display if needed.
5: restored horizons, polygons of horizons for the restoration process if needed.

```
line_id  is an        ACTUAL          TEXT field
       Length = 12 characters,  LEFT justified.
       12 bytes stored per value
```
a field that identifies a polygon belonging to a line segment, if applicable. Not keyed.

```
Locations   is a      FLAT table with   7 fields and   19 records
  Table has no Keys

  Fields:
       Locations_rec Locations_nul  loc_name1          loc_east
       loc_north     loc_id         loc_name2
```

Locations contains the coordinates and attributes of 'locations' for inclusion on maps produced from this databse.

```
Locations_rec is an  AUTOMATIC      INTEGER field
       Expected Minimum = 1  Maximum = 1019
       0 bytes stored per value

Locations_nul is an  AUTOMATIC      INTEGER field
       Expected Minimum = 0  Maximum = 1
       0 bytes stored per value

loc_name1   is an     ACTUAL          TEXT field
       Length = 25 characters,  LEFT justified.
       25 bytes stored per value
```
Name of location, e.g. Mt. Cook, Mikonui-1, 170°E.

```
loc_east   is an      ACTUAL          REAL field
       Expected Minimum = *  Maximum = *
       8 bytes stored per value. Precision 2
       NZMS east coordinates of location.

loc_north   is an     ACTUAL          REAL field
       Expected Minimum = *  Maximum = *
       8 bytes stored per value. Precision 2
       NZMS north coordinates of location.

loc_id is an          ACTUAL          INTEGER field
       Expected Minimum = *  Maximum = *
       4 bytes stored per value
       Identification number of the location for filtering purposes:
       1: wellsite, e.g. Mikonui-1
       2: township, e.g. Hokitika.
       3: geographic, e.g. Haast Pass.
       4: latitude/longitude point.

loc_name2   is an     ACTUAL          TEXT field
       Length = 25 characters,  LEFT justified.
       25 bytes stored per value
       Second accessory name of location, e.g. for lat/long points.
```

```
Regular   is a        FLAT table with  30 fields and 12678 records
  Table has no Keys

  Fields:
       Regular_rec    Regular_nul    line_id          seafloor_twt
       ppa_twt        ppb_twt        topmio_twt       baseoligo_twt
       basement_twt   +seqa_twt      +seqb_twt        +seqc_twt
       +seqd_twt      +seqe_twt      sp_reg           seqa_skel
       seqb_skel      seqc_skel      seqd_skel        seqe_skel
       len_reg        basement_dep2  spreg_east2      spreg_north2
       seqe_thick2    base_locate    seqd_thick2      seqc_thick2
       seqb_thick2    seqa_thick2
```

Regular contains information about the seismic lines once they have been 'regularised', and data is calculated for each shotpoint along the seismic line.

```
Regular_rec is an  AUTOMATIC        INTEGER field
       Expected Minimum = 1  Maximum = 16118
       0 bytes stored per value

Regular_nul is an  AUTOMATIC        INTEGER field
       Expected Minimum = 0  Maximum = 1
       0 bytes stored per value

sp_reg is an          ACTUAL        REAL field
       Expected Minimum = *  Maximum = *
       8 bytes stored per value. Precision 2
       Regularised shot point number.

seafloor_twt is an    ACTUAL        REAL field
       Expected Minimum = *  Maximum = *
       8 bytes stored per value. Precision 2
       Two-way travel time to seafloor horizon at regularised shot point.
```

```
ppa_twt  is an        ACTUAL          REAL field
       Expected Minimum = *  Maximum = *
       8 bytes stored per value. Precision 2
       Two-way travel time to ppa horizon at regularised shot point.

ppb_twt   is an       ACTUAL          REAL field
       Expected Minimum = *  Maximum = *
       8 bytes stored per value. Precision 2
       Two-way travel time to ppb horizon at regularised shot point.

topmio_twt  is an     ACTUAL          REAL field
       Expected Minimum = *  Maximum = *
       8 bytes stored per value. Precision 2
       Two-way travel time to top miocene horizon at regularised shot point.

baseoligo_twt is an   ACTUAL          REAL field
       Expected Minimum = *  Maximum = *
       8 bytes stored per value. Precision 2
       Two-way travel time to oligocene horizon at regularised shot point.

basement_twt is an    ACTUAL          REAL field
       Expected Minimum = *  Maximum = *
       8 bytes stored per value. Precision 2
       Two-way travel time to basement horizon at regularised shot point.

seqa_twt   is a  CALCULATED           REAL field
       Expected Minimum = *  Maximum = *
       0 bytes stored per value. Precision 2
       Equation: ppa_twt seafloor_twt -
       Calculated two way travel time thickness of Sequence A.

seqb_twt   is a  CALCULATED           REAL field
       Expected Minimum = *  Maximum = *
       0 bytes stored per value. Precision 2
       Equation: ppb_twt ppa_twt -
       Calculated two way travel time thickness of Sequence B.

seqc_twt   is a  CALCULATED           REAL field
       Expected Minimum = *  Maximum = *
       0 bytes stored per value. Precision 2
       Equation: topmio_twt ppb_twt -
       Calculated two way travel time thickness of Sequence C.

seqd_twt   is a  CALCULATED           REAL field
       Expected Minimum = *  Maximum = *
       0 bytes stored per value. Precision 2
       Equation: baseoligo_twt topmio_twt -
       Calculated two way travel time thickness of Sequence D.

seqe_twt   is a  CALCULATED           REAL field
       Expected Minimum = *  Maximum = *
       0 bytes stored per value. Precision 2
       Equation: basement_twt baseoligo_twt -
       Calculated two way travel time thickness of Sequence E.

seqa_skel   is an     ACTUAL          REAL field
       Expected Minimum = *  Maximum = *
       8 bytes stored per value. Precision 2
       Skeletal thickness of Seq. A at regularised shot point. Calculated in processing.
```

```
seqb_skel   is an     ACTUAL         REAL field
       Expected Minimum = *  Maximum = *
       8 bytes stored per value. Precision 2
       Skeletal thickness of Seq. B at regularised shot point. Calculated in processing.

seqc_skel   is an     ACTUAL         REAL field
       Expected Minimum = *  Maximum = *
       8 bytes stored per value. Precision 2
       Skeletal thickness of Seq. C at regularised shot point. Calculated in processing.

seqd_skel   is an     ACTUAL         REAL field
       Expected Minimum = *  Maximum = *
       8 bytes stored per value. Precision 2
       Skeletal thickness of Seq. D at regularised shot point. Calculated in processing.

seqe_skel   is an     ACTUAL         REAL field
       Expected Minimum = *  Maximum = *
       8 bytes stored per value. Precision 2
       Skeletal thickness of Seq. E at regularised shot point. Calculated in processing.

len_reg   is an       ACTUAL         REAL field
       Expected Minimum = *  Maximum = *
       8 bytes stored per value. Precision 4
       Length along line to regularised shot point.

basement_dep2 is an   ACTUAL         REAL field
       Expected Minimum = *  Maximum = *
       8 bytes stored per value. Precision 2
       Basement depth, copied from calculated field in Convert.

spreg_east2 is an     ACTUAL         REAL field
       Expected Minimum = *  Maximum = *
       8 bytes stored per value. Precision 2
       East coordinates of regualrised point, copied from calculated field in Convert.

spreg_north2 is an    ACTUAL         REAL field
       Expected Minimum = *  Maximum = *
       8 bytes stored per value. Precision 2
       North coordinates of regualrised point, copied from calculated field in Convert.

seqe_thick2 is an     ACTUAL         REAL field
       Expected Minimum = *  Maximum = *
       8 bytes stored per value. Precision 2
       Sequence E thickness, copied from calculated field in Convert.

seqd_thick2 is an     ACTUAL         REAL field
       Expected Minimum = *  Maximum = *
       8 bytes stored per value. Precision 0
       Sequence D thickness, copied from calculated field in Convert.

seqc_thick2 is an     ACTUAL         REAL field
       Expected Minimum = *  Maximum = *
       8 bytes stored per value. Precision 0
       Sequence C thickness, copied from calculated field in Convert.

seqb_thick2 is an     ACTUAL         REAL field
       Expected Minimum = *  Maximum = *
       8 bytes stored per value. Precision 0
       Sequence B thickness, copied from calculated field in Convert.
```

```
seqa_thick2 is an     ACTUAL          REAL field
       Expected Minimum = *  Maximum = *
       8 bytes stored per value. Precision 0
       Sequence A thickness, copied from calculated field in Convert.

base_locate is an     ACTUAL          INTEGER field
       Expected Minimum = *  Maximum = *
       4 bytes stored per value
      Field acts as a flag for filtering processes. Indicates if shot point is in basin or on
      uplifted block.
```

```
Sequences   is a      FLAT table with  24 fields and   124 records
  Table Keys:
       line_id

  Fields:
       Sequences_rec Sequences_nul *line_id           seqa_kk
       seqb_kk       seqc_kk       seqd_kk           seqe_kk
       seqa_pphi     seqb_pphi     seqc_pphi         seqd_pphi
       seqe_pphi     seqa_vel      seqb_vel          seqc_vel
       seqd_vel      seqe_vel      seafloor_code     ppa_code
       ppb_code      topmio_code   baseoligo_code    basement_code
```

Sequences contains information about the mapped sequences in each line, e.g. original porosity and compaction coefficients for decompaction processing and seismic velocity for depth conversion. Although all the lines are presently treated identically, there is scope for altering the values in individual lines as suits.

```
Sequences_rec is an  AUTOMATIC      INTEGER field
       Expected Minimum = 1  Maximum = 1124
       0 bytes stored per value

Sequences_nul is an  AUTOMATIC      INTEGER field
       Expected Minimum = 0  Maximum = 1
       0 bytes stored per value

seqa_kk   is an       ACTUAL          REAL field
       Expected Minimum = *  Maximum = *
       8 bytes stored per value. Precision 2
       Compaction coefficient of Sequence A.

seqb_kk   is an       ACTUAL          REAL field
       Expected Minimum = *  Maximum = *
       8 bytes stored per value. Precision 2
       Compaction coefficient of Sequence B.

seqc_kk   is an       ACTUAL          REAL field
       Expected Minimum = *  Maximum = *
       8 bytes stored per value. Precision 2
       Compaction coefficient of Sequence C.

seqd_kk   is an       ACTUAL          REAL field
       Expected Minimum = *  Maximum = *
       8 bytes stored per value. Precision 2
       Compaction coefficient of Sequence D.
```

```
seqe_kk   is an      ACTUAL         REAL field
       Expected Minimum = *  Maximum = *
       8 bytes stored per value. Precision 2
       Compaction coefficent of Sequence E.

seqa_pphi   is an    ACTUAL         REAL field
       Expected Minimum = *  Maximum = *
       8 bytes stored per value. Precision 2
       Original porosity of Sequence A.

seqb_pphi   is an    ACTUAL         REAL field
       Expected Minimum = *  Maximum = *
       8 bytes stored per value. Precision 2
       Original porosity of Sequence B.

seqc_pphi   is an    ACTUAL         REAL field
       Expected Minimum = *  Maximum = *
       8 bytes stored per value. Precision 2
       Original porosity of Sequence C.

seqd_pphi   is an    ACTUAL         REAL field
       Expected Minimum = *  Maximum = *
       8 bytes stored per value. Precision 2
       Original porosity of Sequence D.

seqe_pphi   is an    ACTUAL         REAL field
       Expected Minimum = *  Maximum = *
       8 bytes stored per value. Precision 2
       Original porosity of Sequence E.

seqa_vel   is an     ACTUAL         REAL field
       Expected Minimum = *  Maximum = *
       8 bytes stored per value. Precision 2
       Seismic velocity of Sequence A.

seqb_vel   is an     ACTUAL         REAL field
       Expected Minimum = *  Maximum = *
       8 bytes stored per value. Precision 2
       Seismic velocity of Sequence A.

seqc_vel   is an     ACTUAL         REAL field
       Expected Minimum = *  Maximum = *
       8 bytes stored per value. Precision 2
       Seismic velocity of Sequence A.

seqd_vel   is an     ACTUAL         REAL field
       Expected Minimum = *  Maximum = *
       8 bytes stored per value. Precision 2
       Seismic velocity of Sequence A.

seqe_vel   is an     ACTUAL         REAL field
       Expected Minimum = *  Maximum = *
       8 bytes stored per value. Precision 2
       Seismic velocity of Sequence A.

seafloor_code is an  ACTUAL         INTEGER field
       Expected Minimum = *  Maximum = *
       4 bytes stored per value
       The integer code of the seafloor horizon if needed for colouring etc.
```

```
ppa_code  is an       ACTUAL          INTEGER field
       Expected Minimum = *  Maximum = *
       4 bytes stored per value
       The integer code of the ppa horizon if needed for colouring etc.

ppb_code  is an       ACTUAL          INTEGER field
       Expected Minimum = *  Maximum = *
       4 bytes stored per value
       The integer code of the ppb horizon if needed for colouring etc.

topmio_code is an     ACTUAL          INTEGER field
       Expected Minimum = *  Maximum = *
       4 bytes stored per value
       The integer code of the top Miocene horizon if needed for colouring etc.

baseoligo_code is an ACTUAL           INTEGER field
       Expected Minimum = *  Maximum = *
       4 bytes stored per value
       The integer code of the Oligocene horizon if needed for colouring etc.

basement_code is an  ACTUAL           INTEGER field
       Expected Minimum = *  Maximum = *
       4 bytes stored per value
       The integer code of the basement horizon if needed for colouring etc.

line_id  is an        ACTUAL          TEXT field
       Length = 12 characters,  LEFT justified.
       12 bytes stored per value
        Identifies the line segment relating to the attributes. Not keyed.
```

```
Convert   is a        JOIN table with  13 fields
       Table 1: Regular              to Table 2: Sequences

  Fields:
       Convert_rec    Convert_nul    +seqa_thick        +seqb_thick
       +seqc_thick    +seqd_thick    +seqe_thick        +seafloor_dep
       +ppa_dep       +ppb_dep       +topmio_dep        +baseoligo_dep
       +basement_dep
```

Convert is a join table combining the regularised seismic data in Regular with the attributes of each sequence in Sequences, to produce depth converted information for each horizon in each line.

```
Convert_rec is an  AUTOMATIC          INTEGER field
       Expected Minimum = 1  Maximum = *
       0 bytes stored per value

Convert_nul is an  AUTOMATIC          INTEGER field
       Expected Minimum = 0  Maximum = 1
       0 bytes stored per value

seqa_thick  is a  CALCULATED          REAL field
       Expected Minimum = *  Maximum = *
       0 bytes stored per value. Precision 4
       Equation: seqa_twt 2.00 / seqa_vel *
       Calculates the thickness of Seq. A as a product of the twt thickness and velocity.
```

```
seqb_thick  is a  CALCULATED        REAL field
       Expected Minimum = *  Maximum = *
       0 bytes stored per value. Precision 4
       Equation: seqb_twt 2.00 / seqb_vel *
       Calculates the thickness of Seq. B as a product of the twt thickness and velocity.

seqc_thick  is a  CALCULATED        REAL field
       Expected Minimum = *  Maximum = *
       0 bytes stored per value. Precision 4
       Equation: seqc_twt 2.00 / seqc_vel *
       Calculates the thickness of Seq. C as a product of the twt thickness and velocity.

seqd_thick  is a  CALCULATED        REAL field
       Expected Minimum = *  Maximum = *
       0 bytes stored per value. Precision 4
       Equation: seqd_twt 2.00 / seqd_vel *
       Calculates the thickness of Seq. D as a product of the twt thickness and velocity.

seqe_thick  is a  CALCULATED        REAL field
       Expected Minimum = *  Maximum = *
       0 bytes stored per value. Precision 4
       Equation: seqe_twt 2.00 / seqe_vel *
       Calculates the thickness of Seq. E as a product of the twt thickness and velocity.

seafloor_dep is a  CALCULATED       REAL field
       Expected Minimum = *  Maximum = *
       0 bytes stored per value. Precision 2
       Equation: seafloor_twt 2 / 1400 *
       Calculates the seafloor depth as a product of the twt thickness and velocity.

ppa_dep   is a  CALCULATED          REAL field
       Expected Minimum = *  Maximum = *
       0 bytes stored per value. Precision 2
       Equation: seafloor_dep seqa_thick +
       Calculates the depth of PPA Horizon.

ppb_dep   is a  CALCULATED          REAL field
       Expected Minimum = *  Maximum = *
       0 bytes stored per value. Precision 2
       Equation: ppa_dep seqb_thick +
       Calculates the depth of PPB Horizon.

topmio_dep  is a  CALCULATED        REAL field
       Expected Minimum = *  Maximum = *
       0 bytes stored per value. Precision 2
       Equation: ppb_dep seqc_thick +
       Calculates the depth of Top Miocene Horizon.

baseoligo_dep is a  CALCULATED      REAL field
       Expected Minimum = *  Maximum = *
       0 bytes stored per value. Precision 2
       Equation: topmio_dep seqd_thick +
       Calculates the depth of the Oligocene Horizon.

basement_dep is a  CALCULATED       REAL field
       Expected Minimum = *  Maximum = *
       0 bytes stored per value. Precision 2
       Equation: baseoligo_dep seqe_thick +
       Calculates the depth of the Basement Horizon.
```

```
Regloc is a          JOIN table with   5 fields
       Table 1: Regular            to Table 2: Lines

  Fields:
       Regloc_rec     Regloc_nul     +spreg_len          +spreg_east
       +spreg_north
```

Regloc is a join table combining the regularised information of Regular with attributes of individual lines in Lines to provide the coordinates of the regularised shotpoints.

```
Regloc_rec  is an  AUTOMATIC        INTEGER field
       Expected Minimum = 1  Maximum = *
       0 bytes stored per value

Regloc_nul  is an  AUTOMATIC        INTEGER field
       Expected Minimum = 0  Maximum = 1
       0 bytes stored per value

spreg_len   is a   CALCULATED       REAL field
       Expected Minimum = *  Maximum = *
       0 bytes stored per value. Precision 2
       Equation: sp_reg start_sp - abs sp_diff / line_length *
       Calculates the metric length to the regularised shotpoint.

spreg_east  is a   CALCULATED       REAL field
       Expected Minimum = *  Maximum = *
       0 bytes stored per value. Precision 2
       Equation: alpha_x cos spreg_len * start_east +
       Calculates the east coordinate of the regularised shot point.

spreg_north is a   CALCULATED       REAL field
       Expected Minimum = *  Maximum = *
       0 bytes stored per value. Precision 2
       Equation: alpha_y sin spreg_len * start_north +
       Calculates the north coordinate of the regularised shot point.
```

```
Recon  is a            FLAT table with  38 fields and  1068 records
  Table has no Keys

  Fields:
       Recon_rec      Recon_nul      line_id            len_reg
       +bs1_seafloor  +bs2_seafloor  +bs3_seafloor      +bs4_seafloor
       bs1_ppa        +bs2_ppa       +bs3_ppa           +bs4_ppa
       bs1_ppb        bs2_ppb        +bs3_ppb           +bs4_ppb
       bs1_topmio     bs2_topmio     bs3_topmio         +bs4_topmio
       bs1_baseoligo  bs2_baseoligo  bs3_baseoligo      bs4_baseoligo
       bs1_basement   bs2_basement   bs3_basement       bs4_basement
       +bs1_seqb_thick               +bs1_seqc_thick
       +bs1_seqd_thick               +bs1_seqe_thick
       +bs2_seqc_thick               +bs2_seqd_thick
       +bs2_seqe_thick               +bs3_seqd_thick
       +bs3_seqe_thick               +bs4_seqe_thick
```

Recon contains information about the depths of horizons in a particular section at different backstripped and decompacted stages. Information comes from the reconstruction routines in the TECHNICN files.

```
Recon_rec   is an  AUTOMATIC        INTEGER field
       Expected Minimum = 1  Maximum = 2068
       0 bytes stored per value

Recon_nul   is an  AUTOMATIC        INTEGER field
       Expected Minimum = 0  Maximum = 1
       0 bytes stored per value

line_id  is an        ACTUAL        TEXT field
       Length = 12 characters,  LEFT justified.
       12 bytes stored per value
       Identifies the line segment an individual point came from. Not keyed.

len_reg   is an       ACTUAL        REAL field
       Expected Minimum = *  Maximum = *
       8 bytes stored per value. Precision 4
       Length along line to regularised shot point.

bs1_seafloor is a  CALCULATED       REAL field
       Expected Minimum = *  Maximum = *
       0 bytes stored per value. Precision 2
       Equation: NULL
       Depth of the seafloor at Stage 1.

bs1_ppa   is an       ACTUAL        REAL field
       Expected Minimum = *  Maximum = *
       8 bytes stored per value. Precision 2
       Depth of the PPA at Stage 1.

bs1_ppb   is an       ACTUAL        REAL field
       Expected Minimum = *  Maximum = *
       8 bytes stored per value. Precision 2
       Depth of the PPB at Stage 1.

bs1_topmio  is an     ACTUAL        REAL field
       Expected Minimum = *  Maximum = *
       8 bytes stored per value. Precision 2
       Depth of the Top Miocene at Stage 1.
```

```
bs1_baseoligo is an  ACTUAL          REAL field
       Expected Minimum = *  Maximum = *
       8 bytes stored per value. Precision 2
       Depth of the Oligocene at Stage 1.

bs1_basement is an   ACTUAL          REAL field
       Expected Minimum = *  Maximum = *
       8 bytes stored per value. Precision 2
       Depth of the basement at Stage 1.

bs2_seafloor is a  CALCULATED        REAL field
       Expected Minimum = *  Maximum = *
       0 bytes stored per value. Precision 2
       Equation: NULL
       Depth of the seafloor at Stage 2.

bs2_ppa   is a  CALCULATED           REAL field
       Expected Minimum = *  Maximum = *
       0 bytes stored per value. Precision 2
       Equation: NULL
       Depth of the PPA at Stage 2.

bs2_ppb   is an      ACTUAL          REAL field
       Expected Minimum = *  Maximum = *
       8 bytes stored per value. Precision 2
       Depth of the PPB at Stage 2.

bs2_topmio  is an    ACTUAL          REAL field
       Expected Minimum = *  Maximum = *
       8 bytes stored per value. Precision 2
       Depth of the Top Miocene at Stage 2.

bs2_baseoligo is an  ACTUAL          REAL field
       Expected Minimum = *  Maximum = *
       8 bytes stored per value. Precision 2
       Depth of the Oligocene at Stage 2.

bs2_basement is an   ACTUAL          REAL field
       Expected Minimum = *  Maximum = *
       8 bytes stored per value. Precision 2
       Depth of the Basement at Stage 2.

bs3_seafloor is a  CALCULATED        REAL field
       Expected Minimum = *  Maximum = *
       0 bytes stored per value. Precision 2
       Equation: NULL
       Depth of the seafloor at Stage 3.

bs3_ppa   is a  CALCULATED           REAL field
       Expected Minimum = *  Maximum = *
       0 bytes stored per value. Precision 2
       Equation: NULL
       Depth of the PPA at Stage 3.

bs3_ppb   is a  CALCULATED           REAL field
       Expected Minimum = *  Maximum = *
       0 bytes stored per value. Precision 2
       Equation: NULL
       Depth of the PPB at Stage 3.
```

```
bs3_topmio  is an    ACTUAL          REAL field
       Expected Minimum = *  Maximum = *
       8 bytes stored per value. Precision 2
       Depth of the Top Miocene at Stage 3.

bs3_baseoligo is an  ACTUAL          REAL field
       Expected Minimum = *  Maximum = *
       8 bytes stored per value. Precision 2
       Depth of the Oligocene at Stage 3.

bs3_basement is an   ACTUAL          REAL field
       Expected Minimum = *  Maximum = *
       8 bytes stored per value. Precision 2
       Depth of the Basement at Stage 3.

bs4_seafloor is a  CALCULATED        REAL field
       Expected Minimum = *  Maximum = *
       0 bytes stored per value. Precision 2
       Equation: NULL
       Depth of the seafloor at Stage 4.

bs4_ppa   is a  CALCULATED           REAL field
       Expected Minimum = *  Maximum = *
       0 bytes stored per value. Precision 2
       Equation: NULL
       Depth of the PPA at Stage 4.

bs4_ppb   is a  CALCULATED           REAL field
       Expected Minimum = *  Maximum = *
       0 bytes stored per value. Precision 2
       Equation: NULL
       Depth of the PPB at Stage 4.

bs4_topmio  is a  CALCULATED         REAL field
       Expected Minimum = *  Maximum = *
       0 bytes stored per value. Precision 2
       Equation: NULL
       Depth of the Top Miocene at Stage 4.

bs4_baseoligo is an  ACTUAL          REAL field
       Expected Minimum = *  Maximum = *
       8 bytes stored per value. Precision 2
       Depth of the Oligocene at Stage 4.

bs4_basement is an   ACTUAL          REAL field
       Expected Minimum = *  Maximum = *
       8 bytes stored per value. Precision 2
       Depth of the Basement at Stage 4.

bs1_seqb_thick is a  CALCULATED      REAL field
       Expected Minimum = *  Maximum = *
       0 bytes stored per value. Precision 2
       Equation: bs1_ppb bs1_ppa -
       Thickness of Sequence B at Stage 1.

bs1_seqc_thick is a  CALCULATED      REAL field
       Expected Minimum = *  Maximum = *
       0 bytes stored per value. Precision 2
       Equation: bs1_topmio bs1_ppb -
       Thickness of Sequence C at Stage 1.
```

```
bs1_seqd_thick is a  CALCULATED     REAL field
       Expected Minimum = *  Maximum = *
       0 bytes stored per value. Precision 2
       Equation: bs1_baseoligo bs1_topmio -
       Thickness of Sequence D at Stage 1.

bs1_seqe_thick is a  CALCULATED     REAL field
       Expected Minimum = *  Maximum = *
       0 bytes stored per value. Precision 2
       Equation: bs1_basement bs1_baseoligo -
       Thickness of Sequence E at Stage 1.

bs2_seqc_thick is a  CALCULATED     REAL field
       Expected Minimum = *  Maximum = *
       0 bytes stored per value. Precision 2
       Equation: bs2_topmio bs2_ppb -
       Thickness of Sequence C at Stage 2.

bs2_seqd_thick is a  CALCULATED     REAL field
       Expected Minimum = *  Maximum = *
       0 bytes stored per value. Precision 2
       Equation: bs2_baseoligo bs2_topmio -
       Thickness of Sequence D at Stage 2.

bs2_seqe_thick is a  CALCULATED     REAL field
       Expected Minimum = *  Maximum = *
       0 bytes stored per value. Precision 2
       Equation: bs2_basement bs2_baseoligo -
       Thickness of Sequence E at Stage 2.

bs3_seqd_thick is a  CALCULATED     REAL field
       Expected Minimum = *  Maximum = *
       0 bytes stored per value. Precision 2
       Equation: bs3_baseoligo bs3_topmio -
       Thickness of Sequence D at Stage 3.

bs3_seqe_thick is a  CALCULATED     REAL field
       Expected Minimum = *  Maximum = *
       0 bytes stored per value. Precision 2
       Equation: bs3_basement bs3_baseoligo -
       Thickness of Sequence E at Stage 3.

bs4_seqe_thick is a  CALCULATED     REAL field
       Expected Minimum = *  Maximum = *
       0 bytes stored per value. Precision 2
       Equation: bs4_basement bs4_baseoligo -
       Thickness of Sequence E at Stage 4.
```

```
Paleo  is a          FLAT table with  12 fields and   17 records
  Table Keys:
       line_id

  Fields:
       Paleo_rec     Paleo_nul     *line_id          bs1_start_dep
       bs1_end_dep   bs2_start_dep bs2_end_dep       bs3_start_dep
       bs3_end_dep   bs4_start_dep bs4_end_dep       +zero_depth
```

Paleo contains paleodepth information for each line at each stage of reconstruction backstripping. Note paleodepth is given at each end of the line, and interpolated between. Potential exists for digitizing a paleodepth curve for a seismic line to be included at this point.

```
Paleo_rec   is an  AUTOMATIC        INTEGER field
       Expected Minimum = 1  Maximum = 1017
       0 bytes stored per value

Paleo_nul   is an  AUTOMATIC        INTEGER field
       Expected Minimum = 0  Maximum = 1
       0 bytes stored per value

line_id  is an        ACTUAL        TEXT field
       Length = 12 characters,  LEFT justified.
       12 bytes stored per value
       Identifies the line segment. Not keyed.

bs1_start_dep is an  ACTUAL         REAL field
       Expected Minimum = *  Maximum = *
       8 bytes stored per value. Precision 0
       Paleodepth at Stage 1 at the start of the line.

bs1_end_dep is an    ACTUAL         REAL field
       Expected Minimum = *  Maximum = *
       8 bytes stored per value. Precision 0
       Paleodepth at Stage 1 at the end of the line.

bs2_start_dep is an  ACTUAL         REAL field
       Expected Minimum = *  Maximum = *
       8 bytes stored per value. Precision 0
       Paleodepth at Stage 2 at the start of the line.

bs2_end_dep is an    ACTUAL         REAL field
       Expected Minimum = *  Maximum = *
       8 bytes stored per value. Precision 0
       Paleodepth at Stage 2 at the end of the line.

bs3_start_dep is an  ACTUAL         REAL field
       Expected Minimum = *  Maximum = *
       8 bytes stored per value. Precision 0
       Paleodepth at Stage 3 at the start of the line.

bs3_end_dep is an    ACTUAL         REAL field
       Expected Minimum = *  Maximum = *
       8 bytes stored per value. Precision 0
       Paleodepth at Stage 3 at the end of the line.

bs4_start_dep is an  ACTUAL         REAL field
       Expected Minimum = *  Maximum = *
       8 bytes stored per value. Precision 0
       Paleodepth at Stage 4 at the start of the line.

bs4_end_dep is an    ACTUAL         REAL field
       Expected Minimum = *  Maximum = *
       8 bytes stored per value. Precision 0
       Paleodepth at Stage 4 at the end of the line.

zero_depth  is a  CALCULATED        REAL field
       Expected Minimum = 0  Maximum = *
       0 bytes stored per value. Precision 0
       Equation: 0
       Field containing the zero_depth value for calculation  purposes.
```

```
Mikonui   is a        FLAT table with   6 fields and   773 records
  Table has no Keys

  Fields:
       Mikonui_rec    Mikonui_nul    horz_depth(m)    +horz_depth(ft)
       velocity(ms)   +velocity(fts)
```

Mikonui contains interval velocity data from the geophysical airgun report in Mikonui-1. The depths and velocities are converted to Imperial units for use in generating a synthetic seismogram.

```
Mikonui_rec is an  AUTOMATIC        INTEGER field
       Expected Minimum = 1  Maximum = *
       0 bytes stored per value

Mikonui_nul is an  AUTOMATIC        INTEGER field
       Expected Minimum = 0  Maximum = 1
       0 bytes stored per value

horz_depth(m) is an  ACTUAL         REAL field
       Expected Minimum = *  Maximum = *
       8 bytes stored per value. Precision 2
       Interval depth recorded in airgun report, in metres.

horz_depth(ft) is a  CALCULATED     REAL field
       Expected Minimum = *  Maximum = *
       0 bytes stored per value. Precision 0
       Equation: horz_depth(m) 0.305 /
       Calculated interval depth in feet.

velocity(ms) is an   ACTUAL         REAL field
       Expected Minimum = *  Maximum = *
       8 bytes stored per value. Precision 2
       Interval velocity recorded in airgun report, in metres per second.

velocity(fts) is a  CALCULATED      REAL field
       Expected Minimum = *  Maximum = *
       0 bytes stored per value. Precision 2
       Equation: velocity(ms) 0.305 /
       Calculated interval velocity in feet per second.
```

```
Maps   is a          CELL table with  72 fields and  8192 records
  Table attributes:
       Lower-left X coord: 2150000  Column size: 2000  Number: 128
                  Y coord: 5650000  Row size:    2000  Number: 64
       Baseline azimuth:   57.00

  Fields:
       Maps_rec       Maps_nul       Maps_row           Maps_col
       Maps_xc        Maps_csz       Maps_yc            Maps_rsz
       basement_q     map_locate     basement_twt_q
       seqe_thick_q   seqd_thick_q   seqc_thick_q
       seqb_thick_q   seqa_thick_q
       +total_thick   +total_volume
       +paleodepth_0  +paleodepth_1  +paleodepth_2
       +paleodepth_3  +paleodepth_4
       seqa_skel_q    seqb_skel_q    seqc_skel_q
       seqd_skel_q    seqe_skel_q
       +ppa_dep_q     +ppb_dep_q
       +topmio_dep_q  +baseoligo_dep_q
       ppb_dep_1      top_mio_dep_1
       boligo_dep_1   basement_dep_1
       top_mio_dep_2  boligo_dep_2   basement_dep_2
       boligo_dep_3   basement_dep_3
       basement_dep_4
       sea_floor_q
       tectonic_sub_0               tectonic_sub_1
       tectonic_sub_2               tectonic_sub_3
       tectonic_sub_4
       density_1      density_2      density_3
       density_4      density_0
       +basement_1_adj              +basement_2_adj
       +basement_3_adj              +basement_4_adj
       +seq_a_volume  +seq_b_volume  +seq_c_volume      +seq_d_volume
       +seq_e_volume  +seq_volume    +basement_q(km)    +row_dist(km)
```

Maps contains the fields that model the various sequence thicknesses, basement structures, tectonic subsidence etc. that are mapped in the various diagrams in this study.

```
Maps_rec   is an  AUTOMATIC          INTEGER field
       Expected Minimum = 1  Maximum = 9192
       0 bytes stored per value

Maps_nul   is an  AUTOMATIC          INTEGER field
       Expected Minimum = 0  Maximum = 1
       0 bytes stored per value

Maps_row   is an  AUTOMATIC          INTEGER field
       Expected Minimum = 1  Maximum = 32
       0 bytes stored per value

Maps_col   is an  AUTOMATIC          INTEGER field
       Expected Minimum = 1  Maximum = 64
       0 bytes stored per value

Maps_xc   is an  AUTOMATIC           REAL field
       Expected Minimum = 2150000  Maximum = 2293810
       0 bytes stored per value. Precision 0

Maps_csz   is an  AUTOMATIC          REAL field
       Expected Minimum = 4000  Maximum = 4000
       0 bytes stored per value. Precision 0
```

```
Maps_yc   is an  AUTOMATIC          REAL field
       Expected Minimum = 5650000  Maximum = 5891244
       0 bytes stored per value. Precision 0

Maps_rsz   is an  AUTOMATIC         REAL field
       Expected Minimum = 4000  Maximum = 4000
       0 bytes stored per value. Precision 0

basement_q  is an    ACTUAL         REAL field
       Expected Minimum = *  Maximum = *
       8 bytes stored per value. Precision 0
```
This field contains the basement surface modelled from the basement_dep field (in Convert) using MINQ.

```
map_locate  is an    ACTUAL         INTEGER field
       Expected Minimum = *  Maximum = *
       4 bytes stored per value
```
This field acts as a flag for filtering purposes, indicating which cells are within the basin (=0) and those which are over the uplifted block (=1).

```
basement_twt_q is an ACTUAL         REAL field
       Expected Minimum = *  Maximum = *
       8 bytes stored per value. Precision 1


seqe_thick_q is an   ACTUAL         REAL field
       Expected Minimum = *  Maximum = *
       8 bytes stored per value. Precision 0
```
This field contains the Sequence E isopach modelled from the seqe_thick field (in Convert) using MINQ.

```
seqd_thick_q is an   ACTUAL         REAL field
       Expected Minimum = *  Maximum = *
       8 bytes stored per value. Precision 0
```
This field contains the Sequence D isopach modelled from the seqd_thick field (in Convert) using MINQ.

```
seqc_thick_q is an   ACTUAL         REAL field
       Expected Minimum = *  Maximum = *
       8 bytes stored per value. Precision 0
```
This field contains the Sequence C isopach modelled from the seqc_thick field (in Convert) using MINQ.

```
seqb_thick_q is an   ACTUAL         REAL field
       Expected Minimum = *  Maximum = *
       8 bytes stored per value. Precision 0
```
This field contains the Sequence B isopach modelled from the seqb_thick field (in Convert) using MINQ.

```
seqa_thick_q is an   ACTUAL         REAL field
       Expected Minimum = *  Maximum = *
       8 bytes stored per value. Precision 0
```
This field contains the Sequence A isopach modelled from the seqa_thick field (in Convert) using MINQ.

```
total_thick is a  CALCULATED        REAL field
       Expected Minimum = *  Maximum = *
       0 bytes stored per value. Precision 0
       Equation: seqe_thick_q seqd_thick_q + seqc_thick_q
                 +seqb_thick_q + seqa_thick_q +
```
Calculated total thickness of sediments in cell.

```
total_volume is a  CALCULATED       REAL field
       Expected Minimum = *  Maximum = *
       0 bytes stored per value. Precision 2
       Equation: total_thick 2000 * 2000 *
       Calculated total volume of sediments in cell.

paleodepth_0 is a  CALCULATED       REAL field
       Expected Minimum = *  Maximum = *
       0 bytes stored per value. Precision 2
       Equation: 150
       Simple paleodepth adjustment  for Stage 0 of backstripping.

paleodepth_1 is a  CALCULATED       REAL field
       Expected Minimum = *  Maximum = *
       0 bytes stored per value. Precision 2
       Equation: 150
       Simple paleodepth adjustment  for Stage 1 of backstripping.

paleodepth_2 is a  CALCULATED       REAL field
       Expected Minimum = *  Maximum = *
       0 bytes stored per value. Precision 2
       Equation: 300
       Simple paleodepth adjustment  for Stage 2 of backstripping.

paleodepth_3 is a  CALCULATED       REAL field
       Expected Minimum = *  Maximum = *
       0 bytes stored per value. Precision 2
       Equation: 300
       Simple paleodepth adjustment  for Stage 3 of backstripping.

paleodepth_4 is a  CALCULATED       REAL field
       Expected Minimum = *  Maximum = *
       0 bytes stored per value. Precision 2
       Equation: 500
       Simple paleodepth adjustment  for Stage 4 of backstripping.

seqa_skel_q is an    ACTUAL         REAL field
       Expected Minimum = *  Maximum = *
       8 bytes stored per value. Precision 0
      This field contains the Sequence A skeletal thickness modelled from the seqa_skel
      field (in Regular) using MINQ.

seqb_skel_q is an    ACTUAL         REAL field
       Expected Minimum = *  Maximum = *
       8 bytes stored per value. Precision 0
      This field contains the Sequence B skeletal thickness modelled from the seqb_skel
      field (in Regular) using MINQ.

seqc_skel_q is an    ACTUAL         REAL field
       Expected Minimum = *  Maximum = *
       8 bytes stored per value. Precision 0
      This field contains the Sequence C skeletal thickness modelled from the seqc_skel
      field (in Regular) using MINQ.

seqd_skel_q is an    ACTUAL         REAL field
       Expected Minimum = *  Maximum = *
       8 bytes stored per value. Precision 0
      This field contains the Sequence D skeletal thickness modelled from the seqd_skel
      field (in Regular) using MINQ.
```

```
seqe_skel_q is an     ACTUAL          REAL field
       Expected Minimum = *  Maximum = *
       8 bytes stored per value. Precision 0
```
This field contains the Sequence E skeletal thickness modelled from the seqe_skel field (in Regular) using MINQ.

```
ppa_dep_q   is a  CALCULATED          REAL field
       Expected Minimum = *  Maximum = *
       0 bytes stored per value. Precision 0
       Equation: seqa_thick_q
```
Depth to PPA horizon calculated as total of sequence thicknesses above.

```
ppb_dep_q   is a  CALCULATED          REAL field
       Expected Minimum = *  Maximum = *
       0 bytes stored per value. Precision 0
       Equation: seqa_thick_q seqb_thick_q +
```
Depth to PPB horizon calculated as total of sequence thicknesses above.

```
topmio_dep_q is a  CALCULATED         REAL field
       Expected Minimum = *  Maximum = *
       0 bytes stored per value. Precision 0
       Equation: seqa_thick_q seqb_thick_q + seqc_thick_q +
```
Depth to Top Miocene horizon calculated as total of sequence thicknesses above.

```
baseoligo_dep_q is a  CALCULATED      REAL field
       Expected Minimum = *  Maximum = *
       0 bytes stored per value. Precision 0
       Equation: seqa_thick_q seqb_thick_q + seqc_thick_q +
                 seqd_thick_q +
```
Depth to Oligocene horizon calculated as total of sequence thicknesses above.

```
ppb_dep_1   is an     ACTUAL          INTEGER field
       Expected Minimum = *  Maximum = *
       4 bytes stored per value
```
Depth to PPB Horizon at Stage 1 backstripping. Calculated in processing.

```
top_mio_dep_1 is an  ACTUAL           INTEGER field
       Expected Minimum = *  Maximum = *
       4 bytes stored per value
```
Depth to Top Miocene Horizon at Stage 1 backstripping. Calculated in processing.

```
boligo_dep_1 is an    ACTUAL          INTEGER field
       Expected Minimum = *  Maximum = *
       4 bytes stored per value
```
Depth to Oligocene Horizon at Stage 1 backstripping. Calculated in processing.

```
basement_dep_1 is an ACTUAL           INTEGER field
       Expected Minimum = *  Maximum = *
       4 bytes stored per value
```
Depth to Basement Horizon at Stage 1 backstripping. Calculated in processing.

```
top_mio_dep_2 is an  ACTUAL           INTEGER field
       Expected Minimum = *  Maximum = *
       4 bytes stored per value
```
Depth to Top Miocene Horizon at Stage 2 backstripping. Calculated in processing.

```
boligo_dep_2 is an    ACTUAL          INTEGER field
       Expected Minimum = *  Maximum = *
       4 bytes stored per value
```
Depth to Oligocene Horizon at Stage 2 backstripping. Calculated in processing.

```
basement_dep_2 is an ACTUAL          INTEGER field
       Expected Minimum = *  Maximum = *
       4 bytes stored per value
       Depth to Basement Horizon at Stage 2 backstripping. Calculated in processing.

boligo_dep_3 is an   ACTUAL          INTEGER field
       Expected Minimum = *  Maximum = *
       4 bytes stored per value
       Depth to Oligocene Horizon at Stage 3 backstripping. Calculated in processing.

basement_dep_3 is an ACTUAL          INTEGER field
       Expected Minimum = *  Maximum = *
       4 bytes stored per value
       Depth to Basement Horizon at Stage 3 backstripping. Calculated in processing.

basement_dep_4 is an ACTUAL          INTEGER field
       Expected Minimum = *  Maximum = *
       4 bytes stored per value
       Depth to Basement Horizon at Stage 4 backstripping. Calculated in processing.

sea_floor_q is an    ACTUAL          REAL field
       Expected Minimum = *  Maximum = *
       8 bytes stored per value. Precision 0
      This field contains the seafloor surface modelled from the seafloor_dep field (in
      Convert) using MINQ.

tectonic_sub_1 is an ACTUAL          INTEGER field
       Expected Minimum = *  Maximum = *
       4 bytes stored per value
       The tectonic subsidence of the cell at Stage 1. Calculated in processing.

tectonic_sub_2 is an ACTUAL          INTEGER field
       Expected Minimum = *  Maximum = *
       4 bytes stored per value
       The tectonic subsidence of the cell at Stage 2. Calculated in processing.

tectonic_sub_3 is an ACTUAL          INTEGER field
       Expected Minimum = *  Maximum = *
       4 bytes stored per value
       The tectonic subsidence of the cell at Stage 3. Calculated in processing.

tectonic_sub_4 is an ACTUAL          INTEGER field
       Expected Minimum = *  Maximum = *
       4 bytes stored per value
       The tectonic subsidence of the cell at Stage 4. Calculated in processing.

density_1   is an    ACTUAL          REAL field
       Expected Minimum = *  Maximum = *
       8 bytes stored per value. Precision 2
       The density of sediments in the cell at Stage 1. Calculated in processing.

density_2   is an    ACTUAL          REAL field
       Expected Minimum = *  Maximum = *
       8 bytes stored per value. Precision 2
       The density of sediments in the cell at Stage 2. Calculated in processing.

density_3   is an    ACTUAL          REAL field
       Expected Minimum = *  Maximum = *
       8 bytes stored per value. Precision 2
       The density of sediments in the cell at Stage 3. Calculated in processing.
```

```
density_4    is an     ACTUAL          REAL field
       Expected Minimum = *  Maximum = *
       8 bytes stored per value. Precision 2
       The density of sediments in the cell at Stage 4. Calculated in processing.

density_0    is an     ACTUAL          REAL field
       Expected Minimum = *  Maximum = *
       8 bytes stored per value. Precision 2
      The density of sediments in the cell at Stage 0 (present). Calculated in processing.

tectonic_sub_0 is an ACTUAL          REAL field
       Expected Minimum = *  Maximum = *
       8 bytes stored per value. Precision 0
       The tectonic subsidence of the cell at Stage 0 (present). Calculated in processing.

basement_1_adj is a  CALCULATED      REAL field
       Expected Minimum = *  Maximum = *
       0 bytes stored per value. Precision 0
       Equation: basement_dep_1 paleodepth_1 +
       Depth to basement at Stage 1 adjusted for paleodepth.

basement_2_adj is a  CALCULATED      REAL field
       Expected Minimum = *  Maximum = *
       0 bytes stored per value. Precision 0
       Equation: basement_dep_2 paleodepth_2 +
       Depth to basement at Stage 2 adjusted for paleodepth.

basement_3_adj is a  CALCULATED      REAL field
       Expected Minimum = *  Maximum = *
       0 bytes stored per value. Precision 0
       Equation: basement_dep_3 paleodepth_3 +
       Depth to basement at Stage 3 adjusted for paleodepth.

basement_4_adj is a  CALCULATED      REAL field
       Expected Minimum = *  Maximum = *
       0 bytes stored per value. Precision 0
       Equation: basement_dep_4 paleodepth_4 +
       Depth to basement at Stage 4 adjusted for paleodepth.

seq_a_volume is a  CALCULATED        REAL field
       Expected Minimum = *  Maximum = *
       0 bytes stored per value. Precision 0
       Equation: seqa_thick_q 2000 * 2000 *
       Decompacted volume of Sequence A. (m3)

seq_b_volume is a  CALCULATED        REAL field
       Expected Minimum = *  Maximum = *
       0 bytes stored per value. Precision 0
       Equation: ppb_dep_1 2000 * 2000 *
       Decompacted volume of Sequence B. (m3)

seq_c_volume is a  CALCULATED        REAL field
       Expected Minimum = *  Maximum = *
       0 bytes stored per value. Precision 0
       Equation: top_mio_dep_2 2000 * 2000 *
       Decompacted volume of Sequence C. (m3)

seq_d_volume is a  CALCULATED        REAL field
       Expected Minimum = *  Maximum = *
       0 bytes stored per value. Precision 0
       Equation: boligo_dep_3 2000 * 2000 *
       Decompacted volume of Sequence D. (m3)
```

```
seq_e_volume is a  CALCULATED        REAL field
       Expected Minimum = *  Maximum = *
       0 bytes stored per value. Precision 0
       Equation: basement_dep_4 2000 * 2000 *
       Decompacted volume of Sequence E. (m3)

seq_volume  is a  CALCULATED         REAL field
       Expected Minimum = *  Maximum = *
       0 bytes stored per value. Precision 0
       Equation: seq_a_volume seq_b_volume + seq_c_volume +
                 seq_d_volume +  seq_e_volume +
       Total volume of decompacted sediment in each cell. (m3)

basement_q(km) is a  CALCULATED      REAL field
       Expected Minimum = *  Maximum = *
       0 bytes stored per value. Precision 2
       Equation: basement_q 1000 /
       Basement depth expressed in km for display purposes.

row_dist(km) is a  CALCULATED        REAL field
       Expected Minimum = *  Maximum = *
       0 bytes stored per value. Precision 0
       Equation: Maps_row 2 *
       Distance of row from origin in km for display purposes.
```

Appendix C: TECHBASE macros

C.1: TECHNICN and TASK files

TECHBASE has built in productivity aids to handle repetitive tasks, those used in this study have been collectively termed 'macros' and gathered in this Appendix.

Runlogs contain the exact record of key-strokes used when a TECHBASE program is run. These are recorded during a session of the program and can be reproduced by using the runlog as input into the program. A standard word processor may be used to edit the runlogs, but care must be taken to ensure tabs, spaces, escapes and control keys are not altered.

In the following listings, a number of symbols have been used to represent special characters that are included as part of the runlog sequence. Any spaces in the listings are true representations of spaces in the runlogs.

Δ = tab

§ = Control-U, clears the entire field before entering a new value

»h = Home key

»c = Comment (does not affect function of runlog)

☞ = indicates that the line is continuous from the one immediately above.

TECHNICN allows TECHBASE procedures to be subdivided into a series of easily managed projects. A **PROJECT** is a set of procedures, called **TASKS**. In turn the tasks consist of various commands controlling data flow and program execution. Tasks may include runlogs.

A TECHNICN project was created for this study to aid the input and processing of seismic lines. Other runlogs were created for the processing of seismic information and the generation of diagrams resulting from the processing of this data.

```
#
#      This TECHNICN file is for running
#      the Geohistory Analysis Package
#      Keith Sircombe, September 1992
#

#-------------------------------------------------------------------

PROJECT "Seismic data" c:\tbase\wcoast\swlandta\swland
☞ "Enter data from interpreted section"

TASK "Digitize interprtn" c:\tbase\wcoast\swlandta\swland
☞ digitz.tsk  "Digitize interpreted seismic and load into database"

TASK "Input data" c:\tbase\wcoast\swlandta\swland
☞ indig.tsk   "Load digitized data"

#-------------------------------------------------------------------

PROJECT "Depth conversion" c:\tbase\wcoast\swlandta\swland
☞ "Depth convert interpreted section"

TASK "Depth conversion" c:\tbase\wcoast\swlandta\swland
☞ procdat.tsk "Process data from interpreted seismic line"

TASK "create Graphic"   c:\tbase\wcoast\swlandta\swland
☞ dcgrh.tsk   "Create graphic file of interpreted section"

TASK "View conversion"  c:\tbase\wcoast\swlandta\swland
☞ dcview.tsk  "View interpreted seismic line"

#-------------------------------------------------------------------

PROJECT "Reconstruct section" c:\tbase\wcoast\swlandta\swland
☞ "Restore depth converted section"

TASK "Reconstruct section"    c:\tbase\wcoast\swlandta\swland
☞ recon.tsk   "Process data to get reconstructed sections"

TASK "create Graphic"   c:\tbase\wcoast\swlandta\swland
☞ rsgrh.tsk   "Create graphic file of interpreted section"

TASK "View restoration" c:\tbase\wcoast\swlandta\swland
☞ rsview.tsk  "View interpreted seismic line"
```

```
#
#      digitz.tsk
#      for Geohistory Analysis package
#      starts digitizer...
#      All digitising should be done from the start shotpoint to the
#      end shot point, seafloor to basement.
#      The data from the digitiser should be the format expected by
#      the database, e.g. shot_point twt_time line_id horizon_name
#      the line_id and horizon_name are derived from the marker in
#      sdigit.  A space between the two will separate them in the
#      loading process.

RUN sdigit <<-iDONE
oucx
DONE
```

```
#
#      indig.tsk
#      for Geohistory Analysis package
#      loads data
#      The data from the digitiser may be edited between sdigit and
#      here if required, e.g. to patch together long lines etc.

PARAMETER Section = "xx-nn" CT 32

REQUIRE {Section}.dig

RUN load <<-iDONE
ouxdoc:\tbase\wcoast\swlandta\swland
 xsv d{Section}.dig
fshot_point twt_time line_id horizon_name
papp
xl  x
DONE
```

```
#
#      procdat.tsk
#      for South Westland Geohistory Analysis package
#      task creates details and data report of requested section
#      for regularising using a QBASIC program "reg.bas"
#      regularised data is loaded into the database
#      skeletal thicknesses of each sequence is calculated
#      polygons are extracted from the data and tabled in a polygon
#      file
#

#-------------------------------------------------------------------
#      Enter line_id for processing
#

PARAMETER Section = "xx-nn"   CT 32

#-------------------------------------------------------------------
#      Output details of requested section
#      line_id, start shot point and end shot point are extracted via
#      a REPORT runlog.

RUN report <<DONE
»cOutput section details
ouxdoc:\tbase\wcoast\swlandta\swland
 aline_idΔ=Δ{Section}
```

```
 xsr{Section}.det
pΔΔnΔnΔnΔΔnΔy
fline_id "," start_sp "," end_sp
xr x
DONE

#-------------------------------------------------------------------
#     Output digitized information for requested section
#     shotpoints, two way travel time, line id and horizon name are
#     extracted via a REPORT runlog.

RUN report <<DONE
»cOutput horizon data
ouxdoc:\tbase\wcoast\swlandta\swland
 aline_idΔ=Δ{Section}
 xsr{Section}.rep
pΔΔnΔnΔnΔΔnΔy
fshot_point "," twt_time "," line_id "," horizon_name
xr x
DONE

#-------------------------------------------------------------------
#     Check if report outputs completed
#     Run QBASIC routine "reg.bas" to regularise data
#     Check completion of reg.bas
#

REQUIRE {Section}.det
REQUIRE {Section}.rep

ECHO > message.tmp {Section}
RUN qbasic /run reg.bas
ERASE message.tmp

REQUIRE {Section}.reg

#-------------------------------------------------------------------
#     Load regularised data into database
#

RUN load <<DONE
»cLoad regularised data
ouxdoc:\tbase\wcoast\swlandta\swland
 aline_idΔ=Δ{Section}
 xsd{Section}.reg
fline_id sp_reg seafloor_twt ppa_twt ppb_twt topmio_twt
☞ baseoligo_twtΔbasement_twt
pover
xl  x
DONE

#-------------------------------------------------------------------
ERASE {Section}.det
ERASE {Section}.rep
ERASE {Section}.reg

#-------------------------------------------------------------------
#     Calculate section length to each regular shotpoint
#

RUN tbcalc <<DONE
»cCalculate section lengths
oucxdoc:\tbase\wcoast\swlandta\swland
```

```
 aline_idΔ=Δ{Section}
 xsespreg_len = len_reg
xc x
DONE

#-------------------------------------------------------------------
#     Extract data for polygon tabling of depth converted horizons
#

RUN report <<DONE
»cOutput horizons into polygon format
oxoucxdoc:\tbase\wcoast\swlandta\swland
 aline_idΔ=Δ{Section}Δ»h
 xsr{Section}.polΔno»h
p  ΔΔnΔnΔnΔΔnΔy
»cOutput horizons into polygon format: seafloor
flen_reg seafloor_dep "{Section}_seafloor" "1" seafloor_code "4"
 "{Section}"                                                          ☞
xr srΔ§yes»h
»cOutput horizons into polygon format: ppa
xdmΔΔΔ§seqb_thickΔ§!=Δ§0Δ§seqa_thickΔ§!=Δ§0»h
 xsf§len_reg ppa_dep "{Section}_ppa" "1" ppa_code "4" "{Section}"
xr srΔ§yes»h
»cOutput horizons into polygon format: ppb
xdmΔΔΔ§seqc_thickΔ§!=Δ§0Δ§Δ§Δ§»h
 xsf§len_reg ppb_dep "{Section}_ppb" "1" ppb_code "4" "{Section}"
xr srΔ§yes»h
»cOutput horizons into polygon format: topmio
xdmΔΔΔ§seqd_thickΔ§!=Δ§0»h
 xsf§len_reg topmio_dep "{Section}_topmio" "1" topmio_code "4"
☞ "{Section}"
xr srΔ§yes»h
»cOutput horizons into polygon format: baseoligo
xdmΔΔΔ§seqe_thickΔ§!=Δ§0»h
 xsf§len_reg baseoligo_dep "{Section}_baseoligo" "1" baseoligo_code
☞ "4" "{Section}"
xr srΔ§yes»h
»cOutput horizons into polygon format: basement
xdmΔΔΔ§Δ§Δ§»h
 xsf§len_reg basement_dep "{Section}_basement" "1" basement_code "4"
☞ "{Section}"
xr x
DONE

#-------------------------------------------------------------------
#     Load data for polygon tabling of depth converted horizons
#

RUN load <<DONE
»cLoad Polygons into table
oucxdoc:\tbase\wcoast\swlandta\swland
 aline_idΔ=Δ{Section}Δpoly_typeΔ=Δ4
 xsd{Section}.pol
fnull null poly_owner poly_style poly_colour poly_type line_id
☞ (poly)
pover
xl  x
DONE

ERASE {Section}.pol
```

```
#-----------------------------------------------------------------
#
#      dcgrh.tsk
#      for Geohistory Analysis package
#      task creates metafile of depth converted seismic horizons for
#      the requested section
#

PARAMETER Section = "xx-nn" CT 32
PARAMETER X-scale = "10000" CI 8
PARAMETER Y-scale = "10000" CI 8
PARAMETER Max-dep = "3000"  CI 8

RUN report <<DONE
oucxdoc:\tbase\wcoast\swlandta\swland
 aline_idΔ=Δ{Section}
 xsrendbit.repΔnoΔ
pΔΔnΔnΔnΔΔnΔyΔΔΔ
f"SET x_length = " line_lenrnd
xr x
DONE

REQUIRE endbit.rep
INCLUDE endbit.rep
ERASE endbit.rep

RUN poster <<-iDONE
oxoucxdoc:\tbase\wcoast\swlandta\swland
 aline_idΔ=Δ{Section}Δpoly_typeΔ=Δ4
xgm{Section}dc.met
sΔΔΔ2ΔΔΔΔΔΔΔ
xss{X-scale}Δ{Y-scale}Δ
r0Δ{x_length}Δ1Δ{Max-dep}Δ0Δ1
b g0Δ{x_length}Δ500Δ0Δ{Max-
dep}Δ100ΔticksΔblackΔsolidΔ0.25ΔblackΔ0Δ0Δ
gΔΔ§1000ΔΔΔ§500ΔΔΔΔ§0.50ΔΔ1§1.00ΔΔ
xcfPolygons_nul
spoly_colourΔpoly_style
d xaut{Section} Depth ConversionΔ0Δ-700Δ2.00Δ90ΔblackΔ
xx
DONE
```

```
#
#      sdview.tsk
#      for Geohistory Analysis package
#      for viewing interpreted digitized line
#

PARAMETER Section = "xx-nn" CT 32

REQUIRE {Section}dc.met

RUN mftr -i -ze {Section}dc.met
```

```
#
#      RECON.TSK
#      task file for outputing section details for a qbasic program
#      to restore and decompact
#

PARAMETER Section = "xx-nn" CT 32
```

```
#-------------------------------------------------------------------
#     Calculate skeletal thicknesses of the sequences
#     Uses "skelcalc.clc" TBCALC file.

RUN tbcalc <<DONE
»cCalculate skeletal thicknesses
ouxdoc:\tbase\wcoast\swlandta\swland
 aline_idΔ=Δ{Section}
 xse(f,skelcalc.clc)
xc x
DONE

#-------------------------------------------------------------------
#     Report paleodepth details
#

RUN report <<DONE
»cReport paleodepth details
oucxdoc:\tbase\wcoast\swlandta\swland
 aline_idΔ=Δ{Section}
 xsrpaleo.rep
pΔΔnΔnΔnΔΔnΔyΔ
f(f,paleo.fmt)
xr x
DONE

#-------------------------------------------------------------------
#     Report section details
#

RUN report <<DONE
»cOutput section details
oucxdoc:\tbase\wcoast\swlandta\swland
 aline_idΔ=Δ{Section}
 xsrrecon.rep
pΔΔnΔnΔnΔΔnΔy
f(f,recon.fmt)
xr x
DONE

#-------------------------------------------------------------------
#     Run restoration and decompaction QBASIC routine
#

RUN qbasic /run recon.bas
REQUIRE recon.prc

#-------------------------------------------------------------------
#     Load restored and decompacted data
#

RUN load <<DONE
»cLoad restored and decompacted data
oucxdoc:\tbase\wcoast\swlandta\swland
 aline_idΔ=Δ{Section}
 xsdrecon.prc
fline_id len_regΔbs1_ppa bs1_ppb bs1_topmio bs1_baseoligo
☞ bs1_basementΔbs2_ppb bs2_topmio bs2_baseoligo
☞ bs2_basementΔbs3_topmio bs3_baseoligo bs3_basementΔbs4_baseoligo
☞ bs4_basement
poverΔ
xl  x
DONE
```

```
#-----------------------------------------------------------------
#     Extract data for polygon tabling of depth converted horizons
#

RUN report <<DONE
»cOutput restored horizons into polygon format
oxoucxdoc:\tbase\wcoast\swlandta\swland
 aline_idΔ=Δ{Section}»h
 xsr{Section}.polΔno»h
p  ΔΔnΔnΔnΔΔnΔy
»cOutput horizons: Stage 4 ppa
xdmΔΔΔ§bs1_seqb_thickΔ§!=Δ§Δ0§bs1_seqa_thickΔ§!=Δ§0»h
 xsf§len_reg bs1_ppa "{Section}_bs1_ppa" "1Δ8Δ5" "{Section}"
xr srΔ§yes»h
»cOutput horizons: Stage 4 ppb
xdmΔΔΔ§bs1_seqc_thickΔ§!=Δ§0Δ§Δ§Δ§»h
 xsf§len_reg bs1_ppb "{Section}_bs1_ppb" "1Δ5Δ5" "{Section}"
xr srΔ§yes»h
»cOutput horizons: Stage 4 topmio
xdmΔΔΔbs1_seqd_thickΔ!=Δ0»h
 xsf§len_reg bs1_topmio "{Section}_bs1_topmio" "1Δ6Δ5" "{Section}"
xr srΔ§yes»h
»cOutput horizons: Stage 4 baseoligo
xdmΔΔΔ§bs1_seqe_thickΔ§!=Δ§0»h
 xsf§len_reg bs1_baseoligo "{Section}_bs1_baseoligo" "1Δ4Δ5"
☞ "{Section}"
xr srΔ§yes»h
»cOutput horizons: Stage 4 basement
xdmΔΔΔ§Δ§Δ§»h
 xsf§len_reg bs1_basement "{Section}_bs1_basement" "1Δ2Δ5"
☞ "{Section}"
xr srΔ§yes»h
»cOutput horizons: Stage 3 ppb
xdmΔΔΔ§bs2_seqc_thickΔ§!=Δ§0»h
 xsf§len_reg bs2_ppb "{Section}_bs2_ppb" "1Δ5Δ5" "{Section}"
xr srΔ§yes»h
»cOutput horizons: Stage 3 topmio
xdmΔΔΔ§bs2_seqd_thickΔ§!=Δ§0»h
 xsf§len_reg bs2_topmio "{Section}_bs2_topmio" "1Δ6Δ5" "{Section}"
xr srΔ§yes»h
»cOutput horizons: Stage 3 baseoligo
xdmΔΔΔ§bs2_seqe_thickΔ§!=Δ§0»h
 xsf§len_reg bs2_baseoligo "{Section}_bs2_baseoligo" "1Δ4Δ5"
☞ "{Section}"
xr srΔ§yes»h
»cOutput horizons: Stage 3 basement
xdmΔΔΔ§Δ§Δ§ h
 xsf§len_reg bs2_basement "{Section}_bs2_basement" "1Δ2Δ5"
☞ "{Section}"
xr srΔ§yes»h
»cOutput horizons: Stage 2 topmio
xdmΔΔΔ§bs3_seqd_thickΔ§!=Δ§0»h
 xsf§len_reg bs3_topmio "{Section}_bs3_topmio" "1Δ6Δ5" "{Section}"
xr srΔ§yes»h
»cOutput horizons: Stage 2 baseoligo
xdmΔΔΔ§bs3_seqe_thickΔ§!=Δ§0»h
 xsf§len_reg bs3_baseoligo "{Section}_bs3_baseoligo" "1Δ4Δ5"
☞ "{Section}"
xr srΔ§yes»h
»cOutput horizons: Stage 2 basement
xdmΔΔΔ§Δ§Δ§»h
 xsf§len_reg bs3_basement "{Section}_bs3_basement" "1Δ2Δ5"
```

```
☞ "{Section}"
  xr srΔ$yes»h
  »cOutput horizons: Stage 1 baseoligo
  xdmΔΔΔ$bs4_seqe_thickΔ$!=Δ$0»h
   xsf$len_reg bs4_baseoligo "{Section}_bs4_baseoligo" "1Δ4Δ5"
☞ "{Section}"
  xr srΔ$yes»h
  »cOutput horizons: Stage 1 basement
  xdmΔΔΔ$Δ$Δ$»h
   xsf$len_reg bs4_basement "{Section}_bs4_basement" "1Δ2Δ5"
☞ "{Section}"
  xr x
  DONE

  #-------------------------------------------------------------------
  #     Load data into polygon tabling of depth converted horizons
  #

  RUN load <<DONE
  »cLoad Polygons into table
  oucxdoc:\tbase\wcoast\swlandta\swland
   aline_idΔ=Δ{Section}Δpoly_typeΔ=Δ5
   xsd{Section}.pol
  fnull null poly_owner poly_style poly_colour poly_type line_id
☞  (poly)
  pover
  xl  x
  DONE

  ERASE {Section}.pol
```

```
  #
  #     rsgrh.tsk
  #     for Geohistory Analysis package
  #     task creates metafile of restored horizons for the
  #     requested section
  #

  PARAMETER Section = "xx-nn" CT 32
  PARAMETER X-scale = "50000" CI 8
  PARAMETER Y-scale = "50000" CI 8

  RUN report <<DONE
  oucxdoc:\tbase\wcoast\swlandta\swland
   aline_idΔ=Δ{Section}
   xsrendbit.repΔnoΔ
  pΔΔnΔnΔnΔΔnΔyΔΔΔ
  f"SET x_length = " line_lenrnd
  xr x
  DONE

  REQUIRE endbit.rep
  INCLUDE endbit.rep
  ERASE endbit.rep

  SET axis-len = {x-length} {X-scale} / 100

  RUN poster <<DONE
  oxoucxdoc:\tbase\wcoast\swlandta\swland
  »cRestoration Stage 4
   aline_idΔ=Δ{Section}Δpoly_typeΔ=Δ5Δpoly_ownerΔ()Δbs1
  xgm{Section}4.met
```

```
  sΔΔΔ2ΔΔΔΔΔΔΔ
  xss{X-scale}Δ{Y-scale}
  r0Δ{x_length}Δ1Δ2000Δ-100Δ6Δ
  b g0Δ{x_length}Δ500Δ0Δ2000Δ250ΔticksΔblackΔsolidΔ0.15ΔblackΔ0Δ0Δ
  g§0Δ§{x_length}Δ§1000Δ§0§999999999998Δ§999999999999Δ§500Δ§ticks
☞ Δ§blackΔ§solidΔ§0.25Δ§blackΔ§0.00Δ§0Δ
  g§999999999998Δ§999999999999Δ§1Δ§0Δ§2000Δ§500ΔΔΔΔΔΔ§0.35ΔΔ
  x cfPolygons_nul
  spoly_colourΔpoly_style
  d xautLate Nukumaruan (1.2 Ma)Δ§0Δ-300Δ0.50Δ90Δblack»h
  »cRestoration Stage 3
  xgcm§{Section}3.met
  xdmΔΔΔΔΔΔΔΔ§bs2Δ§h
  xsrΔΔΔΔΔ§12Δ
  b g§0Δ§{x_length}Δ§500Δ§0Δ§2000Δ§250Δ§ticksΔ§blackΔ§solidΔ§0.15
☞ Δ§blackΔ§0Δ§0Δ
  g§0Δ§{x_length}Δ§1000Δ§0§999999999998Δ§999999999999Δ§500Δ§ticks
☞ Δ§blackΔ§solidΔ§0.25Δ§blackΔ§0.00Δ§0Δ
  g§999999999998Δ§999999999999Δ§1Δ§0Δ§2000Δ§500ΔΔΔΔΔΔ§0.35ΔΔ
  x cd xat§Waipipian (3.2 Ma)Δ§0Δ§-300Δ§0.50Δ§90Δ§black»h
  »cRestoration Stage 2
  xgcm§{Section}2.met
  xdmΔΔΔΔΔΔΔΔ§bs3Δ§h
  xsrΔΔΔΔΔ§18Δ
  b g§0Δ§{x_length}Δ§500Δ§0Δ§2000Δ§250Δ§ticksΔ§blackΔ§solidΔ§0.15
☞ Δ§blackΔ§0Δ§0Δ
  g§0Δ§{x_length}Δ§1000Δ§0§999999999998Δ§999999999999Δ§500Δ§ticks
☞ Δ§blackΔ§solidΔ§0.25Δ§blackΔ§0.00Δ§0Δ
  g§999999999998Δ§999999999999Δ§1Δ§0Δ§2000Δ§500ΔΔΔΔΔΔ§0.35ΔΔ
  x cd xat§Top Miocene (5.0 Ma)Δ§0Δ§-300Δ§0.50Δ§90Δ§black»h
  »cRestoration Stage 1
  xgcm§{Section}1.met
  xdmΔΔΔΔΔΔΔΔ§bs4Δ§h
  xsrΔΔΔΔΔ§24Δ
  b g§0Δ§{x_length}Δ§500Δ§0Δ§2000Δ§250Δ§ticksΔ§blackΔ§solidΔ§0.15
☞ Δ§blackΔ§0Δ§0Δ
  g§0Δ§{x_length}Δ§1000Δ§0§999999999998Δ§999999999999Δ§500Δ§ticks
☞ Δ§blackΔ§solidΔ§0.25Δ§blackΔ§0.00Δ§0Δ
  g§999999999998Δ§999999999999Δ§1Δ§0Δ§2000Δ§500ΔΔΔΔΔΔ§0.35ΔΔ
  x cd xat§Oligocene (30.0 Ma)Δ§0Δ-300Δ§0.50Δ§90Δ§black»h
  t»h§{Section} RestorationΔ§0Δ§-850Δ§0.70Δ§90Δ§black»h
  »cPresent Section
  xgcm§{Section}0.met
  xdmΔΔΔΔΔ§4Δ§Δ§Δ§Δ§h
  xsrΔΔΔΔΔ§0Δ
  b g§0Δ§{x_length}Δ§500Δ§0Δ§2000Δ§250Δ§ticksΔ§blackΔ§solidΔ§0.15
☞ Δ§blackΔ§0Δ§0Δ
  g§0Δ§{x_length}Δ§1000Δ§0§999999999998Δ§999999999999Δ§500Δ§ticks
☞ Δ§blackΔ§solidΔ§0.25Δ§blackΔ§0.00Δ§0Δ
  g§999999999998Δ§999999999999Δ§1Δ§0Δ§2000Δ§500ΔΔΔΔΔΔ§0.35ΔΔ
  x cd xat§Present sectionΔ§0Δ-300Δ§0.50Δ§90Δ§black»h
  aDistance (m)Δ0Δ2500Δ{axis_len}Δ90ΔblackΔlinearΔrightΔ0Δ{x_length}
☞ Δ1000
  xx
  DONE
```

```
#
#      rsview.tsk
#      for Geohistory Analysis package
#      for viewing restored sections
#

PARAMETER Section = "xx-nn" CT 32

REQUIRE {Section}0.met
REQUIRE {Section}1.met
REQUIRE {Section}2.met
REQUIRE {Section}3.met
REQUIRE {Section}4.met

RUN gview {Section}0 {Section}1 {Section}2 {Section}3 {Section}4.met
```

C.2 TECHBASE Runlogs

Other runlogs were also used to generate maps and diagrams, or processing of data within the study area grid. These situations were generally non-repetitive, but required frequent reprocessing to account for errors and minor modifications.

The following runlog, *map.rlg*, was used to generate the geological base map in Figure 1.4 using POSTER. The numerous `.pol` files used are drawn onto the base map as filled and coloured polygons, with some drawn or redrawn as hollow outlines to create borders.

```
oucxdoc:\tbase\wcoast\swlandta\swland
 xgmmap.met
sΔΔΔ2ΔΔΔΔΔΔΔ
xss1000000Δ1000000Δ
r2100000Δ2350000Δ1Δ5650000Δ5875000Δ1Δ
xf§bath250.polΔ§C10Δ§blankΔ§yΔ§3ΔΔΔ
  f§bath500.polΔ§C11Δ§blankΔ§yΔ§3ΔΔΔ
 f§bath1000.polΔ§C12Δ§blankΔ§yΔ§3ΔΔΔ
 f§bath1500.polΔ§C13Δ§blankΔ§yΔ§3ΔΔΔ
 f§bath2000.polΔ§C14Δ§blankΔ§yΔ§3ΔΔΔ
 f§bath3000.polΔ§C15Δ§blankΔ§yΔ§3ΔΔΔ
 f§metamor.polΔ§C9Δ§blankΔ§yesΔ§3Δ§0.5ΔΔ
 f§basement.polΔ§greenΔ§blankΔ§yesΔ§3Δ§1.00Δ§90Δ
 f§tertiary.polΔ§yellowΔ§blankΔ§yesΔ§3Δ§0.5Δ§90Δ
 f§tertiary.polΔ§blackΔ§solidΔ§yesΔ§hollowΔΔΔ
 f§creta.polΔ§orangeΔ§blankΔ§yesΔ§3Δ§0.5Δ§90Δ
 f§creta.polΔ§blackΔ§solidΔ§yesΔ§hollowΔΔΔ
 f§..\polygons\wcoastl.polΔ§blueΔ§wideΔ§yΔ§Δ§Δ§Δ
 f§..\polygons\afault.polΔ§C2Δ§wideΔ§yesΔΔΔΔ
 f§..\polygons\ffault.polΔ§C2Δ§wideΔ§yesΔΔΔΔ
 f§mfault.polΔ§C2Δ§wideΔ§yesΔΔΔΔ
 f§rivers.polΔ§blueΔ§solidΔ§yΔ§Δ§Δ§Δ
»cf§bathy.polΔ§blueΔ§solidΔ§yΔ§Δ§Δ§Δ
 aupmapleg.picΔ2290000Δ5650000Δ1Δ90ΔΔ
p§scale.picΔ§2230000Δ§5650000Δ§1Δ§90ΔΔ
p§north.picΔ§2147900Δ§5825300Δ§3Δ§87ΔΔ
p§depth.picΔ§2108000Δ§5821000Δ§1Δ§90ΔΔ
p§monogram.picΔ§2100000Δ§5650000Δ§0.5Δ§90ΔΔ
p§crest.picΔ§2330000Δ§5863000Δ§0.025Δ§90ΔΔ
xgsΔΔΔ3ΔΔΔΔΔΔΔ
xda§loc_idΔ§=Δ§4
xpf§loc_eastΔ§loc_northΔloc_name1
m§2Δ§blackΔ§0.5ΔΔ§87ΔΔΔΔΔ
vblackΔ0.30ΔrightΔ87
d
f»h§loc_eastΔ§loc_northΔ§loc_name2»h
m§2Δ§blackΔ§0.0ΔΔΔΔΔΔΔ
v»h§blackΔ§0.30Δ§topΔ§177
d xdm§loc_idΔ§=Δ§2
xpf§loc_eastΔ§loc_northΔ§»h
m§13Δ§blackΔ0.25ΔΔ§90ΔΔΔΔΔ
v»h§blackΔ§0.5Δ§rleftΔ§90
d xatTasman SeaΔ2140704Δ5762737Δ0.50Δ90ΔblackΔ
t§Alpine FaultΔ§2300803Δ§5757050Δ§0.50Δ§55Δ§blackΔ
t§Paringa SectionΔ§2196150Δ§5711555Δ§0.25Δ§57Δ§blackΔ
t§Jackson Head SectionΔ§2130278Δ§5679804Δ§0.25Δ§72Δ§blackΔ
t§Jackson CanyonΔ§2132647Δ§5693546Δ§0.25Δ§73Δ§blueΔ
t§Haast CanyonΔ§2163347Δ§5711133Δ§0.25Δ§90Δ§blueΔ
t§Moeraki CanyonΔ§2169138Δ§5736198Δ§0.25Δ§120Δ§blueΔ
```

```
t§Cook CanyonΔ§2210367Δ§5767950Δ§0.25Δ§103Δ§blueΔ
t§Hokitika CanyonΔ§2270553Δ§5858939Δ§0.25Δ§106Δ§blueΔ
t§HaastΔ§2194729Δ§5694969Δ§0.25Δ§90Δ§blackΔ
t§Franz JosefΔ§2281453Δ§5749046Δ§0.25Δ§90Δ§blackΔ
t§HokitikaΔ§2325526Δ§5829084Δ§0.25Δ§90Δ§blackΔ
xsb xx
```

The following runlog, *map.rlg*, was used to generate the structure contour map in Figure 4.14 using POSTER. The numerous `.pol` files were generated from the polygon option in GRIDCONT and edited in POLYEDIT to conform with the outline of the study area. Other outlines and picture files were produced as standard with minor alterations as needed. The other isopach diagrams displayed in this study used runlogs with a similar format.

```
oucxdoc:\tbase\wcoast\swlandta\swland
 xgmbasement.met
sΔΔΔ2ΔΔΔΔΔΔΔ
xss1000000Δ1000000Δ
r2100000Δ2350000Δ1Δ5650000Δ5875000Δ1
xf..\general\sislfill.polΔC9ΔblankΔyΔsolidΔΔΔ
Δf§..\general\gridbord.polΔ§C15Δ§blankΔ§yΔ§solidΔΔΔ
 f§base3500.polΔ§C14Δ§blankΔ§yΔ§solidΔΔΔ
 f§base3000.polΔ§C13Δ§blankΔ§yΔ§solidΔΔΔ
 f§base2500.polΔ§C12Δ§blankΔ§yΔ§solidΔΔΔ
 f§base2000.polΔ§C11Δ§blankΔ§yΔ§solidΔΔΔ
 f§..\general\swdzfill.polΔ§greenΔ§blankΔ§yΔ§solidΔΔΔ
 f§basegrid.polΔ§blackΔ§solidΔ§yΔ§hollowΔΔΔ
 f§..\general\wcoastl.polΔ§blueΔ§wideΔ§yΔ§hollowΔ§Δ§Δ
 f§..\general\afault.polΔ§redΔ§wideΔ§yΔ§hollowΔΔΔ
 f§..\general\ffault.polΔ§redΔΔwide§yΔ§hollowΔ§1.00ΔΔ
 f§..\general\swdz.polΔ§redΔ§wideΔ§yΔ§hollowΔΔΔ
 aupbasedep.picΔ2290000Δ5650000Δ1Δ90ΔΔ
p§..\general\scale.picΔ§2230000Δ§5650000Δ§1Δ§90ΔΔ
p§..\general\north.picΔ§2147900Δ§5825300Δ§3Δ§87ΔΔ
p§..\general\monogram.picΔ§2100000Δ§5650000Δ§0.5Δ§90ΔΔ
xgsΔΔΔ3ΔΔΔΔΔΔΔ
xda§loc_idΔ§=Δ§4
xpf§loc_eastΔ§loc_northΔloc_name1
m§2Δ§blackΔ§0.5ΔΔ§87ΔΔΔΔΔ
vblackΔ0.00ΔrightΔ87
d
xsb xx
```

C.3 TECHBASE Picture files

During the compilation of metafiles or graphics displaying various aspects of the study area (e.g. geological base map, basement structure contours etc.) some annotations, such as scales, compass directions are used repeatedly. These images are generated using picture files, which are listed below.

Depth.pic produces an image of the bathymetric depth scale seen in Figure 1.4.

```
# bathymetric scale
U cm
S blank 3
C C0
A 4    -0.80 -0.20
       1.80 -0.20
       1.80 5.40
       -0.80 5.40
C C15
A 3    0.00 0.00
       0.50 1.00
       0.00 1.00
C C14
A 4    0.00 1.00
       0.50 1.00
       0.50 2.00
       0.00 2.00
C C13
A 4 0.00 2.00
       0.50 2.00
       0.50 3.00
       0.00 3.00
C C12
A 4    0.00 3.00
       0.50 3.00
       0.50 4.00
       0.00 4.00
C C11
A 4    0.00 4.00
       0.50 4.00
       0.50 4.50
       0.00 4.50
C C10
A 4    0.00 4.50
       0.50 4.50
       0.50 5.00
       0.00 5.00
S solid 1
C black
P 4    0.00 0.00
       0.50 1.00
       0.00 1.00
       0.00 0.00
R 0.00 1.00 0.50 2.00
R 0.00 2.00 0.50 3.00
R 0.00 3.00 0.50 4.00
R 0.00 4.00 0.50 4.50
R 0.00 4.50 0.50 5.00
F 3 1
T 0.60 0.90 0.25 90
2000
T 0.60 1.90 0.25 90
1500
T 0.60 2.90 0.25 90
1000
T 0.60 3.90 0.25 90
500
T 0.60 4.40 0.25 90
250
T 0.60 4.90 0.25 90
0
T -0.30 1.00 0.25 0
Depth in metres
S solid 1
C black
R -0.80 -0.20 1.80 5.40
```

Scale.pic produces the key and title of the plot. Amendments to each metafile may be made as required.

```
#scale bar for basemap
U cm
C BACKGR
S solid 3
A 4 0.00 0.00
       6.00 0.00
       6.00 3.00
       0.00 3.00
C black
S solid
R 0.00 0.00 6.00 3.00
S solid 3
A 4 0.50 1.00
       1.50 1.00
       1.50 1.20
       0.50 1.20
A 4 2.50 1.00
       3.50 1.00
       3.50 1.20
       2.50 1.20
A 4 4.50 1.00
       5.50 1.00
       5.50 1.20
       4.50 1.20
S solid 1
R 0.50 1.00 5.50 1.20
L 1.50 1.10 2.50 1.10
L 3.50 1.10 4.50 1.10
S wide 1
L 0.50 1.00 0.50 1.50
L 5.50 1.00 5.50 1.50
F 3 c
T 0.50 1.60 0.25
0
T 5.50 1.60 0.25
50
T 3.00 1.60 0.20
kilometres
```

C.4 TBCALC files

The calculation steps used in a TBCALC program or runlog can often be better implemented as a separate file called from the TBCALC program as *(f, filename)* as required.

These TBCALC files are listed below. Calculation equations are in Reverse Polish Notation.

---

density.clc calculates the average density of the sediments in a cell. The density is used to help calculate tectonic subsidence.

```
seqa_skel_q seqb_skel_q + seqc_skel_q + seqd_skel_q + seqe_skel_q +
☞ = temp1
total_thick sea_floor_q + = temp2
temp2 temp1 - = temp3
temp1 2.70 * = temp4
temp3 temp4 + temp2 / = density_0

seqb_skel_q seqc_skel_q + seqd_skel_q + seqe_skel_q + = temp1
basement_dep_1 paleodepth_1 + = temp2
temp2 temp1 - = temp3
temp1 2.70 * = temp4
temp3 temp4 + temp2 / = density_1

seqc_skel_q seqd_skel_q + seqe_skel_q + = temp1
basement_dep_2 paleodepth_2 + = temp2
temp2 temp1 - = temp3
temp1 2.70 * = temp4
temp3 temp4 + temp2 / = density_2

seqd_skel_q seqe_skel_q + = temp1
basement_dep_3 paleodepth_3 + = temp2
temp2 temp1 - = temp3
temp1 2.70 * = temp4
temp3 temp4 + temp2 / = density_3

seqe_skel_q = temp1
basement_dep_4 paleodepth_4 + = temp2
temp2 temp1 - = temp3
temp1 2.70 * = temp4
temp3 temp4 + temp2 / = density_4
```

---

tectonic.clc calculates the tectonic subsidence of a cell at each backstripped stage through the sediment column (i.e. as if each horizon was individually back at the surface).

```
3.30      density_0          -         =         temp1
3.30      1.00       -       =         temp2
temp1     temp2      /       =         temp3
basement_q           sea_floor_q       +         =         temp4
temp4     temp3      *       =         temp5
temp4     temp5      -       =         tectonic_sub_0

3.30      density_1          -         =         temp1
3.30      1.00       -       =         temp2
temp1     temp2      /       =         temp3
basement_dep_1       paleodepth_1      +         =         temp
temp4     temp3      *       =         temp5
temp4     temp5      -       =         tectonic_sub_1
```

```
3.30      density_2          -        =        temp1
3.30      1.00       -       =        temp2
temp1     temp2      /       =        temp3
basement_dep_2       paleodepth_2     +        =        temp4
temp4     temp3      *       =        temp5
temp4     temp5      -       =        tectonic_sub_2

3.30      density_3          -        =        temp1
3.30      1.00       -       =        temp2
temp1     temp2      /       =        temp3
basement_dep_3       paleodepth_3     +        =        temp4
temp4     temp3      *       =        temp5
temp4     temp5      -       =        tectonic_sub_3

3.30      density_4          -        =        temp1
3.30      1.00       -       =        temp2
temp1     temp2      /       =        temp3
basement_dep_4       paleodepth_4     +        =        temp4
temp4     temp3      *       =        temp5
temp4     temp5      -       =        tectonic_sub_4
```

---

skelcalc.clc calculates the skeletal thickness of a sequence at a given point along a seismic line. Used in *procdat.tsk* task file.

```
#
# calculate skeletal thickness of sequence a
#
1      seqa_pphi    /      = temp1
1      seqa_kk      /      = temp2
ppa_dep      1000   /      = temp6
seafloor_dep 1000   /      = temp7
seqa_thick   1000   /      = temp8
seqa_kk temp6       *      temp1 +      = temp3
seqa_kk temp7       *      temp1 +      = temp4
temp3 temp4 /       ln     temp2 *      = temp5
temp8 temp5 -       1000   *            = seqa_skel
#
# calculate skeletal thickness of sequence b
#
1      seqb_pphi    /      = temp1
1      seqb_kk      /      = temp2
ppb_dep      1000   /      = temp6
ppa_dep      1000   /      = temp7
seqb_thick   1000   /      = temp8
seqb_kk temp6       *      temp1 +      = temp3
seqb_kk temp7       *      temp1 +      = temp4
temp3 temp4 /       ln     temp2 *      = temp5
temp8 temp5 -       1000   *            = seqb_skel
#
# calculate skeletal thickness of sequence c
#
1      seqc_pphi    /      = temp1
1      seqc_kk      /      = temp2
topmio_dep   1000   /      = temp6
ppb_dep      1000   /      = temp7
seqc_thick   1000   /      = temp8
seqc_kk temp6       *      temp1 +      = temp3
seqc_kk temp7       *      temp1 +      = temp4
temp3 temp4 /       ln     temp2 *      = temp5
temp8 temp5 -       1000   *            = seqc_skel
```

```
#
# calculate skeletal thickness of sequence d
#
1      seqd_pphi    /      = temp1
1      seqd_kk      /      = temp2
baseoligo_dep 1000        /      = temp6
topmio_dep  1000  /      = temp7
seqd_thick  1000  /      = temp8
seqd_kk temp6      *      temp1 +      = temp3
seqd_kk temp7      *      temp1 +      = temp4
temp3 temp4 /      ln     temp2 *      = temp5
temp8 temp5 -      1000   *            = seqd_skel
#
# calculate skeletal thickness of sequence e
#
1      seqe_pphi    /      = temp1
1      seqe_kk      /      = temp2
basement_dep 1000 /      = temp6
baseoligo_dep 1000        /      = temp7
seqe_thick  1000  /      = temp8
seqe_kk temp6      *      temp1 +      = temp3
seqe_kk temp7      *      temp1 +      = temp4
temp3 temp4 /      ln     temp2 *      = temp5
temp8 temp5 -      1000   *            = seqe_skel
```

C.5: Q-BASIC programs

Not all processing of the seismic data can be easily done within the TECHBASE system. A number of small Q-BASIC[1] programs were created to undertake various 'number-crunching' routines that were difficult to implement in TECHBASE. For further information about the Q-BASIC progamming language, refer to the appropriate manuals and on-line help files.

Three Q-BASIC programs used during various aspects of the processing are listed here:

REG.BAS: regularises 'raw' digitised seismic data into data points at regular intervals

RECON.BAS: takes data from a section and proceeds to backstrip and decompact at regular intervals along the section, therefore undertaking a very simple palinspastic reconstruction of the section.

RECONQ.BAS: similar to above, but works across the entire study area array.

```
'
'     REG.BAS
'     for Geohistory Analysis package
'     for regularising an interpreted section
'
'$DYNAMIC

DECLARE SUB Datain ()
DECLARE SUB Standard ()

COMMON SHARED section$  'section id from TECHBASE
COMMON SHARED filename$ 'filename of report file from TECHBASE
COMMON SHARED detfile$  'filename of details file from TECHBASE
COMMON SHARED regfile$  'filename of regularised input for section
COMMON SHARED numline   'number of lines in report file
COMMON SHARED horzcount 'number of horizons in section
COMMON SHARED lloc      'left value of location in report file
COMMON SHARED rloc      'right value of location in report file
COMMON SHARED ltor      'digitizing from left to right = 1
COMMON SHARED spinterval      'distance os shotpoint intervals (m)

DIM SHARED inlocation(1)      'array for location values read in
☞ from report file
DIM SHARED location(10, 250)  'array for location values sorted by
☞ horizons
DIM SHARED indepth(1)   'array for depth values read in from report
☞ file
DIM SHARED depth(10, 250)     'array for depth values sorted by
☞ horizons
DIM SHARED horizonname$(1) 'array for horizon names from report file
DIM SHARED horizonid(1)
DIM SHARED horzname$(20)      'array for horizon names
DIM SHARED horzbreaks(40)     'array for location of horizon changes
☞ within report file
DIM SHARED horzlen(20)  'array for length of horizon data in report
```

[1] Q-BASIC (Quick-Beginners All-purpose Symbolic Instruction Code) is © Microsoft Corporation 1987–1991. It is a general purpose computer language, implemented with a simple compiler in as 'standard' within some installed operating systems.

```
☞file
DIM SHARED seqvel(20)    'array for sequence velocity information
DIM SHARED seqkk(20)     'array for sequence k-value info
DIM SHARED seqpphi(20)   'array for sequence phi-value info
DIM SHARED condepth(horzcount, 1)
DIM SHARED conloc(1)
DIM SHARED hstartloc(20)
DIM SHARED hstartdep(20)
DIM SHARED hendloc(20)
DIM SHARED henddep(20)

Begin:
      CLS

Getsectionid:

      OPEN "message.tmp" FOR INPUT AS #1
      INPUT #1, section$
      CLOSE #1

Getnumberoflines:
      filename$ = section$ + ".rep"
      OPEN filename$ FOR INPUT AS #2

      numline = 0
      DO
      LINE INPUT #2, line$
      numline = numline + 1
      LOOP UNTIL EOF(2)
      CLOSE #2

' redimension arrays
      REDIM SHARED inlocation(numline + 1)
      REDIM SHARED indepth(numline + 1)
      REDIM SHARED horizonname$(numline + 1)
      REDIM SHARED horizonid(numline + 1)

      CALL Datain

      CALL Standard

      SYSTEM

REM $STATIC
SUB Datain

'     Subroutine for inputing and checking datafile from TECHBASE

PRINT "Inputting data from file "; filename$
VIEW PRINT 3 TO 3

OPEN filename$ FOR INPUT AS #2
linept = 0
DO
      linept = linept + 1

      INPUT #2, inlocation(linept), indepth(linept), dummy$,
horizonname$(linept)

      PRINT "●";

LOOP UNTIL (EOF(2))
```

```
CLOSE #2
PRINT ""

'-------------------------------------------------------------------
'
detfile$ = section$ + ".det"

OPEN detfile$ FOR INPUT AS #3
      INPUT #3, dummy$, lloc, rloc
CLOSE #3


'-------------------------------------------------------------------
'     Check for direction of data
'
IF lloc < rloc THEN ltor = 1 ELSE ltor = 0

'-------------------------------------------------------------------
'     Look for number of "main" horizons
'
horzcount = 0
hb = 1
FOR iloop = 1 TO numline
      oldid$ = id$
      id$ = horizonname$(iloop)
      IF id$ <> oldid$ THEN
      horzcount = horzcount + 1
      horzname$(horzcount) = id$
      horzbreaks(hb) = iloop
      hb = hb + 1
      END IF
      horizonid(iloop) = horzcount
NEXT iloop
horzbreaks(hb) = numline + 1

'-------------------------------------------------------------------
'     Separate individual horizons into arrays
'
arraycount = 1
horzcount = 0

FOR iloop = 1 TO numline
      depth(horizonid(iloop), arraycount) = indepth(iloop)
      location(horizonid(iloop), arraycount) = inlocation(iloop)
      arraycount = arraycount + 1
      IF (horizonname$(iloop + 1) <> horizonname$(iloop)) THEN
      horzcount = horzcount + 1
      horzlen(horzcount) = arraycount - 1
      arraycount = 1
      END IF
NEXT iloop

'-------------------------------------------------------------------
END SUB

SUB Standard

' subroutine for standardising input from TECHBASE report file into
' regular intervals for further processing

IF ltor = 1 THEN interval = 1 ELSE interval = -1

regfile$ = section$ + ".reg"
```

```
VIEW PRINT 2 TO 3
CLS
PRINT "Standardising input into regular intervals."
VIEW PRINT 3 TO 3
OPEN regfile$ FOR OUTPUT AS #6

FOR iloop = lloc TO rloc STEP interval
      dist = ABS(lloc - rloc)
      PRINT #6, section$; iloop;

      FOR hloop = 1 TO horzcount

      ' find end and start of horizon
      hstart = location(hloop, 1)
      hend = location(hloop, horzlen(hloop))

      'if iloop before start of horizon
      '     if horizon first part
      '     extrapolate before horizon
      '     print depth
      SELECT CASE ltor
      CASE IS = 1
      IF iloop < hstart THEN
      slope = (depth(hloop, 2) - depth(hloop, 1)) / (location(hloop,
☞2) - location(hloop, 1))
      PRINT #6, ABS(CINT((depth(hloop, 1) -
☞  (slope * (location(hloop, 1) - iloop))) * 1000) / 1000);
      END IF

      CASE IS = 0
      IF iloop > hstart THEN
      slope = (depth(hloop, 2) -
☞  depth(hloop, 1)) / (location(hloop, 2) - location(hloop, 1))
      PRINT #6, ABS(CINT((depth(hloop, 1) -
☞  (slope * (location(hloop, 1) - iloop))) * 1000) / 1000);
      END IF

      END SELECT

      'if iloop after the end of horizon
      '     if horizon last part [sloop = numsubhorz(hloop)]
      '     extrapolate after horizon
      '     print depth
      SELECT CASE ltor
      CASE IS = 1
      IF iloop > hend THEN
      lastdepth = depth(hloop, horzlen(hloop))
      penudepth = depth(hloop, horzlen(hloop) - 1)
      lastloc = location(hloop, horzlen(hloop))
      penuloc = location(hloop, horzlen(hloop) - 1)
      slope = (lastdepth - penudepth) / (lastloc - penuloc)
      PRINT #6, ABS(CINT((lastdepth + (slope * (iloop - lastloc))) *
☞1000) / 1000);
      END IF

      CASE IS = 0
      IF iloop < hend THEN
      lastdepth = depth(hloop, horzlen(hloop))
      penudepth = depth(hloop, horzlen(hloop) - 1)
      lastloc = location(hloop, horzlen(hloop))
      penuloc = location(hloop, horzlen(hloop) - 1)
      slope = (lastdepth - penudepth) / (lastloc - penuloc)
      PRINT #6, ABS(CINT((lastdepth + (slope * (iloop - lastloc))) *
```

```
☞1000) / 1000);
        END IF

        END SELECT


        'if iloop after start and before end of horizon
        '     find points either side of iloop
        '     interpolate between two points
        '     print depth

        IF ((iloop >= hstart) AND (iloop <= hend)) OR
☞((iloop <= hstart) AND (iloop >= hend)) THEN
        icount = 0
        DO
        icount = icount + 1
        LOOP UNTIL ((iloop >= location(hloop, icount)) AND
☞  (iloop < location(hloop, icount + 1))) OR
☞  ((iloop <= location(hloop, icount)) AND (iloop > location(hloop,
  icount + 1)))
        slope = (depth(hloop, icount) - depth(hloop, icount + 1)) /
☞(location(hloop, icount) - location(hloop, icount + 1))
        PRINT #6, ABS(CINT((depth(hloop, icount) - (slope *
☞(location(hloop, icount) - iloop))) * 1000) / 1000);
        END IF

        NEXT hloop

        PRINT #6, ""
        IF CINT(((ABS(lloc - iloop) / dist) * 80)) > oldpt THEN
        PRINT TAB(CINT(((ABS(lloc - iloop) / dist) * 80))); "●";
        oldpt = CINT(((ABS(lloc - iloop) / dist) * 80))
        END IF

  NEXT iloop

  PRINT ""

  CLOSE #6
  END SUB
```

```
  '
  '     RECON.BAS
  '     program for inputting a report file from TECHBASE and
  '     decompacting sediment thicknesses of a section.
  '

  DECLARE FUNCTION ZFUNC! (z#, p#, k#)
  DECLARE FUNCTION COMPFAC (zsk#, ztop#, phi#, k#)
  DECLARE FUNCTION PALEOSEA! (age#)

  CONST reportfile$ = "recon.rep"
  CONST paleofile$ = "paleo.rep"
  CONST procfile$ = "recon.prc"

  TYPE Sequenceinfo
        skel AS DOUBLE
        pphi AS DOUBLE
        kk AS DOUBLE
  END TYPE

  TYPE Pdepth
```

```
      left  AS DOUBLE
      right AS DOUBLE
END TYPE

DIM SHARED sequence(1 TO 5) AS Sequenceinfo
DIM SHARED paleodepth(1 TO 4) AS Pdepth
DIM SHARED depths#(1 TO 6)
DIM SHARED pseal#(154)

' ***** set up paleo sea level array *****
DATA 0., 13., 26., 36., 40., 46., 45., 34., 30., 36., 46., 61., 74.
DATA 75., 71., 66., 53., 42., 35., 31., 29., 28., 33., 35., 46.
DATA 55., 56., 57., 63., 70., 77., 87., 90., 88., 86., 86., 95.
DATA 102., 107., 113., 106., 99., 98., 99., 100., 103., 99., 89.
DATA 81., 77., 88., 103., 112., 118., 113., 109., 112., 119., 133.
DATA 147., 149., 144., 136., 134., 128., 134., 138., 145., 144.
DATA 146., 141., 141., 148., 157., 163., 163., 164., 158., 151.
DATA 140., 140., 141., 146., 154., 164., 167., 167., 161.
DATA 154., 150., 148., 146., 145.,143., 142., 134., 128., 126.
DATA 127., 127., 122., 127., 121., 120., 120., 115., 109., 113.
DATA 110., 115., 117., 118., 118., 112., 112., 113., 118., 125.
DATA 131., 133., 133., 136., 131., 127., 128., 119., 120., 113.
DATA 104., 101., 94., 87., 92., 94., 88., 88., 78., 72., 59., 57.
DATA 56., 62., 67., 80., 83., 92., 103., 109., 112., 115., 112.
DATA 100., 93., 91.

'FOR iloop% = 0 TO 154
'     READ pseal#(iloop%)
'NEXT iloop%

CLS
PRINT "Reconstruction and decompaction program"
VIEW PRINT 2 TO 2

' open report file to count number of lines
OPEN reportfile$ FOR INPUT AS #1
numline = 0
DO
      LINE INPUT #1, dummy$
      numline = numline + 1
LOOP UNTIL EOF(1)
CLOSE #1

'OPEN "message.tmp" FOR INPUT AS #4
'     INPUT #4, section$
'CLOSE #4

OPEN paleofile$ FOR INPUT AS #5
      INPUT #5, section$
      FOR ploop = 1 TO 4
      INPUT #5, paleodepth(ploop).left, paleodepth(ploop).right
      NEXT ploop
CLOSE #5

OPEN reportfile$ FOR INPUT AS #1
OPEN procfile$ FOR OUTPUT AS #2
FOR iloop = 1 TO numline
      PRINT "";
      INPUT #1, length#
      FOR dloop = 1 TO 6
      INPUT #1, depths#(dloop)
      depths#(dloop) = ABS(depths#(dloop) / 1000)
      NEXT dloop
```

```
        depths#(1) = 0
        FOR sloop = 1 TO 5
        INPUT #1, sequence(sloop).skel, sequence(sloop).pphi,
☞ sequence(sloop).kk
        sequence(sloop).skel = sequence(sloop).skel / 1000
        NEXT sloop

        PRINT #2, section$, length#;
        FOR stage = 1 TO 4
        PRINT ".";
        plodepth = ((paleodepth(stage).left -
☞ paleodepth(stage).right) / numline) * iloop
        plodepth = paleodepth(stage).left - plodepth
        PRINT #2, plodepth;      ' work out paleodepth and eustatic
☞ correction
        FOR depalt = (stage + 1) TO 6
        depths#(depalt) = depths#(depalt) - depths#(stage + 1)
        NEXT depalt
        FOR unit = (stage + 1) TO 5
        decompac = COMPFAC(sequence(unit).skel, depths#(unit),
☞ sequence(unit).pphi, sequence(unit).kk)
        PRINT #2, (decompac * 1000) + plodepth;
        depths#(unit + 1) = decompac
        NEXT unit
        NEXT stage
        PRINT #2, ""

  NEXT iloop
  CLOSE #2
  CLOSE #1

  SYSTEM

  FUNCTION COMPFAC (zsk#, ztop#, phi#, k#)

  errmax# = .0001

  zset# = zsk# + ZFUNC(ztop#, phi#, k#)
  zbot# = ztop# + ABS(zsk#)

  DO WHILE (ABS(zbot# - oldzbot#) > errmax#)

        oldzbot# = zbot#
        IF k# = 0 THEN
        zbot# = zset#
        ELSE
        zbot# = ((1 / k#) * LOG((1 / phi#) + (k# * oldzbot#))) + zset#
        END IF

  LOOP

  COMPFAC = zbot#

  END FUNCTION

  FUNCTION PALEOSEA (age#)

        agep# = age# * 10
        IF (ABS(agep#) < .1) THEN
        PALEOSEA = 0
        ELSE
        i% = 2
        DO WHILE ((agep# > i%) AND (i% < 153))
```

```
        i% = i% + 1
        LOOP
        IF (agep# = i% - 1) THEN
        ' agep = exact value in sea level array
        PALEOSEA = pseal#(i% - 1) / 1000
        ELSE
        IF (agep# > 153) THEN    ' agep > than maximum array value
        PALEOSEA = pseal#(154) / 1000
        ELSE  ' interpolate agep from levels on either side
        slope# = pseal#(i%) - pseal#(i% - 1)
        PALEOSEA = (pseal#(i% - 1)
☞+ (slope# * (agep# - (i% - 1)))) / 1000
        END IF
        END IF
        END IF


END FUNCTION

FUNCTION ZFUNC (z#, p#, k#)

        IF (k# <> 0) THEN
        ZFUNC = z# - (LOG((1 / p#) + (k# * z#)) / k#)
        ELSE
        ZFUNC = z#
        END IF

END FUNCTION
```

```
'
'       RECONQ.BAS
'       program for inputting a report file from TECHBASE and
'       decompacting sediment thicknesses across the study area
'       array.
'

DECLARE FUNCTION ZFUNC! (z#, p#, k#)
DECLARE FUNCTION COMPFAC (zsk#, ztop#, phi#, k#)
DECLARE FUNCTION PALEOSEA! (age#)

CONST reportfile$ = "reconq.rpt"
CONST procfile$ = "reconq.prc"

TYPE Sequenceinfo
        skel AS DOUBLE
        pphi AS DOUBLE
        kk AS DOUBLE
        pdepth AS DOUBLE
END TYPE

DIM SHARED sequence(1 TO 5) AS Sequenceinfo
DIM SHARED depths#(1 TO 6)
DIM SHARED pseal#(154)

' ***** set up paleo sea level array *****
DATA 0., 13., 26., 36., 40., 46., 45., 34., 30., 36., 46., 61., 74.
DATA 75., 71., 66., 53., 42., 35., 31., 29., 28., 33., 35., 46.
DATA 55., 56., 57., 63., 70., 77., 87., 90., 88., 86., 86., 95.
DATA 102., 107., 113., 106., 99., 98., 99., 100., 103., 99., 89.
DATA 81., 77., 88., 103., 112., 118., 113., 109., 112., 119., 133.
DATA 147., 149., 144., 136., 134., 128., 134., 138., 145., 144.
DATA 146., 141., 141., 148., 157., 163., 163., 164., 158., 151.
```

```
DATA 140., 140., 141., 146., 154., 164., 167., 167., 161.
DATA 154., 150., 148., 146., 145.,143., 142., 134., 128., 126.
DATA 127., 127., 122., 127., 121., 120., 120., 115., 109., 113.
DATA 110., 115., 117., 118., 118., 112., 112., 113., 118., 125.
DATA 131., 133., 133., 136., 131., 127., 128., 119., 120., 113.
DATA 104., 101., 94., 87., 92., 94., 88., 88., 78., 72., 59., 57.
DATA 56., 62., 67., 80., 83., 92., 103., 109., 112., 115., 112.
DATA 100., 93., 91.

'FOR iloop% = 0 TO 154
'     READ pseal#(iloop%)
'NEXT iloop%

CLS
PRINT "Reconstruction and decompaction program"
VIEW PRINT 2 TO 2

' open report file to count number of lines
OPEN reportfile$ FOR INPUT AS #1
numline = 0
DO
      LINE INPUT #1, dummy$
      numline = numline + 1
LOOP UNTIL EOF(1)
CLOSE #1

'OPEN "message.tmp" FOR INPUT AS #4
'     INPUT #4, section$
'CLOSE #4

OPEN reportfile$ FOR INPUT AS #1
OPEN procfile$ FOR OUTPUT AS #2
FOR iloop = 1 TO numline
      PRINT "";
      FOR dloop = 1 TO 6
      INPUT #1, depths#(dloop)
      depths#(dloop) = ABS(depths#(dloop) / 1000)
      NEXT dloop
      depths#(1) = 0
      FOR sloop = 1 TO 5
      INPUT #1, sequence(sloop).skel, sequence(sloop).pphi,
☞ sequence(sloop).kk, sequence(sloop).pdepth
      sequence(sloop).skel = sequence(sloop).skel / 1000
      NEXT sloop

      PRINT #2, section$, length#;
      FOR stage = 1 TO 4
      PRINT ".";
      FOR depalt = (stage + 1) TO 6
      depths#(depalt) = depths#(depalt) - depths#(stage + 1)
      NEXT depalt
      FOR unit = (stage + 1) TO 5
      decompac = COMPFAC(sequence(unit).skel, depths#(unit),
☞ sequence(unit).pphi, sequence(unit).kk)
      PRINT #2, USING "######."; (decompac * 1000) +
☞ sequence(unit).pdepth;
      depths#(unit + 1) = decompac
      NEXT unit
      NEXT stage
      PRINT #2, ""

NEXT iloop
CLOSE #2
```

```
CLOSE #1

SYSTEM

FUNCTION COMPFAC (zsk#, ztop#, phi#, k#)

errmax# = .0001

zset# = zsk# + ZFUNC(ztop#, phi#, k#)
zbot# = ztop# + ABS(zsk#)

DO WHILE (ABS(zbot# - oldzbot#) > errmax#)

      oldzbot# = zbot#
      IF k# = 0 THEN
      zbot# = zset#
      ELSE
      zbot# = ((1 / k#) * LOG((1 / phi#) + (k# * oldzbot#))) + zset#
      END IF

LOOP

COMPFAC = zbot#

END FUNCTION

FUNCTION PALEOSEA (age#)

      agep# = age# * 10
      IF (ABS(agep#) < .1) THEN
      PALEOSEA = 0
      ELSE
      i% = 2
      DO WHILE ((agep# > i%) AND (i% < 153))
      i% = i% + 1
      LOOP
      IF (agep# = i% - 1) THEN
      'agep = exact value in sea level array
      PALEOSEA = pseal#(i% - 1) / 1000
      ELSE
      IF (agep# > 153) THEN    ' agep > than maximum array value
      PALEOSEA = pseal#(154) / 1000
      ELSE  ' interpolate agep from levels on either side
      slope# = pseal#(i%) - pseal#(i% - 1)
      PALEOSEA = (pseal#(i% - 1) +
☞ (slope# * (agep# - (i% - 1)))) / 1000
      END IF
      END IF
      END IF


END FUNCTION

FUNCTION ZFUNC (z#, p#, k#)

      IF (k# <> 0) THEN
      ZFUNC = z# - (LOG((1 / p#) + (k# * z#)) / k#)
      ELSE
      ZFUNC = z#
      END IF

END FUNCTION
```

Appendix D: Pascal source code listing for GeoHist+

The program GeoHist+ was adapted from GEO_HIST, a geohistory program for the VAX/VMS system programmed by Wood (1989).

GeoHist+ was programmed on a Macintosh™[1] Plus computer using *Lightspeed Pascal*™[2] for the Macintosh™. For further information about Pascal and the Macintosh programming environment the reader is directed towards:

Lightspeed Pascal: User's Guide and Reference Manual, THINK Technologies, Inc., 1986.

The program is subdivided into 8 units, in association with 'standard' libraries. These units are built together in order such that procedures and functions in each unit can be called by units below it. The units and their build order used in GeoHist+ is as follows:

- `Calculations`
- `DataParams`
- `DataHandlers`
- `Decompaction`
- `GraphicsHandlers`
- `ResultHandlers`
- `PlotDriver`
- `Geodcomp`

Longer descriptions of the routines in each unit is given below in the source code listings. GeoHist+ also makes extensive use of resources in the Macintosh environment for dialog, alert, text and graphic display windows. These are found in the file *GeoHist.Rsrc*, and can be 'viewed' and/or edited with a utility like *ResEdit*.

☞ = indicates that the line is continuous from the one immediately above.

---

[1] **Macintosh** is a trademark of McIntosh Laboratory, Inc. and used by Apple Computer, Inc.

[2] **Lightspeed Pascal** is a trademark of THINK Technologies, Inc.

```
{*****************************************************************************}
UNIT Calculations;

{This unit interfaces and implements the calculations required by the program for   }
{decompaction.                                                                      }
{  Programmer: Keith Sircombe                                                       }
{  Date: August 1992                                                                }
{  Number 2 in build order (after SANE and before DataParams)                       }

INTERFACE
   CONST
      maxlayr = 30;       {maximum number of layers permitted by program - nominal}
      maxlayr1 = 31;

   TYPE
      lithology = ( sandstone,
                    siltstone,
                    mudstone,
                    opshales,
                    limestone,
                    volcanics);

      lithdata = ARRAY[sandstone..volcanics] OF real;
      str = STRING;
      unitrec = RECORD
            layernum : integer;     {unit number}
            water : real;           {paleowater depth}
            age : real;             {age of *top* of unit, *base* of previous}
            top : real;             {depth of top of unit}
            base : real;            {depth of base of unit}
            z : real;               {thickness of unit}
            zsum : real;            {cumulative thickness of sequence }
            lith : lithdata;        {array to carry lithology data}
            zsk : real;             {skeletal thickness of unit}
            rate : real;            {sedimentation rate of unit}
            kk : real;              {compaction coeff. of unit}
            pphi : real;            {original porosity of unit}
            dens : real;            {bulk density of unit}
            unitname : str;         {name of unit}
            plotcurve : boolean;    {plot unit on plot}
         END;                       {end of unit record}

      resultsrec = RECORD
            tect : ARRAY[0..maxlayr] OF real;
                        {tectonic curve array}
            totalz : ARRAY[0..maxlayr] OF real;
                        {total thickness of sediments after decompaction}
            curve : ARRAY[0..maxlayr, 0..maxlayr] OF real;
                        { }
            p2 : ARRAY[0..maxlayr] OF real;
                        {bulk density of sedimentary. column}
            zsum : ARRAY[0..maxlayr] OF real;
                        {totalled thickness of sedimentary. column}
            zp : ARRAY[0..maxlayr, 0..maxlayr] OF real;
                        {}
            listz : ARRAY[0..maxlayr] OF real;
                        {array to write out data}
         END; {record}

      nztimescale = RECORD
            age : real;
            stage : char;
         END;

      column = ARRAY[0..maxlayr1] OF unitrec;
```

```
VAR
   k : ARRAY[sandstone..volcanics] OF real;
   phi : ARRAY[sandstone..volcanics] OF real;
   bulkdens : ARRAY[sandstone..volcanics] OF real;
   pseafile : text;                          {pointer to Paleosealevel.data file}
   paleosealevel : ARRAY[0..153] OF real;
                                  {data array of sea levels, from Haq et al.}
   nz : ARRAY[0..12] OF nztimescale;
   nlayr : integer;
   projectname : STRING;
   dataIn : boolean;
   AlertInt : integer;
   CallByEdit : boolean;

FUNCTION datestring (VAR dt : DateTimeRec) : STRING;
   {This function returns a string of the date record passed to it in the form of}
   { hh:mm dayname daynumber month year                                          }

PROCEDURE CalcSetup;
   {This procedure loads the k, phi & bulkdens arrays with constant values for   }
   {each lithology type                                                          }

FUNCTION Zfunc(  z : real;
                 p : real;
                 k : real) : real;
   {This function calculates a often recurring part of the decompaction equation }
   {given the input of z, p & k                                                  }

FUNCTION Skelthick (   z2    : real;
                       z1    : real;
                       k  : real;
                       phi   : real) : real;
   {This function calculates the skeletal thickness of a unit given:            }
   {  z2 - depth to base of unit                                                 }
   {  z1 - depth to top of unit                                                  }
   {  k  - compaction coefficient of unit                                        }
   {  phi - original porosity of unit                                            }

FUNCTION PaleoSea (age : real) : real;
   {This function returns the paleo sea level at a given age (in Myr)           }
   {taken from the long term Haq eustatic curve (Haq et al., 1987)              }

FUNCTION Compfac (  zsk   : real;
                    ztop  : real;
                    phi   : real;
                    k     : real) : real;
   {This function calculates the decompacted thickness of a unit                }
   {given:                                                                       }
   {  zsk - skeletal thickness of the unit                                       }
   {  ztop - depth to the top of the unit                                        }
   {  phi - original porosity of the unit                                        }
   {  k - compaction coefficient of the unit                                     }
```

```
IMPLEMENTATION

{*****************************************************************************}
   FUNCTION datestring;

      VAR
         dayname : STRING;
         monthname : STRING;
         minutestr : STRING;

   BEGIN

      WITH dt DO
         BEGIN

            CASE dayofweek OF
               1 :
                  dayname := 'Sunday';
               2 :
                  dayname := 'Monday';
               3 :
                  dayname := 'Tuesday';
               4 :
                  dayname := 'Wednesday';
               5 :
                  dayname := 'Thursday';
               6 :
                  dayname := 'Friday';
               7 :
                  dayname := 'Saturday';
            END;

            CASE month OF
               1 :
                  monthname := 'January';
               2 :
                  monthname := 'February';
               3 :
                  monthname := 'March';
               4 :
                  monthname := 'April';
               5 :
                  monthname := 'May';
               6 :
                  monthname := 'June';
               7 :
                  monthname := 'July';
               8 :
                  monthname := 'August';
               9 :
                  monthname := 'September';
               10 :
                  monthname := 'October';
               11 :
                  monthname := 'November';
               12 :
                  monthname := 'December';
            END;

            IF minute < 10 THEN
               minutestr := StringOf('0', minute : 1)
            ELSE
               minutestr := StringOf(minute : 2);

            datestring := StringOf(dt.hour : 2, ':', minutestr : 2, ', ', dayname,
```

```
☞ ', ', dt.day : 2, ' ', monthname, ', ', dt.year : 4, '.');

        END;{ with dt }

    END;
{*****************************************************************************}

{*****************************************************************************}
    PROCEDURE CalcSetup;
      VAR
        iloop : integer;
    BEGIN
      k[sandstone] := 1.2;            {Falvey & Deighton, 1982}
      phi[sandstone] := 0.4;          {Falvey & Deighton, 1982}
      bulkdens[sandstone] := 2.65;    {Sclater & Christie, 1980}

      k[siltstone] := 2.18;           {Falvey & Deighton, 1982}
      phi[siltstone] := 0.53;         {Falvey & Deighton, 1982}
      bulkdens[siltstone] := 2.72;    {?? same as ms from S&C, 1980}

      k[mudstone] := 2.43;            {Falvey & Deighton, 1982}
      phi[mudstone] := 0.70;          {Falvey & Deighton, 1982}
      bulkdens[mudstone] := 2.72;     {Sclater & Christie, 1980}

      k[opshales] := 1.15;            {Dickinson, 1953; Wood, 1990}
      phi[opshales] := 0.45;          {Dickinson, 1953; Wood, 1990}
      bulkdens[opshales] := 2.72;     {?? same as ms from S&C, 1980}

      k[limestone] := 1.3;            {Schmoker & Halley, 1982; Wood, 1990}
      phi[limestone] := 0.74;         {Schmoker & Halley, 1982; Wood, 1990}
      bulkdens[limestone] := 2.71;    {Schmoker & Halley, 1982}

      k[volcanics] := 0;              {Wood, 1990}
      phi[volcanics] := 0.1;          {Wood, 1990}
      bulkdens[volcanics] := 3.0;     {?? guess ??}

      reset(pseafile, 'Paleosealevel.data');
      FOR iloop := 0 TO 153 DO
        read(pseafile, pseal[iloop]);

      nz[0].age := 0.0;
      nz[1].age := 0.0;
      nz[1].stage := 'W'; {Wangauni}
      nz[2].age := 5.0;
      nz[2].stage := 'T'; {Taranaki}
      nz[3].age := 10.5;
      nz[3].stage := 'S'; {Southland}
      nz[4].age := 16.0;
      nz[4].stage := 'P'; {Pareora}
      nz[5].age := 22.0;
      nz[5].stage := 'L'; {Landon}
      nz[6].age := 36.5;
      nz[6].stage := 'A'; {Arnold}
      nz[7].age := 48.0;
      nz[7].stage := 'D'; {Dannevirke}
      nz[8].age := 66.5;
      nz[8].stage := 'M'; {Mata}
      nz[9].age := 85.0;
      nz[9].stage := 'R'; {Raukumara}
      nz[10].age := 95.0;
      nz[10].stage := 'C';   {Clarence}
      nz[11].age := 107.0;
      nz[11].stage := 'T';   {Taitai}
      nz[12].age := 136.0;
```

```
   END; {Setup}
{*****************************************************************************}

{*****************************************************************************}
   FUNCTION Zfunc;

      VAR
         zfn : real;

   BEGIN
      IF (k <> 0) THEN
         zfn := z - (ln((1 / p) + (k * z)) / k)
      ELSE
         zfn := z;

      Zfunc := zfn;

   END; {Function Zfunc}
{*****************************************************************************}

{*****************************************************************************}
   FUNCTION Skelthick;

      VAR
         za, zb : real;

   BEGIN
      IF ((z1 < 0) AND (k > 0.01)) THEN
         BEGIN                      {assume deposition of non-volcanics}
            za := 0;                {at or below sea level}
            zb := z2 - z1;
         END {if}
      ELSE                      {assume erosion at sea level}
         BEGIN
            IF (z2 < z1) THEN
               BEGIN
                  za := z1 - z2;
                  zb := 0;
               END {if}
            ELSE
               BEGIN
                  za := z1;
                  zb := z2;
               END {else}
         END; {else}

      Skelthick := Zfunc(zb, phi, k) - Zfunc(za, phi, k);

   END; {Function Skelthick}
{*****************************************************************************}
```

```
{*****************************************************************************}
   FUNCTION PaleoSea;

      VAR
         agep : real;          {exact value in sea level array }
         psl : real;           {paleosealevel variable}
         slope : real;         {slope variable for interpolation}
         iloop : integer;      {counter}

   BEGIN

      agep := age * 10;
      IF (ABS(agep) < 0.1) THEN
         psl := 0
      ELSE
         BEGIN
            iloop := 2;
            WHILE ((agep > iloop) AND (iloop < 153)) DO
               iloop := iloop + 1;
            IF (agep = iloop - 1) THEN
               psl := pseal[iloop - 1] / 1000
            ELSE
               BEGIN
                  IF (agep > 153) THEN   {agep > than maximum array value}
                     psl := pseal[153] / 1000
                  ELSE
                     BEGIN       {interpolate agep from levels on either side}
                        slope := 0;
                        slope := pseal[iloop] - pseal[iloop - 1];
                        psl := (pseal[iloop - 1] + (slope * (agep - (iloop - 1)))) /
☞ 1000;
                     END; {else}
               END; {else}
         END; {else}

      PaleoSea := psl;


   END; {Function PaleoSea}
{*****************************************************************************}

{*****************************************************************************}
   FUNCTION Compfac;
      CONST
         errmax = 0.0001; {iterative margin of error}
      VAR
         zset, zbot, oldzbot : real;
   BEGIN
      zset := zsk + Zfunc(ztop, phi, k);
      zbot := ztop + abs(zsk);
      oldzbot := ztop;
      WHILE (abs(zbot - oldzbot) > errmax) DO
         BEGIN
            oldzbot := zbot;
            IF k = 0 THEN
               zbot := zset
            ELSE
               zbot := ((1 / k) * ln((1 / phi) + (k * oldzbot))) + zset;
         END; {while}
      Compfac := zbot;
   END; {Function Compfac}
{*****************************************************************************}

END. {of unit Calculations}
{*****************************************************************************}
```

```
{*****************************************************************************}
UNIT DataParams;
   {This unit interfaces and implements the procedures that control the entry of    }
   {data into the program via the dialog windows                                    }
   {  Programmer: Keith Sircombe                                                    }
   {  Date: August 1992                                                             }
   {  Number 3 in build order (after Calculations and before DataHandlers)          }

INTERFACE
   USES
      SANE, Calculations;

   CONST
      ReturnKey = $0000240D;
      EnterKey = $00004C03;

   VAR
      numberlayers : integer;
      presentelevation : real;
      layer : unitrec;
      projname : STRING;

   FUNCTION EnterDataParams (  VAR numlayr : integer;
                               VAR preslevel : real) : boolean;
      {This function opens a dialog window to ask for the base parameters of the    }
      {data to be enetered manually.  It returns TRUE if completed with the number  }
      {of layers to be processed.                                                    }

   FUNCTION EnterUnitData (VAR layer : unitrec) : boolean;
      {This function opens dialog windows to enter stratigraphic and                }
      {lithostratigrahic data about each layer.  It returns TRUE if completed, along}
      {with the record of entred data.                                              }

IMPLEMENTATION

{*****************************************************************************}
   FUNCTION EnterDataParams;

      LABEL
         1799;

      CONST
         DataParamDLOG = 23904;
         NoDataALRT = 31866;
         nlayrBox = 3;

      VAR              {these variables are required by the dialog window management}
         dialogdone : boolean;
         dStorage : DialogRecord;
         dia : DialogPtr;
         theEvent : EventRecord;
         itemHit : integer;
         itemtype : integer;
         itemhandle : Handle;
         itemrect : rect;
         item3str, item5str, itemstr : Str255;
         item3int : integer;
         item5real : real;
         AlertInt : integer;

    BEGIN
      dia := GetNewDialog(DataParamDLOG, @dStorage, pointer(-1));
                                  {resource ID of Data Parameters Dialog Resource}
      REPEAT
         EnterDataParams := false;
```

```
      REPEAT
         ModalDialog(NIL, itemHit);
      UNTIL (itemHit = OK) OR (itemHit = 6);

      dialogdone := true;

      IF itemHit = OK THEN
         BEGIN
            GetDItem(dia, 3, itemtype, itemhandle, itemrect);{get and check item 3}
            item3str := '';   {define varaiable}
            GetIText(itemhandle, item3str);
            IF item3str = '' THEN  {check to see if string present }
               BEGIN
                  dialogdone := false;
                  AlertInt := StopAlert(NoDataALRT, NIL);
               END   { alert for no data entered }
            ELSE
               BEGIN
                  item3int := Num2Integer(Str2Num(item3str));  {convert to integer}
                  IF item3int < 2 THEN
                     BEGIN                    {too few layers!}
                        dialogdone := false;
                        AlertInt := StopAlert(NoDataALRT, NIL);
                     END;                     {alert for too few layers }
               END; {check on item3}

            GetDItem(dia, 5, itemtype, itemhandle, itemrect);{get and check item 5}
            item5str := '';                                  {define varaiable}
            GetIText(itemhandle, item5str);
            IF item5str = '' THEN               {check to see if string present}
               item5real := 0                      {assume default value of zero}
            ELSE
               item5real := Num2Real(Str2Num(item5str)); {convert to real }

            GetDItem(dia, 8, itemtype, itemhandle, itemrect);{get and check item 5}
            itemstr := '';    {define variable}
            projectname := '';
            GetIText(itemhandle, itemstr);
            projectname := itemstr;

            IF dialogdone THEN
               EnterDataParams := true;

         END {if itemHit = 1}
       ELSE
         GOTO 1799;  {cancel button pressed}

   UNTIL dialogdone;

   DisposDialog(dia);
   numlayr := item3int;
   numberlayers := item3int;
   preslevel := item5real;

1799 :
   END;

{*****************************************************************************}
```

```
{*****************************************************************************}
   FUNCTION EnterUnitData;

      CONST
         DataUnitDLOG = 12248;

         OK = 1;           {These are the 'id numbers' of resources in the data      }
         Cancel = 2;       {entry dialog window...                                   }
         Previous = 3;
         whichlayer = 3;
         Next = 4;
         NameofUnit = 5;
         Basedepth = 6;
         AgeofBase = 7;
         Paleodepth = 8;
         Plotcurve = 9;
         sstone = 10;
         zstone = 11;
         mstone = 12;
         opstone = 13;
         lstone = 14;
         vstone = 15;
         projname = 16;

      VAR      {These variables are mostly required by dialog window management}
         dialogdone : boolean;
         dStorage : DialogRecord;
         dia : DialogPtr;
         theEvent : EventRecord;
         itemHit : integer;
         layernumstr, nlayrstr, topdepthstr, prevagestr, editstr : str255;
         itemtype, itemint : integer;
         itemstr : Str255;
         itemreal, lithsum : real;
         itemrect : rect;
         itemhandle : Handle;
         AlertInt : integer;
         lloop : lithology;
         tempage : real;

      BEGIN
         layernumstr := StringOf(layer.layernum : 2);
         nlayrstr := StringOf(numberlayers : 2);
         topdepthstr := StringOf(layer.top : 5 : 1);
         prevagestr := StringOf(layer.age : 5 : 1);

         ParamText(layernumstr, nlayrstr, topdepthstr, prevagestr);
         dia := GetNewDialog(DataUnitDLOG, @dStorage, pointer(-1));
                                    {resource ID of Data Parameters Dialog Resource }
         GetDItem(dia, projname, itemtype, itemhandle, itemrect);
         SetIText(itemhandle, projectname);
         EnterUnitData := false;

         REPEAT
            dialogdone := false;
            REPEAT
               ModalDialog(NIL, itemHit);
            UNTIL (itemHit = OK) OR (itemHit = Cancel);

            dialogdone := true;

            IF itemHit = 1 THEN
               BEGIN
               {Get unitname: item 5}
                  GetDItem(dia, NameofUnit, itemtype, itemhandle, itemrect);
```

```
            itemstr := '';    {define varaiable}
            GetIText(itemhandle, itemstr);
            layer.unitname := '';
            layer.unitname := itemstr;

         {Get Depth of base : item 6}
            GetDItem(dia, Basedepth, itemtype, itemhandle, itemrect);
            itemstr := '';
            GetIText(itemhandle, itemstr);
            IF itemstr = '' THEN
               itemstr := '0';
            layer.base := Num2Real(Str2Num(itemstr));
            layer.z := layer.base - layer.top;

         {Get Paleodepth : item 8}
            GetDItem(dia, Paleodepth, itemtype, itemhandle, itemrect);
            itemstr := '';
            GetIText(itemhandle, itemstr);
            IF itemstr = '' THEN
               itemstr := '0';
            layer.water := Num2Real(Str2Num(itemstr));

         {Get Plot Curve : item 9}
            GetDItem(dia, Plotcurve, itemtype, itemhandle, itemrect);
            itemstr := '';
            GetIText(itemhandle, itemstr);
            IF itemstr = '' THEN
               itemstr := 'N';
            IF (itemstr = 'Y') OR (itemstr = 'y') THEN
               layer.plotcurve := true
            ELSE
               layer.plotcurve := false;

         { Get Age : item 7 }
            GetDItem(dia, AgeofBase, itemtype, itemhandle, itemrect);
            itemstr := '';
            GetIText(itemhandle, itemstr);
            IF itemstr = '' THEN
               itemstr := '0';
            itemreal := Num2Real(Str2Num(itemstr));
            IF itemreal <= layer.age THEN
               BEGIN
                  dialogdone := false;
                  AlertInt := StopAlert(31867, NIL); { Alert! age must decrease }
               END
            ELSE
               tempage := itemreal;

         { Checking Lithology % }
            lithsum := 0;
            FOR lloop := sandstone TO volcanics DO
               BEGIN
                  GetDItem(dia, ord(lloop) + sstone, itemtype, itemhandle,
☞ itemrect);
                  itemstr := '';
                  GetIText(itemhandle, itemstr);
                  IF itemstr = '' THEN
                     itemstr := '0';
                  itemreal := Num2Real(Str2Num(itemstr));
                  lithsum := lithsum + itemreal;
                  layer.lith[lloop] := itemreal;
               END;
            IF lithsum <> 100 THEN
               BEGIN
                  dialogdone := false;
```

```
                  AlertInt := StopAlert(31868, NIL);{ALERT! total litho.% <> 100%}
               END;
            IF dialogdone = true THEN
               EnterUnitData := true;

         END; {itemHit = 1 not cancel}

   UNTIL dialogdone;

   layer.age := tempage;

   DisposDialog(dia);
END;

{*****************************************************************************}

END.  {of DataParams}
```

```
{*****************************************************************************}
UNIT DataHandlers;
   {This unit interfaces and implements routines for handling the data once it has  }
   {been entered or is retrieved from file.                                         }
   {Programmer: Keith Sircombe                                                      }
   {Date: August 1992                                                               }
   {Number 4 in build order (after DataParams and before Decompaction)              }

INTERFACE
   USES
      SANE, Calculations, DataParams;

   VAR
      layers : column;
      inputfilename : str;

   PROCEDURE DataInit;
      {This procedure initialises various variables and arrays to 'null' as this is }
      {not done automatically when they are created.                                 }

   FUNCTION FileIn (   VAR layers : column;
                       VAR inputfilename : str) : boolean;
      {This function opens a requested data file and assuming compatability loads    }
      {the data into internal arrays.                                                }

   PROCEDURE FileOut (VAR    layers : column;
                             inputfilename : str);
      {This function opens/creates a data file and writes the section data to it     }
      {in the standard format.                                                       }

   FUNCTION ManualData (VAR layers : column) : boolean;
      {This function calls the data entry routines of DataParams and does some       }
      {minor checking and modifications of the returned data.                        }

   FUNCTION EditData (VAR layers : column) : boolean;
      {This function takes pre-exisiting data for a section and allows the user to   }
      {edit it through a series of dialog windows.  It returns TRUE if editing is    }
      {completed gracefully along with the altered data.                             }

IMPLEMENTATION

{*****************************************************************************}
   PROCEDURE DataInit;

   BEGIN
      layers[0].z := 0;       {initial thickness}
      layers[0].zsum := 0;    { initial total thickness }
      layers[0].age := 0;     { initial age, .i.e. of present surface }
      layers[1].age := 0;
      inputfilename := '';
   END;  {Procedure DataInit}

{*****************************************************************************}

{*****************************************************************************}
   FUNCTION EditData;
      LABEL
         599;
      CONST
         EditDataParamDLOG = 31157;
         EditDataDLOG = 19976;
         NotValidALRT = 25796;

         OK = 1;     {These are the 'id' numbers of the items in the editing dialog}
         Cancel = 2;
```

```
      Previous = 3;
      whichlayer = 3;
      Next = 4;
      NameofUnit = 5;
      Thickness = 6;
      AgeofBase = 7;
      Paleodepth = 8;
      Plotcurve = 9;
      sstone = 10;
      zstone = 11;
      mstone = 12;
      opstone = 13;
      lstone = 14;
      vstone = 15;
      projname = 16;

   VAR  {these are mainly variables required by the dialog management}
      dialogdone, unitdone, EditDatatemp : boolean;
      dStorage : DialogRecord;
      dia : DialogPtr;
      itemHit : integer;
      itemtype : integer;
      itemhandle : Handle;
      itemrect : rect;
      itemstr : str255;
      itemreal : real;
      editint, neweditint : integer;
      AlertInt : integer;
      layer : unitrec;
      lloop : lithology;
      layernumstr, nlayrstr, zstr, prevagestr, editstr : str255;
      lithsum : real;
      iloop : integer;

BEGIN
   dia := GetNewDialog(EditDataParamDLOG, @dStorage, pointer(-1));
                        {resource ID of Data Parameters Dialog Resource }
   REPEAT
      REPEAT
         ModalDialog(NIL, itemHit);
      UNTIL (itemHit = OK);

      dialogdone := true;

      IF itemHit = OK THEN
         BEGIN
            { get and check item 3}
            GetDItem(dia, whichlayer, itemtype, itemhandle, itemrect);
            itemstr := '';    {define varaiable}
            GetIText(itemhandle, itemstr);
            IF itemstr = '' THEN   {check to see if string present }
               BEGIN
                  dialogdone := false;
                  AlertInt := StopAlert(NotValidALRT, NIL);
               END   { alert for no data entered }
            ELSE
               BEGIN
                  editint := Num2Integer(Str2Num(itemstr)); {convert to integer }
                  IF (editint < 1) OR (editint > nlayr) THEN
                     BEGIN              { to few layers! }
                        dialogdone := false;
                        AlertInt := StopAlert(NotValidALRT, NIL);
                     END; {alert for too few layers }
               END; {else}
         END; {if itemHit = OK}
```

```
UNTIL dialogdone;

DisposDialog(dia);      {gracefully dispose the dialog window}
dialogdone := false;

REPEAT {until dialogdone}

   BEGIN

      EditDatatemp := true;

   {set up edit dialog with previous values}
      layer.unitname := layers[editint].unitname;
      layer.layernum := editint;
      layer.age := layers[editint + 1].age * 10;
      layer.plotcurve := layers[editint].plotcurve;
      layer.z := layers[editint].z * 1000;
      layer.water := layers[editint + 1].water * 1000;
      FOR lloop := sandstone TO volcanics DO
         layer.lith[lloop] := layers[editint].lith[lloop];
      layernumstr := StringOf(layer.layernum : 2);
      nlayrstr := StringOf(nlayr : 2);
      prevagestr := StringOf(layers[editint].age * 10 : 5 : 1);
      ParamText(layernumstr, nlayrstr, ' ', prevagestr);

   {resource ID of Data Parameters Dialog Resource }
      dia := GetNewDialog(EditDataDLOG, @dStorage, pointer(-1));

   { projectname = 16}
      GetDItem(dia, projname, itemtype, itemhandle, itemrect);
      SetIText(itemhandle, projectname);

   {unitname = 5}
      GetDItem(dia, NameofUnit, itemtype, itemhandle, itemrect);
      SetIText(itemhandle, layer.unitname);

   {plotcurve = 9}
      GetDItem(dia, Plotcurve, itemtype, itemhandle, itemrect);
      IF layer.plotcurve THEN
         SetIText(itemhandle, 'Y')
      ELSE
         SetIText(itemhandle, 'N');

   { paleowater = 8 }
      editstr := StringOf(layer.water : 5 : 1);
      GetDItem(dia, Paleodepth, itemtype, itemhandle, itemrect);
      SetIText(itemhandle, editstr);

   { thickness = 6 }
      editstr := StringOf(layer.z : 5 : 1);
      GetDItem(dia, Thickness, itemtype, itemhandle, itemrect);
      SetIText(itemhandle, editstr);

   { age = 7}
      editstr := StringOf(layer.age : 5 : 1);
      GetDItem(dia, AgeofBase, itemtype, itemhandle, itemrect);
      SetIText(itemhandle, editstr);

      FOR lloop := sandstone TO volcanics DO
         BEGIN
            editstr := StringOf(layer.lith[lloop] : 5 : 1);
            GetDItem(dia, ord(lloop) + sstone, itemtype, itemhandle, itemrect);
            SetIText(itemhandle, editstr);
         END;
```

```
          {finish set up of edit dialog}

            unitdone := true;

            REPEAT  {until unitdone}

               REPEAT
                  ModalDialog(NIL, itemHit);
               UNTIL (itemHit = OK) OR (itemHit = Previous) OR (itemHit = Next) OR
☞ (itemHit = Cancel);

               CASE itemHit OF

                  OK, Previous, Next :
                     BEGIN {OK, Prev, Next}
                        dialogdone := true;

            {Get unitname: item 5}
                        GetDItem(dia, NameofUnit, itemtype, itemhandle, itemrect);
                        itemstr := '';   {define varaiable}
                        GetIText(itemhandle, itemstr);
                        layer.unitname := '';
                        layer.unitname := itemstr;

            {Get thickness: item 6}
                        GetDItem(dia, Thickness, itemtype, itemhandle, itemrect);
                        itemstr := '';
                        GetIText(itemhandle, itemstr);
                        IF itemstr = '' THEN
                           itemstr := '0';
                        layer.z := Num2Real(Str2Num(itemstr));

            {Get Paleodepth : item 8}
                        GetDItem(dia, Paleodepth, itemtype, itemhandle, itemrect);
                        itemstr := '';
                        GetIText(itemhandle, itemstr);
                        IF itemstr = '' THEN
                           itemstr := '0';
                        layer.water := Num2Real(Str2Num(itemstr));

            {Get Plot Curve : item 9}
                        GetDItem(dia, Plotcurve, itemtype, itemhandle, itemrect);
                        itemstr := '';
                        GetIText(itemhandle, itemstr);
                        IF itemstr = '' THEN
                           itemstr := 'N';
                        IF (itemstr = 'Y') OR (itemstr = 'y') THEN
                           layer.plotcurve := true
                        ELSE
                           layer.plotcurve := false;

            { Get Age : item 7 }
                        GetDItem(dia, AgeofBase, itemtype, itemhandle, itemrect);
                        itemstr := '';
                        GetIText(itemhandle, itemstr);
                        IF itemstr = '' THEN
                           itemstr := '0';
                        itemreal := Num2Real(Str2Num(itemstr));
                        IF itemreal <= (layers[editint].age * 10) THEN
                           BEGIN
                              dialogdone := false;
                              unitdone := false;
                              AlertInt := StopAlert(31867, NIL); { age must decrease }
                           END
                        ELSE
```

```
                        layer.age := itemreal;

            { Checking Lithology % }
                        lithsum := 0;
                        FOR lloop := sandstone TO volcanics DO
                           BEGIN
                              GetDItem(dia, ord(lloop) + sstone, itemtype, itemhandle,
☞ itemrect);
                              itemstr := '';
                              GetIText(itemhandle, itemstr);
                              IF itemstr = '' THEN
                                 itemstr := '0';
                              itemreal := Num2Real(Str2Num(itemstr));
                              lithsum := lithsum + itemreal;
                              layer.lith[lloop] := itemreal;
                           END;

                        IF lithsum <> 100 THEN
                           BEGIN
                              dialogdone := false;
                              unitdone := false;
                              AlertInt := StopAlert(31868, NIL);
                           END;

                        IF itemHit = Previous THEN
                           BEGIN
                              unitdone := true;
                              dialogdone := false;
                              IF editint - 1 > 0 THEN
                                 neweditint := editint - 1
                              ELSE
                                 BEGIN
                                    FlashMenuBar(0);
                                    FlashMenuBar(0);
                                 END;
                           END;

                        IF itemHit = Next THEN
                           BEGIN
                              unitdone := true;
                              dialogdone := false;
                              IF editint + 1 < nlayr + 1 THEN
                                 neweditint := editint + 1
                              ELSE
                                 BEGIN
                                    FlashMenuBar(0);
                                    FlashMenuBar(0);
                                 END;
                           END;

                     END; {case of ::OK, Prev, Next ::}

                  2 :
                     BEGIN
                        EditDatatemp := false;
                        unitdone := true;
                        dialogdone := true;
                        GOTO 599;
                     END;

               END;     {case of itemHit}

            UNTIL unitdone;
```

```
            IF EditDatatemp THEN
               BEGIN

                  layers[editint].layernum := layer.layernum;
                  layers[editint].unitname := layer.unitname;
                  layers[editint + 1].water := layer.water / 1000;
                  layers[editint + 1].age := layer.age / 10;
                  layers[editint].z := layer.z / 1000;
                  FOR iloop := 1 TO nlayr DO
                     layers[iloop].zsum := layers[iloop - 1].zsum + (layers[iloop].z);
                  layers[editint].kk := 0;
                  layers[editint].pphi := 0;
                  FOR lloop := sandstone TO volcanics DO
                     BEGIN
                        layers[editint].lith[lloop] := layer.lith[lloop];
                        layers[editint].kk := layers[editint].kk + ((k[lloop] *
☞ layer.lith[lloop]) / 100);
                        layers[editint].pphi := layers[editint].pphi + ((phi[lloop] *
☞ layer.lith[lloop]) / 100);
                     END;
                  layers[editint].plotcurve := layer.plotcurve;

               END;

            editint := neweditint;

            DisposDialog(dia);

         END; { begin repeat until dialogdone }

      UNTIL dialogdone;

599 :
      IF Editdatatemp = false THEN
         DisposDialog(dia);
      EditData := Editdatatemp;

   END;
{*****************************************************************************}

{*****************************************************************************}
   FUNCTION FileIn;

      LABEL
         999;

      VAR
         lloop : lithology;
         lithsum : real;
         inputfileptr : text;
         dummyline : STRING;
         plotchar : char;
         dia : DialogPtr;
         itemtype : integer;
         itemhandle : Handle;
         itembox : rect;
         nlayrstr : str255;

      BEGIN
         FileIn := true;
         inputfilename := OldFileName('Open datafile');
         IF inputfilename = '' THEN
            GOTO 999;

         reset(inputfileptr, inputfilename);
```

```
IF eof(inputfileptr) THEN
   BEGIN
     AlertInt := StopAlert(31384, NIL);
     FileIn := false;
   END;

nlayr := 1;

readln(inputfileptr, dummyline);                    { header 1 }
readln(inputfileptr, dummyline);                    { header 2 }
readln(inputfileptr, dummyline);                    { header 3 }
readln(inputfileptr, projectname);                  { project name }
readln(inputfileptr, layers[1].water);
                          {header of data file = present water depth}
layers[1].water := layers[1].water / 1000.0;        {reduce to km}
readln(inputfileptr, dummyline);                    { separator }

dia := GetNewDialog(30189, NIL, pointer(-1));
GetDItem(dia, 1, itemtype, itemhandle, itembox);

WHILE NOT eof(inputfileptr) DO
   BEGIN

     nlayrstr := 'Layer ';
     nlayrstr := concat(nlayrstr, StringOf(nlayr : 2));
     SetIText(itemhandle, nlayrstr);
     DrawDialog(dia);

     readln(inputfileptr, layers[nlayr].layernum);   {read layer #}
     readln(inputfileptr, layers[nlayr].unitname);   {read unitname}
     readln(inputfileptr, layers[nlayr].z);          {read unit thickness}
     readln(inputfileptr, layers[nlayr + 1].age);    {read unit base age}

     FOR lloop := sandstone TO volcanics DO
        readln(inputfileptr, layers[nlayr].lith[lloop]); {read lith%}

     readln(inputfileptr, layers[nlayr].kk);         {read unit kk}
     readln(inputfileptr, layers[nlayr].pphi);       {read unit pphi}
     readln(inputfileptr, layers[nlayr + 1].water);  {read paleowater depth}
     readln(inputfileptr, plotchar);                 {read plotcurve (Y/N)}

     IF plotchar = 'Y' THEN
        layers[nlayr].plotcurve := true
     ELSE
        layers[nlayr].plotcurve := false;

     readln(inputfileptr, dummyline);  {read in separator}

     lithsum := 0; { check if lithologies = 100 }
     FOR lloop := sandstone TO volcanics DO
        lithsum := lithsum + layers[nlayr].lith[lloop];
     IF lithsum <> 100 THEN
        BEGIN
           AlertInt := StopAlert(31385, NIL); {improper data}
           FileIn := false;
           GOTO 999;
        END; {if lithsum}
     layers[nlayr + 1].water := layers[nlayr + 1].water / 1000; {reduce to km}
     layers[nlayr].z := layers[nlayr].z / 1000;                 {reduce to km}
     layers[nlayr + 1].age := layers[nlayr + 1].age / 10;{reduce to 100,000 yr}
  {sum thicknesses}
     layers[nlayr].zsum := layers[nlayr].z + layers[nlayr - 1].zsum;
     nlayr := nlayr + 1;
  END; {while not eof}
```

```
      DisposDialog(dia);  {gracefully dispose of dialog window}
      nlayr := nlayr - 1;
      close(inputfileptr);{close input file}
999 :
   END;
{*****************************************************************************}

{*****************************************************************************}
   PROCEDURE FileOut;
      LABEL
         899;
      VAR
         lloop : lithology;
         outputfilename : str;
         outputfileptr : text;
         iloop : integer; {loop counter }
         dummy : STRING;
         date : DateTimeRec;

   BEGIN
      outputfilename := NewFileName('Name of output file:', inputfilename);
      IF outputfilename = '' THEN
         GOTO 899;

      rewrite(outputfileptr, outputfilename);    { creates and opens new file }

      writeln(outputfileptr, 'University of Waikato, Department of Earth Sciences,
☞ GeoHist+');
      GetTime(date);
      writeln(outputfileptr, datestring(date));
      writeln(outputfileptr, 'Input Data File for:');
      writeln(outputfileptr, projectname);
      writeln(outputfileptr, layers[1].water * 1000 : 6 : 1);
      writeln(outputfileptr, '============');

      FOR iloop := 1 TO nlayr DO
         BEGIN
            writeln(outputfileptr, layers[iloop].layernum : 5);
            writeln(outputfileptr, layers[iloop].unitname);
            writeln(outputfileptr, (layers[iloop].z * 1000) : 6 : 2);
            writeln(outputfileptr, (layers[iloop + 1].age * 10) : 5 : 2);

            FOR lloop := sandstone TO volcanics DO
               writeln(outputfileptr, layers[iloop].lith[lloop] : 5 : 2);

            writeln(outputfileptr, layers[iloop].kk : 6 : 4);
            writeln(outputfileptr, layers[iloop].pphi : 6 : 4);
            writeln(outputfileptr, (layers[iloop + 1].water * 1000) : 5 : 2);
            CASE layers[iloop].plotcurve OF
               true :
                  writeln(outputfileptr, 'Y');
               false :
                  writeln(outputfileptr, 'N');
            END; {case}
            writeln(outputfileptr, '=======');
         END; {iloop}
      close(outputfileptr);  { close output file }
899 :
   END;  {Procedure FileOut }
{*****************************************************************************}
```

```
{*****************************************************************************}
   FUNCTION ManualData;    { Subroutine to input data from user }

      LABEL
         111, 112, 199;
      VAR
         ans : char;
         dummy : char;
         iloop : integer;
         lithsum : real;
         lloop : lithology;
         dataUnitsOK : boolean;
         loopstart, loopend : integer;

   BEGIN
      ManualData := false;
111 :
   {call routine to enter data parameters}
      IF NOT EnterDataParams(nlayr, layers[1].water) THEN
         GOTO 199;  {cancel button pressed}

      layers[1].top := layers[1].water;
      layers[1].water := layers[1].water / 1000;
      layers[0].base := layers[1].water;
      layers[1].age := 0;

      FOR iloop := 1 TO nlayr DO
         BEGIN
112 :

            WITH layer DO
               BEGIN
                  unitname := layers[iloop].unitname;
                  layernum := iloop;
                  age := layers[iloop].age * 10;
                  plotcurve := false;
                  top := layers[iloop - 1].base * 1000;
                  base := layers[iloop + 1].top;
                  FOR lloop := sandstone TO volcanics DO
                     lith[lloop] := layers[iloop].lith[lloop];
               END;
         {call routine to enter data information}
            IF NOT EnterUnitData(layer) THEN
               GOTO 199; {cancel button pressed }

            WITH layer DO
               BEGIN
                  layers[iloop].layernum := layernum;
                  layers[iloop].unitname := unitname;
                  layers[iloop + 1].water := water / 1000;
                  layers[iloop + 1].age := age / 10;
                  layers[iloop + 1].top := base;
                  layers[iloop].base := base / 1000;
                  layers[iloop].z := z / 1000;
                  layers[iloop].zsum := layers[iloop - 1].zsum + z / 1000;
                  layers[iloop].kk := 0;
                  layers[iloop].pphi := 0;
                  FOR lloop := sandstone TO volcanics DO
                     BEGIN
                        layers[iloop].lith[lloop] := lith[lloop];
                        layers[iloop].kk := layers[iloop].kk + ((k[lloop] *
☞ lith[lloop]) / 100);
                        layers[iloop].pphi := layers[iloop].pphi + ((phi[lloop] *
☞ lith[lloop]) / 100);
                     END;
```

```
                layers[iloop].plotcurve := plotcurve;

              END;

         END; {for iloop}
      ManualData := true;
199 :
   END;  {Procedure ManaualData}
{*****************************************************************************}

END.  {of DataHandlers}
```

```
{*****************************************************************************}
UNIT Decompaction;
   {This unit interfaces and implements the routine that actual does the 'guts'     }
   {of the program and progressively removes layers, decompacts remaining layers    }
   {and adjusts for paleobathymetry and eustatic sea level changes                  }
   {Programmer: Keith Sircombe                                                      }
   {Date: August 1992                                                               }
   {Number 5 in build order (after DataHandlers and before GraphicHandlers)         }

INTERFACE
   USES
      Calculations, DataParams, DataHandlers;

   FUNCTION Solution (    VAR layers : column;
                          VAR results : resultsrec) : boolean;
      {This function takes a column of stratigraphic information and produces a     }
      {list of decompacted and adjusted thicknesses through time                    }
      {This is the real guts of the program.                                        }
      {The rest is merely fancy 'window' dressing.                                  }

IMPLEMENTATION

{*****************************************************************************}
   FUNCTION Solution;

      LABEL
         499;  {end of procedure}

      CONST
         ps = 2.7;      { density of sediments }
         pm = 3.3;      { density of mantle }
         wload = 'Y';
                    {water load assumed for the calculation of tectonic subsidence}

      VAR
         zskp : ARRAY[0..maxlayr] OF real;
         zlimit, zmax, zskmin, ztop, zt : real;
         zskt : real;
         eroded : boolean;
         iloop, jloop, kloop : integer; {loop counters}
         pl : real;                     { density of displaced material }
         dummy : char;
         erodedlayerstr, progressstr : str255;
         dia : DialogPtr;
         itemtype : integer;
         itemhandle : Handle;
         itembox : rect;

   BEGIN
      Solution := true;
      progressstr := '';
      dia := GetNewDialog(24910, NIL, pointer(-1));
      GetDItem(dia, 2, itemtype, itemhandle, itembox);

      progressstr := 'Checking...';
      SetIText(itemhandle, progressstr);
      DrawDialog(dia);

      progressstr := '';

      FOR iloop := 1 TO nlayr DO
         BEGIN
            IF layers[iloop].z <= 0 THEN
               BEGIN
                  IF layers[iloop].kk > 0 THEN
```

```
                zlimit := -1 / (layers[iloop].pphi * layers[iloop].kk)
             ELSE
                zlimit := -999999;
             IF (layers[iloop].z < zlimit) THEN
                BEGIN
                   NumToString(iloop, erodedlayerstr);
                   ParamText(erodedlayerstr, ' ', ' ', ' ');
                   AlertInt := StopAlert(32505, NIL);{too much erosion in layer }
                   Solution := false;
                   GOTO 499;
                END;  {if}
             layers[iloop].plotcurve := false; {can't plot unconformities }
          END; {if }
       END; {if}
    results.totalz[1] := layers[nlayr].zsum; {total thickness of present sequence}
    IF ((layers[nlayr].z < 0) OR (results.totalz[1] < 0)) THEN     {}
       BEGIN
          AlertInt := StopAlert(32504, NIL); { too overall erosion}
          Solution := false;
          GOTO 499;
       END; {if}

    zmax := 0;

    FOR iloop := 1 TO nlayr DO
       BEGIN
          IF (layers[iloop].zsum >= zmax) THEN
             BEGIN    { deposition occurred }
                zmax := layers[iloop].zsum;{raise zmax to new total thickness value}
                results.zp[iloop, 1] := layers[iloop].zsum;
             {save for plotting }
                results.curve[1, iloop] := layers[iloop].zsum + layers[1].water;
             END {if}
          ELSE
             BEGIN                              { eroded }
                jloop := iloop - 1;             { backup one layer }
                WHILE ((layers[jloop].zsum < zmax) AND (jloop >= iloop)) DO
                { find positive depth }
                   jloop := jloop - 1;
                IF (layers[jloop].zsum >= zmax) THEN
                   BEGIN    { [?] }
                      results.curve[1, iloop] := layers[jloop].zsum +
☞ layers[1].water;
                      results.zp[iloop, 1] := layers[jloop].zsum;
                   END {if}
                ELSE
                   BEGIN
                      results.curve[1, iloop] := zmax + layers[1].water;
                      results.zp[iloop, 1] := zmax;
                   END; {else}
             END; {else}
       END; {iloop}

    FOR jloop := 1 TO nlayr DO
       layers[jloop].zsk := Skelthick(layers[jloop].zsum, layers[jloop - 1].zsum,
☞ layers[jloop].kk, layers[jloop].pphi);

  {initial sedimentation rate }
    layers[1].rate := abs((layers[1].zsum * 1000) / layers[2].age);
    FOR iloop := 2 TO nlayr DO
       BEGIN            { time index for curve }
          results.curve[iloop, iloop - 1] := layers[iloop].water-
☞ PaleoSea(layers[iloop].age);
          zmax := layers[iloop - 1].zsum;
          results.zp[iloop - 1, iloop] := 0;          { strip off top layer }
```

```
            eroded := false;        {check for erosion }
            zskmin := 0;
            ztop := 0;

            FOR jloop := iloop TO nlayr DO
               BEGIN       {layer index for curve }
                  IF (layers[jloop].zsum >= zmax) THEN
                     BEGIN
                        IF (eroded) THEN
                           BEGIN
                              zskp[jloop] := zskmin + layers[jloop].zsk;
                              kloop := jloop - 1;       { avoid uplift decompaction }
                              WHILE ((layers[kloop].zsum < zmax) AND (kloop > 1)) DO
                                 kloop := kloop - 1;
                              {proper depth for compaction }
                              ztop := results.zp[kloop, iloop]
                           END {if}
                        ELSE
                           BEGIN
                              zskp[jloop] := layers[jloop].zsk;
                              ztop := results.zp[jloop - 1, iloop];
                           END; {else}
                        zskmin := 0;
                        zmax := layers[jloop].zsum
                     END
                  ELSE
                     BEGIN    { eroded }
                        zskp[jloop] := 0;
                        ztop := results.zp[jloop - 1, iloop];
                        eroded := true;
                        zskmin := zskmin + layers[jloop].zsk;
                     END; {else}

         {given skeletal thickness and depth of top of unit calculate depth            }
         {of bottom of unit...this is it!                                              }
                     results.zp[jloop, iloop] := Compfac(zskp[jloop], ztop,
☞ layers[jloop].pphi, layers[jloop].kk);
                     results.zp[jloop, iloop] := results.zp[jloop, iloop] - ztop +
☞ results.zp[jloop - 1, iloop];   { find proper depth }

                     FOR kloop := (iloop - 1) DOWNTO 1 DO
                        IF (results.zp[jloop, iloop] - results.zp[jloop - 1, iloop]) <
☞ (results.zp[jloop, kloop] - results.zp[jloop - 1, kloop]) THEN
                           results.zp[jloop, iloop] := results.zp[jloop - 1, iloop] +
☞ results.zp[jloop, kloop] - results.zp[jloop - 1, kloop];
                     IF (jloop = iloop) THEN
                        layers[iloop].rate := (results.zp[jloop, iloop] * 1000) /
☞ (layers[iloop + 1].age - layers[iloop].age);
                     results.curve[iloop, jloop] := results.zp[jloop, iloop] +
☞ results.curve[iloop, iloop - 1];

                  {draw progress dialog to remind the user that it hasn't crashed - yet }
                     progressstr := concat(progressstr, '.');
                     SetIText(itemhandle, progressstr);
                     DrawDialog(dia);

                  END; {jloop}

               results.totalz[iloop] := results.zp[nlayr, iloop]; { sediment thickness }
               eroded := false;
               progressstr := concat(progressstr, '|');
               SetIText(itemhandle, progressstr);
               DrawDialog(dia);
```

```
          END; {iloop}

       results.curve[nlayr + 1, nlayr] := layers[nlayr + 1].water -
☞ PaleoSea(layers[nlayr + 1].age);

     {now compute tectonic curve, allowing for subsidence due to sediment loading,     }
     {water loading and changes in sea level                                           }
     {assumes water density = 1.0, sediment density = 2.5, mantle density = 3.3        }

        {draw progress dialog to remind the user that it hasn't crashed - yet }
        progressstr := 'Tectonic Curve...';
        SetIText(itemhandle, progressstr);
        DrawDialog(dia);

        IF (wload = 'Y') THEN
           p1 := 0  { assume air in hole}
        ELSE
           p1 := 1;    { assume water in hole }

        FOR iloop := 1 TO nlayr DO
           BEGIN
              zt := results.totalz[iloop] + layers[iloop].water;
              zskt := 0;
              FOR jloop := iloop TO nlayr DO
                 zskt := zskt + layers[jloop].zsk;
        { effective p = skeletal z*sed dens + porosity+water z / total z }
              IF (zt > 0) THEN
                 results.p2[iloop] := ((zskt * ps) + zt - zskt) / zt
              ELSE
                 results.p2[iloop] := 0;
              results.tect[iloop] := (zt * ((pm - results.p2[iloop]) / (pm - p1))) -
☞ PaleoSea(layers[iloop].age);

           END; {iloop}
        results.tect[nlayr + 1] := results.curve[nlayr + 1, nlayr];

        DisposDialog(dia);

   499 :
      END; {Procedure Solution}

   {*****************************************************************************}

   END. {Decompaction}
```

```
{*****************************************************************************}
UNIT GraphicsHandlers;
   {This unit interfaces and implements routines for constructing a graphic      }
   {representation of the decompacted section, i.e. a geohistory plot!           }
   {Programmer: Keith Sircombe                                                   }
   {Date: August 1992                                                            }
   {Number 5 in build order (after Decompaction and before ResultHandlers)       }

INTERFACE
   USES
      Calculations;

   FUNCTION EnterPlotParams (  VAR Plottitle : STRING;
                               VAR Ref : boolean;
                               VAR AgeScale : real;
                               VAR DepthScale : real;
                               DefAgeScale : real;
                               DefDepthScale : real) : boolean;
      {This function opens a dialog window to get information from the user about  }
      {desired size/scale and title of the geohistory plot seen on the screen.     }

   PROCEDURE Graphics (  layers : column;
                         results : resultsrec);
      {This procedure creates the graphic display of the geohistory plot of the    }
      {processed section.                                                          }

IMPLEMENTATION

{*****************************************************************************}
   FUNCTION EnterPlotParams;

      LABEL
         2399;

      CONST   {These are the id # of dialog items}
         PlotParamsDLOG = 30998;
         OK = 1;
         Cancel = 2;
         PlotTitleBox = 3;
         RefYNBox = 4;
         AgeScaleBox = 5;
         DepthScaleBox = 6;

      VAR   {these variables are mainly required by the dialog manager}
         dialogdone : boolean;
         dStorage : DialogRecord;
         dia : DialogPtr;
         itemHit : integer;
         itemtype : integer;
         itemhandle : Handle;
         itemrect : rect;
         itemstr : str255;
         itemint : integer;
         itemchar : char;
         itemreal : real;

   BEGIN
      EnterPlotParams := false;

      dia := GetNewDialog(PlotParamsDLOG, @dStorage, pointer(-1));
      GetDItem(dia, PlotTitleBox, itemtype, itemhandle, itemrect);
      SetIText(itemHandle, projectname);
      GetDItem(dia, AgeScaleBox, itemtype, itemhandle, itemrect);
      SetIText(itemHandle, StringOf(DefAgeScale : 4 : 2));
      GetDItem(dia, DepthScaleBox, itemtype, itemhandle, itemrect);
```

```
      SetIText(itemHandle, StringOf(DefDepthScale : 4 : 2));

      REPEAT
         dialogdone := false;
         REPEAT
            ModalDialog(NIL, itemHit);
         UNTIL (itemHit = OK) OR (itemHit = Cancel);

         IF itemHit = OK THEN
            BEGIN

               GetDItem(dia, PlotTitleBox, itemtype, itemhandle, itemrect);
               itemstr := '';
               GetIText(itemhandle, itemstr);
               Plottitle := itemstr;

               GetDItem(dia, RefYNBox, itemtype, itemhandle, itemrect);
               itemstr := '';
               GetIText(itemhandle, itemstr);
               IF itemstr = 'Y' THEN
                  ref := true
               ELSE
                  ref := false;

               GetDItem(dia, AgeScaleBox, itemtype, itemhandle, itemrect);
               itemstr := '';
               GetIText(itemhandle, itemstr);
               ReadString(itemstr, AgeScale);

               GetDItem(dia, DepthScaleBox, itemtype, itemhandle, itemrect);
               itemstr := '';
               GetIText(itemhandle, itemstr);
               ReadString(itemstr, DepthScale);

               dialogdone := true;

            END
         ELSE
            GOTO 2399;

      UNTIL dialogdone;

      EnterPlotParams := true;

2399 :
      DisposDialog(dia);
   END; {EnterPlotParams}
{*****************************************************************************}

{*****************************************************************************}
   PROCEDURE Graphics;

      LABEL
         1999;

      CONST
         leftW = 5;                {global coordinates of text display window}
         topW = 40;
         rightW = 600;
         bottomW = 500;
         lmargin = 20;
         tmargin = 30;
         rmargin = 50;
         bmargin = 20;
         topaxismargin = 35;
```

```
        CourierFont = 22;
        fsize = 12;

      VAR   {these variables are reuired by the window manager and inbuilt graphics}
        wRecord : WindowRecord;
        myWindow : WindowPtr;
        whichWindow : WindowPtr;
        windowrect : rect;
        bounds : rect;
        instr : STRING;
        instrlen, instrheight : integer;
        instrinfo : FontInfo;
        penloc : Point;
        displaydone : boolean;
        anEvent : EventRecord;
        mwhere : integer;

        xmin, xmax, ymin, ymax : real;       { outer coordinates of the plot }
        rage, slope : real;     { }
        x, oldx, y : real;      { plot coordinates }
        plottitle : str;
        iloop, jloop, ploop : integer;     { loop counters }
        dummy : char;
        xscale, yscale : real;
        tstr : STRING;
        tlen : integer;
        finfo : FontInfo;
        theight, cwidth : integer;
        stripes : Pattern;
        pseabot : Pattern;
        xorigin, yorigin : integer;
        pictrec : Picture;
        pictptr : PicPtr;
        picthand : PicHandle;
        scraplong : longint;

        {Plottitle : string;}
        ref : boolean;
        AgeScale, DepthScale : real;

    BEGIN

        IF NOT EnterPlotParams(Plottitle, ref, AgeScale, DepthScale, 5.0, 0.5) THEN
          GOTO 1999;

        SetRect(windowrect, leftW, topW, rightW, bottomW);
        myWindow := NewWindow(@wRecord, windowrect, 'GeoHist+ Graphic Display', true,
☞ 0, pointer(-1), true, 999);
        SetPort(myWindow);

        SetOrigin(0, 0);

        TextFont(CourierFont);        {sets up font for window display}
        TextSize(Fsize);              {sets up font size for window display}
        GetFontInfo(finfo);
        theight := finfo.ascent + finfo.descent;

        StuffHex(@stripes, 'E4E4E4E4E4E4E4E4');    {sets up stipes for a line type}
        StuffHex(@pseabot, 'FCFCFCFCFCFCFCFC');    {set up pattern for paleobathymetry}

        xmin := 0;
        xmax := -99999;
        ymax := -99999;
        ymin := 99999;
```

```
      FOR iloop := 1 TO (nlayr + 1) DO
         BEGIN       { find extremes }
           IF (layers[iloop].age > xmax) THEN
              xmax := layers[iloop].age;
           FOR jloop := 1 TO nlayr DO
              BEGIN
                 IF (results.curve[iloop, jloop] > ymax) THEN
                    ymax := results.curve[iloop, jloop];
                 IF (results.curve[iloop, jloop] < ymin) THEN
                    ymin := results.curve[iloop, jloop];
              END; {jloop}
         END; {iloop}

      FOR iloop := 1 TO (nlayr + 1) DO
         BEGIN
           IF (results.tect[iloop] > ymax) THEN
              ymax := results.tect[iloop];
           IF (results.tect[iloop] < ymin) THEN
              ymin := results.tect[iloop];
         END; {iloop}

      xmin := round(xmin);
      xmax := round(xmax + 0.51);

      ymin := round(ymin);
      ymax := round(ymax + 0.51);

      xscale := (rightW - leftW - (lmargin + rmargin)) / (15.4 * AgeScale) * 10;
      yscale := (bottomW - topW - (tmargin + bmargin) - topaxismargin) / (7.6 *
☞ DepthScale);

      picthand := OpenPicture(windowrect);
      ShowPen;

   {Plot X-axis}
      MoveTo(rightW - rmargin, tmargin);
      Line(-round(xmax * xscale), 0);

   {Plot X-axis ticks}
      FOR iloop := 0 TO round(xmax) DO
         BEGIN
           Move(-round(iloop * xscale), 0);
           Line(0, -5);
           tstr := StringOf(iloop * 10 : 3);
           tlen := StringWidth(tstr);
           Move(-round(tlen / 2), -1);
           DrawString(tstr);
           MoveTo(rightW - rmargin, tmargin);
         END;

   {Plot NZ stages}
      iloop := 1;
      WHILE (nz[iloop + 1].age / 10) <= xmax DO
         BEGIN
           x := nz[iloop + 1].age / 10;
           oldx := nz[iloop].age / 10;
           Move(-round(x * xscale), 0);
           Line(0, 4);
           Move(round(((x - oldx) * xscale) / 2), 5);
           TextSize(Fsize - 2);
           DrawChar(nz[iloop].stage);
           MoveTo(rightW - rmargin, tmargin);
           iloop := iloop + 1;
         END;
```

```
{Plot X-axis label}
      TextSize(Fsize);
      tstr := StringOf('Age (Myr)' : 9);
      tlen := StringWidth(tstr);
      Move(-round(((xmax / 2) * xscale) + (tlen / 2)), -(6 + theight));
      DrawString(tstr);
      MoveTo(rightW - rmargin, tmargin);

{Plot Y-axis}
      MoveTo(rightW - rmargin, tmargin);
      Line(0, round((ymax - ymin) * yscale) + topaxismargin);
      MoveTo(rightW - rmargin, tmargin + topaxismargin);

{Plot Y-ticks}
      MoveTo(rightW - rmargin, tmargin + topaxismargin);
      FOR iloop := 0 TO round(ymax * 2) DO
         BEGIN
            Move(0, round((iloop / 2) * yscale));
            Line(5, 0);
            tstr := StringOf(iloop / 2 : 3 : 1);
            tlen := StringWidth(tstr);
            Move(1, round(theight / 2));
            DrawString(tstr);
            MoveTo(rightW - rmargin, tmargin + topaxismargin);
         END;

{Plot Y-label}
      cwidth := CharWidth('D');
      MoveTo(rightW - leftW - cwidth - 2, tmargin + round((((ymax - ymin) * yscale) +
☞ topaxismargin) / 2));
      Move(0, -4 * (theight + 1));
      DrawChar('D');
      Move(-cwidth, theight + 1);
      DrawChar('e');
      cwidth := CharWidth('e');
      Move(-cwidth, theight + 1);
      DrawChar('p');
      cwidth := CharWidth('p');
      Move(-cwidth, theight + 1);
      DrawChar('t');
      cwidth := CharWidth('t');
      Move(-cwidth, theight + 1);
      DrawChar('h');
      cwidth := CharWidth('h');
      Move(-cwidth, theight + 1);
      DrawChar(' ');
      cwidth := CharWidth(' ');
      Move(-cwidth, theight + 1);
      DrawChar('(');
      cwidth := CharWidth('(');
      Move(-cwidth, theight + 1);
      DrawChar('k');
      cwidth := CharWidth('k');
      Move(-cwidth, theight + 1);
      DrawChar('m');
      cwidth := CharWidth('m');
      Move(-cwidth, theight + 1);
      DrawChar(')');

      SetOrigin(-3, 0);

{Plot Layers}
      FOR iloop := 1 TO nlayr DO
         BEGIN
            PenSize(1, 1);
```

```
            ForeColor(magentaColor);
            IF iloop = nlayr THEN
               BEGIN
                  layers[iloop].plotcurve := true;
                  PenPat(black);
                  PenSize(2, 2);
               END;
            IF layers[iloop].plotcurve THEN
               BEGIN
                  x := layers[1].age;
                  y := results.curve[1, iloop] - ymin;
                  MoveTo(round(rightW - leftW - rmargin - (x * xscale)),
☞ round(tmargin + topaxismargin + (y * yscale)));
                  FOR jloop := 2 TO (iloop + 1) DO
                     BEGIN
                        x := layers[jloop].age;
                        y := results.curve[jloop, iloop] - ymin;
                        LineTo(round(rightW - leftW - rmargin - (x * xscale)),
☞ round(tmargin + topaxismargin + (y * yscale)));
                     END; {jloop}
               END; {if}
         END; {iloop}
      PenSize(1, 1);

   {PlotPaleoSeaBottom}
      PenPat(pseabot);
      PenSize(1, 1);
      ForeColor(greenColor);
      x := layers[1].age;
      y := layers[1].water;
      MoveTo(round(rightW - leftW - rmargin - (x * xscale)),
☞ round(tmargin + topaxismargin + (y * yscale)));
      FOR iloop := 2 TO 101 DO
         BEGIN
            rage := (layers[nlayr + 1].age / 100) * (iloop - 1);
            x := rage;
            jloop := 1;
            WHILE ((rage > layers[jloop].age) AND (jloop < nlayr + 1)) DO
               BEGIN
                  jloop := jloop + 1;
               END;
            slope := (layers[jloop].water - layers[jloop - 1].water) /
☞ (layers[jloop].age - layers[jloop - 1].age);
            y := layers[jloop - 1].water + (slope * (rage - layers[jloop - 1].age));
            y := y - PaleoSea(rage);
            LineTo(round(rightW - leftW - rmargin - (x * xscale)),
☞ round(tmargin + topaxismargin + (y * yscale)));
         END; {iloop}

   {PlotPaleoSeaLevel}
      PenPat(dkGray);
      PenSize(1, 1);
      ForeColor(redColor);
      x := layers[1].age;
      y := -PaleoSea(layers[1].age);
      MoveTo(round(rightW - leftW - rmargin - (x * xscale)),
☞ round(tmargin + topaxismargin + (y * yscale)));
      FOR iloop := 1 TO 101 DO
         BEGIN
            rage := (layers[nlayr + 1].age / 100) * (iloop - 1);
            x := rage;
            y := (-PaleoSea(rage) - ymin);
            LineTo(round(rightW - leftW - rmargin - (x * xscale)),
☞ round(tmargin + topaxismargin + (y * yscale)));
         END; {iloop}
```

```
{PlotTectonic}
      PenPat(stripes);
      PenSize(1, 1);
      ForeColor(blueColor);
      x := layers[1].age;
      y := results.tect[1];
      MoveTo(round(rightW - leftW - rmargin - (x * xscale)),
☞ round(tmargin + topaxismargin + (y * yscale)));
      FOR iloop := 2 TO (nlayr + 1) DO
         BEGIN
            x := layers[iloop].age;
            y := results.tect[iloop];
            LineTo(round(rightW - leftW - rmargin - (x * xscale)),
☞ round(tmargin + topaxismargin + (y * yscale)));
         END;

{PlotReference}
      ForeColor(blackColor);
      IF ref THEN
         BEGIN
            IF AgeScale >= 1 THEN
               xorigin := lmargin
            ELSE
               xorigin := round(rightW - leftW - rmargin - round(xmax * xscale));
            IF DepthScale >= 1 THEN
               yorigin := bottomW - topW - bmargin
            ELSE
               yorigin := tmargin + topaxismargin + round(ymax * yscale);
            TextSize(12);
            MoveTo(xorigin, yorigin);
            DrawString('Tectonic Curve  :');
            PenPat(stripes);
            PenSize(1, 1);
            ForeColor(blueColor);
            Move(2, -round(theight / 2));
            Line(20, 0);

            ForeColor(blackColor);
            MoveTo(xorigin, yorigin);
            Move(0, -(theight + 1) * 1);
            DrawString('Total Subsidence:');
            PenPat(black);
            PenSize(2, 2);
            ForeColor(magentaColor);
            Move(2, -round(theight / 2));
            Line(20, 0);

            ForeColor(blackColor);
            MoveTo(xorigin, yorigin);
            Move(0, -(theight + 1) * 2);
            DrawString('Unit Subsidence :');
            PenPat(black);
            PenSize(1, 1);
            ForeColor(magentaColor);
            Move(2, -round(theight / 2));
            Line(20, 0);

            ForeColor(blackColor);
            MoveTo(xorigin, yorigin);
            Move(0, -(theight + 1) * 3);
            DrawString('Paleo Sea Bottom:');
            PenPat(pseabot);
            PenSize(1, 1);
            ForeColor(greenColor);
```

```
            Move(2, -round(theight / 2));
            Line(20, 0);

            ForeColor(blackColor);
            MoveTo(xorigin, yorigin);
            Move(0, -(theight + 1) * 4);
            DrawString('Paleo Sea Level :');
            PenPat(dkGray);
            PenSize(1, 1);
            ForeColor(redColor);
            Move(2, -round(theight / 2));
            Line(20, 0);
         END;

{Plot Title}
      ForeColor(blackColor);
      IF AgeScale >= 1 THEN
         MoveTo(lmargin, 0)
      ELSE
         MoveTo(round(rightW - leftW - rmargin - round(xmax * xscale)), 0);
      IF DepthScale >= 1 THEN
         Move(0, bottomW - topW - bmargin)
      ELSE
         Move(0, tmargin + topaxismargin + round((ymax - ymin) * yscale));

      Move(160, 0);
      TextSize(14);
      DrawString(PlotTitle);

   {place a PICT copy of the geohistory plot in the clipboard}
      ClosePicture;
      scraplong := ZeroScrap;
      scraplong := PutScrap(picthand^^.picsize, 'PICT', pointer(picthand^));
      scraplong := UnloadScrap;
      displaydone := false;

      REPEAT
         IF GetNextEvent(mDownMask, anEvent) THEN
            CASE anEvent.what OF
               mouseDown :
                  BEGIN
                     mwhere := FindWindow(anEvent.where, myWindow);
                     CASE mwhere OF
                        {mwhere}
                        inGoAway :
                           BEGIN
                              IF TrackGoAway(myWindow, anEvent.where) THEN
                                 displaydone := true;
                           END; {inGoAway}
                        {mwhere}
                        OTHERWISE
                           REPEAT
                           UNTIL NOT WaitMouseUp;
                     END; {case mwhere of}
                  END; {mouseDown}
               OTHERWISE
                  REPEAT
                  UNTIL NOT WaitMouseUp;
            END; {case anEvent.what}
      UNTIL displaydone = true;
      CloseWindow(myWindow); { close window AND controls }
1999 :
   END; { procedure Graphics}
{*****************************************************************************}
END.  {GraphicHandlers}
```

```
{*****************************************************************************}
UNIT ResultHandlers;
   {This unit interfaces and implements the procedures to handle and display the    }
   {processed data.                                                                 }
   {Programmer: Keith Sircombe                                                      }
   {Date: August 1992                                                               }
   {Number 7 in build order (after GraphicsHandlers and before Plot)                }

INTERFACE
   USES
     Calculations;

   CONST   {constant 'headers' are set up for the display of the processed data}
     header1 = 'GeoHist+, University of Waikato, Department of Earth Sciences';
     {header2 = 'Date goes here';}
     {header3 = 'separator goes here';}
     header4 = 'Project: ';
     {header5 = 'Empty line here';}
     header6 = 'GeoHist+ INPUT SUMMARY.';
     header7 = 'Water depth or elevation : ';
     {header8 = 'Empty line here';}
     header9 = '   Thickness of  Age of Unit                  Lithology %
☞                          Paleodepth';
     header10 = '     Unit (m)     base (My)    SS     ZS     MS     OP     LS
☞      VO      KK     ø    of Unit (m)   Plot Layer';
     {header11 = 'Empty line here';}
     {header12 = 'Empty line here';}
     {header13 = 'separator goes here';}
     header14 = 'GeoHist+ BACKSTRIPPING SUMMARY.';
     {header15 = 'Empty line here';}
     header16a = 'Time (Myr)';
     header16b = 'Zsk    Sed.';
     header16c = 'Rate';
     header17 = 'Water Depth (m)';
     header17b = '(m/My)';
     {header18 = 'separator goes here';}
     {header19 = 'separator goes here';}
     header20 = 'Total Depth (m)';
     header21 = 'Density (Mg/m3)';
     header22 = 'Tectonic Sub. (m)';
   {header24 = 'separator goes here';}

   VAR
     CallbyCurrentDisplay : boolean;

   PROCEDURE DisplayData (CallByCurrentDisplay : boolean);
     {This procedure displays the processed data in a text window.  The data can    }
     {then be moved with scroll bars.                                               }

   PROCEDURE SaveResultsProc ( layers : column;
                               results : resultsrec);
     {This procedure saves the currently processed results in a text file for later
}
     {use.  Unprocessed data is also stored.                                        }

   FUNCTION LoadResultsProc (  VAR layers : column;
                               VAR results : resultsrec) : boolean;
     {This function loads a data and results file as required.                      }
```

```
IMPLEMENTATION

{*****************************************************************************}
   FUNCTION makespacer (  spacer : char;
                          numspacers : integer) : STRING;
   {This function is internal to ResultHandlers and returns a string of spacer      }
   {characters as specified by the requesting code.                                  }

      VAR
         t : integer;
         tempstr : STRING;

   BEGIN
      makespacer := '';
      tempstr := '';
      FOR t := 1 TO numspacers DO
         tempstr := concat(tempstr, spacer);
      makespacer := tempstr;
   END;
{*****************************************************************************}

{*****************************************************************************}
   FUNCTION LoadResultsProc;

      LABEL
         1099;
      VAR
         resfilename : STRING;
         resfileptr : text;
         fillerstr, linestr, lithstr, namestr : STRING;
         erodedlayerstr : str255;
         iloop, jloop : integer;
         dummychar : char;
         dummystr : STRING;
         dummyint, namelen, cutpos, plotpos : integer;
         zmax, zlimit : real;
         dia : DialogPtr;
         itemtype : integer;
         itemHandle : Handle;
         itembox : rect;
         progress : str255;

   BEGIN
      LoadResultsProc := false;
      linestr := '';
      resfilename := OldFileName('Results file to be loaded:');
      IF resfilename = '' THEN
         GOTO 1099;
      reset(resfileptr, resfilename);
      dia := GetNewDialog(30189, NIL, pointer(-1));
      GetDItem(dia, 1, itemtype, itemhandle, itembox);
      progress := 'Input Summary';
      SetIText(itemhandle, progress);
      DrawDialog(dia);
      readln(resfileptr, fillerstr);                {1}
      readln(resfileptr, fillerstr);                {2}
      readln(resfileptr, fillerstr);                {3}
      readln(resfileptr, linestr);                        {4}
      projectname := omit(linestr, 1, length(header4));  {remove "Project:" }
      readln(resfileptr, fillerstr);                {5}
      readln(resfileptr, fillerstr);                {6}
      readln(resfileptr, linestr);                        {7}
      linestr := omit(linestr, 1, length(header7));      {get present water depth }
      ReadString(linestr, layers[1].water);
      layers[1].water := layers[1].water / 1000;
```

```
        readln(resfileptr, fillerstr);                {8}
        readln(resfileptr, fillerstr);                {9}
        readln(resfileptr, fillerstr);                {10}
        readln(resfileptr, fillerstr);                {11}
        nlayr := 0;
        readln(resfileptr, linestr);
        REPEAT
           BEGIN
              nlayr := nlayr + 1;
              lithstr := copy(linestr, 25, 45);
              linestr := omit(linestr, 25, 45);
              ReadString(linestr, layers[nlayr].layernum, dummychar, layers[nlayr].z,
☞ layers[nlayr + 1].age, layers[nlayr].kk, layers[nlayr].pphi,
☞  layers[nlayr + 1].water);
              ReadString(lithstr, layers[nlayr].lith[sandstone],
☞  layers[nlayr].lith[siltstone], layers[nlayr].lith[mudstone],
☞  layers[nlayr].lith[opshales], layers[nlayr].lith[limestone],
☞  layers[nlayr].lith[volcanics]);
              layers[nlayr].z := layers[nlayr].z / 1000;
              layers[nlayr].zsum := layers[nlayr].z + layers[nlayr - 1].zsum;
              layers[nlayr + 1].age := layers[nlayr + 1].age / 10;
              layers[nlayr + 1].water := layers[nlayr + 1].water / 1000;

              plotpos := pos('Y', linestr);
              IF plotpos = 0 THEN
                 plotpos := pos('N', linestr);
              dummystr := copy(linestr, plotpos, 1);
              IF dummystr = 'Y' THEN
                 layers[nlayr].plotcurve := true
              ELSE
                 layers[nlayr].plotcurve := false;

              readln(resfileptr, linestr);
           END;
           progress := concat(progress, '.');
           SetIText(itemhandle, progress);
           DrawDialog(dia);
        UNTIL length(linestr) = 0;

        readln(resfileptr, fillerstr);                {'13'}
        readln(resfileptr, fillerstr);                {'14'}
        readln(resfileptr, fillerstr);                {'15'}
        readln(resfileptr, fillerstr);                {'16'}
        readln(resfileptr, linestr);                  { ages }
        namelen := pos('.', linestr) - 6;             { find length of names }
        readln(resfileptr, linestr);                  { paleowater }
        readln(resfileptr, fillerstr);                {'18'}
        FOR iloop := 1 TO nlayr DO
           BEGIN
              IF layers[iloop].z <= 0 THEN
                 BEGIN
                    IF layers[iloop].kk > 0 THEN
                       zlimit := -1 / (layers[iloop].pphi * layers[iloop].kk)
                    ELSE
                       zlimit := -999999;
                    IF (layers[iloop].z < zlimit) THEN
                       BEGIN
                          NumToString(iloop, erodedlayerstr);
                          ParamText(erodedlayerstr, ' ', ' ', ' ');
                          AlertInt := StopAlert(32505, NIL);{too much erosion in layer }
                          GOTO 1099;
                       END;  {if}
                    layers[iloop].plotcurve := false; {can't plot unconformities }
                 END; {if }
           END; {if}
```

```
      results.totalz[1] := layers[nlayr].zsum;{total thickness of present sequence }
      IF ((layers[nlayr].z < 0) OR (results.totalz[1] < 0)) THEN     {}
         BEGIN
            AlertInt := StopAlert(32504, NIL); { too overall erosion}
            GOTO 1099;
         END; {if}

      zmax := 0;
      FOR iloop := 1 TO nlayr DO
         BEGIN
            IF (layers[iloop].zsum >= zmax) THEN
               BEGIN    { deposition occurred }
                  zmax := layers[iloop].zsum;{raise zmax to new total thickness value}
                  results.zp[iloop, 1] := layers[iloop].zsum;
                  { save for plotting }
                  results.curve[1, iloop] := layers[iloop].zsum + layers[1].water;
               END {if}
            ELSE
               BEGIN                              { eroded }
                  jloop := iloop - 1;             { backup one layer }
                  { find positive depth }
                  WHILE ((layers[jloop].zsum < zmax) AND (jloop >= iloop)) DO
                     jloop := jloop - 1;
                  IF (layers[jloop].zsum >= zmax) THEN
                     BEGIN
                        results.curve[1, iloop] := layers[jloop].zsum +
☞ layers[1].water;
                        results.zp[iloop, 1] := layers[jloop].zsum;
                     END {if}
                  ELSE
                     BEGIN
                        results.curve[1, iloop] := zmax + layers[1].water;
                        results.zp[iloop, 1] := zmax;
                     END; {else}
               END; {else}
            results.curve[iloop, iloop - 1] := layers[iloop].water -
☞ PaleoSea(layers[iloop].age);
         END; {iloop}

      progress := 'Backstripping Summary';
      SetIText(itemhandle, progress);
      DrawDialog(dia);

      FOR jloop := 1 TO nlayr DO   {layer loop}
         BEGIN
            readln(resfileptr, linestr);
            namestr := copy(linestr, 1, namelen);
            namestr := omit(namestr, 1, 5);            {get rid of layernumber }
            layers[jloop].unitname := namestr;
            linestr := omit(linestr, 1, namelen);      { get rid of unitname}

            FOR iloop := 1 TO jloop DO
               BEGIN
                  cutpos := pos('.', linestr) + 2;
                  ReadString(linestr, results.listz[iloop]);
                  IF jloop = 1 THEN
                     results.curve[iloop, jloop] := ((results.listz[iloop] / 1000) +
☞ layers[iloop].water - PaleoSea(layers[iloop].age))
                  ELSE
                     results.curve[iloop, jloop] := (results.listz[iloop] / 1000) +
☞ results.curve[iloop, jloop - 1];
                  linestr := omit(linestr, 1, cutpos);
               END; {iloop}

            ReadString(linestr, layers[jloop].zsk, layers[jloop].rate);
```

```
            layers[jloop].zsk := layers[jloop].zsk / 1000;
            layers[jloop].rate := layers[jloop].rate * 10;
            progress := concat(progress, '.');
            SetIText(itemhandle, progress);
            DrawDialog(dia);
         END; {jloop}
      results.curve[nlayr + 1, nlayr] := layers[nlayr + 1].water -
☞  PaleoSea(layers[nlayr + 1].age);
      results.tect[nlayr + 1] := results.curve[nlayr + 1, nlayr];
      readln(resfileptr, fillerstr);                {'19'}

      progress := 'Final Results...';
      SetIText(itemhandle, progress);
      DrawDialog(dia);

      readln(resfileptr, linestr);                          { Total Depth }
      linestr := omit(linestr, 1, namelen);
      FOR iloop := 1 TO nlayr DO
         BEGIN
            cutpos := pos('.', linestr) + 2;
            ReadString(linestr, results.curve[iloop, nlayr]);
            results.curve[iloop, nlayr] := (results.curve[iloop, nlayr] -
☞  PaleoSea(layers[iloop].age)) / 1000;
            linestr := omit(linestr, 1, cutpos);
         END;

      readln(resfileptr, linestr);                          { Density }
      linestr := omit(linestr, 1, namelen);
      FOR iloop := 1 TO nlayr DO
         BEGIN
            cutpos := pos('.', linestr) + 2;
            ReadString(linestr, results.p2[iloop]);
            linestr := omit(linestr, 1, cutpos);
         END;

      readln(resfileptr, linestr);                          { Tectonic sub }
      linestr := omit(linestr, 1, namelen);
      FOR iloop := 1 TO nlayr DO
         BEGIN
            cutpos := pos('.', linestr) + 2;
            ReadString(linestr, results.tect[iloop]);
            results.tect[iloop] := results.tect[iloop] / 1000;
            linestr := omit(linestr, 1, cutpos);
         END;


      readln(resfileptr, fillerstr);                {'24'}

      close(resfileptr);
      LoadResultsProc := true;
      DisposDialog(dia);
   1099 :
      END;
   {*****************************************************************************}

   {*****************************************************************************}
      PROCEDURE DisplayData;

         CONST
            leftW = 5;                {global coordinates of text display window}
            topW = 40;
            rightW = 495;
            bottomW = 320;

         VAR      {these variables are mostly required by the text window manager}
```

```
        dragRect : rect;
        txRect : rect;
        textH : TEHandle;
        wRecord : WindowRecord;
        myWindow : WindowPtr;
        whichWindow : WindowPtr;
        windowrect : rect;
        bounds : rect;
        resultfilename : STRING;
        resultfileptr : text;
        instr : STRING;
        instrlen, instrheight : integer;
        instrinfo : FontInfo;
        penloc : Point;
        displaydone : boolean;
        anEvent : EventRecord;
        mwhere, numlines : integer;
        vscrollrect, hscrollrect : rect;
        vscrollhandle, hscrollhandle, wscrollhandle : ControlHandle;
        controlpart : integer;
        displayrect : rect;
        visheight, viswidth : real;
        scrolldist : real;
        voldloc, holdloc : real;
        maxwidth : real;

    BEGIN
      IF CallByCurrentDisplay THEN
        resultfilename := 'display.temp'
      ELSE
        resultfilename := OldFileName('Enter name of results file');

      reset(resultfileptr, resultfilename);

    {Set up text display window}
      SetRect(windowrect, leftW, topW, rightW, bottomW);
      SetRect(displayrect, 5, 5, 3000, 3000);
      myWindow := NewWindow(@wRecord, windowrect, 'GeoHist+ Summary', true, 0,
☞ pointer(-1), true, 999);
      SetPort(myWindow);
      SetRect(txRect, 5, 5, rightW - leftW - 20, bottomW - topW - 20);
      textH := TENew(displayrect, txRect);
      textH^^.txFont := 22;     { Courier font }
      textH^^.txSize := 12;     { Size 12 }
      numlines := 0;
      maxwidth := 0;

      REPEAT
        BEGIN
          numlines := numlines + 1;
          instr := '';
          readln(resultfileptr, instr);
          instr := concat(' ', instr, ' ', chr(13));
          instrlen := StringWidth(instr);
          IF instrlen > maxwidth THEN
            maxwidth := instrlen;
          TEInsert(pointer(ord(@instr) + 1), length(instr), textH);
        END;
      UNTIL eof(resultfileptr);

      close(resultfileptr);

      visheight := (bottomW - topW - 20) / textH^^.lineheight;
      viswidth := rightW - leftW - 20;
      displaydone := false;
```

```
        SetRect(vscrollrect, (rightW - leftW - 16), 0, (rightW - leftW),
☞   (bottomW - topW - 16));
        vscrollhandle := NewControl(myWindow, vscrollrect, '', true, 0, 0,
☞   round(numlines - visheight + 2), 16, 99);
        SetRect(hscrollrect, 0, (bottomW - topW - 16), (rightW - leftW - 16),
☞   (bottomW - topW));
        hscrollhandle := NewControl(myWindow, hscrollrect, '', true,
☞   round(viswidth / 5), round(viswidth / 5), round(maxwidth / 5), 16, 998);

        REPEAT
           IF GetNextEvent(mDownMask + updateMask, anEvent) THEN
             CASE anEvent.what OF

                mouseDown :
                   BEGIN
                      mwhere := FindWindow(anEvent.where, myWindow);
                      CASE mwhere OF
             {MouseDown}
                         inGoAway :
                            BEGIN
                               IF TrackGoAway(myWindow, anEvent.where) THEN
                                  displaydone := true;
                            END; {inGoAway}
             {MouseDown}
                         inContent :
                            BEGIN
                               GlobaltoLocal(anEvent.where);
                               voldloc := GetCtlValue(vscrollhandle);
                               holdloc := GetCtlValue(hscrollhandle);
                               controlpart := FindControl(anEvent.where, myWindow,
☞   wscrollhandle);
                               IF controlpart > 0 THEN
                                  BEGIN
                                     controlpart := TrackControl(wscrollhandle,
☞   anEvent.where, NIL);
                                     IF controlpart > 0 THEN
                                        BEGIN
                                           CASE controlpart OF
                                              inUpbutton :
                                                 SetCtlValue(wscrollhandle,
☞   GetCtlValue(wscrollhandle) - 1);
                                              inDownButton :
                                                 SetCtlValue(wscrollhandle,
☞   GetCtlValue(wscrollhandle) + 1);
                                              inPageUp :
                                                 SetCtlValue(wscrollhandle,
☞   GetCtlValue(wscrollhandle) - 5);
                                              inPageDown :
                                                 SetCtlValue(wscrollhandle,
☞   GetCtlValue(wscrollhandle) + 5);
                                              OTHERWISE
                                                 REPEAT
                                                 UNTIL NOT WaitMouseUp;
                                           END; {case controlpart of}
                                        END {if controlpart after TrackControl}
                                     ELSE
                                        REPEAT
                                        UNTIL NOT WaitMouseUp;
                                  END {if controlpart before TrackControl }
                               ELSE
                                  REPEAT
                                  UNTIL NOT WaitMouseUp;

                               IF wscrollhandle = vscrollhandle THEN
                                  BEGIN
```

```
                                    scrolldist := voldloc - GetCtlValue(vscrollhandle);
                                    TEScroll(0, round(scrolldist * textH^^.lineheight),
☞ textH);
                                    voldloc := GetCtlValue(vscrollhandle);
                                 END {wscrollhandle = vscrollhandle}
                              ELSE
                                 BEGIN
                                    scrolldist := holdloc - GetCtlValue(hscrollhandle);
                                    TEScroll(round(scrolldist * 5), 0, textH);
                                    holdloc := GetCtlValue(hscrollhandle);
                                 END; { wscrollhandle = hscrollhandle}
                           END; {inContent}
                        OTHERWISE
                           REPEAT
                           UNTIL NOT WaitMouseUp;
                     END; {case mwhere}
                  END;{mouseDown}

               updateEvt :
                  BEGIN
                     BeginUpdate(WindowPtr(anEvent.message));
                     EraseRect(thePort^.portrect);
                     TEUpdate(thePort^.portRect, textH);
                     DrawControls(myWindow);
                     EndUpdate(WindowPtr(anEvent.message));
                  END; {updateEvt}
            END;{case Event.what}
      UNTIL displaydone = true;
      TEDispose(textH);          { close and dispose text }
      CloseWindow(myWindow); { close window AND controls }

   END;
{*****************************************************************************}

{*****************************************************************************}
   PROCEDURE SaveResultsProc;

      LABEL
         2299;

      VAR
         iloop, jloop : integer;
         lloop : lithology;
         dummy : char;
         bounds : rect;
         outputfilename : str;
         outputfileptr : text;
         maxlen : integer;
         date : DateTimeRec;
         seplen : integer;

         dia : DialogPtr;
         itemtype : integer;
         itemHandle : Handle;
         itembox : rect;
         progress : str255;

   BEGIN
      IF CallByCurrentDisplay THEN
         outputfilename := 'display.temp'
      ELSE
         outputfilename := NewFileName('Name of output file:', '');
      IF outputfilename = '' THEN
         GOTO 2299;
```

```
      rewrite(outputfileptr, outputfilename);    { creates and opens new file }

      maxlen := 15;
      FOR jloop := 1 TO nlayr DO
         IF length(layers[jloop].unitname) > maxlen THEN
            maxlen := length(layers[jloop].unitname);
      IF (6 + maxlen + ((nlayr + 1) * 8) + 15) > 112 THEN
         seplen := (6 + maxlen + ((nlayr + 1) * 8) + 15)
      ELSE
         seplen := 112;
      dia := GetNewDialog(30189, NIL, pointer(-1));
      GetDItem(dia, 2, itemtype, itemhandle, itembox);
      IF CallByCurrenTDisplay THEN
         SetIText(itemhandle, 'Working')
      ELSE
         SetIText(itemhandle, 'Saving');
      GetDItem(dia, 1, itemtype, itemhandle, itembox);
      progress := 'Input Summary';
      SetIText(itemhandle, progress);
      DrawDialog(dia);
      writeln(outputfileptr, header1);
      GetTime(date);
      writeln(outputfileptr, datestring(date));
      writeln(outputfileptr, makespacer('=', seplen));
      writeln(outputfileptr, header4, projectname);
      writeln(outputfileptr, '');
      writeln(outputfileptr, header6);
      writeln(outputfileptr, header7, layers[1].water * 1000 : 6 : 2, 'm');
      writeln(outputfileptr, '');
      writeln(outputfileptr, header9);
      writeln(outputfileptr, header10);
      writeln(outputfileptr, '');
      FOR iloop := 1 TO nlayr DO
         BEGIN
            write(outputfileptr, iloop : 3, ': ');
            write(outputfileptr, layers[iloop].z * 1000 : 6 : 1);
            write(outputfileptr, '      ', layers[iloop + 1].age * 10 : 5 : 1,
☞ '    ');
            FOR lloop := sandstone TO volcanics DO
               write(outputfileptr, '  ', layers[iloop].lith[lloop] : 5 : 1);
            write(outputfileptr, '    ', layers[iloop].kk : 3 : 2);
            write(outputfileptr, '  ', layers[iloop].pphi : 3 : 2);
            write(outputfileptr, '    ', layers[iloop + 1].water * 1000 : 6 : 1);
            IF layers[iloop].plotcurve THEN
               write(outputfileptr, '            Y')
            ELSE
               write(outputfileptr, '            N');
            writeln(outputfileptr, '');
            progress := concat(progress, '.');
            SetIText(itemhandle, progress);
            DrawDialog(dia);
         END;
      writeln(outputfileptr, '');
      writeln(outputfileptr, makespacer('=', seplen));
      progress := 'Backstripping Summary';
      SetIText(itemhandle, progress);
      DrawDialog(dia);
      writeln(outputfileptr, header14);
      writeln(outputfileptr, '');
      write(outputfileptr, makespacer(' ', trunc(((nlayr * 8) -
☞ length(header16a)) / 2) + maxlen + 6)), header16a);
      write(outputfileptr, makespacer(' ', trunc(((nlayr * 8) -
☞ length(header16a)) / 2)) + 2), header16b);
      writeln(outputfileptr, '');
      write(outputfileptr, makespacer(' ', maxlen + 5));
```

```
      FOR iloop := 1 TO nlayr DO
         write(outputfileptr, '  ', layers[iloop].age * 10 : 6 : 1);
      write(outputfileptr, makespacer(' ', 10), header16c);
      writeln(outputfileptr, '');
      write(outputfileptr, header17, makespacer('.', (maxlen + 5) - 15));
      FOR iloop := 1 TO nlayr DO
         write(outputfileptr, '  ', layers[iloop].water * 1000 : 6 : 1);
      write(outputfileptr, makespacer(' ', 9), header17b);
      writeln(outputfileptr, '');
      writeln(outputfileptr, makespacer('-', 6 + maxlen + (nlayr * 8) + 15));
      FOR jloop := 1 TO nlayr DO      { layer loop }
         BEGIN
            write(outputfileptr, jloop : 3);
            write(outputfileptr, ': ', layers[jloop].unitname,
☞ makespacer(' ', maxlen - length(layers[jloop].unitname)));
            FOR iloop := 1 TO jloop DO   { time loop }
               BEGIN
                  IF (jloop = 1) THEN
                     results.listz[iloop] := trunc((results.curve[iloop, jloop] -
☞ layers[iloop].water + PaleoSea(layers[iloop].age)) * 1000)
                  ELSE
                     results.listz[iloop] := trunc((results.curve[iloop, jloop] -
☞ results.curve[iloop, jloop - 1]) * 1000);
                  write(outputfileptr, '  ', results.listz[iloop] : 6 : 1);
               END; { iloop }
            write(outputfileptr, makespacer(' ', (nlayr - jloop) * 8 + 1),
layers[jloop].zsk * 1000 : 6 : 1);
            write(outputfileptr, '  ', layers[iloop - 1].rate / 10 : 6 : 1);
            writeln(outputfileptr, '');
            progress := concat(progress, '.');
            SetIText(itemhandle, progress);
            DrawDialog(dia);
         END; {jloop}
      progress := 'Final Results...';
      SetIText(itemhandle, progress);
      DrawDialog(dia);
      writeln(outputfileptr, makespacer('-', (6 + maxlen + (nlayr * 8) + 15)));
      write(outputfileptr, header20, makespacer('.', (maxlen + 5) -
☞ length(header20)));
      FOR iloop := 1 TO nlayr DO
         write(outputfileptr, '  ', (results.curve[iloop, nlayr] +
☞ PaleoSea(layers[iloop].age)) * 1000 : 6 : 1);
      writeln(outputfileptr, '');

      write(outputfileptr, header21, makespacer('.', (maxlen + 5) -
☞ length(header21)));
      FOR iloop := 1 TO nlayr DO
         write(outputfileptr, '  ', results.p2[iloop] : 6 : 2);
      write(outputfileptr, '  Initial depth:');
      writeln(outputfileptr, '');

      write(outputfileptr, header22, makespacer('.', (maxlen + 5) -
☞ length(header22)));
      FOR iloop := 1 TO nlayr DO
         write(outputfileptr, '  ', results.tect[iloop] * 1000 : 6 : 1);
      write(outputfileptr, '    ', results.tect[nlayr + 1] * 1000 : 6 : 1);
      writeln(outputfileptr, '');

      writeln(outputfileptr, makespacer('-', (6 + maxlen + (nlayr * 8) + 15)));
      close(outputfileptr);
2299 :
      DisposDialog(dia);
   END;
{*****************************************************************************}
END.  {ResultHandlers}
```

```
{*****************************************************************************}
UNIT PlotDriver;
   {This unit interfaces and implements the procedure that controls the output of   }
   {results graphic to a hardcopy pen plotter, in particular a Graphtec MP4200 in   }
   {HP-GL Emulation mode.                                                           }
   {Consult relevant instruction and command reference manuals for further info     }
   {on the use of the Graphtec MP4200 plotter.                                      }
   {Programmer: Keith Sircombe                                                      }
   {Date: August 1992                                                               }
   {Number 8 in build order (after ResultHAndlers and before Geodecomp)             }

INTERFACE
   USES
     Calculations, DataHandlers, GraphicsHandlers;

   PROCEDURE Plot (    layers : column;
                       results : resultsrec);
     {This procedure conducts simple serial communication with the plotter and      }
     {plots a geohistory plot of the current results in a similar fashion to the    }
     {screen graphic display of the ResultHandlers.                                 }
     {Note:  the communication between computer and plotter is *very* simple.       }
     {The computer merely 'dumps' all the instructions and required data to the     }
     {presumably listening (& functioning) plotter via the serial port.             }
     {No error checking or correction is attempted.                                 }

IMPLEMENTATION
{*****************************************************************************}
   PROCEDURE Plot;

     LABEL
        701, 702, 703, 704, 705, 706, 707, 708, 709, 710, 711, 712, 713, 799;
   {InitPlotter}
   {PlotXaxis}
   {PlotXlabel}
   {PlotYaxis}
   {PlotYlabel}
   {PlotLayers}
   {PlotPaleoSeaLevel}
   {Pausing}
   {PlotPaleoSeaBottom}
   {PlotTect}
   {PlotRef}
   {PlotTitle}
   {EndPlotting}

     CONST
        PausingALRT = 22407;
        Lplot = 2000.0;
        Bplot = 2000.0;
        Rplot = 14000.0;
        Tplot = 9000.0;
        DefAgeScale = 2.50;
        DefDepthScale = 0.50;
        loopdelay = 10000;

     VAR
        xmin, xmax, ymin, ymax : real;     { outer coordinates of the plot }
        rage, slope : real;                { }
        x, y, oldx : real;                 { plot coordinates }
        plottitle : str;
        iloop, jloop, ploop : integer;     { loop counters }
        dummy : char;
        plotterptr : text;
        AgeScale, DepthScale, xlen, ylen : real;
        ref : boolean;
        topaxismargin : real;
```

```
    BEGIN
       ref := true;
       IF NOT EnterPlotParams(Plottitle, ref, AgeScale, DepthScale, DefAgeScale,
☞ DefDepthScale) THEN
          GOTO 799;
       xmin := 0;
       xmax := -99999;
       ymax := -99999;
       ymin := 99999;
       FOR iloop := 1 TO (nlayr + 1) DO
          BEGIN      { find extremes }
             IF (layers[iloop].age > xmax) THEN
                xmax := layers[iloop].age;
             FOR jloop := 1 TO nlayr DO
                BEGIN
                   IF (results.curve[iloop, jloop] > ymax) THEN
                      ymax := results.curve[iloop, jloop];
                   IF (results.curve[iloop, jloop] < ymin) THEN
                      ymin := results.curve[iloop, jloop];
                END; {jloop}
          END; {iloop}
       FOR iloop := 1 TO (nlayr + 1) DO
          BEGIN
             IF (results.tect[iloop] > ymax) THEN
                ymax := results.tect[iloop];
             IF (results.tect[iloop] < ymin) THEN
                ymin := results.tect[iloop];
          END; {iloop}

       xmin := round(xmin);
       xmax := round(xmax + 0.51) * 10;
       ymin := round(ymin);
       ymax := round(ymax + 0.51);
       xlen := (30.0 * AgeScale);
       ylen := 17.5 * DepthScale;
       topaxismargin := (ylen - ymin) * 0.1;

  701 :   {InitPlotter}
       rewrite(plotterptr, 'Printer:');  { opens line to plotter }

       write(plotterptr, 'IN;');            { initilises plotter to default settings }
       write(plotterptr, 'IP2000,2000,14000,9000;');
                                 { sets out P1, P2 points on plotter in plotter units }
       write(plotterptr, 'SC', xmin : 6 : 2, xlen : 7 : 3, (ymin - 0) : 6 : 2,
☞ ylen : 7 : 3, chr(3));{ sets P1, P2 in user coordinates }
       FOR iloop := 1 TO loopdelay DO
          ploop := iloop;
       write(plotterptr, 'SI.2,.3;DI-1.0,0.0;VS5;');
     {sets width of character size TO 1 of (p2-p1) AND height TO outputfileptr (p2-p1)}
       write(plotterptr, 'SP1;PU;PA', xmin : 6 : 2, (ymin - topaxismargin) : 6 : 2,
☞ chr(3)); { select pen; pen up; plot absolute TO " origin "of axes }
       FOR iloop := 1 TO loopdelay DO
          ploop := iloop;

  702 :   {PlotXaxis}
       write(plotterptr, 'PD;PA', xmax : 7 : 4, (ymin - topaxismargin) : 7 : 4,
☞ 'PU;');   { pen down; plot absolute "age" axis; pen up }
       write(plotterptr, 'PA', xmin : 7 : 4, (ymin - topaxismargin) : 7 : 4, chr(3));
     { return to origin of axes }
       write(plotterptr, 'TL0,2;LO5;');
     {set length of graduation ticks to -2% of |P2y - P1y| }
       FOR ploop := 0 TO round(xmax / 10) DO
          BEGIN
             write(plotterptr, 'PA', (ploop * 10) : 5, (ymin - topaxismargin) : 7 : 4,
☞ ';XT;CP0,1;LB', ((ploop / 10) * 100) : 5 : 1, chr(3), ';PU;');{ plot tick on axis }
```

```
         END; {ploop}
      FOR iloop := 1 TO loopdelay DO
         ploop := iloop;
      {Plot NZ Series}
      iloop := 1;
      write(plotterptr, 'TL0,-2;LO5;');
   { set length of graduation ticks to -2% of |P2y - P1y| }
      WHILE (nz[iloop + 1].age) <= xmax DO
         BEGIN
            x := nz[iloop + 1].age;
            oldx := nz[iloop].age;
            write(plotterptr, 'PA', xmin : 7 : 4, (ymin - topaxismargin) : 7 : 4,
☞ chr(3));  { return to origin of axes }
            write(plotterptr, 'PA', x : 5 : 1, (ymin - topaxismargin) : 7 : 4,
☞ ';XT;');
            write(plotterptr, 'PR', -((x - oldx) / 2) : 7 : 4, 0, ';CP0,-0.5;');
            write(plotterptr, 'LB', nz[iloop].stage, chr(3), ';PU;');
            iloop := iloop + 1;
         END;
      FOR iloop := 1 TO loopdelay DO
         ploop := iloop;

703 :    { PlotXlabel }
      write(plotterptr, 'PA', (xmax - xmin) / 2 : 7 : 4, (ymin - topaxismargin) :
☞ 7 : 4, ';CP0,2;LBAge (Myr)', chr(3), ';PU;');  { move to axislabel POINT }
      FOR iloop := 1 TO loopdelay DO
         ploop := iloop;
      GOTO 704;

704 :    { PlotYaxis }
      write(plotterptr, 'PU;PA', xmin : 7 : 4, (ymin - topaxismargin)
☞ : 7 : 4, chr(3));     { return to origin }
      write(plotterptr, 'PD;PA', xmin : 7 : 4, ymax : 7 : 4, ';PU;');
                              { pen down; plot absolute "depth" axis; pen up }
      write(plotterptr, 'TL0,2;');
   { set length of graduation ticks to -2% of |P2y - P1y| }
      FOR iloop := 0 TO round((ymax * 2)) DO
         BEGIN
            write(plotterptr, 'PA', xmin : 7 : 4, (iloop / 2) : 7 : 1, 'YT;');
   { plot tick on axis }
            write(plotterptr, 'LO2;DI-1.0,0.0;');
   { label origin; label direction=effectively upsidedown }
            write(plotterptr, 'CP2,0;LB', (iloop / 2) : 5 : 1, chr(3));
   { plot label }
         END; {iloop}
      FOR iloop := 1 TO loopdelay DO
         ploop := iloop;

705 :    { PlotYlabel }
      write(plotterptr, 'PA', xmin : 7 : 4, (ymax - ymin) / 2 : 7 : 4, chr(3));
   { move to axis label POINT }
      write(plotterptr, 'CP8,0;LO5;DI0, 1;LBDepth (km)', chr(3)); { plot axis label }
      write(plotterptr, 'PU;PA', xmin : 7 : 4, (ymin - topaxismargin)
☞ : 7 : 4, chr(3));     { return to origin }
      FOR iloop := 1 TO loopdelay DO
         ploop := iloop;

706 :    { PlotLayers}
      FOR iloop := 1 TO nlayr DO
         BEGIN
            write(plotterptr, 'SP8;');          { select unit colour }
            IF iloop = nlayr THEN
               BEGIN
                  layers[iloop].plotcurve := true;
                  write(plotterptr, 'SP6;');    {select colour for total subsidence }
```

```
            END; {if}
         IF (layers[iloop].plotcurve = true) OR (iloop = nlayr) THEN
            BEGIN
               x := layers[1].age * 10;
               y := (results.curve[1, iloop] - ymin);
               write(plotterptr, 'PU;PA', x : 7 : 4, y : 7 : 4, 'PD;');
               FOR jloop := 2 TO (iloop + 1) DO
                  BEGIN
                     x := layers[jloop].age * 10;
                     y := results.curve[jloop, iloop] - ymin;
                     write(plotterptr, 'PA', x : 7 : 4, y : 7 : 4, chr(3));
                  END; {jloop}
            END; {if}
      END; {iloop}
   FOR iloop := 1 TO loopdelay DO
      ploop := iloop;

707 :    { PlotPaleoSeaLevel }
   write(plotterptr, 'PU;PA0,0;SP4;');
   x := layers[1].age * 10;
   y := -PaleoSea(layers[1].age) - ymin;
   write(plotterptr, 'PA', x, y, chr(3));
   FOR iloop := 1 TO 101 DO
      BEGIN
         rage := (layers[nlayr + 1].age / 100) * (iloop - 1);
         x := rage * 10;
         y := (-PaleoSea(rage) - ymin);
         write(plotterptr, 'PD;PA', x : 7 : 4, y : 7 : 4, chr(3));
      END; {iloop}
   FOR iloop := 1 TO loopdelay DO
      ploop := iloop;

708 :    {Pausing, so computer doesn't overfill the plotters buffer}
   AlertInt := StopAlert(PausingALRT, NIL);

709 :    { PlotPaleoSeaBottom}
   write(plotterptr, 'PU;PA0,0;SP2;');  {select pen 2 for Paleo Sea Bottom colour }
   x := layers[1].age * 10;
   y := layers[1].water - ymin;
   write(plotterptr, 'PA', x : 7 : 4, y : 7 : 4, 'PD;');
   FOR iloop := 2 TO 101 DO
      BEGIN
         rage := (layers[nlayr + 1].age / 100) * (iloop - 1);
         x := rage * 10;
         jloop := 1;
         WHILE ((rage > layers[jloop].age) AND (jloop < nlayr + 1)) DO
            BEGIN
               jloop := jloop + 1
            END; {while }
         slope := (layers[jloop].water - layers[jloop - 1].water) /
☞ (layers[jloop].age - layers[jloop - 1].age);
         y := layers[jloop - 1].water + (slope * (rage - layers[jloop - 1].age));
         y := y - PaleoSea(rage) - ymin;
         write(plotterptr, 'PA', x : 7 : 4, y : 7 : 4, chr(3));
      END; {iloop}
   FOR iloop := 1 TO loopdelay DO
      ploop := iloop;

710 :    {PlotTect}
   write(plotterptr, 'PU;SP5;PA0,0;');  { pen up; select pen 5; return to origin }
   write(plotterptr, 'LT2,1;');         { set line to broken pattern }
   x := layers[1].age * 10;
   y := results.tect[1] - ymin;
   write(plotterptr, 'PA', x : 7 : 4, y : 7 : 4, 'PD;');
   FOR iloop := 2 TO (nlayr + 1) DO
```

```
            BEGIN
               x := layers[iloop].age * 10;
               y := results.tect[iloop] - ymin;
               write(plotterptr, 'PA', x : 7 : 4, y : 7 : 4, chr(3));
            END; {iloop}
         write(plotterptr, 'PU;PA0, 0;');
         FOR iloop := 1 TO loopdelay DO
            ploop := iloop;

   711 :    {PlotRef}
         IF ref THEN
            BEGIN
               write(plotterptr, 'PA', xmax : 5 : 1, ymax : 5 : 1, chr(3));
               write(plotterptr, 'LO2;DI-1,0;LT;');
      { label origin; label direction= effectively upsidedown }
               write(plotterptr, 'SI.2,.25;');          { sets width of character size }
               write(plotterptr, 'SP1;CP0,10;LBPaleo Sea Level  : ', chr(3),
☞  'SP4;PR-.01,0;PD;PR', -(0.05 * xmax) : 6 : 3, ',0;PU;PA', xmax : 7 : 4,
☞  ymax : 7 : 4, chr(3));
               write(plotterptr, 'SP1;CP0,8;LBPaleo Sea Bottom : ', chr(3),
☞  'SP2;PR-.01,0;PD;PR', -(0.05 * xmax) : 6 : 3, ',0;PU;PA', xmax : 7 : 4,
☞  ymax : 7 : 4, chr(3));
               write(plotterptr, 'SP1;CP0,6;LBUnit Subsidence  : ', chr(3),
☞  'SP8;PR-.01,0;PD;PR', -(0.05 * xmax) : 6 : 3, ',0;PU;PA', xmax : 7 : 4,
☞  ymax : 7 : 4, chr(3));
               write(plotterptr, 'SP1;CP0,4;LBTotal Subsidence : ', chr(3),
☞  'SP6;PR-.01,0;PD;PR', -(0.05 * xmax) : 6 : 3, ',0;PU;PA', xmax : 7 : 4,
☞  ymax : 7 : 4, chr(3));
               write(plotterptr, 'SP1;CP0,2;LBTectonic Curve   : ', chr(3),
☞  'SP5;LT2,1;PR-.01,0;PD;PR', -(0.05 * xmax) : 6 : 3, ',0;PU;PA', xmax : 7 : 4,
☞  ymax : 7 : 4, chr(3));
               FOR iloop := 1 TO loopdelay DO
                  ploop := iloop;
            END;
         GOTO 712;

   712 :    {PlotTitle}
         FOR iloop := 1 TO loopdelay DO
            ploop := iloop;
         plottitle := concat(plottitle, chr(3), 'PU;');
         write(plotterptr, 'SI0.3,0.6;SP1;PA', (xmax - xmin) / 2 : 7 : 4, ymax : 7 : 4,
☞  chr(3), ';LO5;DI-1.0,0.0;LB', plottitle);
         FOR iloop := 1 TO loopdelay DO
            ploop := iloop;
         write(plotterptr, 'SP;PA', xlen : 7 : 4, ylen : 7 : 4, chr(3));
         GOTO 713;

   713 :    {EndPlotting}
         FOR iloop := 1 TO loopdelay DO
            ploop := iloop;
         write(plotterptr, 'PU;PA', xlen : 7 : 4, ylen : 7 : 4, chr(3));
         FOR iloop := 1 TO loopdelay DO
            ploop := iloop;
         close(plotterptr);

   799 :
      END; {Procedure Plot}
   {*****************************************************************************}
   END.  {Plot}
```

```
{*****************************************************************************}
PROGRAM Geodcomp;
   {This program is largely based on a the GEO_HIST program for a VAX/VMS system    }
   {written by Ray Wood of the then Geophysics division of DSIR Geology and         }
   {Geophysics, now the Crown Research Institute of Geological and Nuclear Sciences }
   {This is the main part of the whole program.  From here the calls to the         }
   {procedures and functions outlined in the above units are made.                  }
   {The menus are set up here and managed during the running of the program.        }
   {This program is designed to input stratigraphic data from exploration well or   }
   {outcrop section sites.  The sedimentary units are then progressively removed    }
   {to build a plot of the depths and decompacted thicknesses of those units        }
   {backwards through time.  The amount of tectonic subsidence is also calculated.  }
   {Programmer: Keith Sircombe                                                      }
   {Date: August 1992                                                               }
   {Number 9 in build order (after PlotDriver)                                      }

   USES
     Calculations, DataHandlers, Decompaction, GraphicsHandlers, ResultHandlers,
☞  PlotDriver;

   CONST   {these are menu id numbers for menu items appearing in the menus}
     appleId = 1;
     geohistId = 22768;

     appleM = 1;
     geohistM = 2;
     projectM = 3;

     menuCount = 3;

     AboutGeoHist = 1;

     EnterDataManually = 1;
     EditDataid = 2;
     RestoreDataFromFile = 3;
     OutputDataToFile = 4;
     ProcessData = 6;
     SaveResults = 8;
     LoadResults = 9;
     ResultGraphics = 10;
     PlotResults = 11;
     DisplayCurrentResults = 13;
     DisplaySavedResults = 14;
     Quit = 16;
   VAR
     myMenus : ARRAY[1..menuCount] OF MenuHandle; {array of handles to menus}
     bounds : rect;
     results : resultsrec;
     iloop, jloop : integer;        { loop counters}
     lloop : lithology;
     dummy : char;
     menuId : integer;
     anEvent : EventRecord;
     ev : boolean;
     where : integer;
     whichWindow : WindowPtr;
     menuchoice : longint;
     keyint : integer;
     continue, doneFlag : boolean;
     dragRect : rect;
     extended : boolean;
     textH : TEHandle;
     theChar : char;
     oldprojname : STRING;
     memsize, growsize : Size;
```

```
{*****************************************************************************}

{*****************************************************************************}
   PROCEDURE About;
      {This procedure simply calls up a alert dialog window with information 'about'}
      {the GeoHist+ program.                                                    }

      VAR
         Alertint : integer;
   BEGIN
      Alertint := Alert(31200, NIL);
   END;
{*****************************************************************************}

{*****************************************************************************}
   PROCEDURE SetUpMenus;
      {This procedure sets up the menus and menu bar used during the program.   }

      VAR
         i : integer;

   BEGIN

      myMenus[appleM] := GetMenu(appleId);    {read Apple menu}
      AddResMenu(myMenus[appleM], 'DRVR');    {add desk acc}
      myMenus[geohistM] := GetMenu(geohistId);  {read geohist menu}
      myMenus[projectM] := NewMenu(707, 'None');

      FOR i := 1 TO menuCount DO
         InsertMenu(myMenus[i], 0);

      DrawMenuBar;
   END; {SetUpMenus}
{*****************************************************************************}

{*****************************************************************************}
   FUNCTION QuitApp : boolean;
      {This function gives a second chance when quitting the application to prevent }
      {unintentional quitting (& data loss).  If quitting is the desired option,    }
      {then the menus are gracefully disposed of.                                   }

      CONST
         QuitDLOG = 31234;
         No = 1;
         Yes = 2;

      VAR
         dStorage : DialogRecord;
         dia : DialogPtr;
         itemHit : integer;
         i : integer;
   BEGIN
      QuitApp := false;

      dia := GetNewDialog(QuitDLOG, @dStorage, pointer(-1));
      REPEAT
         ModalDialog(NIL, itemHit);
      UNTIL (itemHit = No) OR (itemHit = Yes);

      IF itemHit = Yes THEN
         BEGIN
            QuitApp := true;
            FOR i := 1 TO menuCount DO
               BEGIN
                  DeleteMenu(myMenus[i]^^.menuID);
```

```
                DisposeMenu(myMenus[i]);
             END; { for i }
          END   { if itemHit=Yes)
       ELSE
          QuitApp := false;
       DisposDialog(dia);
    END;
{*****************************************************************************}

{*****************************************************************************}
    PROCEDURE DoCommand (mResult : longint);
       {This procedure, given the result of a request from the menu will action that }
       {request and alter the menu appearance accordingly.                           }

       VAR
          theItem : integer;
          theMenu : integer;
          name : str255;
          temp : integer;
          ManualDataOK : boolean;

    BEGIN
       theItem := LoWord(mResult);
       theMenu := HiWord(mResult);
       CASE theMenu OF
          appleId :
             BEGIN
                IF theItem = AboutGeoHist THEN
                   About
                ELSE
                   BEGIN
                      GetItem(myMenus[appleM], theItem, name);
                      temp := OpenDeskAcc(name);  {open a desk accessory if requested}
                   END;
             END; {appleId}
          geohistId :
             BEGIN
                CASE theItem OF
                   EnterDataManually :
                      BEGIN
                         IF ManualData(layers) THEN
                            BEGIN
                               EnableItem(myMenus[geohistM], EditDataid);
                               EnableItem(myMenus[geohistM], ProcessData);
                               EnableItem(myMenus[geohistM], OutputDataToFile);
                               DisableItem(myMenus[geohistM], SaveResults);
                               DisableItem(myMenus[geohistM], DisplayCurrentResults);
                               DisableItem(myMenus[geohistM], PlotResults);
                               DisableItem(myMenus[geohistM], ResultGraphics);
                            END;
                      END;
                   EditDataid :
                      BEGIN
                         IF EditData(layers) THEN
                            BEGIN
                            END;
                      END;
                   RestoreDataFromFile :
                      BEGIN
                         IF FileIn(layers, inputfilename) THEN
                            BEGIN
                               EnableItem(myMenus[geohistM], EditDataid);
                               EnableItem(myMenus[geohistM], ProcessData);
                               EnableItem(myMenus[geohistM], OutputDataToFile);
                               DisableItem(myMenus[geohistM], SaveResults);
```

```
                        DisableItem(myMenus[geohistM], DisplayCurrentResults);
                        DisableItem(myMenus[geohistM], PlotResults);
                        DisableItem(myMenus[geohistM], ResultGraphics);
                     END;
               END;
            OutputDataToFile :
               FileOut(layers, inputfilename);
            ProcessData :
               BEGIN
                  IF Solution(layers, results) THEN
                     BEGIN
                        EnableItem(myMenus[geohistM], SaveResults);
                        EnableItem(myMenus[geohistM], DisplayCurrentResults);
                        EnableItem(myMenus[geohistM], PlotResults);
                        EnableItem(myMenus[geohistM], ResultGraphics);
                        DisableItem(myMenus[geohistM], ProcessData);
                     END;
               END;
            SaveResults :
               BEGIN
                  CallByCurrentDisplay := false;
                  SaveResultsProc(layers, results);
               END;
            LoadResults :
               BEGIN
                  IF LoadResultsProc(layers, results) THEN
                     BEGIN
                        EnableItem(myMenus[geohistM], SaveResults);
                        EnableItem(myMenus[geohistM], DisplayCurrentResults);
                        EnableItem(myMenus[geohistM], PlotResults);
                        EnableItem(myMenus[geohistM], EditDataid);
                        EnableItem(myMenus[geohistM], ResultGraphics);
                        EnableItem(myMenus[geohistM], ProcessData);
                     END;
               END;
            ResultGraphics :
               Graphics(layers, results);
            PlotResults :
               Plot(layers, results);
            DisplayCurrentResults :
               BEGIN
                  CallByCurrentDisplay := true;
                  SaveResultsProc(layers, results);
                  DisplayData(CallByCurrentDisplay);
               END;
            DisplaySavedResults :
               BEGIN
                  CallByCurrentDisplay := false;
                  DisplayData(CallByCurrentDisplay);
               END;
            Quit :
               BEGIN
                  doneFlag := QuitApp;
               END;
         END; {case theItem}
      END; {case geohistId}
   OTHERWISE
      BEGIN
      END; {otherwise}
END; {case theMenu}
HiliteMenu(0);
END; {Procedure}
{*****************************************************************************}
```

```
{********************************** MAIN PROGRAM ***********************************}

BEGIN

   MaxApplZone;
   FOR iloop := 1 TO 10 DO
      MoreMasters;

   InitCursor;

   CallByEdit := false;
   projectname := '';

   FOR iloop := 0 TO maxlayr DO
      BEGIN                        {initilise data arrays to 'null'}
         WITH layers[iloop] DO
            BEGIN
               layernum := 0;
               water := 0;
               age := 0;
               top := 0;
               base := 0;
               z := 0;
               zsum := 0;
               zsk := 0;
               rate := 0;
               kk := 0;
               pphi := 0;
               dens := 0;
               plotcurve := true;
               unitname := '';
               FOR lloop := sandstone TO volcanics DO
                  lith[lloop] := 0;
            END;

         WITH results DO
            BEGIN
               tect[iloop] := 0;
               totalz[iloop] := 0;
               p2[iloop] := 0;
               zsum[iloop] := 0;
               listz[iloop] := 0;
               FOR jloop := 0 TO maxlayr DO
                  BEGIN
                     curve[iloop, jloop] := 0;
                     zp[iloop, jloop] := 0;
                  END;
            END;
      END;

    SetUpMenus;       {assemble and display menus}

    CalcSetup;        {more data initilisation}
    DataInit;

    doneFlag := false;

    REPEAT
       SystemTask;
       oldprojname := projectname;

       IF GetNextEvent(everyEvent, anEvent) THEN
          CASE anEvent.what OF
```

```
            mouseDown :
               CASE FindWindow(anEvent.where, whichWindow) OF
                  inSysWindow :
                     SystemClick(anEvent, whichWindow);
                  inMenuBar :
                     DoCommand(MenuSelect(anEvent.where));
                  OTHERWISE
                     REPEAT
                     UNTIL NOT WaitMouseUp;
               END; {mouseDown}

            keyDown, autoKey :
               BEGIN
                  theChar := chr(BitAnd(anEvent.message, charCodeMask));
                  IF BitAnd(anEvent.modifiers, cmdKey) <> 0 THEN
                     DoCommand(MenuKey(theChar))
                  ELSE
                     BEGIN
                     END;
               END;

            activateEvt :
               REPEAT
               UNTIL NOT WaitMouseUp;

            updateEvt :
               BEGIN
                  BeginUpdate(WindowPtr(anEvent.message));
                  EndUpdate(WindowPtr(anEvent.message));
               END;

            OTHERWISE
               REPEAT
               UNTIL NOT WaitMouseUp;

         END; {of event case}

      IF oldprojname <> projectname THEN
         BEGIN
            DeleteMenu(707);
            myMenus[projectM] := NewMenu(707, projectname);
            InsertMenu(myMenus[projectM], 0);
            DrawMenuBar;
         END;

   UNTIL doneFlag;

END. {Geodecomp}
```

Appendix E: Petrographic details

No petrographic analysis of samples was undertaken in this study. For the compilation of the QFL diagram in Fig. 4.16, modal analyses from other studies were used. These analyses and their literature sources are listed here.

Sample	Feld. %	Lithic %	Quartz %	Literature source
Otumotu Formation	4.41	22.06	73.53	Table 5.1, Adams, 1987.
Otumotu Formation	8.33	25.00	66.67	Table 5.1, Adams, 1987.
Otumotu Formation	1.64	57.38	40.98	Table 5.1, Adams, 1987.
Otumotu Formation	1.39	48.61	50.00	Table 5.1, Adams, 1987.
Otumotu Formation	11.76	39.22	49.02	Table 5.1, Adams, 1987.
Otumotu Formation	1.96	19.61	78.43	Table 5.1, Adams, 1987.
Otumotu Formation	10.71	17.86	71.43	Table 5.1, Adams, 1987.
Butler Formation	25.00	23.81	51.19	Table 5.2, Adams, 1987.
Butler Formation	18.89	27.78	53.33	Table 5.2, Adams, 1987.
Butler Formation	27.42	32.26	40.32	Table 5.2, Adams, 1987.
Moeraki Mem, Tauperikaka	9.09	34.09	56.82	Table 5.3, Adams, 1987.
Moeraki Mem, Tauperikaka	15.38	15.38	69.23	Table 5.3, Adams, 1987.
Moeraki Mem, Tauperikaka	5.56	50.00	44.44	Table 5.3, Adams, 1987.
Moeraki Mem, Tauperikaka	8.05	22.99	68.97	Table 5.3, Adams, 1987.
Moeraki Mem, Tauperikaka	16.67	27.78	55.56	Table 5.3, Adams, 1987.
Moeraki Mem, Tauperikaka	13.33	33.33	53.33	Table 5.3, Adams, 1987.
Moeraki Mem, Tauperikaka	2.60	19.48	77.92	Table 5.3, Adams, 1987.
Paringa Mem, Tauperikaka	24.53	6.29	69.18	Table 5.4, Adams, 1987.
Paringa Mem, Tauperikaka	6.67	6.67	86.67	Table 5.4, Adams, 1987.
Paringa Mem, Tauperikaka	24.39	12.20	63.41	Table 5.4, Adams, 1987.
Rasselas M., Tauperikaka	31.25	6.25	62.50	Table 5.5, Adams, 1987.
Rasselas M., Tauperikaka	30.20	13.42	56.38	Table 5.5, Adams, 1987.
Rasselas M., Tauperikaka	17.20	6.37	76.43	Table 5.5, Adams, 1987.
Long Reef M., Tititira Frm.	28.6	13.9	57.5	Table 3, Nathan, 1978.
Long Reef M., Tititira Frm.	17.5	0.5	82.0	Table 3, Nathan, 1978.
Long Reef M., Tititira Frm.	26.4	13.3	60.3	Table 3, Nathan, 1978.
Long Reef M., Tititira Frm.	24.9	17.2	57.9	Table 3, Nathan, 1978.
Long Reef M., Tititira Frm.	32.8	17.0	50.2	Table 3, Nathan, 1978.

References

References

Abers, G.A. & Lyon-Caen, H., 1990: Regional Gravity Anomalies, Depth of the Foreland Basin and Isostatic Compensation of the New Guinea Highlands. *Tectonics,* **9**(6): 1479-1493.

Adams, D.P.M., 1987: *Cretaceous and Eocene Geology of South Westland,* unpublished M.Sc thesis, University of Canterbury, Christchurch, New Zealand.

Adams, J., 1980: Comtemporary uplift and erosion of the Southern Alps, New Zealand, *Geological Society of America Bulletin,* **91:** 1–114.

Aliprantis, M.D., 1987: *Tertiary Geology of the Paringa Region, South Westland, with special attention to the structurally deformed coastal section,* unpublished M.Sc thesis, University of Canterbury, Christchurch, New Zealand.

Allen, P.A., & Allen, J.R., 1990: *Basin analysis -principles and applications.* Blackwell Scientific, Oxford, 451p.

Allen, P.A.; Homewood, P. & Willams, G.D. 1986: Foreland basins: an Introduction *in* **Allen, P.A. & Homewood, P.** (Eds.) *Foreland Basins,* Special Publication of the International Association of Sedimentologists **8**:3–12.

Allis, R.G., 1981: Continental underthrusting beneath the Southern Alps of New Zealand, *Geology,* **9:** 303–307.

Allis, R.G., 1986: Mode of crustal shortening adjacent to the Alpine Fault, New Zealand, *Tectonics,* **5:** 15–32.

Allis, R.G.; Henley, R.W., & Carman, A.F., 1979: The thermal regime beneath the Southern Alps, *in* **Walcott, R.I., & Cresswell, M.M.,** (Eds.) *The Origin of the Southern Alps,* Royal Society of New Zealand Bulletin 18, 79–85.

Audet, D.M., & Fowler, A.C., 1992: A mathematical model for compaction in sedimentary basins, *Geophysical Journal International,* **110:** 577–590.

Audley-Charles, M.G., 1991: Tectonics of the New Guinea area. *Annual Review of Earth and Planetary Sciences* **19:** 17–41.

Australian Gulf Oil Co., 1973: Basic geophysical data from M.V. *Gulfrex* cruises 94–98, October 1972–January 1973, *New Zealand Geological Survey open-file petroleum report 614.*

Baarli, B.G., 1990: Peripheral bulge of a foreland basin in the Oslo Region during the early Silurian. *Palaeogeography, Palaeoclimatology, Palaeoecology,* **78:** 149–161.

Baldwin, B., & Butler, C.O., 1985: Compaction curves. *American Association of Petroleum Geologists Bulletin,* **69**(4): 622–626.

Bally, A.W., (Ed.), 1987: *Atlas of Seismic Stratigraphy,* Volume 1, AAPG Studies in Geology **27**.

Beaumont, C., 1981: Foreland Basins. *Royal Astronomical Society Geophysical Journal,* **65**: 291–329.

Beggs, J.M., 1990: Seismic Stratigraphy of the Plio-Pliestocene Giant Foresets, Western Platform, Taranaki Basin, *in* **Ministry of Commerce**, *1989 New Zealand Oil Exploration Conference Proceedings.* Petroleum and Geothermal Unit, Energy and Resources Division, Ministry of Commerce, New Zealand, p.201–207.

Biddle, K.T.; Uliana, M.A.; Mitchum, R.M.; Fitzgerald, M.G. & Wright, R.C. 1986: The stratigraphic and structural evolution of the central and eastern Magallanes Basin, southern South America, *in* **Allen, P.A. & Homewood, P.** (Eds.) *Foreland Basins*, Special Publication of the International Association of Sedimentologists **8**:41–61.

Bond, G.C., & Kominz, M.A., 1984: Construction of tectonic subsidence curves for the early Paleozoic miogeocline, southern Canadian Rocky mountains: Implications for subsidence mechanisms, age of breakup, and crustal thinning, *Geological Society of America Bulletin*, **94:**155–173.

Boyer, S.E., & Elliot, D., 1982: Thrust systems, *American Association of Petroleum Geologists,* **66:** 1196–1230.

Brown, L.F. Jr., & Fisher, W.L., 1977: Seismic-Stratigrapic Interpretation of Depositional Systems: Examples from Brazilian Rift and pull-apart basins, *See* **Payton**, 1977, pp. 213–248.

Butler, R.W.H., 1989: The influence of pre-existing basin structure on thrust system evolution in the Western Alps *in* **Cooper, M.A. & Williams, G.D.** (Eds), *Inversion Tectonics*, Geological Society Special Publications **44:** 105–122.

Cant, D.J., & Stockmal, G.S., 1989: The Alberta foreland basin: relationship between stratigraphy and Cordilleran terrane-accretion events. *Canadian Journal of Earth Sciences* **26:** 1964–1975.

Carter, L., 1981: Jackson Bathymetry, *New Zealand Coastal Institute Chart, Coastal Series, 1:200 000.*

Clews, J.E., 1989: Structural controls on basin evolution: Neogene to Quaternary of the Ionian zone, Western Greece. *Journal of the Geological Society,* **146:** 447–457.

Cochran, J.R., 1983: A model for the development of the Red Sea, *American Association of Petroleum Geologists Bulletin*, **67**: 41–69.

Cook, R.A.; Wood, R.A., & Campbell, H.J., 1990: The Chatham Rise: An Exploration Frontier, *in* **Ministry of Commerce**, *1989 New Zealand Oil Exploration Conference Proceedings.* Petroleum and Geothermal Unit, Energy and Resources Division, Ministry of Commerce, New Zealand, p.35–41.

Cooper, A.F.; Barriero, B.A.; Kimbrough, D.L., & Mattinson, J.M., 1987: Lamprophyre dyke intrusion and the age of the Alpine Fault, New Zealand, *Geology,* **15:** 941–944.

Cotton, C.A., 1956: Coastal history of Southern Westland and Northern Fiordland, *Transactions of the Royal Society of New Zealand*, **83**(3): 483–488.

Covey, M., 1986: The evolution of foreland basins to steady state: evidence from the western Taiwan foreland basin *in* **Allen, P.A. & Homewood, P.** (Eds.) *Foreland Basins*, Special Publication of the International Association of Sedimentologists **8**: 77–90.

Cross, T.A., & Lessenger, M.A., 1988: Seismic Stratigraphy, *Annual Review of Earth and Planetary Sciences*, **16**:319–354.

Cross, T.A., 1986: Tectonic controls of foreland basin subsidence and Laramide style deformation, western United States *in* **Allen, P.A. & Homewood, P.** (Eds.) *Foreland Basins*, Special Publication of the International Association of Sedimentologists **8**: 15–39.

Dahlstrom, C.D.A., 1969: Balance cross sections, *Canadian Journal of Earth Sciences*, **6:** 743–757.

Davey, F.J., & Smith, E.G.C., 1983: The tectonic setting of the Fiordland region, southwest New Zealand, *Geophysical Journal of the Royal Astronomical Society*, **72:** 23–38.

Davy, B.W., & Davey, F.J., 1985: Bounty Gravity Anomaly Map, Oceanic Series, 1:1 000 000. Wellington, New Zealand, Department of Scientific and Industrial Research.

De Graciansky, P.C.; Dardeau, G.; Lemoine, M. & Tricart, P., 1989: The inverted margin of the French Alps and foreland basin inversion, *in* **Cooper, M.A. & Williams, G.D.** (Eds), *Inversion Tectonics*, Geological Society Special Publications **44:** 87–104.

De Paor, D.G., 1988: Balanced section in thrust belts Part 1: Construction, *American Association of Petroleum Geologists Bulletin*, **72**(1): 73–90.

DeCelles, P.G., & Hertel, F., 1989: Petrology of fluvial sands from the Amazonian foreland basin, Peru and Bolivia. *Geological Society of America Bulletin*, **101**(12): 1552–1562.

DeCelles, P.G., 1986: Sedimentation in a tectonically partitioned, non-marine foreland basin: The lower Cretaceous Kootenai Formation, southwestern Montana. *Geological Society of America Bulletin*, **97**(18): 911–931.

Dewey, J.F., 1982: Plate tectonics and the evolution of the British Isles, *Journal of the Geological Society of London*, **139:** 371–414.

Diamond Shamrock Oil Company (N.Z.) Ltd., 1981: Mikonui no.1 well completion report, *New Zealand Geological Survey open-file petroleum report 836.*

Dickinson, W.R. 1974a: Plate tectonics and sedimentation, *in* **Dickinson, W.R.** (Ed.) *Tectonics and Sedimentation*, Special Publication of the Society of Economic Paleontologists and Mineralogists **22**:1–27.

Dickinson, W.R., & Suczek, C.A., 1979: Plate Tectonics and Sandstone Compositions. *The American Association of Petroleum Geologists Bulletin*, **63**(12): 2164–2182.

Dickinson, W.R., 1974b: Subduction and Oil migration. *Geology*, **2:** 421–424.

Dickinson, W.R.; Beard, L.S.; Brakenridge, G.R.; Erjavec, J.L.; Ferguson, R.C.; Inman, K.F.; Knepp, R.A.; Lindberg, F.A., & Ryberg, P.T., 1983: Provenance of North America Phanerozoic sandstones in relation to tectonic setting. *Geological Society of America Bulletin*, **94:** 222–235.

Dunbar, C.O., & Rogers, J., 1957: *Principles of Stratigraphy*, Wiley, New York, 356 pp.

Eade, J.V., 1972: Hokitika Provisional Bathymetry, *New Zealand Coastal Institute Chart, Coastal Series, 1:200 000.*

Edwards, A.R.; Hornibrook, N. de B.; Raine, J.I., Scott, G.H.; Stevens G.R.; Strong, C.P. & Wilson, G.J., 1988: A New Zealand Cretaceous–Cenozoic time scale, *New Zealand Geological Survey Record* **35:** 135–149.

Esso Exploration and Production (New Zealand) Ltd., 1968: Geophysical report PPL 712 (South Greymouth), *New Zealand Geological Survey open-file petroleum report 400.*

Falvey, D.A., & Deighton, I., 1982: Recent Advances in Burial and Thermal Geohistory Analysis, *Australian Petroleum Exploration Association Journal,* **22**(1): 65–81.

Fleming, P.B. & Jordan, T.E., 1989: A Synthetic Stratigraphic Model of Foreland Basin Development. *Journal of Geophysical Research,* **94**(B4): 3851–3866.

Fowler, C.M.R., 1990: *The solid earth: an introduction to global geophysics.* Cambridge University Press, Cambridge, 472p.

Gair, H.S., 1967: Sheet 20 — Mt. Cook (1st ed.), *Geological Map of New Zealand 1:250,000,* Department of Scientific and Industrial Research, Wellington, New Zealand.

Griffiths, G.A., & Glasby, G.P., 1985: Input of river-derived sediment to the New Zealand continental shelf: 1. Mass, *Estuarine, Coastal and Shelf Science,* **21:** 773–787.

Griffiths, G.A., & McSaveney, M.J., 1983: Distribution of mean annual precipitation across some steepland regions of New Zealand, *New Zealand Journal of Science,* **26:** 197–209.

Guidish, T.M.; Kendall, C.G.St.C; Lerche, I.; Toth, D.J.; & Yarzab, R.F., 1985: Basin evaluation using burial history calculations: an overview. *American Association of Petroleum Geologists Bulletin,* **69**(1): 92–105.

Haq, B.U.; Hardenbohl, J., & Vail, P.R., 1987: Chronology of fluctuating sea levels since the Triassic. *Science,* **235:** 1165–1167.

Hayward, B.W., & Wood, R.A., 1989: Computer-generated geohistory plots for Taranaki Drillhole sequences. *New Zealand Geological Survey Report* PAL 147.

Hayward, B.W., 1987: Paleobathymetry and structural and tectonic history of Cenozoic drillhole sequences in Taranaki Basin. *New Zealand Geological Survey Report* PAL **122.**

Hayward, B.W., 1990: Use of foraminiferal data in analysis of Taranaki Basin, New Zealand. *Journal of Foraminiferal Research,* **20**(1): 71–83.

Hegarty, K.A.; Weissel, J.K., & Mutter, J.C., 1988: Subsidence history of Australia's southern margin: constraints on basin models, *American Association of Petroleum Geologists Bulletin,* **72**(5): 615–633.

Heidlauf, D.T.; Hsui, A.T., & Klein, G. deV., 1986: Tectonic Subsidence Analysis of the Illinois Basin, *The Journal of Geology,* **94**(6):779–794.

Hellinger, S.J., & Sclater, J.G., 1983: Some comments on two-layer extension models for the evolution of sedimentary basins, *Journal of Geophysical Research,* **88:** 8251–8270.

Hill, K.C., 1991: Structure of the Papuan Fold Belt, Papua New Guinea. *The American Association of Petroleum Geologists Bulletin* **75**(5): 857–872.

Hirst, J.P.P. & Nichols, G.J., 1986: Thrust tectonic controls on Miocene alluvial distribution patterns, southern Pyrenees*in* **Allen, P.A. & Homewood, P.** (Eds.) *Foreland Basins*, Special Publication of the International Association of Sedimentologists **8**: 247–258.

Holt, W.E., & Stern, T.A., 1991: Sediment loading on the Western Platform of the New Zealand continent: implications for the strength of a continental margin, *Earth and Planetary Science Letters*, **107:** 523–538.

Homewood, P.; Allen, P.A. & Williams, G.D., 1986: Dynamics of the Molasse Basin of western Switzerland *in* **Allen, P.A. & Homewood, P.** (Eds.) *Foreland Basins*, Special Publication of the International Association of Sedimentologists **8**: 199–217.

Hornibrook, N. de B.; Brazier, R.C., & Strong, C.P., 1989: *Manual of New Zealand Permian to Pliestocene Foraminiferal Biostratigraphy*, New Zealand Geological Survey Paleontological Bulletin 56. Department of Scientific and Industrial Research, Lower Hutt, 175p.

Hoskins, R.H., (Ed.), 1982: Stages of the New Zealand marine Cenozoic: a synopsis, *New Zealand Geological Survey Report 107.*

Hossack, J.R., 1979: The use of balnced cross-sections in the calculation of orogenic contraction: A review, *Journal of the Geological Society of London*, **136:** 705–711.

Houseknecht, D.W., 1986: Evolution from passive margin to foreland basin: the Atoka Formation of the Arkoma Basin, south-central U.S.A. *in* **Allen, P.A. & Homewood, P.** (Eds.) *Foreland Basins*, Special Publication of the International Association of Sedimentologists **8**: 327–345.

Jarvis, G.T., & McKenzie, D.P., 1980: Sedimentary basin formation with finite extension rates, *Earth and Planetary Science Letters,* **48:** 42–52.

Jervey, M.T., 1988: Quantitative geological modeling of siliciclastic rock sequences and their seismic expression, *See* **Wilgus** *et al.*, 1988, pp.47–69.

Jervey, M.T., 1991: GeoMOD: Stratigraphic modeling programs for sequence development in foreland basins, *SEPM Computer Contribution* **2.**

Jordan, T.E., 1981: Thrust Loads and Foreland Basin Evolution, Cretaceous, Western United States. *American Association of Petroleum Geologists Bulletin*, **65**(12): 2506–2520.

Kamp, P.J.J., & Hegarty, K.A., 1989: Multigenic gravity couple across a modern convergent margin: inheritance from Cretaceous asymmetric extension, *Geophysical Journal,* **96:** 33–41.

Kamp, P.J.J., 1986a: Late Cretaceous–Cenozoic tectonic development of the southwest Pacific region, *Tectonophysics*, **121:** 225–251.

Kamp, P.J.J., 1986b: The mid-Cenozoic Challenger Rift System of western New Zealand and its implications for the age of the Alpine Fault inception, *Geological Society of America Bulletin,* v.97, p.255-281.

Kamp, P.J.J., 1991: Late Oligocene Pacific-wide tectonic event, *Terra Nova,* **3:** 65–69.

Kamp, P.J.J.; Green, P.F., & Tippett, J.M., 1992: Tectonic architecture of the mountain front-foreland basin transition, South Island, New Zealand, assessed by Fission track analysis, *Tectonics,* **11**(1): 98–113.

Karner, G.D. & Watts, A.B. 1983: Gravity anomalies and flexure of the lithosphere at mountain ranges. *Journal of Geophysical Research*, **88**(B): 10449–10477.

Karner, G.D.; Steckler, M.S., & Thorne, J.A., 1983: Long-term thermo-mechanical properties of the continental lithosphere, *Nature*, **304**:250–253.

Katz, H.R., 1979: Alpine uplift and subsidence of foredeeps, *in* **Walcott, R.I., & Cresswell, M.M.,** (Eds.) *The Origin of the Southern Alps,* Royal Society of New Zealand Bulletin 18, 121–130.

King, P.R., 1990: Polyphase evolution of the Taranaki Basin, New Zealand: Changes in sedimentary and structural style, *in* **Ministry of Commerce,** *1989 New Zealand Oil Exploration Conference Proceedings,* Petroleum and Geothermal Unit, Energy and Resources Division, Ministry of Commerce, p.134–150.

Klein, G. deV., 1987: Current Aspects of Basin Analysis, *Sedimentary Geology*, **50**:95–118.

Kominz, M.A. & Bond, G.C., 1986: Geophysical modelling of the thermal history of foreland basins. *Nature,* **320**: 252–256.

Koons, P.O., 1989: The topographic evolution of collisional mountain belts: a numerical look at the Southern Alps, New Zealand, *American Journal of Science*, **289:** 1041–1069.

Koons, P.O., 1990: Two-side orogen: Collision and erosion from the sandbox to the Southern Alps, New Zealand, *Geology*, **18:** 679–682.

Kusznir, N. & Karner, G.D., 1985: Dependence of the flexural rigidity of the continental lithosphere on rheology and temperature. *Nature,* **316:** 138–142.

Laird, M.G., & Shelley, D., 1974: Sedimentation and early tectonic history of the Greenland Group, Reefton, *New Zealand Journal of Geology and Geophysics*, **17**: 839–854.

Laird, M.G., 1972: Sedimentology of the Greenland Group in the Paparoa Range, West Coast, South Island, *New Zealand Journal of Geology and Geophysics*, **15**: 372–393.

Loutit, T.S, Hardenbol, J., Vail, P.R., & Baum, G.R., 1988: Condensed sections: The key to age determination and correlation of continental margin sequences, *See* **Wilgus** *et al.*, 1988, pp.183–213.

Lucchi, F.R., 1986: The Oligocene to Recent foreland basins of the northern Apennines *in* **Allen, P.A. & Homewood, P.** (Eds.) *Foreland Basins*, Special Publication of the International Association of Sedimentologists **8**: 105–139.

Lyon-Caen, H., & Molnar, P., 1985: Gravity anomalies, flexure of the Indian plate, and the structure, support and evolution of the Himalaya and Ganga Basin, *Tectonics*, **4:** 513–538.

Magellan Petroleum New Zealand Ltd., 1971: Marine seismic survey—Westland area review incorporating New Zealand Petroleum Co. data of a 1971 survey (by F.A. Gibson), *New Zealand Geological Survey open-file petroleum report 575.*

Marshak, S., & Woodward, N., 1988: Introduction to cross-section balancing, *In* **Marshak, S., & Mitra, G.,** (Eds), *Basic methods of structural geology,* Prentice Hall, New Jersey, pp.303–332.

Massari, F.; Grandesso, P.; Stefani, C., & Jobstraibizer, P.G., 1986: A small polyhistory foreland basin evolving in a context of oblique convergence: the Venetian basin (Chattian to Recent, Southern Alps, Italy) *in* **Allen, P.A. & Homewood, P.** (Eds.) *Foreland Basins*, Special Publication of the International Association of Sedimentologists **8**: 141–168.

Matthews, E.R., 1984: Geological evaluation with recommendations for further exploration—PPL 38075, NZ Oil and Gas/Petroleum Resources Ltd., *DSIR Geology and Geophysics unpublished open-file Petroleum Report No.1055.*

McKenzie, D., 1978: Some Remarks on the Development of Sedimentary Basins, *Earth and Planetary Letters*, **40**:25–32.

McNaughton, D.A., & Gibson, F.A., 1970: Reef play developing in New Zealand, *The Oil and Gas Journal*, **68**(45): 89-95.

McNutt, M.K., 1980: Implications of regional gravity for the state of stress in the earth's crust and upper mantle, *Journal of Geophysical Research*, **85**:6377–6396.

McNutt, M.K.; Diament, M., & Kogan, M.G., 1988: Variations of Elastic Plate Thickness at Continental Thrust Belts, *Journal of Geophysical Research*, **93**(B8):8825–8838.

McSaveney, M.J., Chinn, T.J., & Hancox, G.T., 1992: The Mount Cook rock avalanche of 14 December, 1991, abstract in *Joint Annual Conference, Geological Society of New Zealand, New Zealand Geophysical Society, Programme and Abstracts,* Geological Society of New Zealand Miscellaneous Publication 63A, p.104.

MINEsoft, 1991: *TECHBASE User's Manual Version 2.1*, MINEsoft Ltd, Denver.

Mitchum, R.M. Jr.; Vail, P.R., & Sangree, J.B., 1977: Seismic stratigraphy and global changes of sea level, Part 6: Stratigraphic interpretation of seismic reflection patterns in depositional sequences, *See* **Payton**, 1977, pp. 177–133.

Mitchum, R.M. Jr.; Vail, P.R., & Thompson, S. III, 1977: Seismic stratigraphy and global changes of sea level, Part 2: The depositional sequence as a basic unit for stratigraphic analysis, *See* **Payton**, 1977, pp. 55–62.

Molnar, P., & Lyon-Caen, H., 1988: Some simple physical aspects of the support, structure and evolution of mountain belts *in* **Clark, S.P.; Burchfiel, B.C., & Suppe, J.,** (Eds.) *Processes in Continental Lithospheric Deformation,* Geological Society of America, Special Paper **218:** 179–207.

Moussavi-Harami, R., & Brenner, R.L., 1992: Geohistory Analysis and Petroleum Reservior Characteristics of Lower Cretaceous (Neocomian) Sandstones, Eastern Kopet-Dagh Basin, Northeastern Iran, *American Association of Petroleum Geologists Bulletin*, **76**(8): 1200–1208.

Mutch, A.R., & McKellar, I.C., 1964: Sheet 19 — Haast, *Geological Map of New Zealand 1:250,000*, Department of Scientific and Industrial Research, Wellington, New Zealand.

Nathan, S., 1977: Cretaceous and Lower Tertiary stratigraphy of the coastal strip between Buttress Point and Ship Creek, South Westland, New Zealand, *New Zealand Journal of Geology and Geophysics*, **20**(4): 615–654.

Nathan, S., 1978: Upper Cenozoic stratigraphy of South Westland, New Zealand, *New Zealand Journal of Geology and Geophysics*, **21**(3): 329–361.

Nathan, S.; Anderson, H.J.; Cook, R.A.; Herzer, R.H.; Hoskins, R.H.; Raines, J.I.; & Smale, D., 1986: Cretaceous and Cenozoic sedimentary basins of the West Coast Region, South Island, New Zealand. *New Zealand Geological Survey Basin Studies 1.* 90p.

New Zealand Petroleum Co. Ltd., 1971: Harihari no. 1 well completion report, *New Zealand Geological Survey open-file petroleum report 528.*

New Zealand Petroleum Co. Ltd., 1972: Waiho no. 1 well completion report, *New Zealand Geological Survey open-file petroleum report 529.*

New Zealand Petroleum Exploration Co. Ltd., 1971: Westland offshore seismic survey 1971, *New Zealand Geological Survey open-file petroleum report 523.*

New Zealand Petroleum Exploration Co. Ltd., 1974: Marine seismic survey PPL 683 and PPL 1004 (Prakla-Seismos), *New Zealand Geological Survey open-file petroleum report 629.*

Nichols, G., 1989: Structural and sedimentological evolution of part of the west central Spanish Pyrenees in the Late Tertiary. *Journal of the Geological Society*, **146:** 851–857.

Norris, R.J., Koons, P.O., & Cooper, A.F., 1990: The obliquely-convergent plate boundary in the South Island of New Zealand: implications for ancient collision zones. *Journal of Structural Geology*, **12:** 715–725.

Norris, R.M., 1978: Late Cenozoic geology of the West Coast shelf between Karamea and the Waiho River, South Island, New Zealand, *New Zealand Oceanographic Institute Memoir* **81**.

Nunns, A.G., 1991: Structural restoration of seismic and geologic sections in extensional regimes, *American Association of Petroleum Geologists Bulletin*, **75**(2): 278–297.

Oliver, J., 1986: Fluids expelled tectonically from orogenic belts: Their role in hyrdocarbon migration and other geologic penomena. *Geology,* **14:** 99-102.

Ori, G.G. & Friend, P.F., 1984: Sedimentary basins formed and carried piggyback on active thrust sheets. *Geology*, **12:** 475-478.

Parsons, B., & Sclater, J.G., 1977: An analysis of the variation of ocean floor bathymetry with heat flow and age, *Journal of Geophysical Research*, **82:** 803–827.

Payton, C.E., (Ed.), 1977: Seismic Stratigraphy — applications to hydrocarbon exploration, *AAPG Memoir* 26, 516p.

Peper, T., Beekman, F., & Cloetingh, S., 1992: Consequences of thrusting and intraplate stress fluctuations for vertical movements in foreland basins and peripheral areas, *Geophysical Journal International,* **111:** 104–126.

Pfiffner, O.A., 1986: Evolution of the north Alpine foreland basin in the Central Alps *in* **Allen, P.A. & Homewood, P.** (Eds.) *Foreland Basins*, Special Publication of the International Association of Sedimentologists **8**: 219–228.

Pigram, C.J.; Davies, P.J.; Feary, D.A. & Symonds, P.A. 1989: Tectonic controls on carbonate platform evolution in southern Papua New Guinea: Passive margin to foreland basin. *Geology*, **17**(3): 199–202.

Posamentier, H.W., & Vail, P.R., 1988: Eustatic controls on clastic deposition II—sequence and systems tract models, *See* **Wilgus** *et al.*, 1988, pp.125–154.

Posamentier, H.W.; Jervey, M.T., & Vail, P.R., 1988: Eustatic controls on clastic deposition I—conceptual framework, *See* **Wilgus** *et al.*, 1988, pp.109–124.

Rattenbury, M.S., 1986: Late low-angle thrusting and the Alpine Fault, central Westland, New Zealand, *New Zealand Journal of Geology and Geophysics*, **29**: 437–447.

Rich, J.L, 1951: Three critical environments of deposition and criteria for recognition of rocks deposited in each of them, *Geological Society of America Bulletin,* **18:** 17–45.

Rodgers, J., 1990: Fold-and-Thrust Belts in Sedimentary Rocks. Part 1: Typical examples. *American Journal of Science,* **290**(4): 321–359.

Rodgers, J., 1991: Fold-and-Thrust Belts in Sedimentary Rocks. Part 2: Other examples, especially variants. *American Journal of Science,* **291**(9): 825–886.

Rose, K.H., & Davey, F.J., 1985: Sheet 378—Paringa, *Gravity Anomaly Map, Coastal Series, 1:250,000.* Wellington, New Zealand. Department of Scientific and Industrial Research.

Rose, K.H., 1986: Sheet 359—Greymouth, *Gravity Anomaly Map, Coastal Series, 1:250,000.* Wellington, New Zealand. Department of Scientific and Industrial Research.

Rowan, M.G., & Kligfield, R., 1989: Cross section restoration and balancing as aid to seismic interpretation in extensional terranes, *American Association of Petroleum Geologists Bulletin*, **73**(8): 955–966.

Royden, L., & Karner, G.D., 1984: Flexure of the lithosphere beneath the Appennine and Carpathian fordeep basins, *Nature*, **309:** 142–144.

Royden, L., & Keen, C.E., 1980: Rifitng processes and thermal evolution of the continental margin of eastern Canada determined from subsidence curves, *Earth and Planetary Science Letters,* **51:** 343–361.

Sangree, J.B., & Widmier, J.M., 1979: Interpretation of depositional facies from seismic data, *Geophysics,* **44**(2)**:** 131–160.

Sarg, J.F., 1988: Carbonate sequence stratigraphy, *See* **Wilgus** *et al.*, 1988, pp.155–181.

Schmitt, J.G., & Steidtmann, J.R., 1990: Interior ramp-supported uplifts: Implications for sediment provenance in foreland basins. *Geological Society of America Bulletin,* **102**(4): 494–501.

Schmoker, J.W., & Gautier, D.L., 1989: Compaction of Basin Sediments: Modeling Based on Time-Temperature History, *Journal of Geophysical Research*, **94**(B6)**:**7379–7386.

Schmoker, J.W., & Halley, R.B., 1982: Carbonate porosity versus depth: a predictable relation for south Florida. *American Association of Petroleum Geologists Bulletin*, **66**(12): 2561–2570.

Schwab, F.L., 1986: Sedimentary 'signatures' of foreland basin assemblages: real or counterfeit? *in* **Allen, P.A. & Homewood, P.** (Eds.) *Foreland Basins*, Special Publication of the International Association of Sedimentologists **8**: 395–410.

Sclater, J.G., & **Christie, P.A.F.**, 1980: Continental stretching: an explanation of the post-mid-Cretaceous subsidence of the central North Sea basin. *Journal of Geophysical Research*, **85**(B7): 3711–3739.

Sewell, R.J., & **Nathan, S.**, 1987: Geochemistry of Late Cretaceous and Early Tertiary basalts from South Westland, *New Zealand Geological Survey Record* **18:** 87–94.

Shell BP & Todd Oil Services Ltd., 1967: Marine seismic reconnaissance survey—Greymouth offshore, New Zealand (by M.H.Flandin), *New Zealand Geological Survey open-file petroleum report 548.*

Sheriff, R.E., 1989: *Geophysical methods*, Prentice-Hall, New Jersey, 605p.

Sinclair, H.D.; **Coakley, B.J.**; **Allen, P.A.** & **Watts, A.B.**, 1991: Simulation of Foreland Basin stratigraphy using a diffusion model of mountain belt uplift and erosion: an example from the Central Alps, Switzerland. *Tectonics*, **10**(3): 599–620.

Sloss, L.L., 1963: Sequences in the cratonic interior of North America, *Geological Society of America Bulletin,* **74:** 93–114.

Sloss, L.L., 1988: Forty years of sequence stratigraphy, *Geological Society of America Bulletin,* **100:** 1661–1665.

Spörli, K.B., & **Ballance, P.F.**, 1989: Mesozoic ocean floor/continent interaction and terrane configuration, southwest Pacific area around New Zealand, *in* **Ben-Avraham, Z.**, (Ed.), *The evolution of the Pacific ocean margins*, Oxford University Press, p.176–190.

Stagg, H.M.J.; **Willcox, J.B.**, & **Needham, D.J.L.**, 1992: The Polda Basin—a seismic interpretation of a Proterozoic–Mesozoic rift in the Great Australian Bight, *BMR Journal of Australian Geology and Geophysics*, **13:**1–13.

Steckler, M.S., & **Watts, A.B.**, 1978: Subsidence of the Atlantic-type continental margin off New York, *Earth and Planetary Science Letters*, **41:** 1–13.

Stern, T., 1990: The application of deep seismic reflection profiling to petroleum exploration: an example from the South Taranaki Basin, *in* **Ministry of Commerce**, *1989 New Zealand Oil Exploration Conference Proceedings.* Petroleum and Geothermal Unit, Energy and Resources Division, Ministry of Commerce, New Zealand, p.42–54.

Stern, T.A., & **Davey, F.J.**, 1990: Deep seismic expression of a foreland basin: Taranaki basin, New Zealand. *Geology*,**18:** 979–982.

Stock, J., & **Molnar, P.**, 1982: Uncertainties in the relative positions of the Australia, Antartica, Lord Howe, and Pacific plates since the Late Cretaceous, *Journal of Geophysical Research,* **87:** 4679–4717.

Stockmal, G.S.; **Beaumont, C.** & **Boutilier, R.**, 1986: Geodynamic Models of Convergent Margin Tectonics: Transition from Rifted Margin to Overthrust Belt and Consequences for Foreland-Basin Development. *American Association of Petroleum Geologists Bulletin*, **70**(2): 181–190.

Suggate, R.P., 1990: Late Pliocene and Quaternary glaciations of New Zealand, *Quaternary Science Reviews*, **9:** 175–197.

Suggate, R.P., Stevens, G.R., Te Punga, M.T. (Eds.) 1978: *The geology of New Zealand*, Wellington, Government Printer, 2 vols, 820 p.

Sutherland, R., 1992: Constraints on Late Cenozoic Tectonics in Southwest New Zealand, abstract in *Joint Annual Conference, Geological Society of New Zealand, New Zealand Geophysical Society, Programme and Abstracts,* Geological Society of New Zealand Miscellaneous Publication 63A, p.151.

Swift, D.J.P.; Hudelson, P.M.; Brenner, R.L., & Thompson, P., 1987: Shelf construction in a foreland basin: storm beds, shelf sandbodies, and shelf-slope depositional sequences in the Upper Cretaceous Mesaverde Group, Book Cliffs, Utah. *Sedimentology*, **34:** 423–457.

Syms, M.C., 1978: Sheet 20 — Mt. Cook (1st ed.), *Gravity Map of New Zealand 1:250,000 Bouguer Anomalies / Isostatic Anomalies / Isostatic Vertical Gradient Anomalies*, Department of Scientific and Industrial Research, Wellington, New Zealand.

Syms, M.C., 1979: Sheet 19 — Haast (1st ed.), *Gravity Map of New Zealand 1:250,000 Bouguer Anomalies / Isostatic Anomalies*, Department of Scientific and Industrial Research, Wellington, New Zealand.

Tang, J., & Lerche, I., 1992: Analysis of the Beaufort-Mackenzie Basin, Canada: burial, thermal & hydrocarbon histories, *Marine & Petroleum Geology*, **9**(5):510–525.

Tankard, A.J., 1986: On the depositional response to thrusting and lithospheric flexuring: Examples from the Applachians and the Rocky Mountain basins, *in* **Allen, P.A. & Homewood, P.** (Eds.) *Foreland Basins*, Special Publication of the International Association of Sedimentologists **8**: 369-394.

Thorne, J.A., & Watts, A.B., 1989: Quantitative Analysis of North Sea Subsidence, *American Association of Petroleum Geologists Bulletin*, **73**(1): 88–116.

Tippett, J.M., & Kamp, P.J.J., (*in press*): Fission track analysis of the late Cenozoic vertical kinematics of continental Pacific crust, South Island, New Zealand, *Journal of Geophysical Research.*

Tippett, J.M., 1992: *Uplift history and geomorphic development of the Southern Alps, New Zealand*, assessed by fission track analysis, unpublished D.Phil. thesis, University of Waikato, Hamilton, New Zealand.

Tissot, B.P.; Pelet, R., & Ungerer, P.H., 1987: Thermal History of Sedimentary Basins, Maturation Indices, and Kinetics of Oil and Gas Generation, *American Association of Petroleum Geologists Bulletin*, **71**(12): 1445–1466.

Turcotte, D.L., & Schubert, G., (1982): *Geodynamics: Applications of Continuum Mechanics to Geological Problems*, Wiley, New York, 450 p.

Vail, P.R., 1987: Part 1: Seismic Stratigraphy interpretation procedure, *See* **Bally**, 1987, pp. 1–10.

Vail, P.R., Mitchum, R.M. Jr., & Thompson, S. III., 1977a: Seismic stratigraphy and global changes of sea level, Part 3: Relative changes of sea level from coastal onlap,*See* **Payton**, 1977, pp.63–81.

Vail, P.R., Mitchum, R.M. Jr., & Thompson, S. III., 1977b: Seismic stratigraphy and global changes of sea level, Part 4: Cycles of relative changes of sea level,*See* **Payton**, 1977, pp.63–81.

Vail, P.R., Todd, R.G., Sangree, J.B., 1977: Seismic stratigraphy and global changes in sea-level, Part 5: Chronostratigraphic significance of seismic reflections, *See* **Payton**, 1977, pp.99–116.

Van Hinte, J.E., 1978: Geohistory Analysis—Application of Micropaleontology in Exploration Geology, *American Association of Petroleum Geologists Bulletin*, **62**(2): 201–222.

Van Wagoner, J.C., Mitchum, R.M. Jr., Posamentier, H.W., & Vail, P.R., 1987: Part 2: Key definitions of sequence stratigraphy, *See* **Bally,** 1987, pp. 11–14.

Van Wagoner, J.C., Posamentier, H.W., Mitchum, R.M., Vail, P.R., Sarg, J.F., Loutit, T.S., & Hardenbol, J., 1988: An overview of the fundamentals of sequence stratigraphy and key definitions, *See* **Wilgus** *et al.*, 1988, pp.39–45.

Van Wagoner, J.C., Posamentier, H.W., Mitchum, R.M., Vail, P.R., Sarg, J.F., Loutit, T.S., & Hardenbol, J., 1988: An overview of the fundamentals of stratigraphy and key definitions, *In: Sea Level Changes: an Integrated Approach, Special Publication, Society Economic Paleontologists and Mineralogists,* **42:** 39–45.

Van Wagoner, J.C.; Mitchum, R.M., Jr.; Campion, K.M.; & Rahmanian, V.D., 1990: Siliciclastic sequence stratigraphy in well logs, cores, and outcrops: concepts for high-resolution correlation of time and facies, *AAPG Methods in Exploration Series,* no.7, 55p.

Walcott, R.I., & Cresswell, M.M., (Eds.), 1979:*The Origin of the Southern Alps,* Royal Society of New Zealand Bulletin 18.

Walcott, R.I., 1970: Flexural rigidity, thickness and viscosity of the lithosphere, *Journal of Geophysical Research*, **75**:3941–3954.

Walcott, R.I., 1979: Plate motion and shear strain rates in the vicinity of the Southern Alps, *in* **Walcott, R.I., & Cresswell, M.M.,** (Eds.) *The Origin of the Southern Alps,* Royal Society of New Zealand Bulletin 18, 5–12.

Walcott, R.I., 1984a: Reconstructions of the New Zealand Region for the Neogene, *Paleogeography, Paleoclimatology, Paleoecology,* **46:** 217–231.

Walcott, R.I., 1984b: The kinematics of the plate boundary zone through New Zealand: a comparison of short- and long-term deformations, *Geophysical Journal of the Royal Astronomical Society,* **79:** 613–633.

Walcott, R.I., 1987: Geodetic strain and the deformational history of the North Island of New Zealand during the late Cainozoic, *Philosophical Transactions of the Royal Society, London,* **321:** 163–181.

Wang, Z., & Stein, C.A., 1992: Subsidence of the Gulf of Papua in the Cenozoic, *Tectonophysics*, **205:** 409–426.

Waples, D.W., 1980: Time and Temperature in Petroleum Formation: Application of Lopatin's Method to Petroleum Exploration, *American Association of Petroleum Geologists Bulletin*, **64**(6): 916–926.

Waples, D.W., Kamata, H., & Suizu, M., 1992: The Art of Maturity modelling. Part 1: Finding a satisfactory geologic model. *American Association of Petroleum Geologists Bulletin*, **76**(1): 31–46.

Warren, G., 1967: Sheet 17 — Hokitika (1st ed.), *Geological Map of New Zealand 1:250,000*, Department of Scientific and Industrial Research, Wellington, New Zealand.

Watts, A.B., & Ryan, W.B.R., 1976: Flexure of the lithosphere at continental margin basins, *Tectonophysics*, **36:** 25–44.

Watts, A.B., & Talwani, M., 1974: Gravity anomalies seaward of deep-sea trenches and their tectonic implications, *Geophysical Journal of the Royal Astronomical Society*, **36:** 57–90.

Watts, A.B.; Karner, G.D. & Steckler, M.S., 1982: Lthospheric flexure and the evolution of sedimentary basins. *Philosophical Transactions of the Royal Scoiety of London A,* **305:** 249-281.

Wellman, H.W., & Willett, R.W., 1942: The geology of the West Coast from Abut Head to Milford Sound—Part 1, *Transactions of the Royal Society of New Zealand*, **71**(4): 282–306.

Wellman, H.W., 1955: The geology between Bruce Bay and Haast River, south Westland (2nd edition), *New Zealand Geological Survey bulletin n.s. 48.*

Wellman, H.W., 1979: An uplift map for the South Island of New Zealand, and a model for the uplift of the Southern Alps, *Bulletin of the Royal Society of New Zealand*, **18:** 13–20.

Welte, D.H., & Yalçin, M.N., 1988: Basin modelling—A new comprehensive method in petroleum geology, *Organic Geochemistry*, **13**(1–3): 141–151.

Wheeler, H.E., 1958: Time stratigraphy, *American Association of Petroleum Geologists Bulletin*, **42:** 1047–1063.

Wilgus, C.K.; Posamentier, H.W.; Ross, C.A., & Kendall, C.G.St.C., (Eds.) 1988: Sea level changes—an integrated approach, *SEPM Special Publication* **42**, 407p.

Wilkerson, M.S., & Hsui, A.T., 1989: Application of sediment backstripping corrections for basin analysis using microcomputers, *Journal of Geological Education*, **37:** 337–340.

Wilson, T.J., 1991: Transition from back-arc to foreland basin development in the southernmost Andes: Stratigraphic record from the Ultima Esperanza District, Chile. *Geological Society of America Bulletin*, **103**(1): 98–111.

Wood, R.A., 1989: *Geohistory Analysis.* Technical Report No.104. Geophysics Division, Department of Scientific and Industrial Research, Wellington, New Zealand.

Woodward, D.J., 1975: Sheet 19 — Haast (1st ed.), *Magnetic Map of New Zealand 1:250,000 Total Force Anomalies*, Department of Scientific and Industrial Research, Wellington, New Zealand.

Woodward, N.B., Boyer, S.E., & Suppe, J., 1989: *Balanced Geological Cross-Sections—an essential technique in geological research and exploration*, Short Course in Geology, Volume 6, American Geophysical Union, Washington, 132p.

Young, D.J., 1968: Engineering geology of the Paringa–Haast section of State Highway 6, South Westland, *New Zealand Journal of Geology and Geophysics*, **11**(5): 1134–1158.

Zoetemeijer, R.; Desegaulx, P.; Cloetingh, S.; Roure, F. & Moretti, I., 1990: Lithospheric Dynamics and Tectonic-Stratigraphic Evolution of the Ebro Basin. *Journal of Geophysical Research*, **95**(B3): 2701–2711.